The Synthesis of Glucosamine-Based Derivatives with Potential as Immunomodulators, Kinase Inhibitors, and Prodrugs

Carol Elizabeth Buggy, B.Sc.

NUI MAYNOOTH

Ollscoil na hÉireann Má Nuad

A thesis submitted to the University of Ireland Maynooth in accordance with the requirements for the Degree of Doctor of Philosophy in the Faculty of Science

March 2012

Department of Chemistry

NUI Maynooth

Supervisor: Dr. Trinidad Velasco-Torrijos

Head of Dept.: Prof. John Lowry

Table of Contents

To my parents and to Colm

Memorandum

I declare that the work in this thesis dissertation was carried out in accordance with the regulations of NUI Maynooth. The work is original, except where indicated by reference, and has not been submitted for any other degree. Any views expressed in the dissertation are those of the author and in no way represent those of NUI Maynooth.

Signed: _____ Date: _____

Carol Buggy

Abstract

Chapter 1 gives a brief outline of the relevance of carbohydrates in biological systems. Special attention has been given to the roles of glucosamine and *N*-acetyl glucosamine.

Chapter 2 details the synthesis of novel glucosamine-based serine glycolipids, which were tested for their immunomodulatory ability. The experimental conditions investigated are discussed in detail.

Chapter 3 describes the synthesis of a glucosamine-based serine building block, and its incorporation into a series of glycopeptides, via SPPS techniques, with potential as a kinase inhibitor. The experimental conditions for the synthesis and purification of these peptides are discussed in detail.

Chapter 4 describes an investigation into the introduction of functionalities at the C-6 position of the sugar moiety, with the aim of synthesising an azido-functionalised glucosamine derivative. The experimental details of this investigation are described.

Chapter 5 describes the synthesis of a glucosamine-based dopamine derivative, which has potential as a dopamine prodrug. The various approaches taken in this synthesis, and the experimental conditions are discussed in detail.

Chapter 6 gives the experimental details and characterisations for the compounds reported throughout this thesis.

Chapter 7 contains appendices describing ^{1}H NMR assignation, and also experimental details of attempted experiments.

Chapter 8 contains the bibliographic information used as references in this thesis.

Acknowledgements

I would like to thank Prof. John Lowry for the opportunity to carry out this research.

I would sincerely like to thank my supervisor, Dr. Trinidad Velasco-Torrijos, for her dedicated support, advice, kind words, and friendship over the past four years.

I would like to thank John O' Brien, at Trinity College, Dublin, for the beautiful NMRs which he carried out on my glycolipids. I also want to thank Dr. Derek Doherty, and his students, Andrea Petrasca and Niamh Murphy at St. James' Hospital, Dublin, for the immunological evaluation of these glycolipids. Thanks to Martain Feaney for mass spec analysis of my glycolipids.

My parents, for their continued support and love, it is forever appreciated. Your encouragement and love mean so much to me.

My family and friends, Kim, Liam, Carrie, Claire, Sarah, Zara, and the O'Mearas, for their friendship, support, and forgiveness for my absences!

To Colm, for his constant love and support, the too frequent counselling sessions, and for being the brightness in my days. Without your strength to borrow I couldn't have made it through.

To Niamh, Trish, Alanna, and Louise a special thank you. Thank you for listening, for your advice, and the bucketloads of encouragement. Without your friendship and smiles the last four years would surely have made me insane!

To Noel, for the life-saving operations carried out on computers, and for the chats.

To the technicians Ollie, Orla, Ria and Ken, for patience analysing our difficult samples, and for all the advice.

A special thank you to Barbara, for your patience, advice, and friendship.

To the members of my research group, Roisín, Lorna and Gama. To the postgrads and postdocs, past and present, who have helped, advised, and lent an ear to listen over the past four years, thank you.

Abbreviations

[α]: Specific rotation [expressed without units, the units are (deg·mL)/(g·dm)]

AA: Amino acid

Ac: Acetyl

AcOH: Acetic acid

ACN: Acetonitrile

AD: Alzheimer's disease

Ala: Alanine

aq: Aqueous

Ar: Aryl

Asn: Asparagine

Asp: Aspartic acid

ATP: Adenosine 5'-triphosphate

BBB: Blood brain barrier

Bn: Benzyl

Boc: *tert*-Butoxycarbonyl

bs: Broad singlet

t-Bu: *tert*-Butyl

°C: Degrees Celsius

Cbz: Benzyloxycarbonyl

cm^{-1}: Wavenumber

$CDCl_3$: Deuterated chloroform

COSY: Correlation spectroscopy

CTC: Chlorotrityl chloride

Cys: Cysteine

δ: Chemical shift in parts per million downfield from tetramethylsilane

d: doublet

DBTO: Dibutyltin oxide

DBU: 1,8-diazabicyclo(5.4.0)undec-7-ene

DCC: *N,N'*-dicyclohexylcarbodiimide

DIPEA: Diisopropylethylamine

DCM : Dichloromethane

DEPT: Distortionless enhancement by polarisation transfer

DMAP: 4-(*N*,*N*-dimethylamino)pyridine

DMF: Dimethylformamide

DMSO: Dimethyl sulfoxide

Equiv: Equivalent

ESI: Electrospray ionisation

Et: Ethyl

Et_3N: Triethylamine

EtOAc: Ethyl acetate

Fmoc: 9-Fluorenylmethoxycarbonyl

g: Grams

GlcNAc: *N*-Acetylglucosamine

GlcN: Glucosamine

Glc: Glucose

Gln: Glutamine

Gly: Glycine

Glu: Glutaminc acid

h: Hour(s)

H_2: Hydrogen gas

H_2O: Water

HBr/AcOH: Hydrobromic acid in acetic acid

HCl: Hydrochloric acid

Hex: Hexane

HOBt: Hydroxybenzotriazole

HPLC: High-performance liquid chromatography

HSQC: Heteronuclear single quantum correlation

Hz: Hertz

Ile: Isoleucine

IR: Infrared

J: Coupling constant

KBr: Potassium bromide

L: Litre(s)

Leu: Leucine

Lit: Literature value

Lys: Lysine

m: multiplet (spectral), milli

$MgSO_4$: Magnesium sulphate

M: Molar (moles per litre)

M^+: Parent molecular ion

Me: Methyl

MeOH: Methanol

MHz: Megahertz

min: minute

mol: moles

mmol: Milimoles

MOM: Methoxymethyl

m.p.: Melting point

MS: Mass Spectrometry

N_2: Nitrogen gas

$NaHCO_3$: Sodium hydrogen carbonate

NaH: Sodium hydride

NaCl: Sodium chloride

NBS: *N*-Bromosuccinimide

NMR: Nuclear Magnetic Resonance

NOESY: Nuclear Overhauser enhancement spectroscopy

Pd/C: Palladium on carbon

Pet. Ether: Petroleum ether

Ph: Phenyl

ppm: parts per million

ppt: Precipitate

Pro: Proline

pyr: Pyridine

q: Quartet

R_f: Retention factor

RNA: Ribonucleic acid

rt: Room temperature

s: Singlet

SAR: Structure activity relationship

Sat.: Saturated

Ser: Serine

t: triplet

TBDMS: *tert*-Butyl dimethylsilyl

TBTU: *O*-(Benzotriazol-1, yl) *N,N,N',N'*-tetramethyluronium tetrafluoroborate

TFA: Trifluoroacetic acid

THF: Tetrahydrofuran

Thr: Threonine

TLC: Thin-layer chromatography

TMS: Trimethyl silyl

TMSOTf: Trimethylsilyl trifluoromethane sulfonate

TOF: Time of flight

pTSOH: *para*- Toluene sulphonic acid

Tr: Trityl (Triphenylmethyl)

Troc: Trichloroethoxy carbonyl

Ts: tosyl (*para*-Toluenesulfonyl)

UV: Ultraviolet

v: Volts

Val: Valine

WT: Wild type

Chapter 1: An Introduction to *N*-Acetyl Glucosamine

1.1 Introduction: Carbohydrates in the Development of Novel Therapeutics

Sugars are ubiquitous in the human body, and in nature. They have been found to be integral to many different processes in living organisms such as cell recognition, development, growth, function and survival.[1, 2] For these reasons, oligosaccharides have become interesting in the search for new therapeutics.

Glycosylation is the process of attachment of a sugar moiety to the hydroxy, or other group, of another molecule. In the body, the sugar moiety is attached enzymatically to lipids (glycolipids), other sugars (oligosaccharides), or proteins (glycoproteins). Glycosylation of proteins is one of the most important post translational modifications (PTM) in the human body. The resulting linkage can lead to either the α or β stereoisomer. This linkage can be one of several different kinds when attached to a protein. One type is an *N*-glycosidic linkage, in which the oligosaccharide moiety is bound to the nitrogen of an asparagine amino acid residue. A second is an *O*-glycosidic linkage, where the sugar is attached to the hydroxy group of an amino acid, usually serine or threonine.[3] Each of these glycoproteins serve different purposes in the body, such as forming a protective biofilm on epithelial cells, or as anchors for proteins in cell membranes. For the purposes of this discussion only the *O*-glycoproteins will be addressed.

Glycoproteins derived from natural sources are a complex mixture, due to the process of PTM. The glycoproteins in this mixture are composed of the same peptide backbone, but have slight variations in the nature and site of glycosylation. These are known as glycoforms. A pure glycoform is, therefore, hard to obtain from natural sources, and a synthetic approach is one of the ways in which to achieve a pure, homogenous glycan. These pure forms are necessary for investigation of structure-activity relationships, and also due to the different properties which these glycoforms exhibit.[4] New synthetic techniques and methods have made this feat more achievable.[5-7]

Changes in the glycosylation pattern of cell surface proteins can be a marker for disease. Cancer cells have been found to have altered cell surface glycosylation patterns compared to normal cells. A high abundance of abnormal glycans have been detected on these cells, such as sialyl-Le^x, Globo-H and TF.[8] These antigens are known as tumor-associated carbohydrate antigens (TACA), and are associated with adhesion and invasion of cancer cells, contributing to the metastasis process. Although normal cells do express some of these antigens in low levels, they are much more abundant in abnormal cells. These facts make TACAs a good target for diagnostic purposes, and also as a therapeutic template. Globo-H has been evaluated as an anticancer vaccine in the treatment of breast and prostate cancer (Fig. 1.1).[9]

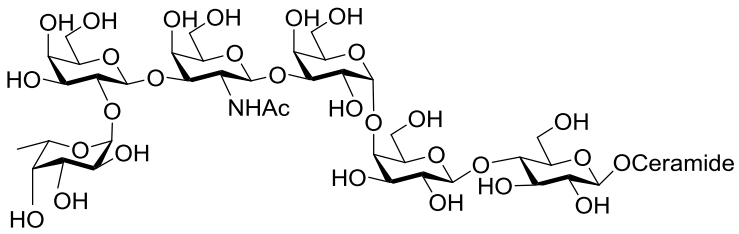

Figure 1.1 Globo-H

Cell-surface carbohydrates play a major role in recognition of antibodies, as receptors for bacterial adhesion, and in cell-cell interactions. HNK-1 glycan is a glucuronylated and sulphated carbohydrate, which is expressed in a cell-type specific manner. Studies have been carried out into the tumor suppressant activity of HNK-1 glycan. This glycan has been shown to play an important role in cell-cell interaction and in cell migration. Studies have found that, in patients suffering from astrocytic tumors, higher HNK-1 expression was associated with increased survival of patients. C6 glioma cells were engineered with HNK-1 positive cells, and these were injected into mouse brains in a controlled study. It was observed that, in the HNK-1 positive mice, the size of tumors were 60 % smaller than in the control mice, which had just been injected with the glioma cells. These results all indicate that HNK-1 glycan functions as a tumor suppressant.[10]

1.2 *N*-Acetyl-D-Glucosamine

The 2-deoxy-2-amino pyranoses are widely found in nature. These sugars have been found to play important roles in vital processes. D-Glucosamine (**1.1**) is the most

abundant of these amino sugars, and it exists as the *N*-acetyl derivative (**1.2**) in most cases (Fig. 1.2). The β-glycosidic linkage has been found to be prevalent in many glycoproteins (**1.3**).[11]

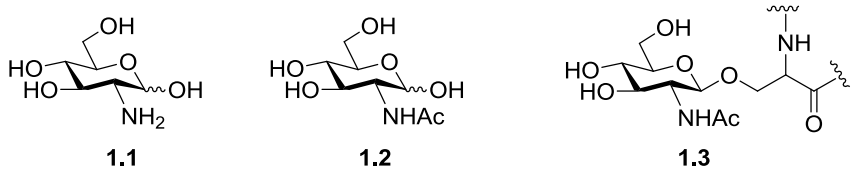

Figure 1.2 D-Glucosamine, *N*-aceytl-D-glucosamine and β-glycoprotein

D-Glucosamine (GlcN) has become of interest to the pharmaceutical and neutraceutical industries over the past few decades.[12] One of the areas of high interest is in the treatment of osteoporosis and osteoarthritis (OA). OA is a disease which affects the joints of the elderly. The cartilage matrix of the joints is mainly composed of collagen and proteoglycan, which GlcN is a large constituent of. This disease is characterized by inflammation, pain and swelling of cartilage. *In-vitro* studies have shown GlcN to suppress mediators which cause these effects. GlcN has been classified as a neutraceutical supplement in many countries, although some controversy exists as to the beneficial effects touted by manufacturers of these supplements.[13]

GlcN has also been investigated for its anti-oxidative and immunostimulating properties. Studies have found that GlcN exhibited strong chelating effects on ferrous ions, and inferred protection onto some macromolecules, such as proteins, from oxidative damage by hydroxyl radicals. These antioxidative activities make GlcN an attractive candidate for therapeutic development. *N*-Acetyl glucosamine (GlcNAc) was investigated, but showed almost no chelating effects. GlcN demonstrated impressive immunostimulating properties also, by enhancement of serum antibody levels in mice.[12]

Glycoproteins possessing the *O*-linked β-*N*-acetylglucosamine (*O*-GlcNAc) modification were discovered relatively recently by Torres and Hart in 1984.[14] They described it as a new PTM which is found abundantly on cytoplasmic and nuclear proteins. There are several reasons for this late discovery of such an integral player in most biological systems. Firstly, the *O*-GlcNAc moiety is small and uncharged,

and so is not picked up by many detection systems. It does not usually alter the migration of proteins in gel electrophoresis. The second reason is that all cells contain hydrolases which cleave *O*-GlcNAc from intracellular proteins once the cells are damaged. Yet another reason is that the degree of protein glycosylation is substoichiometric at each site, and so is difficult to detect by means such as mass spectrometry. Finally, the glycosidic linkage of *O*-GlcNAc is very labile, especially upon ionisation. This means that the sugar is often lost at the ionisation source, and not detected.[15] Developments in detection methods have made this task more manageable.

O-GlcNAc is part of some structural polysaccharides, such as chitin (Fig. 1.3). Chitin forms part of the exoskeleton of invertebrates such as insects and arthropods, and also is a constituent of fungal cell walls.

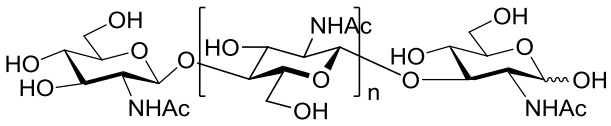

Figure 1.3 The polysaccharide chitin

Enzymes which can hydrolyse chitin are known as chitinases, but humans are deficient in these enzymes. These chitinases could be candidates in the development of insecticides and drugs against pathogens such as *Candida albicans* or *Pseudomonas falciparum*.[16] Chitinase inhibitors have also been investigated for their anti-fungal properties. Chitinases play an essential role in the life cycle of pathogenic fungi, degrading the chitin found in the cell wall. They can also cleave random β-(1,4)-glycosidic bonds within the oligosaccharide, resulting in fragments of varying lengths. Introduction of a chitinase inhibitor could potentially disrupt the natural processes in fungal cells.[16]

Human milk contains many soluble oligosaccharides, such as lacto-*N*-neotstraose (Fig. 1.4). These are known as human milk oligosaccharides (HMO). This collection of sugars is not found in the milk of other mammals. HMOs mainly consist of a lactose moiety as the reducing terminal, and a lactosamine/ isolactosamine at the non-reducing terminal. They are a mixture of linear and branched structures. These oligosaccharides are of major interest due to the properties they infer on the milk.

They can reach the large intestine, where they are easily absorbed into the bloodstream, as they are resistant to hydrolysis. They play roles as prebiotics, and as competitive ligands to pathogenic microorganisms.[11] Adherence is the first step in the pathogenic cycle of invading bacteria. Many of these HMOs have been shown to act as soluble receptor analogues of epithelial cell-surface carbohydrates, and so act as receptor decoys, preventing bacterial adhesion.[17]

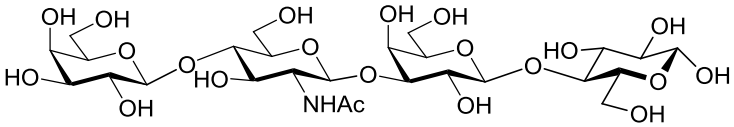

Figure 1.4 Human milk oligosaccharide lacto-*N*-neotstraose

1.3 The Role of *O*-GlcNAcylation in the Regulation of Protein Function

To date more than 1000 proteins have been found to be glycosylated with *O*-GlcNAc residues.[18] This dynamic process is carried out by *O*-GlcNAc transferase (OGT), which glycosylates the hydroxy side chain of serine and threonine residues of proteins (Fig. 1.5). The gene which encodes for OGT is located near the centromere Xq13, which is a chromosomal region linked to several neurological diseases, such as Parkinson's dystonia.[15] The substrate for OGT attachment of *O*-GlcNAc is known as UDP-*O*-GlcNAc (uridine-5'-diphosphate *O*-GlcNAc). Cleavage of *O*-GlcNAc residues from an amino acid is facilitated by a glycosidase enzyme, known as *O*-GlcNAcase. The interplay between these two enzymes allows regulation of many different processes in the body.

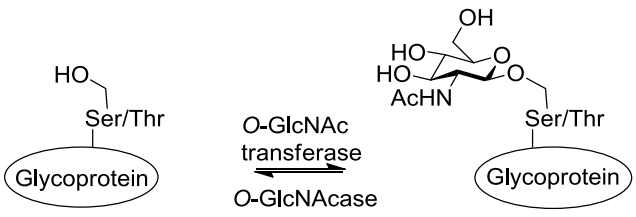

Figure 1.5 Dynamic action of *O*-GlcNAc transferase and *O*-GlcNAcase

O-GlcNAcylation plays an essential role in cell signalling pathways which regulate nuclear and cytoplasmic proteins. Demonstration of the vital nature of *O*-GlcNAcylation is noted in studies where *O*-GlcNAc cycling has been blocked. In

one investigation, galactosyl transferase was used to cap the *O*-GlcNAc moieties with a galactose residue, thereby blocking recognition by enzymes like OGT and *O*-GlcNAcase. This modification to the cell resulted in apoptosis.[19] In another study carried out by O'Donnell *et al*, OGT knockout mice were engineered. Embryonic cells were modified to be deficient in the gene encoding for OGT. This alteration resulted in mice lacking in *O*-GlcNAc, with the outcome of T-cell apoptosis, neuronal tau hyperphosphorylation, and fibroblast growth arrest. Another interesting part of this study was found within the female mouse population. OGT is an X-linked enzyme, and, in female mice, there was no observed alteration in OGT production. This suggests that cells preferentially deactivate the OGT gene deficient chromosome in early development, further demonstrating the necessity of *O*-GlcNAcylation.[20]

Numerous proteins from many functional classes have been found to be *O*-GlcNAcylated, including kinases, transcriptional factors, and even some viral proteins (Fig. 1.6).

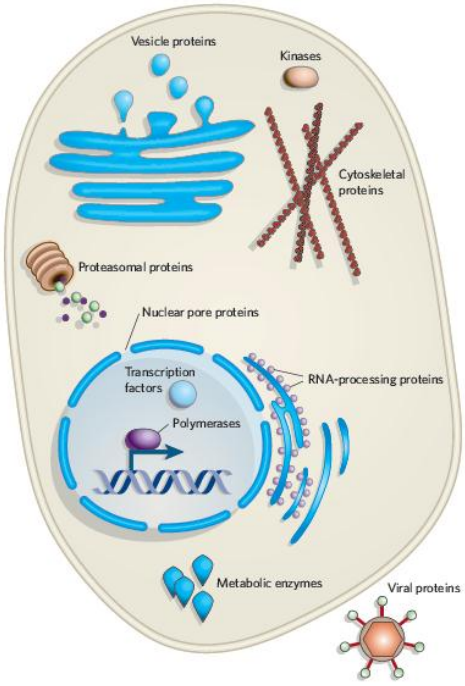

Figure 1.6 Different functional classes of proteins found to be *O*-GlcNAcylated[15]

Regulation of protein function is controlled by several different mechanisms. These include mediating protein phosphorylation, protein degradation, protein-protein interactions, adjusting localisation of proteins, and mediation of transcription.[21]

O-GlcNAcylation has a reciprocal nature with phosphorylation (Fig. 1.6). Both are important PTM, and occur on serine/threonine residues of proteins. A complex relationship exists between these two processes, and each is seen as a regulatory mechanism for the other.

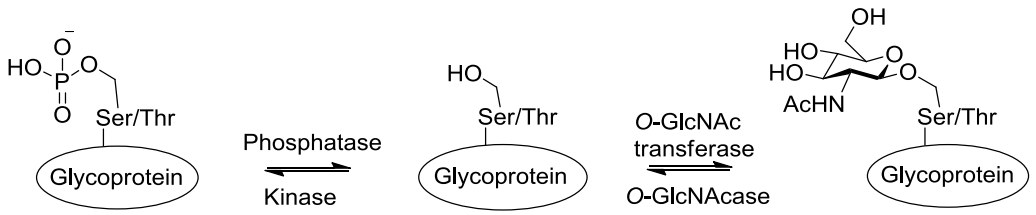

Figure 1.6 Dynamic interplay between glycosylation and phosphorylation

There are at least four different types of interplay which have been identified between *O*-GlcNAcylation and phosphorylation. These include competitive occupancy, where phosphorylation occurs at the same residue as glycosylation (Fig. 1.4), and alternative occupancy, where different residues are targeted by each process.[15] Numerous studies have been carried out to investigate this relationship, with the observation that activation of phosphate kinases resulted in a decrease in *O*-GlcNAcylation. Conversely, when those same kinases were inhibited, an increase in *O*-GlcNAcylation was observed.[22] This relationship can be seen in patients who suffer with Alzheimer's disease (AD). Hyperphosphorylation of the microtubule bundling protein tau is a hallmark of AD, while tau is known to be heavily *O*-GlcNAcylated in the normal human brain.[23]

Protein degradation is required to regulate cell function. *O*-GlcNAcylation can alter the rate of protein degradation in two ways. The first is by altering the targeting of certain proteins to the proteasome, and the second is by altering the activity of the proteasome. Many sites of *O*-GlcNAcylation are located in sequences possessing a high PEST score. These sequences are rich in proline, glutamic acid, serine and threonine residues, which has been shown to mediate protein degradation.[24, 25] A study carried out into murine estrogen receptor-β (mER-β) demonstrated the importance of *O*-GlcNAcylation and phosphorylation in protein degradation. It was shown that Ser^{16} of mER-β is the site for both PTMs to occur. Mutant strains of mER-β, in which the hydroxyl amino acid had been removed at this locus, were glycosylation and phosphorylation deficient. The result of this was a slower rate of

degradation of mER-β, showing the importance of glycosylation and phosphorylation to protein degradation and activity.[26]

Many transcription factors have been found to be *O*-GlcNAc modified. When extracellular concentrations of glucose/glucosamine are altered, the transcription of multiple genes is up- and down-regulated.[21] β-Catenin is a protein which has a vital role in intracellular adhesion and regulating gene expression. Increased transcriptional activity of β-catenin has been associated with the progression of many cancers. Sayat *et al* have shown that *O*-GlcNAcylation of β-catenin negatively regulates its levels in the nucleus. They found that normal prostate cells display higher amounts of *O*-GlcNAcylated β-catenin than prostate cancer cells. *O*-GlcNAcylation of β-catenin significantly reduced its transcriptional activity, making this modification interesting in the development of cancer treatments.[27]

UDP-*O*-GlcNAc is a terminal by-product of the hexosamine biosynthetic pathway (HBP), and is a donor substrate for *O*-GlcNAcylation, as mentioned earlier (Scheme 1.1).[23]

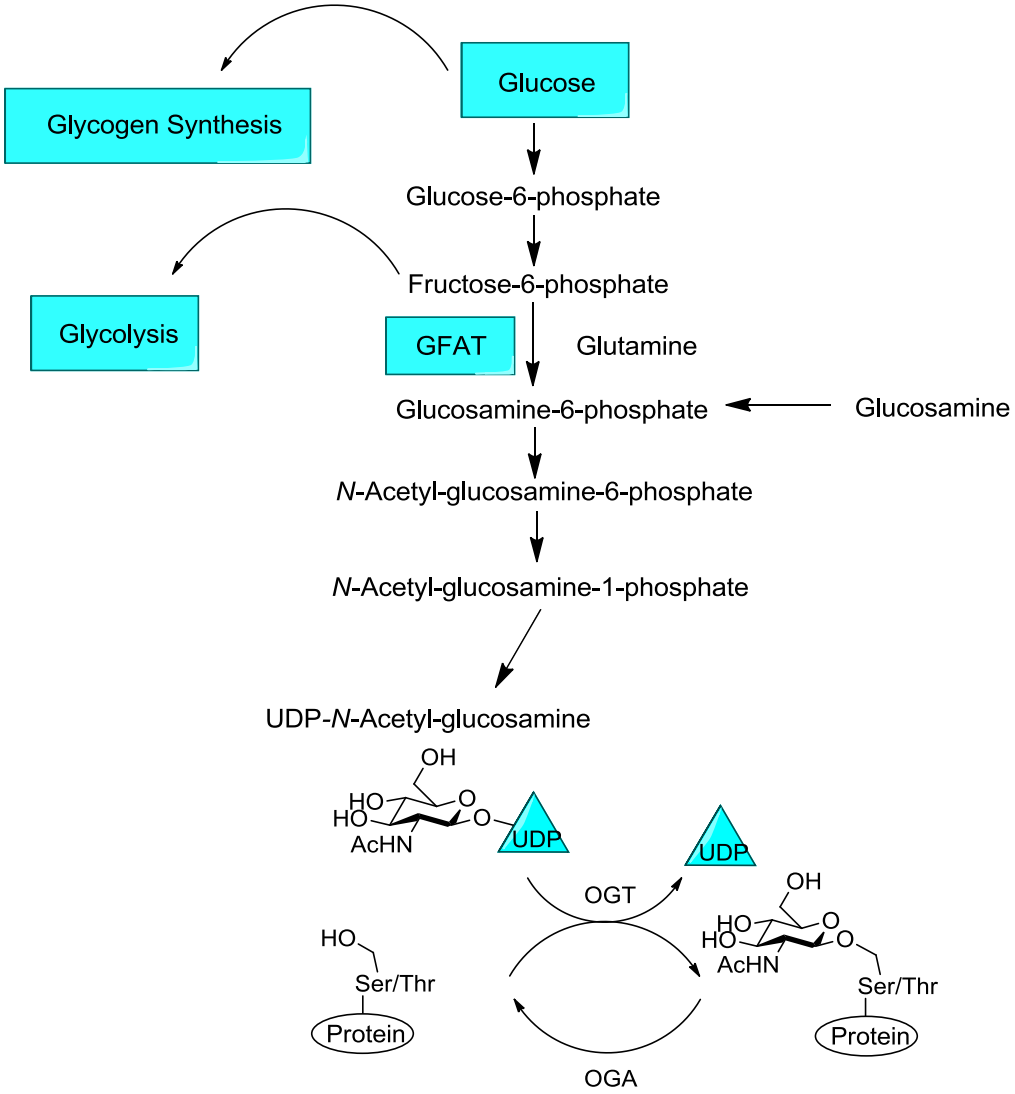

Scheme 1.1 Hexosamine biosynthetic pathway[15]

When the rate of HBP flux varies, this causes changes in the level of UDP-*O*-GlcNAc, which in turn alters the extent of *O*-GlcNAcylation of numerous proteins. HBP is an important pathway in the regulation of insulin levels in the body, acting as a "fuel sensor". It senses the levels of glucose and free fatty acids, and breaks them down into substrates which can be stored within the body. Glucose is rapidly converted to glucose-6-phosphate, and then to fructose-6-phosphate. This is followed by conversion to glucosamine-6-phosphate, which is catalysed by glutamine: fructose-6-phosphate amidotransferase (GFAT). Glucosamine-6-phosphate is next converted to UDP-*O*-GlcNAc, which is the endpoint of the HBP pathway (Scheme 1.1).[28] UDP-*O*-GlcNAc is then used as the donor substrate for *O*-GlcNAcylation of proteins. If there is an abnormal increase in the degree of *O*-GlcNAcylation, this

disrupts the normal dynamic between *O*-GlcNAcylation and *O*-phosphorylation. This, in turn, disturbs signalling, transcription, and other cellular functions, leading to the toxicity associated with type II diabetes, and other diseases.[15] When the HBP flux is increased for prolonged periods of time, over-glycosylation has been shown to occur. This may contribute to impaired cardiac contractile function during the onset of insulin resistance. High circulating free fatty acids observed in obese individuals may chronically activate the HBP, leading to development of insulin resistance. In a study carried out by Rajamani *et al*, it was observed that increasing the HBP flux in a rat model of diet-induced hyperglycaemia/insulin resistance elicited myocardial apoptosis.[28]

The presence of *O*-GlcNAc has been shown to play many vital roles in the functioning of the cell, and regulation of numerous processes. Its integral part in such diverse and important areas make it interesting as a therapeutic target, or as a template for drug design. The prevalence of the labile β-glycosidic bond in nature, and also the added complication of four hydroxy groups of similar reactivity, mean that each step of any synthesis must be carefully planned and carried out. New developments in synthetic carbohydrate chemistry are paving the way for this task,[7] for example, the introduction of less labile, non-native linkages, such as *C*-glycans.[29, 30] In any case, the synthesis of GlcNAc derivatives is of interest in order to study biological processes, and in the search for new therapeutics.

Chapter 2: The Synthesis of Glycosylated-Serine Glycolipid Derivatives

2.1 Introduction: Glycolipids

In biological systems, lipids exist as amphiphilic molecules, which consist of a hydrophilic and a lipophilic portion. The hydrophilic part can be either a phosphate group, in the case of phospholipids, or a carbohydrate moiety in the case of glycoglycerolipids or glycosphingolipids. The lipophilic part is composed of either 1,2-di-*O*-diacylglycerol or *N*-acylsphingosine (Fig. 2.1).[3]

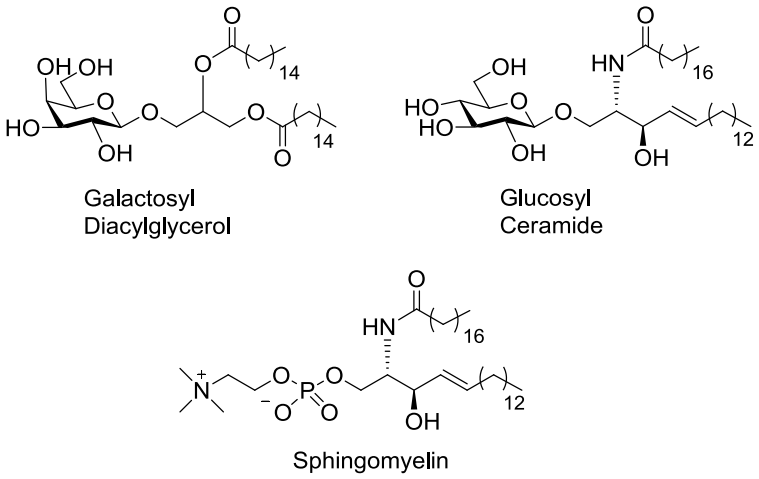

Figure 2.1 Structures of some phospholipids and glycolipids

2.1.1 Sphingolipids

Sphingolipids contain an amine functionality, and when this is acylated it results in the hydrophobic family of compounds, called ceramides, which are a component of most glycosphingolipids (GSLs). The majority of ceramides contain a *trans* C4-C5 double bond in the lipid chain. Sphingolipids which lack this double bond are known as sphinganines, and those which are hydroxylated on C-4 are known as phytosphingosines (Fig. 2.2).[31]

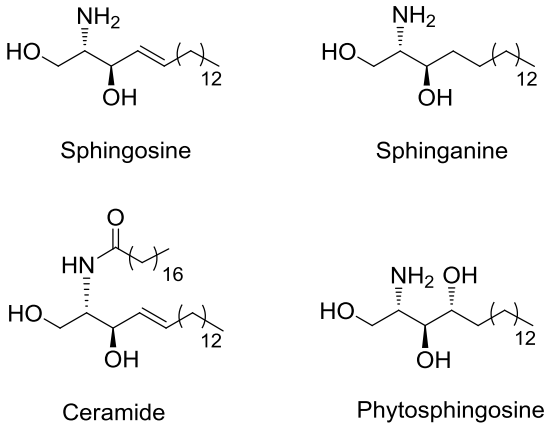

Figure 2.2 Structures of the different sphingolipids

Sphingolipids are produced in the body by either of two different mechanisms. The first is by *de novo* biosynthesis from L-serine and fatty acids, the second is through a salvage pathway, which involves the recycling of building blocks (sphingosine from lysosomal degradation).[32]

2.1.2 Glycosphingolipids

Glycosylated sphingolipids are known as glycosphingolipids (GSL). These are bioactive molecules which are ubiquitous in eukaryotic cell membranes. They are essential to many biological processes such as cellular trafficking, signalling,[33] proliferation, apoptosis,[34] and cell recognition.

Hundreds of different GSLs have been characterised, which vary greatly in respect to the nature of the hydrophobic chains in the ceramide moiety, and also in regard to the carbohydrate portion. GSLs have been loosely divided into several classifications. Cerebrosides contain one sugar residue per ceramide, and are widely distributed in the plasma membranes of neuronal cells. Sulphatides, or sulphoglycosphingosines, consist of a sugar residue which has been sulphated. Gangliosides are complex GSLs, which contain sialic acid residues. And finally, neutral GSLs, or globosides, which contain only neutral oligosaccharides, two or more sugar residues in length.[3]

The composition of GSLs is cell-type specific. For example, gangliosides are a large component of the nervous system, making up 10-12 % of the lipid content, and playing an important part in its crucial processes.[35] The lipid chains of the gangliosides are embedded into the outer leaflet of the plasma membrane, with the

complex glycan moiety extending out into the extracellular space.[36] Gangliosides are involved in regulation of the immune system, metabolic regulation, and in cancer progression. They play an important role in cell-cell recognition, due to binding interactions between the extended glycan and complementary glycan binding proteins (lectins) on other cells. An example of this is the interaction between the sialic acid residues of a ganglioside, and the inhibitory Siglec-7 receptor on natural killer cells, which regulates their cytotoxicity. They can also regulate signalling proteins in their own membranes, as in the case of epidermal growth factor, by interacting laterally.[37] Brain gangliosides GD1a and GT1b bear a sequence (NeuAcα-2-3Galβ1-3GalNAc) which is recognised by myelin-associated glycoprotein (MAG). This cell-cell interaction is required for axon-myelin stability and axon regeneration. Further study of this interaction may provide a way to aid recovery after nerve damage.[38]

2.1.3 The Role of Glycosphingolipids in Disease

The enzymatic degradation of glycosphingolipids by lysosomal hydrolases takes place in endosomes and lysosomes. This is a process which involves several steps, and the failure of any one step can cause accumulation of the lipid substrates in the endosomal compartment. Many symptoms of different diseases have been attributed to this build-up of material, such as Krabbe disease and Fabry disease, and these diseases are collectively known as sphingolipidoses.[39]

Krabbe disease is an inherited autosomal disorder which is caused by a deficiency of galactosylcerebrosidase. This enzyme catalyses hydrolysis of galactose from galactosylceramide and galactosylsphingosine, and its absence causes an accumulation of these glycolipids. An excess of galactosylsphingosine results in the loss of myelin and oligodendrites in the brains of Krabbe disease sufferers. A study was carried out by Pannuzzo *et al* into a galactose free diet for twitcher mice (the mouse model for Krabbe disease). The dietary regime resulted in delayed onset of symptoms in the mice, and may show promise for management of certain forms of the disease.[40]

While being implicated in various disorders, glycosphingolipids have also been investigated as a potential treatment for disease. Sulfatide (Fig. 2.3) and its precursor β-galactosylceramide (β-GalCer) are native GSLs found in pancreatic β-cells. It has

been shown that sulfatide decreases, and β-GalCer increases, the production of proinflammatory cytokines, such as IL-1 β and TNF-α.[41]

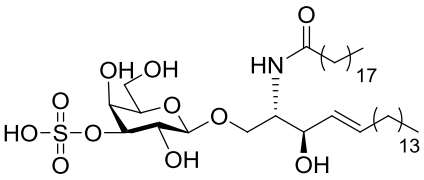

Figure 2.3 Sulfatide

2.2 Non-Ceramide Containing Glycolipids as Therapeutics

Synthetic non-ceramide analogues have been made which display anti-human immunodeficiency virus (HIV) activity. These derivatives appear to be mainly sulfated glycolipids. Dextran sulphate, heparin, and other sulphated polysaccharides have been reported to be highly selective inhibitors of HIV replication.[42]

Achiwa and co-workers have synthesised a number of non-ceramide analogues, which were tested for their anti-HIV activity. They made several different sugar derivatives, which displayed varying amounts of activity. The activity of these compounds was determined by measuring the concentration of the compound (μg/mL) at which 50 % of MT-4 cells expressed HIV-1 antigens. Glycolipids shown in Fig. 2.4 were the most active in this study, and were non-cytotoxic. The glucose derivative **2.1** was the most potent. In the same study, sulphated galactose and glucose serine-based glycolipids were also tested, but showed no anti-HIV activity.[43]

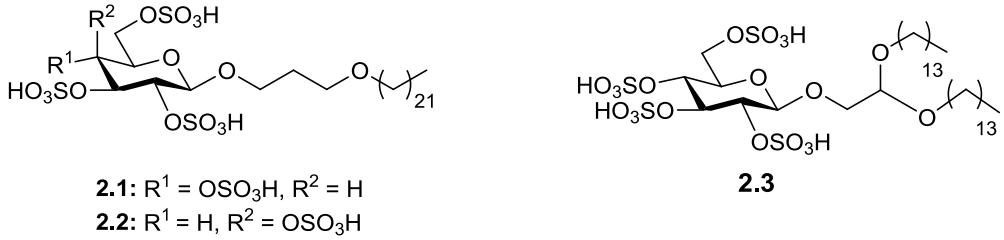

2.1: $R^1 = OSO_3H$, $R^2 = H$
2.2: $R^1 = H$, $R^2 = OSO_3H$

2.3

Figure 2.4 Glycolipid derivatives which display anti-HIV activity

Several glycolipid derivatives have been described so far, with potential for use in the treatment of disease. The area of immune stimulation has attracted huge interest

in recent years, with work being carried out into the development of glycolipid therapeutics.

2.3 Glycolipids as Immunomodulators

2.3.1 The Immune Response

There are two elements to the human immune response; the innate and the adaptive immune systems. The innate immune system deals with many of the pathogens and foreign molecules which the body encounters. It includes physical barriers such as the skin, or epithelia covering vital organs, and also cells like macrophages, dendritic cells, neutrophils, and natural killer (NK) cells. These lymphocytes have the ability to recognise an invading molecule as foreign, and to mount a non-specific attack in order to remove the pathogen from the body. It is a fast response to an unknown pathogen, and is a sufficient barrier in most cases. If the innate immune system becomes overwhelmed, or circumvented, the adaptive immune response is activated. The adaptive immune system is a more specific response, it recognises almost any pathogen. The response is a slower one, as the adaptive system needs to produce lymphocytes with specific antigen receptors, such as T-cell receptors (TCR) and immunoglobulins. These lymphocytes, such as memory T-cells, retain a memory of the invading pathogen. This response provides the host with the ability to recognise these pathogens in the case of reinfection, and so a faster response can be mounted.[44]

2.3.2 Natural Killer T Cells

Natural killer T (NKT) cells are a class of T-lymphocytes which can be considered a hybrid of natural killer (NK) cells and memory T-cells. T-Cells are produced in the thymus, and usually detect peptide antigens which are presented by conventional major histocompatibility (MHC) molecules. NKT cells possess a T-cell receptor (TCR), but differ from traditional T-cells, in that they recognise lipid antigens presented by the non-traditional MHC molecule, CD1d.[45] CD1d is carried by antigen presenting cells, such as dendritic cells or macrophages. NKT cells play an important role in the regulation of the immune response. They have been shown to be involved in host defence against microbial infections, in maintaining immune tolerance,[46] and in the elimination or control of malignant cancers.[45] These

regulatory properties are due to the release of a variety of different cytokines, and activation of cells in the innate and adaptive immune systems. NKT cells are CD1d reactive. The production of cytokines is stimulated by the presentation of specific classes of glycolipids, by the CD1d receptor, to the NKT cells (Fig. 2.5).[47]

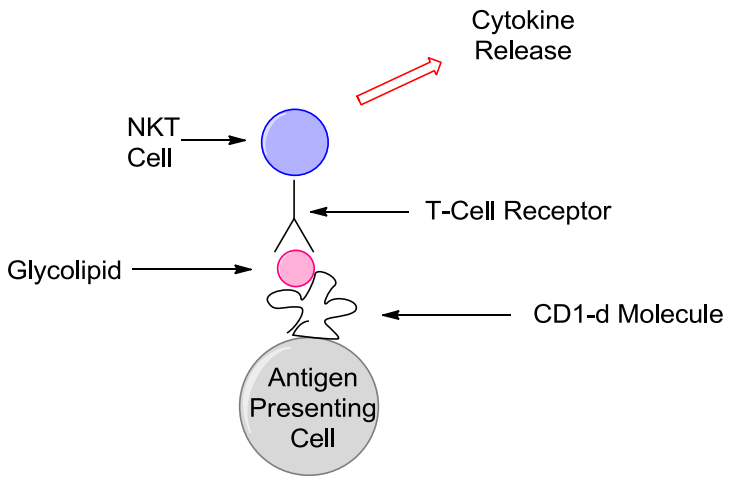

Figure 2.5 A simplified illustration of NKT cell stimulation by binding to CD1d/Glycolipid complex

The CD1d molecule is composed of an α1 helix and an α2 helix, which flank a β-sheet floor. There are two hydrophobic pockets, or channels, in the molecule. Binding of specific glycolipid antigens to CD1d is facilitated by the insertion of the lipophilic glycolipid tails into these pockets. The binding is further strengthened by hydrogen bonds formed between the external polar sugar moiety and amino acid residues at the mouth of the binding pocket. It is this protruding glycan which acts as the TCR binding region. Several features contribute to the specificity of CD1d towards the glycolipid ligand. The lipid chains of the ligand must be of a certain length to fit snugly into the hydrophobic channels; too short and the binding will not be tight enough, too long and the lipid tail will not fit into the pocket. The second factor is the amino acid residues at the binding pocket; these infer specificity for the sugar functionality.[48, 49]

Once NKT cells are activated by binding to this CD1d/glycolipid complex, they can activate the release of different cytokines. The pattern of cytokine release is associated with different immune responses, for example the type 1 and 2 helper T cell based (Th1 and Th2) pathways. It is these two pathways which have received the main focus in the literature. Stimulation of the Th1 response results in the release of

cytokines such as Interferon-γ (IFN-γ) and Interleukin-12 (IL-12), which have been shown to have positive effects on mouse models of malaria and tumor metastasis.[50] Activation of the Th2 pathway induces the release of cytokines such as IL-4 and IL-5, which are regulators of inflammation.[51] As the effects of these two pathways are opposing, the search for a glycolipid which could induce a biased response has become important. Selective activation of either the Th1 or Th2 pathway could be vital for the treatment of many diseases, such as type 1 diabetes or multiple sclerosis.[52]

The native ligand for CD1d mediated activation of NKT cells is not known, but several glycolipids have been suggested. One such glycolipid is isoglobotrihexosylceramide (iGb3), which has been shown to increase the CD1d restricted immune response of human and mouse NKT cells (Fig. 2.6). Using this evidence, synthetic analogues were investigated in order to test the importance of certain parts of the iGb3 molecule to CD1d binding. A structure-activity relationship study showed that the hydroxyl groups on C-2 and C-3 of the galactose moiety were vital for recognition by NKT cells, while the hydroxy groups on C-4 and C-6 were not as important.[53] The α-anomer of iGb3 was found to be recognised by NKT cells, and also to stimulate a more potent *in-vitro* response than the natural β-anomer.[54] Recent research has suggested that iGb3 is not the natural ligand, as it has not yet been found in either mice or humans. Another piece of evidence is the lack of iGb3 synthase in humans, but perhaps the synthesis of iGb3 may be carried out by another enzyme in the absence of iGb3 synthase.[55]

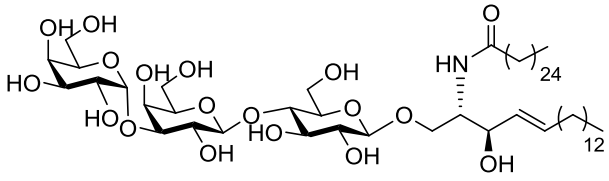

Figure 2.6 Structure of iGb3

Very recent work carried out by Brennan *et al* has described another possible endogenous ligand for CD1d, β-D-glucosylceramide (β-GlcCer). This ligand was tested on mouse and human NKT cells, and was found to stimulate release of both IFN-γ and IL-4. The activity of β-GlcCer was found to be dependent on the composition of the *N*-acyl chain. Several naturally occurring forms of β-GlcCer were

tested, with some derivatives, such as **2.4**, displaying potent stimulatory activity, and **2.5** showing no activity (Fig. 2.7).[56] Some other studies by Stanic *et al* have reported β-GlcCer as being non-antigenic, but the length and degree of saturation of the hydrocarbon chains was different to those tested here.[57]

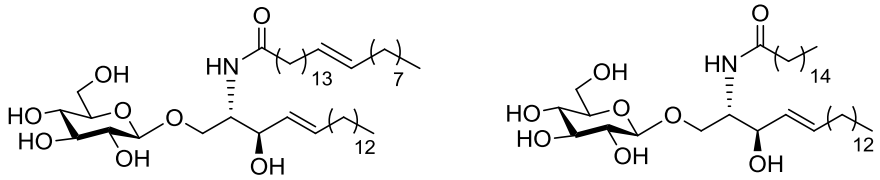

Figure 2.7 Endogenous β-GlcCer derivatives

While the endogenous ligand for CD1d is almost certainly a β-linked glycolipid, much evidence in the literature points to the potent NKT stimulatory abilities of α-glycolipids. The glycoside which has received the most attention in recent years is α-galactosylceramide.

2.3.3 α-Galactosylceramide

α-Galactosylceramide (α-GalCer) is an α-anomeric glycolipid, which is not present in the mammalian body (Fig. 2.8). It was originally isolated from the marine sponge *Agelas mauritianus*, but α-GalCer used in most biological studies is now synthesised in the lab instead, and is known as KRN7000. KRN7000 is usually referred to as α-GalCer, and this convention will be used for the purposes of this discussion. It has been demonstrated that α-GalCer has potent immunomodulatory activity, and much investigation has gone into the use of this glycolipid for the treatment of diseases such as tuberculosis, cancer, and malaria.[58, 59]

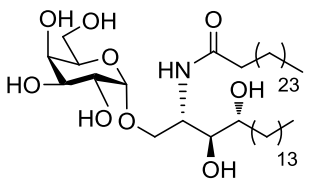

Figure 2.8 Structure of α-GalCer

The stimulation of NKT cells by CD1d molecule presentation of α-GalCer rapidly produces various cytokines, such as IL-4, IL-10, IFN-γ, and tumor-necrosis factor (TNF). *In-vivo* administration of α-GalCer to mice has shown a characteristic

pattern. IL-4 tends to be the main cytokine secreted in the first 24 h, changing to an IFN-γ dominated population after this time.[60]

While α-GalCer has shown promise as a potent immunomodulator, studies have shown that administration can stimulate both the Th1 and Th2 immune responses. This is a problem in the treatment of many diseases, such as autoimmune conditions, where Th1 cytokines are thought to exacerbate symptoms.[53] Other unwanted side-effects such as liver toxicity and aggravation of atherogenesis in mice have also been recorded.[61]

Copious studies have been carried out into the response generated by α-GalCer administration to mouse and human subjects. The potential of α-GalCer is widely acknowledged, but a biased immune response is required for therapeutic applications. This has spurred work into the development of analogues of α-GalCer and other glycolipids.

2.3.4 Synthetic Analogues; The Nature of the Lipid Chains

One point of structural variation is the length of the lipid chains. The hydrophobic pockets of the CD1d molecule are of a specific size, and, by altering the length of the lipid chain, the "fit" of the glycolipid tails can be modified. The length of the hydrocarbon chain may also cause changes in the conformation of CD1d, which could result in a different immune response upon NKT cell activation. Small structural changes could help to generate a biased Th1 or Th2 response. One of the first truncated glycolipid analogues which was tested is known as OCH (Fig. 2.9). This glycolipid contains a shorter sphingosine chain; C_5H_{11} compared to that of α-GalCer, which is $C_{14}H_{29}$.

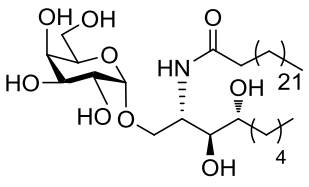

Figure 2.9 Structure of the truncated analogue OCH[62]

OCH has been shown to skew the release of cytokines towards a Th2 profile, with IL-4 being the main cytokine produced. This kind of bias has been beneficial in suppressing the myelin-antigen specific Th1 response in the mouse model of

multiple sclerosis. There is an obvious difference in cytokine stimulation by OCH, compared to the unbiased response of α-GalCer administration.[62] This is thought to be because the shorter sphingosine chain of OCH is not as tightly bound into the hydrophobic pocket of the CD1d molecule. The sugar moiety is then angled differently, lessening interactions with amino acid residues of CD1d, resulting in a shorter association time for the glycolipid/CD1d complex. The release of Th1 cytokines appears to require a longer period of NKT stimulation.[63, 64]

Other truncated analogues of α-GalCer have been synthesised, with several showing a biased Th2 response. Shortening of the acyl chain, for example to C_7H_{15}, also stimulates an increase in the release of Th2 cytokines.[65]

Care must be taken when considering much of the results of these tests. Often a skewed response is noted when working with mouse cell lines, but when the testing is carried out on human cell lines this skewing is not observed. An example of this can be seen in a study carried out by Veerapen *et al*. This group synthesised several truncated OCH glycolipid analogues (Fig. 2.10). They found that several were active, and displayed a biased Th2 response with mouse iNKT (invariant NKT) cells. The same compounds were active when tested with human iNKT cells, but a nonbiased response was stimulated, with secretion of both IL-4 and IFN-γ.[66] It has been found that mouse NKT cells are phenotypically different to those expressed by humans, with a different subset of NKT cells being present. This is especially noted among human iNKT cells, which can be $CD4^+$, $CD8^+$, or $CD4^-CD8^-$. Mouse iNKT cells lack the $CD8^+$ subtype. Healthy mice also possess more iNKT cells than healthy humans. These differences can account for the variation in activity between mouse and human NKT cells.[67]

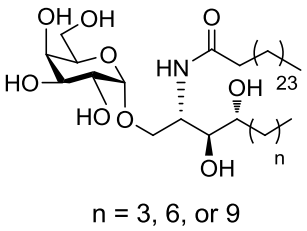

n = 3, 6, or 9

Figure 2.10 Truncated OCH analogues synthesised by Veerapen *et al*[66]

Changes in the nature of the lipid chains described so far have mostly elicited a biased Th2 response, but analogues have also been synthesised which encourage a

Th1, or IFN-γ, based response. Work carried out by Wong and co-workers has produced compounds which stimulate a biased Th1 response in human iNKT cells. They have carried out modifications to introduce a more polar phenyl ring onto the end of the hydrophobic chain, with several compounds displaying the desired activity (Fig. 2.11). These glycolipids were the first of such compounds to stimulate a more potent release of IFN-γ than α-GalCer, and could have potential as adjuvants, or antiviral agents. They also synthesised shorter chain derivatives, but these did not show a biased response, indicating the need for the spacer chain.[68]

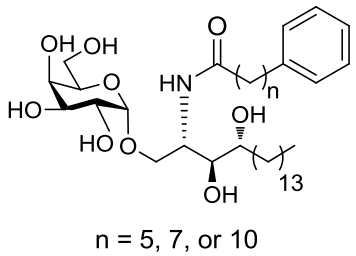

Figure 2.11 Glycolipid derivatives synthesised by Wong and co-workers[68]

Serine-based analogues have been investigated, such as that synthesised by Fan *et al* (Fig. 2.12). This glycolipid was found to activate mouse NKT cells, but the response was non-biased, and mild, with release of small amounts of both IL-4 and IFN-γ. The fucosyl ceramide, and glucosyl-serine derivatives were also synthesised, but showed no immune-activity.[69]

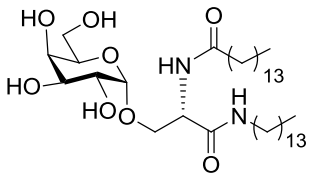

Figure 2.12 Serine-based glycolipid synthesised by Fan *et al*[69]

2.3.5 Synthetic Analogues; Glycosidic Bond Derivatives

Another modification which has been carried out is the replacement of the glycosidic oxygen with a different atom, such as carbon, nitrogen, or sulphur.

One of the first such analogues was α-*C*-GalCer, **2.6**, synthesised by Schmieg *et al* (Fig. 2.13). In this derivative carbon replaces the more electrophilic oxygen atom. In mouse studies α-*C*-GalCer was found to be 1000-fold more potent than its oxygen

counterpart, stimulating a biased Th1 cytokine response. The efficacy of this analogue has been attributed to the resistance of the non-native carbon linkage to enzymatic hydrolysis.[70] When α-*C*-GalCer was tested with human iNKT cells the results were a lot less promising. Further modifications involving *C*-glycosides include the introduction of an alkene at the glycosidic linkage as in **2.7** (Fig. 2.13). This derivative was shown to have potent human NKT stimulating effects, with a bias towards a Th1 response.[71]

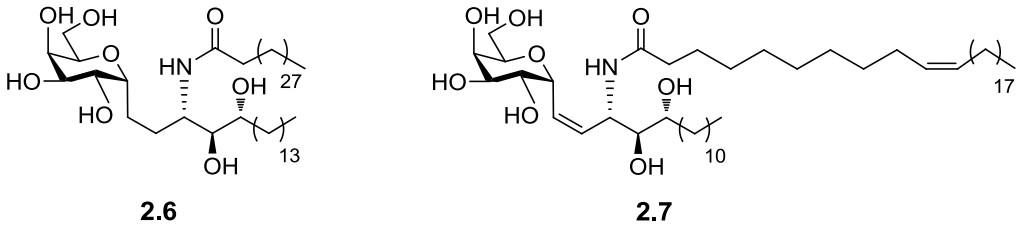

Figure 2.13 *C*-Glycosidic derivatives

Thio-derivatives have also been of interest. Thioglycoside analogues are those in which the glycosidic oxygen has been replaced by a sulphur atom. An α-*S*-GalCer derivative, synthesised by Zhu and co-workers, was found to stimulate the production of cytokines by human NKT cells, with a comparable potency to α-GalCer (Fig. 2.14). It was found that the thioglycoside did not stimulate mouse NKT cells. This analogue shows promise as a positive control in biological studies, and may be a more suitable derivative than α-GalCer, which also stimulates mouse NKT cells. Although this derivative did stimulate cytokine release, a biased response was not obtained.[72]

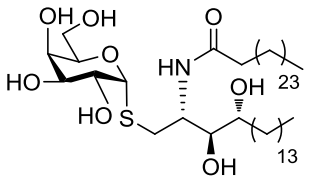

Figure 2.14 Thioglycoside derivative synthesised by Zhu and co-workers[72]

Another popular modification of the glycosidic linkage is to synthesise β-glycolipid analogues. These are of great importance, as, although α-glycolipids have been shown to be potent immunostimmulators, there are no α-glycosphingolipids known in the human body, to date. The native ligand for CD1d must, therefore, be a β-

glycolipid, as discussed earlier, for example β-GlcCer.[56, 73] Much investigation has been carried out into the stimulation of NKT cells by β-glycolipids, and it has been found that they are capable of this activation, albeit in a lower potency than their α-linked analogues. In the binding cleft of the CD1d molecule α- and β-linked sugars adopt different orientations. Observations by Pellicci *et al* show that, even though the sugars orientation at the binding cleft is different, the TCR of the NKT cell is capable of flattening the glycan so that both anomers possess a similar conformation. This is also true for oligosaccharides, like iGb3. The less potent activity of β-glycolipids is attributed to the energetic penalty which is incurred in order to distort them into the shape of an α-linked glycoside.[74] These results were strengthened by Yu *et al* who carried out a similar study.[75]

2.3.6 Synthetic Analogues; β-Glucosylceramides

β-Glucosylceramides (β-GlcCer) are a naturally occurring family of glycolipids found in the human body. β-GlcCer occurs in many different, closely related forms, with variations on the hydrocarbon chains. Only certain forms are found in the body, and, as discussed earlier, endogenous β-GlcCer derivatives have been found to have NKT stimulatory properties.[56]

Kobayashi *et al* examined the effects of synthetic β-GalCer and β-GlcCer derivatives on murine NKT cells. They found that the β-glycolipids did stimulate NKT cells, but at a much lower level than their α-equivalents.[76]

Work carried out by Oku *et al* has shown that β-GlcCer (**2.8**) displays specific cytotoxicity to tumor cells *in-vivo*. They also found that β-GalCer (**2.9**) has the same effect, suggesting that the mode of action is not dependent on the specific sugar structure (Fig. 2.15). These glycolipids were derived from malt feed. The effect of the ceramide portion alone was investigated, and these compounds showed no cytotoxicity towards cancer cells, indicating the need for the glycan component. This may also be due to the hydrophobicity of the ceramide, which would alter its solubility. Glycosylation of the ceramide would introduce a more hydrophilic nature to the compound. This cytotoxicity is not attributed to the production of IFN-γ, as is the case with some other glycolipid derivatives.[77]

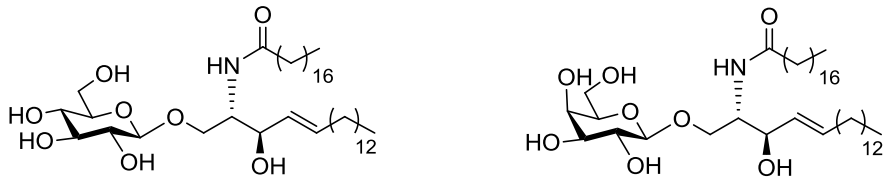

2.8 **2.9**

Figure 2.15 β-Glycolipid derivatives which display cytotoxicity to tumor cells

Ya'acov *et al* have synthesised a thio-derivative of β-GlcCer, and have tested both the *O*- and *S*- glycosides for their immunoregulatory activity (Fig. 2.16). They found that both β-GlcCer and β-*S*-GlcCer led to a decrease in STAT-1 phosphorylation, and a decrease in IFN-γ levels. This result is of importance in the treatment of auto-immune diseases, for example in the alleviation of ConA immune-mediated hepatitis. The thio-analogue was less susceptible to enzymatic degradation, and was shown to increase the suppression of intra-hepatic NKT lymphocytes.[73]

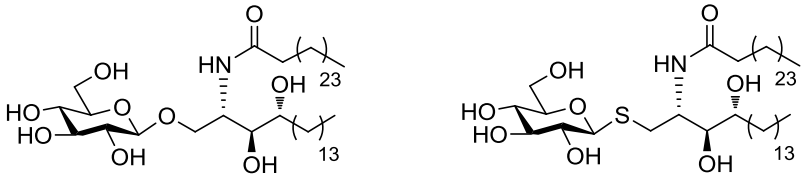

2.10 **2.11**

Figure 2.16 The structures of β-GlcCer 2.10 and β-*S*-GlcCer 2.11

Several β-linked glycolipid derivatives have been tested for their immunostimulatory ability, but, for the main part, they have shown weaker activity than their α-linked counterparts. This should not be seen as a deterrent, as, even with weak activity, as long as the immune response generated is biased, there may still be a use for β-glycosides as immunomodulators.

2.3.7 Synthetic Analogues; Modification of the Carbohydrate Moiety

Modification of the sugar moiety is another area which has been investigated. Several 6'-modified α-GalCer derivatives have been shown to stimulate cytokine release from mouse NKT cells. The analogue synthesised by Trappeniers *et al*, shown in Fig. 2.17, was found to induce a strong Th1 biased response.[78] This compound was later tested for activation of human NKT cells, and was found to stimulate the release of cytokines.[79]

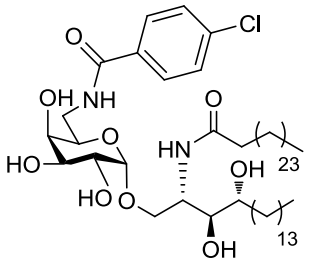

Figure 2.17 6'-Modified analogue synthesised by Trappeniers *et al*[78]

Substitution of the galactose sugar moiety for a different sugar has been carried out. An example of this is β-mannosylceramide (β-ManCer), which has been shown to activate both mice and human NKT cells (Fig. 2.18). Unusually, β-ManCer infers some tumor immunity in mouse studies, but does not stimulate the release of IFN-γ, which is thought to be the source of most analogues anti-tumor properties. It also does not induce release of IL-4, or other commonly stimulated cytokines. The mode of action of β-ManCer was investigated, and found to be due to the stimulation of NOS (Nitric Oxide Synthase) and TNF-α. Mouse models were given an NOS inhibitor called *N*-nitro-D-arginine-methyl ester. This NOS inhibition had no effect on the tumor formation in mice treated with α-GalCer, showing that the immunity given by α-GalCer is not dependent on NOS production. Conversely, the protection brought about by β-ManCer was completely eradicated in these mice, showing the NOS-dependent manner of protection by this analogue. NOS can be induced by TNF-α. Blocking of TNF-α was also found to reverse tumor immunity.[80]

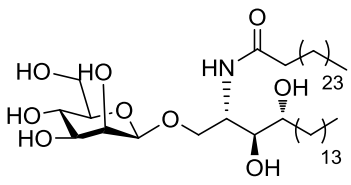

Figure 2.18 The structure of β-mannosylceramide

A non-glycosidic analogue, known as threitolceramide, has also been synthesised (Fig 2.19). This derivative demonstrates stimulation of NKT cells, even without the sugar moiety. The levels of cytokine release were lower than that of α-GalCer, but the levels of NKT cell-mediated lysis of the antigen bearing cells (dendritic cells) was also lowered. This is due to the lower affinity of the NKT cell TCR for threitolceramide than for a glycan.[81]

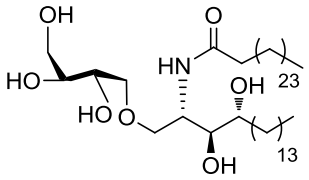

Figure 2.19 Non-glycosidic analogue threitolceramide

2.3.8 A Multitude of Analogues

The glycolipid analogues discussed above are just a small selection of the work which has been carried out in this area. Several reviews exist which detail many more derivatives, some with promising effects.[53, 82] It is a field which holds great potential in the treatment of disease, and work will continue in the effort to synthesise, or discover, a glycolipid which induces a strong biased response in human models.

2.4 L-Serine

Serine is a naturally occurring amino acid, and is found in many proteins (Fig. 2.20). Glycosylated serine is not often found in glycolipids, but is very common in glycoproteins.[8]

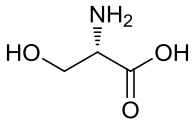

Figure 2.20 The structure of L-Serine

Serine provides an attractive option to develop ceramide analogues, as it allows the use of simple, well established peptide coupling methodology to introduce different functionalities. Several serine-based glycolipids have emerged, which have been demonstrated to be bioactive.

Achiwa and co-workers synthesised galactosamine and glucosamine serine-based glycolipids (Fig. 2.21). The non-sulphated derivatives, **2.12** and **2.13**, displayed no anti-HIV activity, but the sulphated analogues, **2.14** and **2.15**, showed good anti-HIV activity, and were non-cytotoxic.[83]

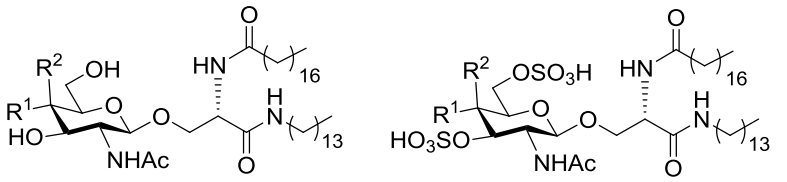

2.12: R^1 = OH, R^2 = H
2.13: R^1 = H, R^2 = OH

2.14: R^1 = OSO_3H, R^2 = H
2.15: R^1 = H, R^2 = OSO_3H

Figure 2.21 Serine-based glycolipid derivatives

Huang *et al* have synthesised some serine-based glycolipids, and tested their activity as Toll-like receptor 4 (TLR4) activators (Fig. 2.22). Lipopolysaccharides (LPS) are amphiphilic glycolipid component of the outer membrane of Gram-negative bacteria. When these bacteria enter the body, they are recognised by TLR4, which stimulates the innate and adaptive immune systems. Compounds **2.16**, **2.17** and **2.18** were all shown to activate TLR4. Changes in the sugar moiety, and conversion to the β-linkage in the glucosyl derivative **2.18** were tolerated. The β-anomer of the galactosyl derivative resulted in a loss of activity.[84]

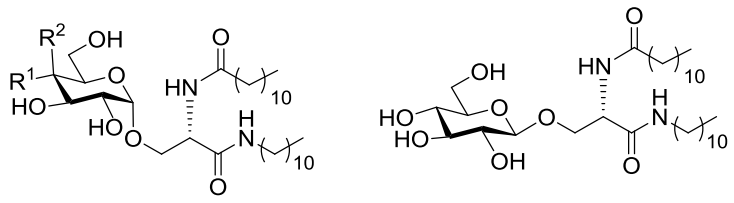

2.16: R^1 = OH, R_2 = H
2.17: R^1 = H, R^2 = OH

2.18

Figure 2.22 Serine-based glycolipids showing TLR4 activation

Anionic β-glycolipids **2.19** and **2.20** were synthesised by Faroux-Corlay *et al*, and were found to display anti-HIV activity (Fig. 2.23). Binding studies carried out on these glycolipids found that, on addition of gp120 (the envelope glycoprotein of HIV), the gp120 inserted into monolayers of the galactolipids. This binding may be responsible for the anti-HIV properties of these analogues.[85]

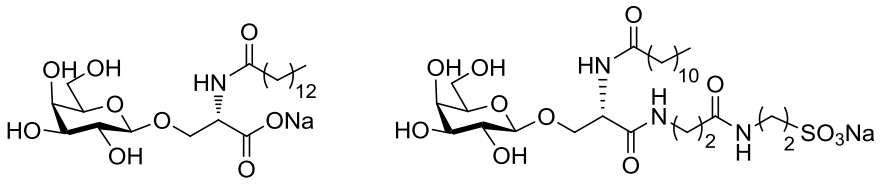

2.19 **2.20**

Figure 2.23 Anti-HIV glycolipids synthesised by Faroux-Corlay *et al*[85]

Serine-based glycolipid derivatives have also been used for a slightly different purpose, with the β-GalCer analogue shown in Fig. 2.24 displaying potential for inclusion in cosmetics and medicines, to improve skin barrier function. This derivative increases β-glucocerebrosidase activity *in-vitro*, which is associated with the skin barrier function. β-Glucocerebrosidase produces acylceramide, which is an important lipid in the prevention of various skin diseases, such as dermatitis.[86]

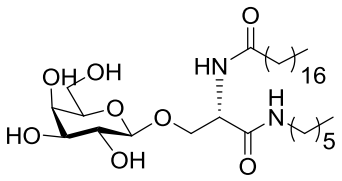

Figure 2.24 β-GalCer derivative synthesised by Fukunaga *et al*[86]

2.5 Aim

The aim of this section was to synthesise some glucosamine-based serine glycolipid derivatives (Fig. 2.25), and to have them tested on human NKT cell lines to assess their potential as immunomodulators.

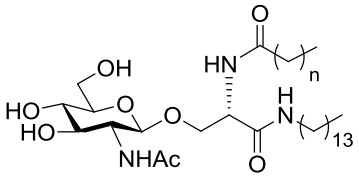

Figure 2.25 Glucosamine based serine glycolipid derivatives (n = 8 or 22)

As mentioned earlier, there are several advantages to incorporating serine into glycolipids. The hydrocarbon chains can be introduced using peptide coupling methodology of TBTU/HOBt, which is a well-established procedure. Serine is

structurally similar to ceramide, and it was postulated that small changes in this part of the molecule may induce favorable differences in activation of NKT cells.

Glucosamine has been demonstrated to be involved with many regulatory processes in the body.[18] We wanted to synthesise glucosamine-based glycolipids in order to investigate the effect that the acetamide group, at the C-2 position of GlcNAc, would have on the glycolipids affinity for the CD1d molecule. It is thought that the acetamide functionality may change the binding affinity, and may also alter the profile of cytokine release by the activated NKT cell, as compared to that of galactose or glucose-based analogues.

As discussed previously, it has recently emerged that the endogenous ligand for CD1d cells could be β-GlcCer, and so it is important for new, synthetic β-glycolipid analogues to be made.[56]

2.6 Synthesis of Glycosyl Building Block 2.22

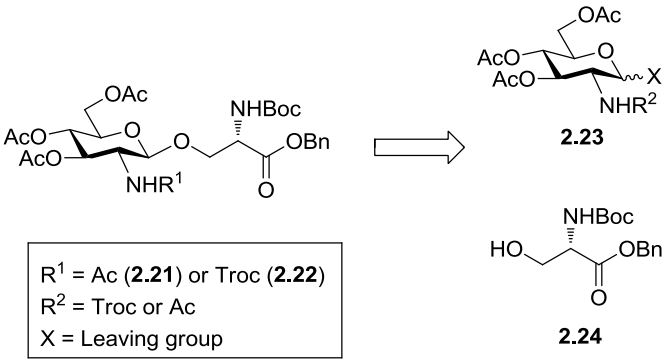

Scheme 2.1 Retrosynthetic approach to the synthesis of glycosyl building block

The retrosynthetic scheme for the synthesis of a suitable building block is shown in Scheme 2.1. These glycosides, **2.21** and **2.22**, have been synthesised by multistep procedures in the literature, but it was thought that a more succinct synthesis could be possible.[87] The protected serine acceptor, **2.24**, was synthesised following literature procedures, by alkylation of the carboxylic acid functionality of commercially available L-Boc serine, with benzyl bromide, to produce the benzyl ester **2.24** (Scheme 2.2).[88] The free acid is protected to prevent undesired glycosylation from occurring at the carboxylic acid position.

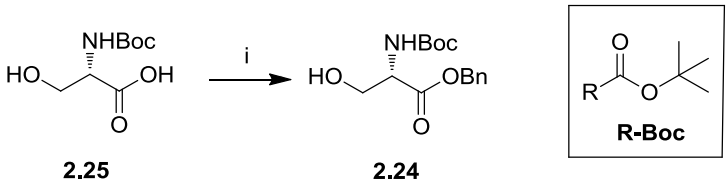

2.25 **2.24**

Scheme 2.2 Synthesis of glycosyl acceptor 2.24. Reagents and conditions: i) BnBr, K_2CO_3, DMF, overnight, rt, 68 %

N-Troc glucosamine derivative **2.26**, the first glycosyl donor prepared for the synthesis of **2.21**, was obtained following literature procedures.[89] The *N*-Troc protecting group was chosen for its stability to mildly acidic and basic conditions. It is removed under very specific conditions, and is orthogonal to the other protecting groups used. D-Glucosamine hydrochloride was first *N*-Troc protected at the amine functionality, by reacting with trichloroethoxycarbonyl chloride (TrocCl), in the presence of $NaHCO_3$. This was followed by acetylation of the hydroxy groups with acetic anhydride, in the presence of pyridine, to give the anomeric mixture of **2.26** (Scheme 2.3). This protection is necessary, as D-glucosamine contains four hydroxy groups, each of which could act as the glycosyl acceptor, although the hydroxy group at the C-1 position is the most reactive.

Peracetylated donors are well documented in the literature,[90] and glycosylation of **2.24** directly from **2.26** was attempted, using $BF_3.OEt_2$ as the promoter. This was unsuccessful from our donor, with full recovery of starting materials (Scheme 2.3).

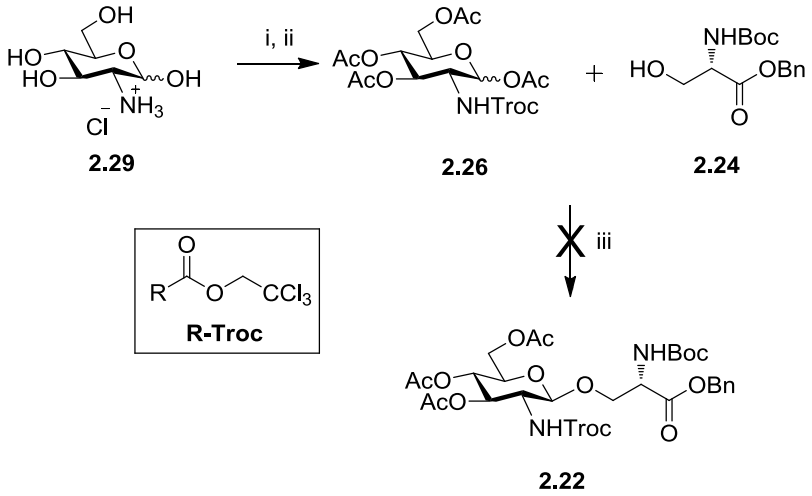

2.29 **2.26** **2.24** **2.22**

Scheme 2.3 Glycosylation directly from *N*-Troc protected donor 2.26. Reagents and conditions: i) TrocCl, H_2O, $NaHCO_3$, 2.5 h, rt; ii) Ac_2O, pyr, overnight, rt, 87 % over two steps; iii) $BF_3.OEt_2$, DCM, rt, overnight

As the above route was unsuccessful, an alternative donor was investigated. Glycosyl halides are popular donors for the Köenigs-Knorr reaction.[91] The glycosyl halide is activated with metal salts, and the halide (Br or Cl) is substituted by an alcohol. If there is neighboring group participation with the functionality at C-2, the new glycosidic bond will be in the β configuration. Peracetylated glucosamine **2.30** was synthesised by reacting D-glucosamine hydrochloride with acetic anhydride, in the presence of pyridine. **2.30** was treated with HBr/AcOH in an attempt to form glycosyl donor **2.31** (Scheme 2.4). Some glycosyl halides, such as glycosyl iodides, are very reactive and unstable, they are generally reacted *in-situ*.[92] In contrast, glycosyl bromides are usually relatively stable, and, for most sugars, can be prepared in advance.[93] In this case, using *N*-acetyl glucosamine, the bromide was never isolated. It was found that, instead of detecting the bromine containing compound **2.31** as expected, the oxazoline derivative **2.32** was formed. This was confirmed by MS, and also ^{1}H NMR data was in agreement with reported values.[94] It has been reported in the literature that this oxazoline ring can be opened, in the presence of a Lewis acid, to react with an alcohol acceptor.[95] This reaction was attempted using two different Lewis acid promoters, TMSOTf or $BF_3.OEt_2$. These reactions were unsuccessful, and the starting material was recovered (Scheme 2.4).

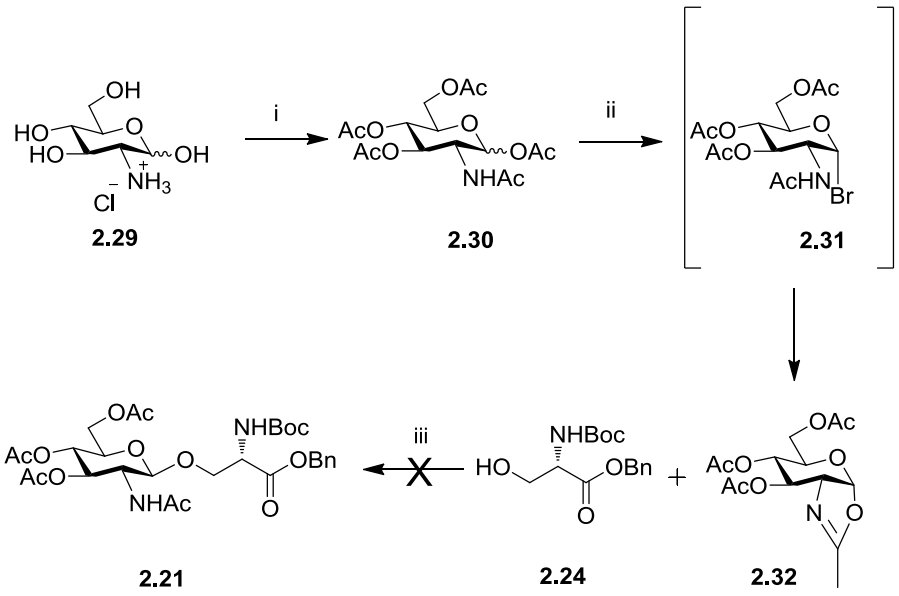

Scheme 2.4 Attempted synthesis of glycosyl building block 2.21. Reagents and conditions:i) Ac_2O, pyr, rt, overnight, 34 %; ii) 33 % HBr/HOAc, DCM, 0 ˚C → rt, overnight, 44 % of **2.32**; iii) TMSOTf or $BF_3.OEt_2$, DCM, rt, overnight

As these syntheses were unsuccessful, it was decided to follow the well-established trichloroacetimidate donor route. This synthesis involves several more steps than those previously attempted, but the use of the imidate donor, by Schmidt and coworkers, lends itself well to glucosamine.[87]

Although the reactions to synthesise glucosyl building block **2.22** have been reported in literature,[87, 89] some optimization was required. *N*-Troc protected **2.26** was synthesised as described above. Selective deacetylation at the anomeric position resulted in an anomeric mixture of hemiacetal **2.33**. This reaction was initially carried out in the presence of benzylamine. Dimethylamine later replaced benzylamine, as an alternative nucleophile. This improved the purification of compound **2.33**. Synthesis of hemiacetal **2.33** was also carried out using hydrazine acetate, which reduced the reaction time from overnight to 4 h. The free hydroxyl group of **2.33** was treated with trichloroacetonitrile and sodium hydride to give exclusively the α-imidate **2.34**, which would serve as the glycosyl donor (Scheme 2.5). The α-anomer is the expected product of this reaction, due to the influence of the anomeric effect on an electronegative substituent, and also encouraged by the use of a strong base for deprotonation of the anomeric hydroxyl group. Imidate **2.34** was also synthesized using DBU as an alternative base to NaH. The yields obtained were comparable to the synthesis carried out with NaH (86 % with NaH, compared to 72 % with DBU), but DBU would be preferable to work with, as NaH is highly flammable when exposed to water. Glycosylation of Boc protected serine acceptor **2.24** by glycosyl donor **2.34** was then carried out, using a 0.04 N solution of TMSOTf in DCM as the promoter (Scheme 2.5).

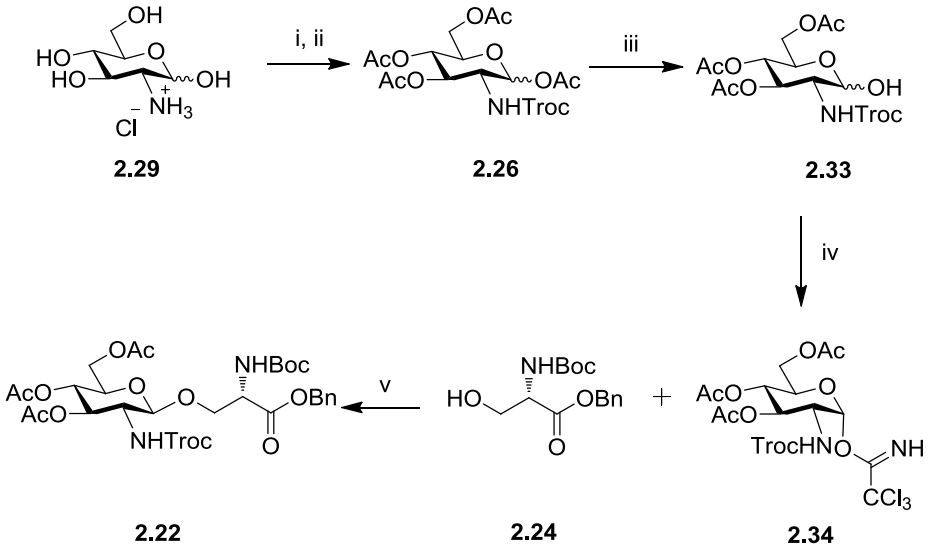

2.29 **2.26** **2.33**

2.22 **2.24** **2.34**

Scheme 2.5 Synthesis of glycosyl building block 2.22. Reagents and conditions: i) TrocCl, H_2O, $NaHCO_3$, 2.5 h, rt; ii) Ac_2O, pyr, overnight, rt, 87 % over two steps; iii) $NH(CH_3)_2$, THF, overnight, reflux, 81 %; iv) Cl_3CCN, DBU or NaH, 2h, rt, 86 %; v) 0.04 N TMSOTf, DCM, overnight, rt, 49 %

It is important that the glycosylation reaction is carried out under anhydrous conditions. The presence of water can severely reduce the yield of the desired product by attacking the activated glycosyl donor, in place of the glycosyl acceptor, and decomposing it to hemiacetal **2.33**. To minimise the amount of moisture in the reaction several steps were taken; the glassware was dried in an oven overnight, the reaction was carried out under a nitrogen atmosphere, and the reactants **2.34** and **2.24** were dried under vacuum for several hours. The glycosylation mechanism is shown in Scheme 2.6, and examination of this mechanism illustrates how an unwanted side reaction could occur in the presence of water. The water molecule could also attack the glycosyl cation which is formed during the reaction, resulting in the synthesis of hemiacetal **2.33**.

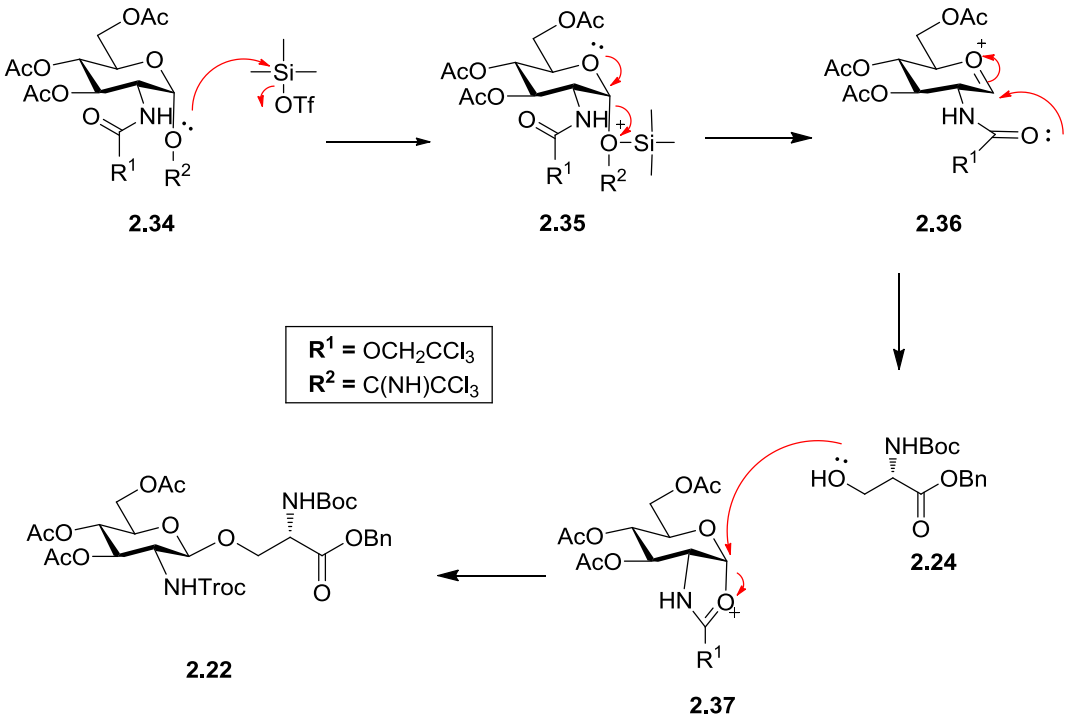

Scheme 2.6 Mechanism of TMSOTf promoted glycosylation

The first step in the reaction involves attack on the silicon by the anomeric oxygen. This places a positive charge onto the oxygen, in turn making the anomeric center more electrophilic. The lone pair on the ring oxygen aids the departure of the leaving group, and stabilises the oxocarbenium ion, **2.36**, which is formed. The reaction proceeds in an S_N1 type fashion. The presence of the *N*-Troc protected neighbouring group on C-2 of the sugar ensures that a β-glycosidic linkage is formed. The oxygen lone pair of the *N*-Troc group attacks the anomeric center, forming an oxazoline-type intermediate, **2.37**. This neighbouring group participation only allows the alcohol acceptor **2.24** to attack at the upper face of C-1, resulting in the β-glycoside **2.22** (Scheme 2.6).

2.7 Synthesis of Glycolipids 2.71 and 2.74

2.7.1 Route A

Orthogonal protecting groups are those which can be selectively removed, without interfering with other protecting groups present in the molecule. This allows for selective adaption of a specific functional group. The next stage in the synthesis

involved removal of these orthogonal protecting groups, from the glucosyl building block, **2.22**, to allow introduction of the hydrocarbon chains.

Selective removal of the benzyl ester protecting group from **2.22** was carried out by hydrogenolysis, using a Pd/C catalyst, under H_2, to give acid **2.38**. This was followed by introduction of the tetradecylamide chain, using standard coupling conditions of TBTU and HOBt, in the presence of Et_3N, resulting in **2.39** (Scheme 2.7).

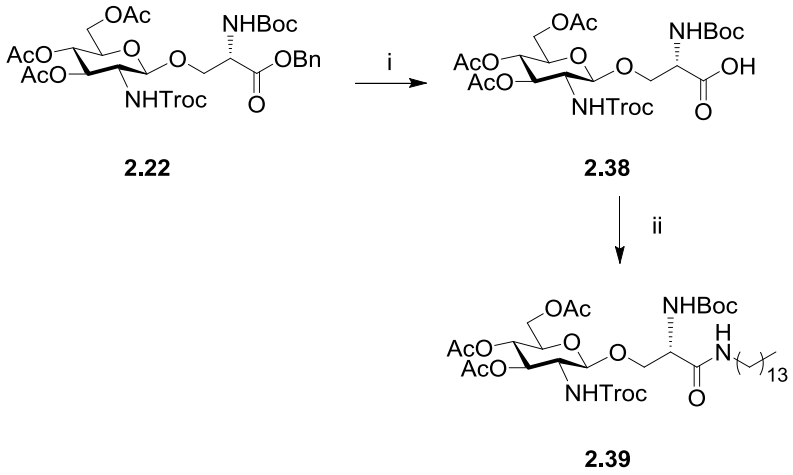

2.22 **2.38** **2.39**

Scheme 2.7 Synthesis of hydrocarbon chain amide derivative 2.39. Reagents and conditions: i) Pd/C, H_2,EtOAc, 2 h, rt, 75 %; ii) HOBt, TBTU, $NH_2C_{14}H_{29}$, DCM, overnight, rt, 77 %

TBTU is often used in peptide synthesis methodologies as it greatly reduces the risk of racemisation, and is useful for hindered couplings. The rate of reaction is quite fast, preventing unwanted side reactions from occurring.[96] The use of HOBt also helps to prevent racemisation, and speeds up the rate of the reaction.[97]

TBTU is known as a "uronium" based coupling reagent, but it has been demonstrated that, in the crystalline state, TBTU exists as the guanidinium *N*-oxide derivatives **2.41** and **2.40**.[98] Another closely related reagent, HATU, also exhibits this property. In solution both forms of the TBTU molecule are thought to be present, and either can react with a carboxylate to form an activated ester.[99] The mechanism proceeds with attack of the carboxylate nucleophile **2.40** on the TBTU carbocation to form the acyloxyuronium species **2.43**. This intermediate immediately reacts with the released BtO^- **2.44**, at the carbonyl carbon, to form the activated ester **2.45**. The amino containing compound **2.46** can now attack the carbonyl carbon of

2.45 to form the amide bond, resulting in **2.48** (Scheme 2.8). The acid is generally activated by stirring with base and the activating agent, i.e. TBTU, for 5-10 mins, to ensure formation of the activated ester before addition of the amine.

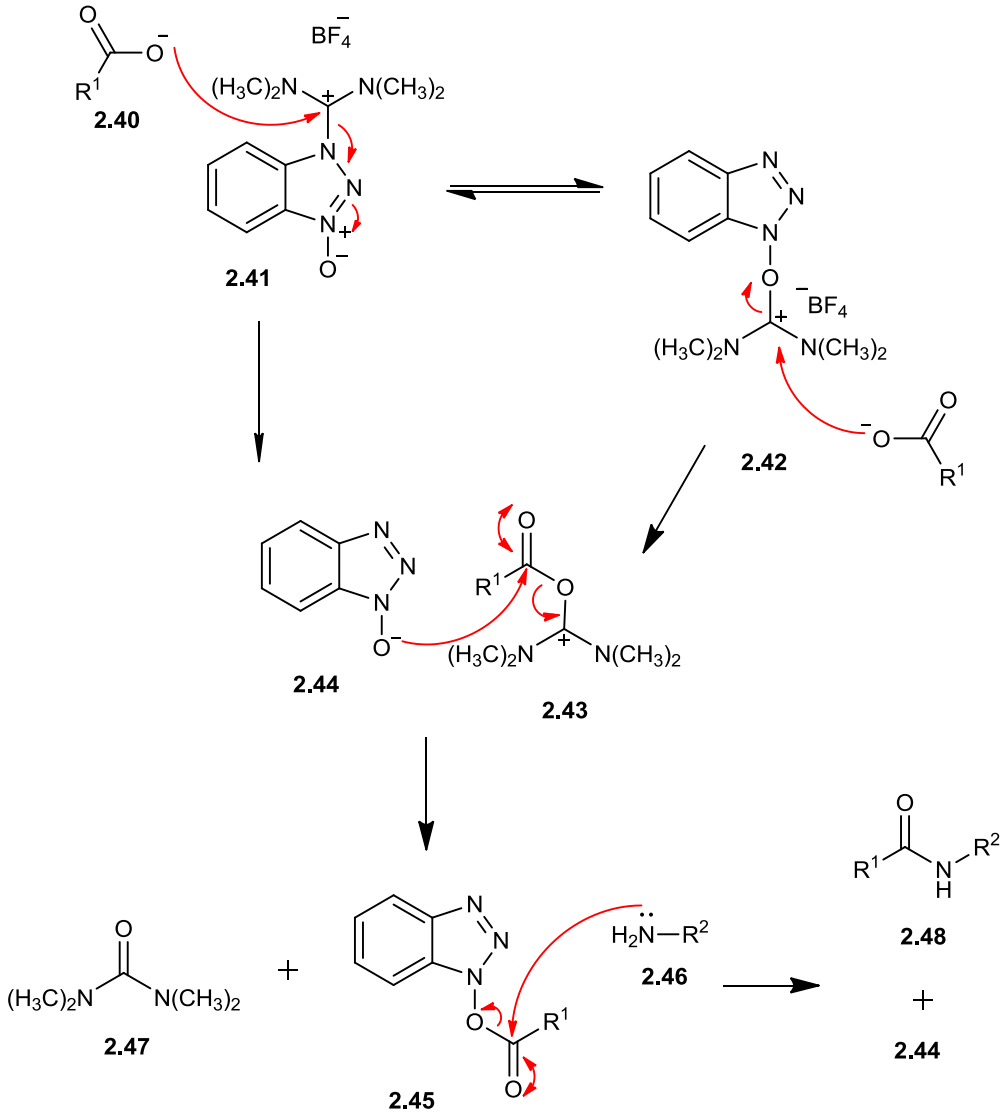

Scheme 2.8 Mechanism of amide formation using the TBTU coupling reagent

Initially, *N*-Boc deprotection of **2.39** was attempted using the standard reaction conditions of TFA in DCM (Scheme 2.9). The *N*-Boc group is an acid labile protecting group, and should be easily removed under these conditions. The reaction was carried out by adding a solution of 50 % TFA in DCM to a solution of **2.39**, in DCM, on ice, then allowing the reaction mixture to reach rt and stir for 2 h. Free amine **2.49** was not produced in this reaction, with full recovery of the starting material. The reaction was repeated, adding neat TFA to a solution of **2.39** in DCM

at rt, and left to stir overnight at rt. Starting material was still present after this treatment, and none of the deprotected **2.49** was observed.

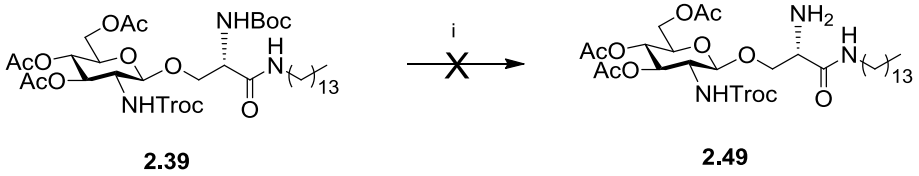

Scheme 2.9 Attempted deprotection of the *N*-Boc protecting group of 2.39. Reagents and conditions: i) 50 % TFA, DCM, 1-24 h

It was postulated that the orientation of the long hydrocarbon chain may have been presenting a steric hindrance, and so preventing removal of the *N*-Boc group. In order to confirm this, a shorter chain propyl derivative, **2.50**, was synthesised. The *N*-Boc group was easily removed from this derivative, under the standard conditions of TFA at rt overnight, to give **2.51** (Scheme 2.10). This was confirmed by MS analysis, and also by the disappearance of the characteristic *N*-Boc CH_3 peak at 1.4 ppm in the ^{1}H NMR spectrum.

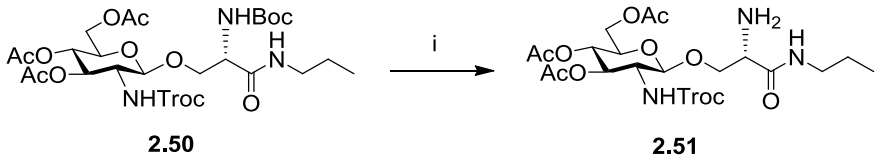

Scheme 2.10 Removal of *N*-Boc protecting group from propyl derivative 2.50. Reagents and conditions: i) 50 % TFA, DCM, overnight, rt, 97 %

2.7.2 Route B

As the presence of the long hydrocarbon chain appeared to have prevented *N*-Boc deprotection, the order of introduction of the hydrocarbon chains was modified. From building block **2.22**, *N*-Boc deprotection was carried out, with the addition of TFA in DCM carried out on ice, and the reaction mixture allowed to stir at 0 ˚C for 1 h. The reaction was successful, resulting in compound **2.52** in good yield. This was followed by coupling of decanoic acid to the amine **2.52**, using the TBTU/ HOBt methodology to give **2.53**. Hydrogenolysis of the benzyl ester **2.53** was then carried out, using Pd/C and H_2, resulting in acid **2.54**. Introduction of the second hydrocarbon chain was attempted using the standard TBTU/HOBt coupling conditions, but this reaction was unsuccessful (Scheme 2.11).

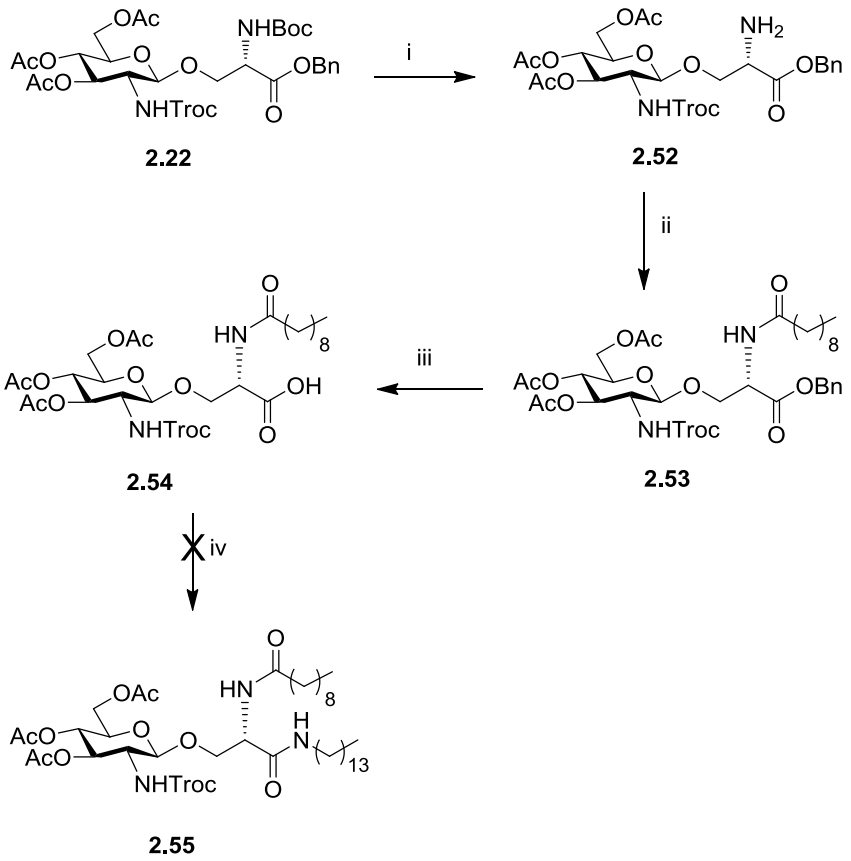

Scheme 2.11 Synthesis of protected glycolipid derivative 2.55. Reagents and conditions: i) 50 % TFA, DCM, 0 ˚C, 1 h, 90 %; ii) HOBt, TBTU, Et_3N, $C_9H_{19}C(O)OH$, DCM, overnight, rt, 88 %; iii) Pd/C, H_2, EtOAc, 2 h, rt, 98 %; iv) HOBt, TBTU, Et_3N, $NH_2C_{14}H_{29}$, DCM, overnight, rt

*2.7.3 Various Coupling Conditions Investigated From Free Acid **2.54***

The initial attempts to introduce a second hydrocarbon chain at the free acid, using the standard coupling conditions shown above, were unsuccessful (Scheme 2.11). The attempted coupling reaction resulted in degradation of compound **2.54**. On examination of the ^{1}H NMR spectral data, and also by TLC analysis, hemiacetal **2.33** was identified. This was isolated by column chromatography, and was confirmed by MS. The presence of **2.33** indicated that degradation had occurred during the reaction. It was postulated that this degradation could have resulted from either cleavage of the glycosidic bond by hydrolysis at the anomeric centre, or by α-H elimination via a retro-Michael-type mechanism. Hydrolysis of **2.54** would result in hemiacetal **2.33** and the functionalised serine **2.56** (Scheme 2.12). However, hydrolysis of an acetal is normally observed under strongly acidic conditions, while

this reaction was carried out in a basic environment. Compound **2.56** was not isolated, and was not detected in MS analysis of the crude reaction material.

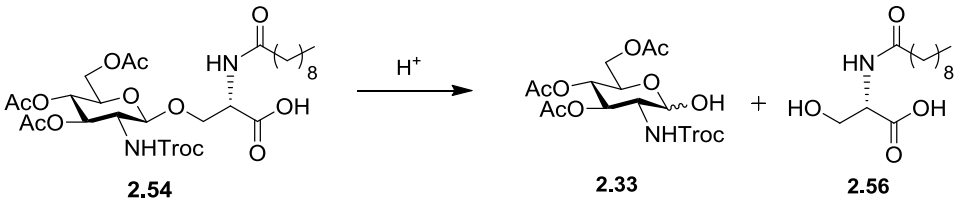

2.54 **2.33** **2.56**

Scheme 2.12 Degradation mediated by hydrolysis at the anomeric center

On the other hand, the retro-Michael reaction would yield a dehydroalanine type product, **2.57**, as well as hemiacetal, **2.33**. The presence of the dehydroalanine compound **2.57** was confirmed by MS analysis, which indicated that this degradation was due to α-elimination (Scheme 2.13). On further examination of the literature, it was found that these types of glycosylated serine compounds are indeed base sensitive, with degradation occurring over ~ pH 10.5.[100, 101] In fact, some groups carry out this elimination on purpose, as the dehydroalanine acts as a protected form of serine, which can be used in peptide synthesis.[102] **2.54** was stirred overnight in DCM, in the presence of Et_3N, without addition of the coupling reagents (HOBt/TBTU). Degradation to the hemiacetal did not occur, with recovery of starting material. This experiment demonstrated that the α-proton of **2.54** was not acidic enough to be removed before being converted into the activated ester by TBTU. The mechanism of the elimination observed with **2.54** is known as E1cB. E1cB elimination is usually catalysed by a strong base, like KOH or Et_3N, and is made possible by an anion-stabilising group, like a carbonyl. The proton which is adjacent to the activated carbonyl is very acidic. The base can remove this proton, without a leaving group departing at the same time, due to delocalisation of the negative charge onto the carbonyl group. The carbonyl stabilises the anion which is formed, but elimination of a leaving group will still occur. The electrons flow back down from the carbonyl oxygen, and the result is formation of an alkene containing compound, and an elimination of the adjacent group (Scheme 2.13). This elimination is promoted by the formation of the activated ester during the first stages of the coupling reaction. The α-proton is made more acidic, and is easily deprotonated, even in the presence of a mild base like pyridine (pKa_H ~5.2). The activated ester will quickly hydrolyse to the corresponding carboxylic acid, **2.57**.

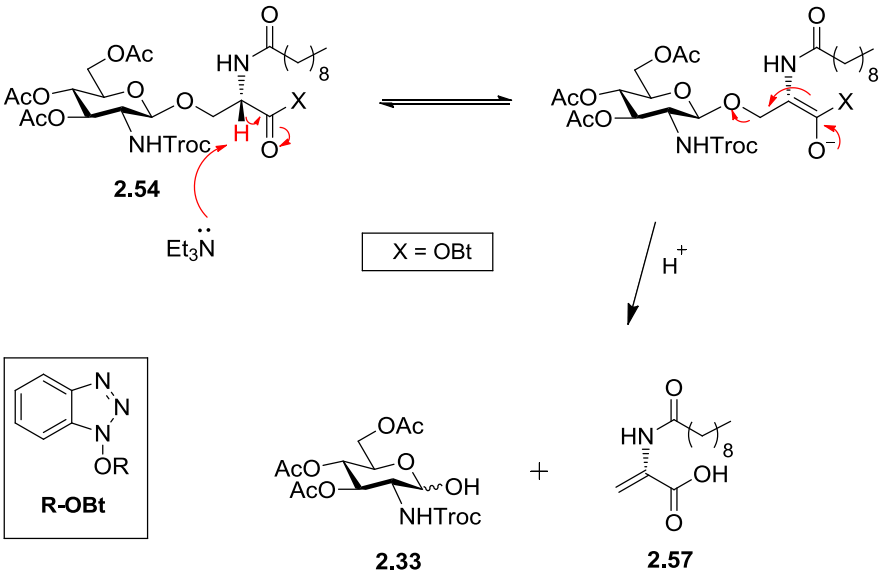

Scheme 2.13 Mechanism of E1cB elimination

In order to further confirm the presence of the dehydroalanine degradation compound **2.57**, a trapping experiment was performed, which involved carrying out the standard coupling reaction in the presence of 2.2 equivalents of NBS (Scheme 2.14). The dehydroalanine compound, **2.57**, can be unstable, due to addition reactions at the double bond. The NBS acted as a source of electrophilic bromine, which could "trap" the dehydroalanine as it is formed, by addition of bromine across the alkene bond to give compound **2.58**.[103] The presence of this compound was confirmed by MS.

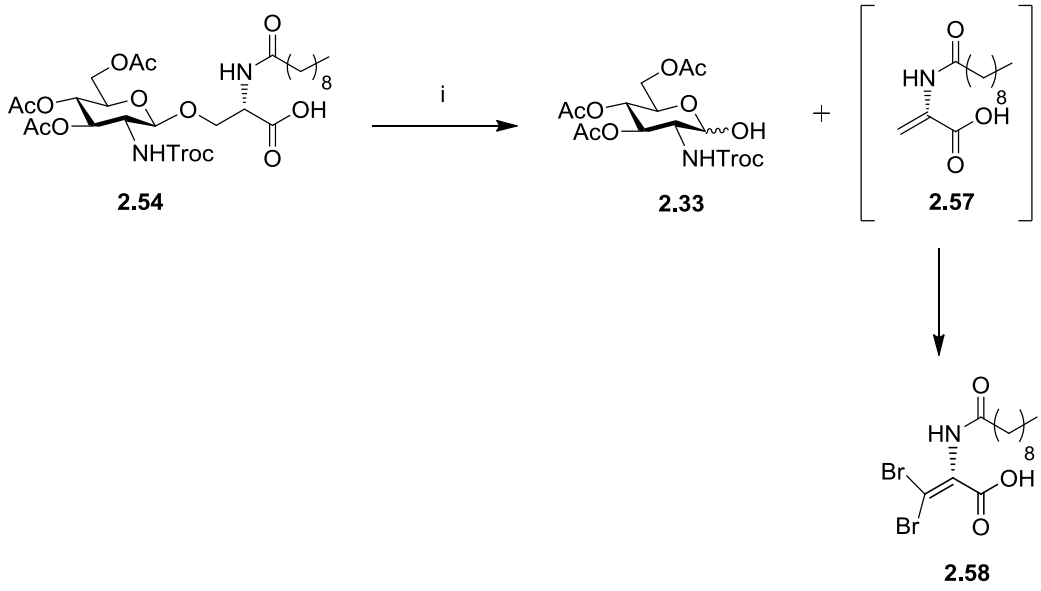

Scheme 2.14 NBS trapping of dehydroalanine 2.57. Reagents and conditions: i) HOBt, TBTU, Et_3N, DMF, NBS, 2 h, rt

Various different conditions to avoid the undesired elimination, as outlined in Table 2.1, were investigated for this coupling reaction. Entry **1** shows the standard conditions which were initially investigated. Entry **2** was carried out in the absence of HOBt, to investigate if this additive may be enhancing the degradation, but hemiacetal **2.33** was still detected after the reaction. Entry **3** shows the reaction carried out with less equivalents of the base Et_3N, which made no difference to the reaction, with MS showing the presence of hemiacetal **2.33**, and also some remaining starting acid **2.54**. Entry **4** was carried out in the presence of a more hindered base, DIPEA, to see if this would prevent the elimination, but hemiacetal was again detected in this experiment. Entries **5** and **6** show the reaction carried out in less basic conditions, using pyridine and *N*-methyl morpholine respectively, but hemiacetal **2.33** was again produced in both reactions. From this data it is clear that the nature of the base is not important. Deprotonation of the α-H occurred in all cases where the activated carboxylic acid, **2.58**, described earlier, was being generated using the TBTU and HOBt coupling conditions. It was then decided to change the method of coupling, and the acid chloride of **2.54** was synthesised. This was carried out by reaction of the acid **2.54** with oxalyl chloride, in DMF, followed by addition of the long chain tetradecylamide, in the presence of pyridine (entry **7**). These alternative conditions did not yield the desired product, **2.55**, but, again, the presence of starting acid **2.54** and dehydroalanine **2.57** were confirmed by MS.

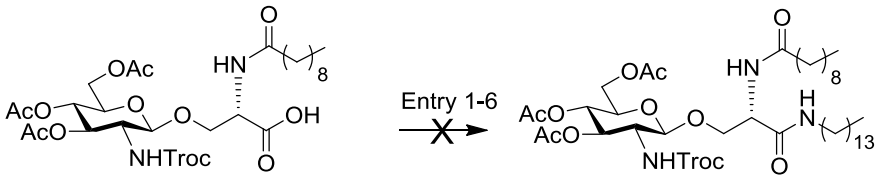

2.54 **2.55**

Entry	Coupling reagent	HOBt	Base (equiv.)
1	TBTU	Y	NEt_3 (2)
2	TBTU	N	NEt_3 (2)
3	TBTU	Y	NEt_3 (1.2)
4	TBTU	N	DIPEA (2)
5	TBTU	N	Pyridine (2)
6	TBTU	N	*N*-methyl-morpholine(2)
7	$(COCl)_2$	N	Pyridine (2)

Table 2.1 Investigation of the coupling conditions using compound 2.54

In order to investigate if the observed E1cB elimination would occur with any functionality in the amide position, lysine derivative **2.59** was synthesised. Introduction of the tetradecylamine chain was attempted using the standard TBTU/HOBt conditions (Scheme 2.15). This was also unsuccessful, with hemiacetal **2.33** again being isolated. This suggested that activation of any amide containing derivative of **2.54** would result in degradation.

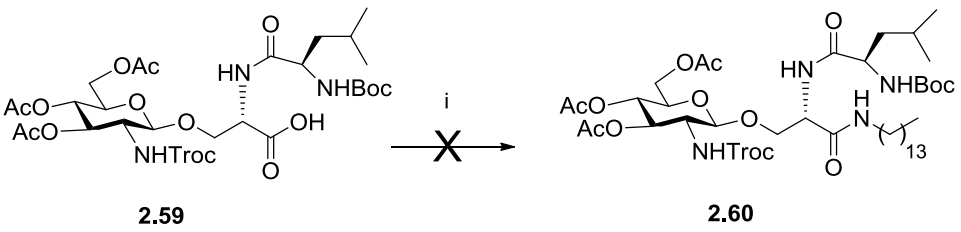

Scheme 2.15 Attempted coupling of second chain to lysine derivative 2.59. Reagents and conditions: i) HOBt, TBTU, Et_3N, $NH_2C_{14}H_{29}$, DCM, overnight, rt

Another approach which was taken in the synthesis of **2.55** was to carry out the glycosylation on an acceptor which had already been functionalised with both hydrocarbon chains, **2.63** (Scheme 2.17). The synthesis of this acceptor is shown in Scheme 2.16, below. The tetradecylamine chain was introduced using TBTU and Et_3N, to give **2.61**. This was followed by deprotection of the *N*-Boc group, using a 50 % solution of TFA (v/v) in DCM, to give the free amine, **2.62**. Interestingly, this deprotection did not present the difficulty which had been encountered in the presence of the sugar moiety in **2.39**. The second hydrocarbon chain was introduced into the molecule, again using TBTU and Et_3N, resulting in **2.63** (Scheme 2.16).

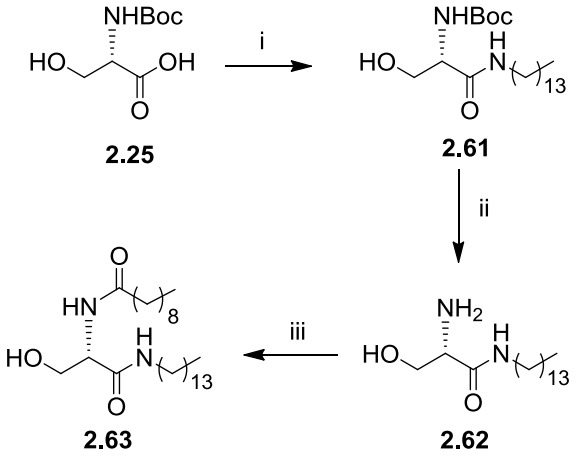

Scheme 2.16 Synthesis of lipid 2.63. Reagents and conditions: i) TBTU, Et_3N, DCM, $NH_2C_{14}H_{29}$, rt, overnight, 75 %; ii) 50 % TFA, DCM, 5 h, rt, 91 %; iii) TBTU, $C_9H_{19}C(O)OH$, DMF, Et_3N, overnight, rt, 32 %

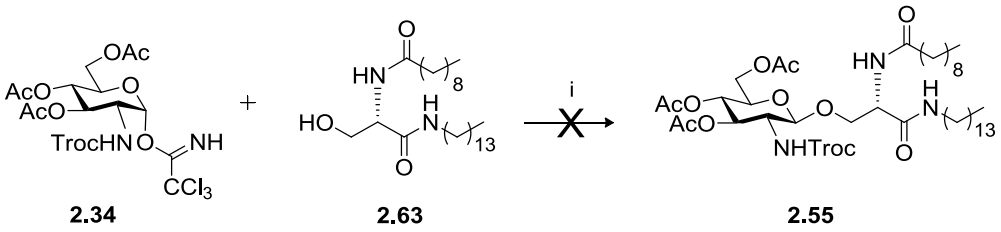

2.34 **2.63** **2.55**

Scheme 2.17 Attempted glycosylation of acceptor 2.63. Reagents and conditions: i) 0.04 N TMSOTf or $BF_3.OEt_2$, DCM, overnight, rt

Direct glycosylation of a serine acceptor, which had been functionalised with one hydrocarbon chain, has shown success in the literature,[43] using $BF_3.OEt_2$ as the promoter. For our acceptor the reaction did not yield any of the desired product, with recovery of hemiacetal **2.33**, and the functionalised serine. It was postulated that this reaction did not progress due to a steric hindrance caused by the presence of the second hydrocarbon chain.

In view that degradation was observed, even in the presence of a very mild base such as pyridine, introduction of the second chain to the free acid was carried out in the absence of base (Scheme 2.18). This reaction produced the desired product **2.55**, which was confirmed by MS, but in low yield of 13 %.

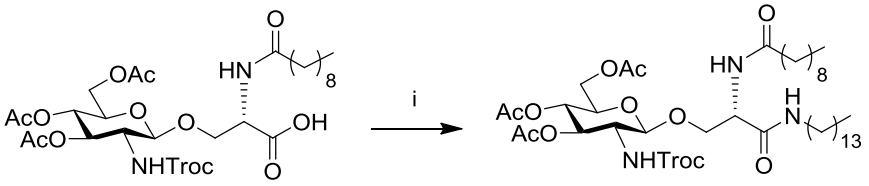

2.54 **2.55**

Scheme 2.18 Coupling of tetradecyl chain in the absence of base. Reagents and conditions: i) TBTU, HOBt, $NH_2C_{14}H_{29}$, DCM, overnight, rt, 13 %

From glycolipid **2.55** the removal of the *N*-Troc protecting group was attempted, using the standard conditions of Zn, Ac_2O and Et_3N described by Zhu and Schmidt (Scheme 2.19).[104] This reaction was unsuccessful, and starting material was recovered. It was thought that, again, the presence of the long hydrocarbon chains was posing a steric hindrance.

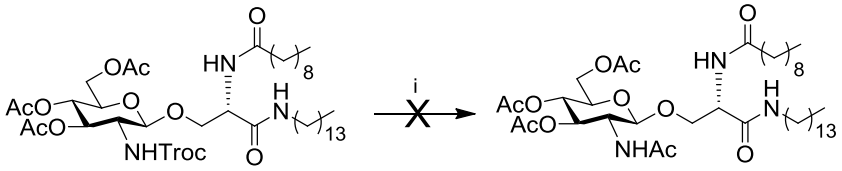

2.55 **2.64**

Scheme 2.19 Attempted deprotection of *N*-Troc from 2.55. Reagents and conditions: i) Zn, Ac_2O, Et_3N, overnight, rt

2.7.4 Route C

It was observed in route B that degradation occurred when activating the carboxylic acid of **2.54** to introduce the second hydrocarbon chain. It had also been observed, as discussed in route A, using the *N*-Boc protected building block **2.22**, that functionalisation could not be carried out at the acid functionality first, due to problems with *N*-Boc deprotection. For this reason *N*-Cbz protected glycosyl acceptor **2.65** was synthesised. Only one hydrocarbon chain was introduced into this acceptor, and so the problem encountered with acceptor **2.63** could be avoided. The *N*-Cbz protecting group is removed by hydrogenolysis, which would not be orthogonal to the benzyl protecting group of the serine acceptor, **2.24**, utilised in earlier syntheses. For this reason, introduction of the tetradecyl chain was carried out before glycosylation, removing the need for benzyl ester protection (Scheme 2.20).

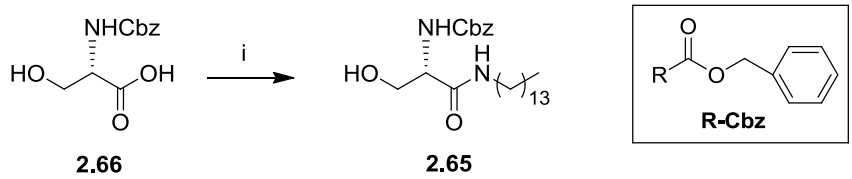

2.66 **2.65**

Scheme 2.20 Coupling of the tetradecyl chain to *N*-Cbz serine. Reagents and conditions: i) TBTU, HOBt, Et_3N, $NH_2C_{14}H_{29}$, DCM, overnight, rt, 55 %

Imidate glycosyl donor **2.34** was used for the glycosylation reaction. TMSOTf was again used as the promoter for the reaction, resulting in **2.67**. This was followed by deprotection of the *N*-Troc protecting group using standard conditions of freshly activated zinc, and acetic anhydride to give **2.68**. Hydrogenolysis of the *N*-Cbz protecting group was then carried out, using Pd/C under a H_2 atmosphere, to give amine **2.69** (Scheme 2.21). The order of deprotection is crucial to this synthesis. When hydrogenolysis of the *N*-Cbz group was attempted from **2.67**, prior to

reduction of the *N*-Troc group, this step was unsuccessful, with return of starting material (Scheme 2.22). Also, it was previously noted in compound **2.55** (Route B) that reduction of the *N*-Troc protecting group could not be carried out once the compound was functionalised with both lipid chains.

Coupling of decanoic acid to the free amine **2.69** was carried out using TBTU and HOBt, in the presence of Et_3N, to give the protected glycolipid **2.70**. This was followed by selective hydrolysis of the *O*-acetyl protecting groups, leaving the *N*-acetyl group intact, using $MeOH/H_2O/Et_3N$ (Scheme 2.21). Standard Zemplén conditions of NaOMe/MeOH for deacetylation were not used, as these were anticipated to be too harsh, and may also remove the *N*-acetyl protecting group. Fig. 2.26 shows the ^1H NMR spectrum of the deprotected glycolipid **2.71**. The doublet at approx. 8.8 ppm is attributed to the N*H*Ac amide proton, with the signal at 8.5 ppm being attributed to the amide protons of both hydrocarbon chains. The resonance of the α-anomeric *H*-1 is observed at 5.3 ppm, while the β-anomeric *H*-1 is seen at a lower ppm of 5.1, which is characteristic of each of these anomers. The singlet at 2.1 ppm represents the methyl protons of the NHAc group, and integrates for three protons. Most of the long hydrocarbon chain CH_2 protons are observed as a multiplet at 1.2 ppm. The analysis was carried out in deuterated pyridine, as residual solvent peaks from deuterated DMSO would have obscured the sugar peaks. Solubility was also poor in other solvents, and a sharp, clear spectrum was obtained in pyridine.

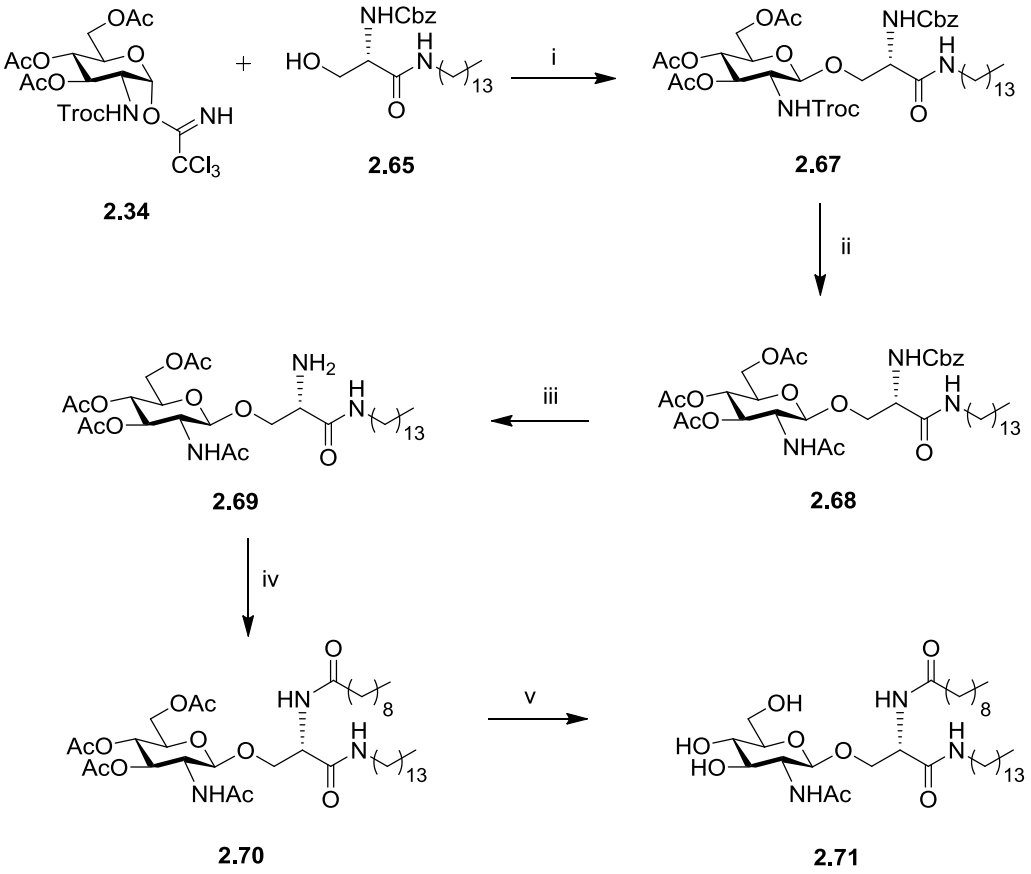

Scheme 2.21 Synthesis of glycolipid 2.71. Reagents and conditions: i) 0.04 N TMSOTf, DCM, rt, overnight, 53 %; ii) Zn, Et_3N, Ac_2O, rt, 5 h, 70 %; iii) H_2, Pd/C, EtOAc, 2 h, rt, 95 %; iv) HOBt , TBTU, Et_3N, $C_9H_{19}C(O)OH$, DMF, overnight, rt, 40 %; v) Et_3N/MeOH/H_2O, 40 °C, overnight, 41 %

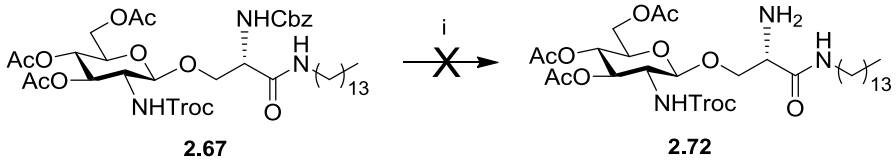

Scheme 2.22 *N*-Cbz deprotection from 2.67. Reagents and conditions: i) H_2, Pd/C, EtOAc, overnight, rt

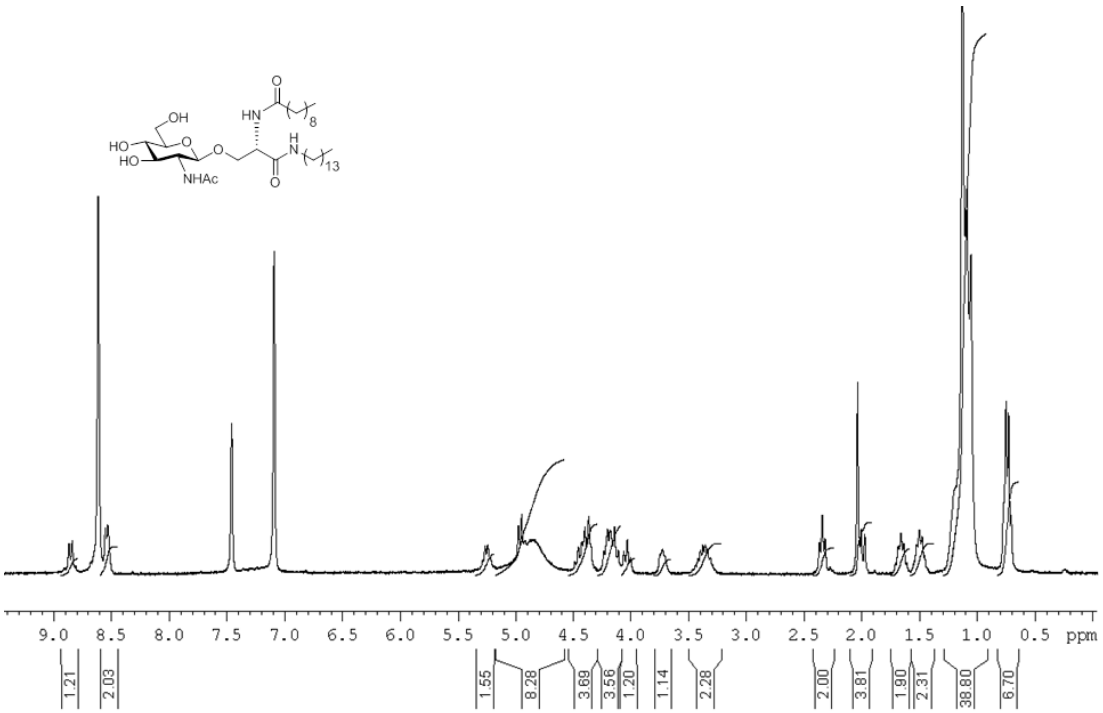

Figure 2.26 ^{1}H NMR spectrum of deprotected glycolipid 2.71 in C_5D_5N

A longer hydrocarbon chain derivative, **2.74**, was synthesised, which would be more comparable to other glycolipids which have been tested for their immunomodulatory activities, like α-GalCer. Tetracosanoic acid was coupled to **2.69**, using TBTU and HOBt, in the presence of Et_3N, to give glycolipid **2.73**. The low yield of this reaction is due to the poor solubility of tetracosanoic acid in either DCM or DMF. This glycolipid analogue was then subjected to the same deprotection conditions as the shorter chain derivative, resulting in deprotected glycolipid **2.74** (Scheme 2.23).

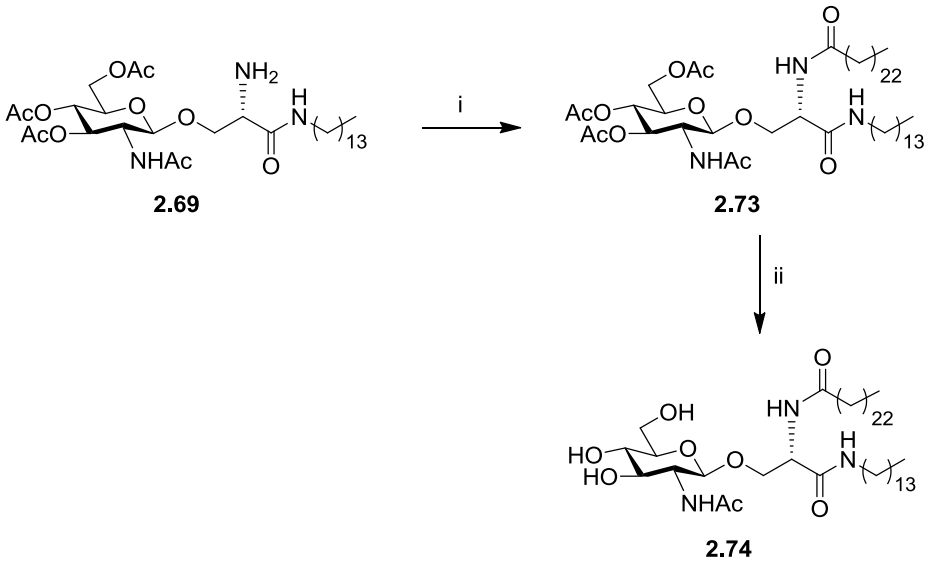

Scheme 2.23 Synthesis of tetracosonoyl glycolipid derivative 2.74. Reagents and conditions: i) TBTU, HOBt, Et_3N, $C_{23}H_{57}C(O)OH$, DMF, overnight, rt, 17 %; ii) $Et_3N/MeOH/H_2O$, 45 °C, overnight, 57 %

2.8 Biological Evaluation of Glycolipids 2.71 and 2.74 as Immunomodulators

Deprotected glycolipids **2.71** and **2.74**, and also lipid **2.63** were tested by Dr. Derek Doherty, Andreea Petrasca, and Niamh Murphy at St. James' Hospital, Dublin for their potential as immunostimulators (Fig. 2.27). Glycolipids **2.71** and **2.74** are novel glycolipids and differ only in the length of one hydrocarbon chain, while **2.63** has been recorded in the literature,[105] and does not contain the sugar moiety. **2.63** was included in the testing to investigate if the sugar moiety was required for iNKT stimulation and cytokine release, or if a different cytokine profile would be induced by the glycosides.

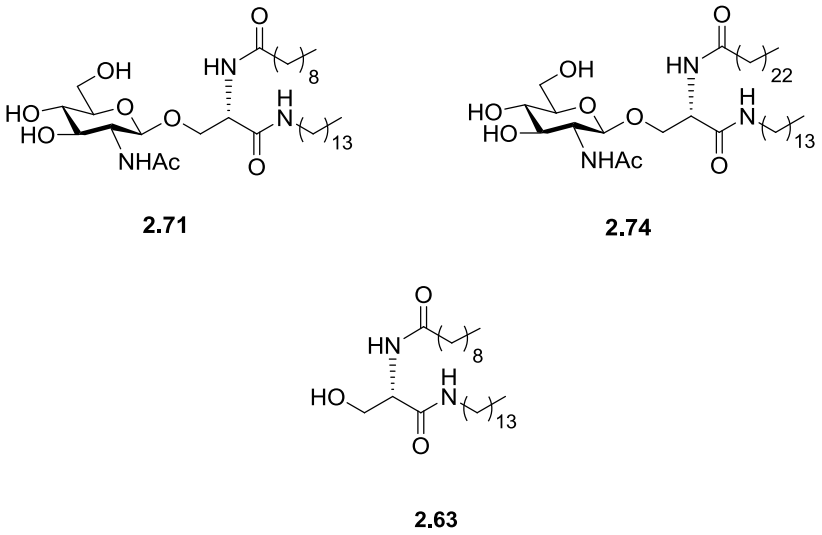

Figure 2.27 Lipids tested for immunostimulatory activity

The aim of this study was to investigate the potential of these glycolipids to stimulate iNKT cells to mediate cytotoxicity, T helper function and cytokine secretion.

2.8.1 Materials and Methods used for Testing[106]

iNKT cell lines were co-cultured with cancer cells in the presence of the above glycolipids, and assessed using flow cytometry and ELISAs (enzyme-linked immunosorbent assays). Two different types of cell line were transfected with CD1d; HeLa cells were derived from cervical cancer cells, and C1R cells are a mutant lymphoblastoid cell line. Testing was carried out using literature procedures, described by Hogan *et al*.[72] α-GalCer was used as the positive control, and gave a positive result for all ELISAs. The negative control was HeLa-CD1d cells with iNKT cells but no compound added (vehicle). This gave a baseline result with which to compare the results of the novel glycolipids.

2.8.2 Ability of Glycolipids to Induce Cytotoxicity

iNKT cells have the ability to induce an immune response and also to mediate cytotoxicity, which accounts for their antitumor activity. In this study, cytotoxicity was evaluated by flow cytometric analysis of CD107a positive cells. CD107a is a lysosomal protein which lines the surface of cytolytic granules and lysosomes, and it becomes exposed to the surface during degranulation. This makes it an ideal marker for assessing cytotoxic activity.[107] Glycolipids **2.71** and **2.74**, and lipid **2.63** were tested for their ability to prime iNKT cell lines for cytotoxicity, using iNKT cells

from four different donors. In the presence of C1R cells only α-GalCer was able to cause CD107a externalisation, the other lipids did not induce any cytotoxicity against this cell line. In the presence of CD1d-HeLa cells, **2.71** and **2.74** were able to externalise CD107a in just one iNKT cell line, while **2.64** induced CD107a expression by two cell lines (Fig. 2.28). These results indicate that the cells are undergoing degranulation, and so are mediating cytotoxicity.

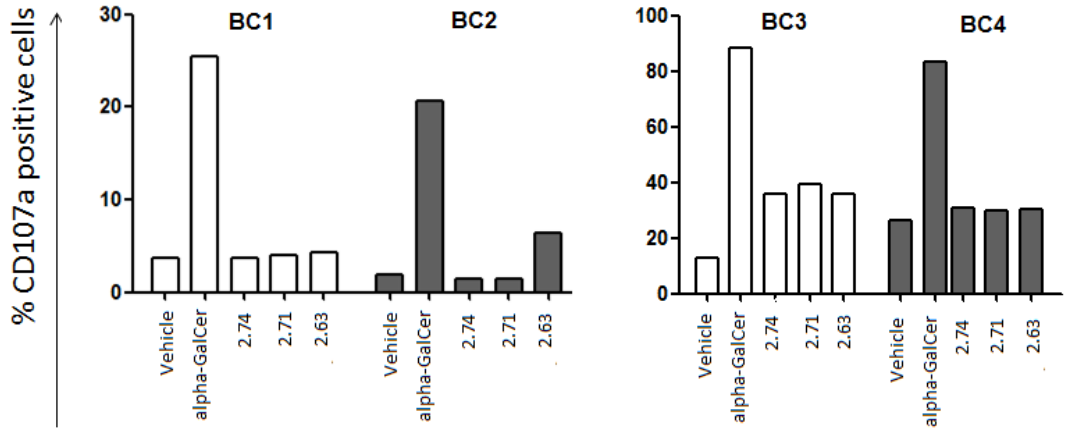

Figure 2.28 iNKT cell cytotoxicity in four different donors (BC1-4) after exposure to HeLa cells presenting various lipids

These lipids were also tested for induction of CD40L expression by iNKT cells, which is located on B-cells, dendritic cells and macrophages. This protein is important in T-cell activation and also plays other roles in immune stimulation.[108] **2.71**, **2.74** and **2.63** did not induce expression of CD40L, indicating that these compounds would not play a part in induction of T-helper function (data not shown).

The iNKT cell lines which gave a $CD107a^+$ result were examined to find out what subsets they contained. It has been reported that therapeutic outcomes can vary in patients expressing different subset compositions. iNKT cells can be $CD4^+$, $CD8^+$ or $CD4^-CD8^-$ (Double negative, DN); $CD4^+$ iNKT cells expand more readily than the others upon mitogen stimulation, while $CD8^+$ and $CD4^-CD8^-$ iNKT cells most potently killed $CD1d^+$ cell lines and primary leukaemia cells.[109] In this study the $CD107a^+$ cells were found to be mostly $CD8^+$, and CD107a expression for each of the subsets is illustrated in Fig. 2.29 below. $CD40L^+$ cells were found to be mainly

$CD4^+$, which could account for the lack of CD40L expression by the glycolipids tested.

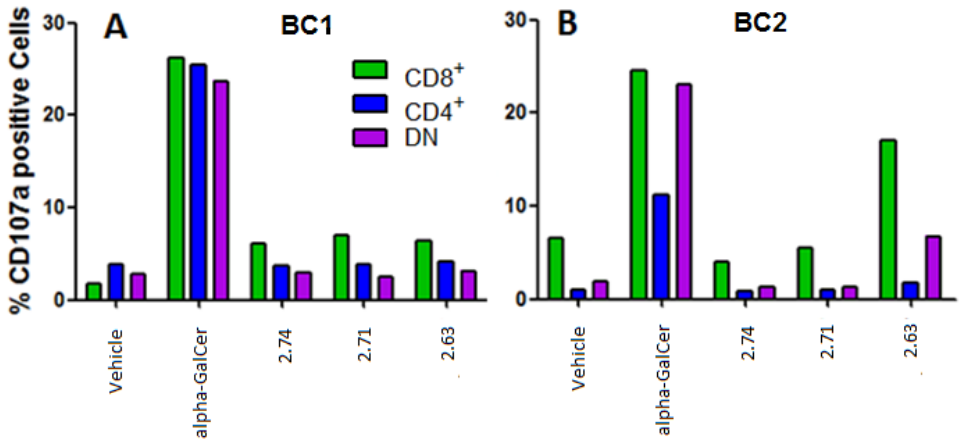

Figure 2.29 Expression of CD107a by iNKT subsets in two cell lines

2.8.3 Analysis of the Cytokine Release Profile Induced by Glycolipids

The extracellular cytokine expression induced by the different lipids was determined using ELISAs to measure cytokine concentrations in the supernatant, 24 h after lipid stimulation of iNKT cells. α-GalCer was the only lipid tested that showed evidence of IL-4, IFN-γ, IL-13 and GM-CSF secretion (Fig. 2.30).

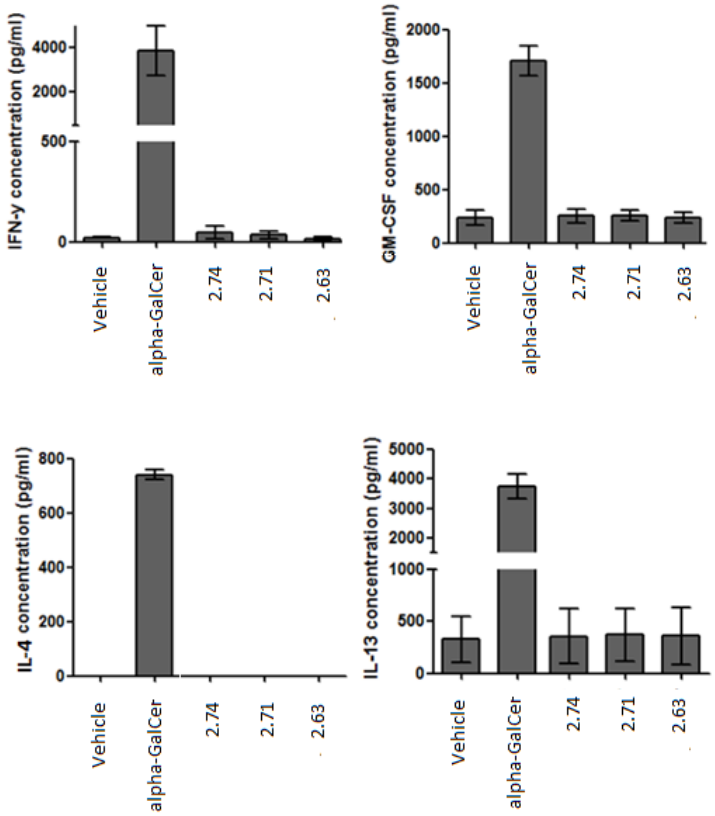

Figure 2.30 Effect of glycolipid stimulation on extracellular cytokine secretion

The intracellular cytokine profile was also examined by flow cytometry. This intracellular cytokine assay only measures the percentage of cytokine-secreting cells, and so does not actually quantify how much cytokine secretion is induced. Glycolipid **2.71**, which is the shorter chain derivative tested, was shown to weakly induce secretion of Th2 cytokine IL-4 in each of the four cell lines (BC1-4), and also IFN-γ and TNF-α secretion in two cell lines (BC1-2). The percentage of IFN-γ positive cells induced by **2.71** was higher than that induced by α-GalCer in cell lines BC1-2. The longer chain derivative **2.74** and the non-glycosidic **2.63** failed to induce an intracellular secretion of any of these cytokines (Fig. 2.31).

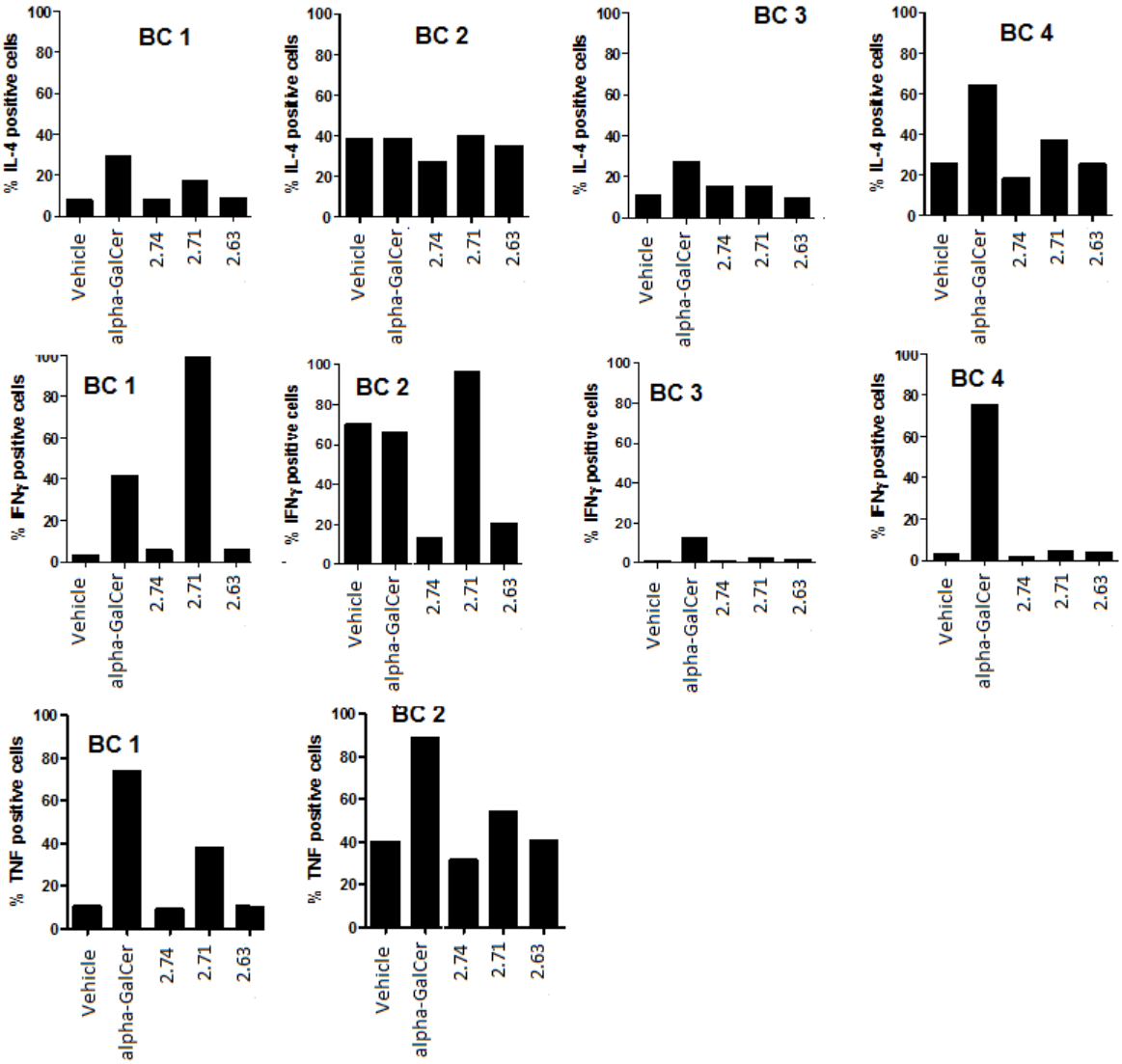

Figure 2.31 Intracellular cytokine profile

As our glycolipids did not illicit a strong release of the typical cytokines examined for immunostimulation, they were tested for their ability to produce IL-10. This cytokine has become of interest in the area of immunoregulation, and is known as a suppressor cytokine.[110] IL-10 has been found to display immunosuppressive properties, including inhibition of inflammatory cytokine production (such as IL-4), which could be used in the treatment of certain diseases, such as allergic responses. Immunostimulatory abilities of IL-10 were also noted, for example proliferation and differentiation of B cells.[111] All of our glycolipids tested induced secretion of IL-10, with **2.74** showing the highest release of IL-10, followed by **2.71**, and a lesser stimulation was noted with the non-glycosidic derivative **2.63** (Fig. 2.32). This again shows the importance of the sugar moiety in cytokine release. **2.71** induced a more

potent response than α-GalCer at a concentration of 100 ng/mL. **2.73** also induced a strong response, but, as the 100 ng/mL measurement was not carried out, it cannot be said with certainty that the level of IL-10 released was higher than α-GalCer. The suppressive nature of IL-10 could account for the failure of these lipids to stimulate the release of IL-4 in the earlier studies. The testing was carried out at different concentrations of the lipids to investigate if the response was dose dependant. Some measurements were not carried out due to the amount of sample available. From Fig. 2.32 it can be observed that the response did not increase with higher dosage levels. In this study medium alone was used as the negative control, and phorbol myristate acetate (PMA) with ionomycin was used alongside α-GalCer as the positive control.

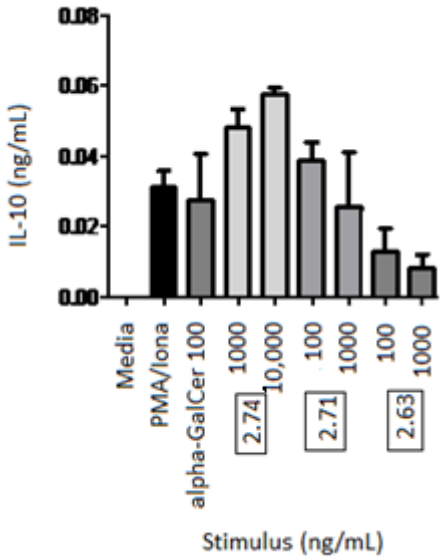

Figure 2.32 Stimulation of IL-10 production by novel glycolipids

2.8.4 Summary of Immunological Results

2.71, the decanoic acid derivative, was shown to illicit a non-biased release of cytokines, with induction of both Th1 (IFN-γ and TNF-α) and Th2 (IL-4) responses. **2.71** was found to lack strong cytotoxicity. This lack of cytotoxicity may be due to a structural change induced when **2.71** binds to the CD1d molecule, which stimulates cytokine release, but makes it non-cytotoxic. The tetracosanoic acid derivative, **2.74**, and the non-glycosidic **2.63** both failed to activate the iNKT cells in this study. As **2.63** is structurally similar to **2.71**, with equivalent lipid length and character, the lack of iNKT cell activation by this compound demonstrates the necessity of the glycan moiety.

All of the lipids **2.63**, **2.71** and **2.74** induced release of IL-10, the suppressor cytokine. The non-glycosidic **2.63** did not illicit as potent a response as the glycosyl derivatives. This result indicates a possible use in the treatment of Th2 aggravated diseases.

2.9 Chapter Conclusion

To summarise, two glycolipid derivatives, **2.71** and **2.74**, were successfully synthesised, and showed some interesting biological results, such as the stimulation of the release of Il-10. Several barriers were overcome throughout the synthesis, including the problems presented by the lipid chains in the removal of protecting groups. Another issue which was encountered during the synthesis of these derivatives was the elimination of the sugar moiety, under basic coupling conditions. This synthesis demonstrated the importance of the order of reactions in the synthetic scheme.

Future work could include the synthesis of a derivative in which the length of the other hydrocarbon chain, tetradecyl in each of our glycolipids, is modified. The α-anomeric analogue could also be synthesised, in order to compare the biological activity of this glycolipid.

As will be discussed in chapter 4, functionalisation at the C-6 position of the sugar could be carried out. The introduction of other biologically relevant groups at this position may enhance the immunomodulatory activity of the glycolipid.

Chapter 3: The Synthesis of a Series of Glycopeptides

3.1 Introduction: Glycopeptides

A large amount of peptides in the body have been found to be glycosylated. Glycosylation involving *N*-acetyl glucosamine (GlcNAc) plays an important part in the regulation of protein function, for example in the stability or targeting of a glycoprotein. This has already been discussed in detail in chapter 1. The protein which we will be focusing on is the tau protein, which has been implicated in the development of neurodegenerative disorders, such as Alzheimer's disease.

3.2 Alzheimer's Disease

Alzheimer's disease (AD) is the most common form of dementia, accounting for 50-60 % of all cases. It is a progressive neurological condition, which is manifested by debilitating effects. It can become more and more difficult for sufferers of AD to remember, reason and use language. The loss of memory of recent events is often one of the first difficulties to be noticed. The person may also become disorientated, be at a loss for a word when speaking, and have increasing difficulty with simple daily tasks, such as using the phone. The risk of developing AD increases with age, with more than 25 % of those over the age of 80 suffering from the disease. Although it is rare, AD can also occur in people under 65.[112]

AD is a complicated disease, with multiple factors influencing its onset. The brains of people that suffer from AD display pathological hallmarks of the disease: Neuronal and synaptic loss, neurofibrillary tangles, and β-amyloid (Aβ) plaques. These plaques were first reported in 1907 by Alois Alzheimer.[113] Neurofibrillary tangles (NFT) are twisted, stringy fibres of tau protein, which accumulate inside brain cells, and disrupt normal brain cell function. These will be discussed in more detail later. Aβ plaques are insoluble deposits of β-amyloid peptide, and are thought to accumulate due to mutations in the amyloid precursor protein. Studies carried out by Shankar *et al* have shown that the plaques did not impair cognitive function, but that soluble Aβ dimers which were released from the plaques could cause AD-like symptoms.[114] Misfolding of Aβ may trigger events which result in aggregation of

the tau protein.[115] A third abnormality, degeneration of cholinergic neurons, has also been reported. This neuronal death leads to the cognitive impairment associated with AD. Therapies targeting this pathological marker of AD aim to promote the activity of surviving cholinergic neurons.[116]

For the purposes of this discussion, the molecular target which is focused on will be the hyperphosphorylation of the tau protein, and development of NFT.

The treatment of AD is complicated for several reasons. The first is the contribution of different factors to the development and progression of the disease, as mentioned above. The second reason is the lack of diagnostic techniques. A person suffering from AD is often not diagnosed until the later stages, when the disease has progressed, and symptoms, such as memory loss, have become pronounced. New techniques are being pioneered for the diagnosis of AD. The use of neuroimaging-biomarkers will allow for earlier diagnosis, although the pathological markers of AD mentioned above need to have developed. Techniques such as high-field MRI of brain atrophy, and *in-vivo* amyloid plaque imaging, using radio-labelled ligands, may allow for diagnosis of AD at a stage where its progression could be curbed.[117]

3.3 Tau Protein

Tau is a microtubule-associated protein (MAP) which is expressed throughout the central nervous system (CNS), but is mostly found in neuronal axons. Tau plays an important part in the organisation of microtubules in these axons. Microtubules are involved in cell shape maintenance and serve as channels for axonal transport. Tau association reduces the probability that a microtubule will shift from the growing phase to the shrinking phase. Partial phosphorylation of serine and threonine residues of tau is important to regulate the growth of microtubules by decreasing the affinity that tau has for the microtubule lattice. It has been shown that hyperphosphorylation of the tau protein causes destabilisation of microtubules by preventing binding.[118] Phosphorylation of tau is carried out by phosphate kinases, such as glycogen synthase kinase 3 (GSK-3), extracellular signal-regulated kinase 2 (ERK-2), and cyclin-dependant kinase 5 (CDK-5) (Scheme 3.1). Phosphate kinases use adenosine-5’-triphosphate (ATP) as their source of phosphate.[119]

The tau protein is also modified by addition of *O*-GlcNAc to specific serine or threonine residues in the sequence.[120] As mentioned in chapter 1, glycosylation is carried out by the enzyme *O*-GlcNAc transferase (OGT). Glycosylation has been shown to occur at many of the same sites as phosphorylation, and also to regulate the phosphorylation of adjacent sites. Studies have demonstrated that inhibition of tau phosphorylation results in increased glycosylation, and that targeted deletion of OGT causes hyperphosphorylation of tau.[121] This is yet another example of the dynamic interplay observed between glycosylation and phosphorylation of proteins, which was discussed in chapter 1 (Scheme 3.1).

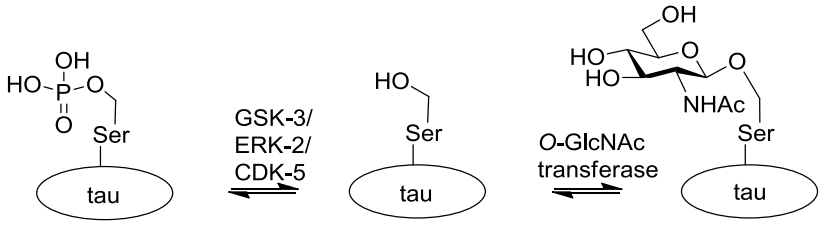

Scheme 3.1 The dynamic relationship between tau phosphorylation and glycosylation

Tau protein is translated from a single gene located on chromosome 17. Six different isoforms of tau have been found, each generated from alternative mRNA splicing at chromosome 17. These isoforms range from 352-441 amino acids in length. A highly conserved repeat region of 31 or 32 amino acids has been determined in all of these isoforms. This region also repeats itself several times within a single isoform.[122] Further study into the repeat region has revealed a strong Pro-Gly-Gly-Gly motif, which has been shown to represent the tubulin binding domain. The longest isoforms of tau contain up to 79 serine and threonine residues at which phosphorylation can occur. Only about 30 of these residues are actually phosphorylated at one time under normal physiological conditions.[123]

3.4 Tau and AD

In patients with AD, tau shows abnormal hyperphosphorylation, which causes it to aggregate into paired helical filaments (PHF) and form neurofibrillary tangles (NFT). When this happens, the microtubules disintegrate, collapsing the neuron's transport system. This may result first in communication malfunctions between neurons, and later in cell death (Fig. 3.1).[115] Tau has also been implicated in other

neurodegenerative diseases, such as Parkinson's disease and Pick's disease. These diseases are collectively known as tauopathies.[124]

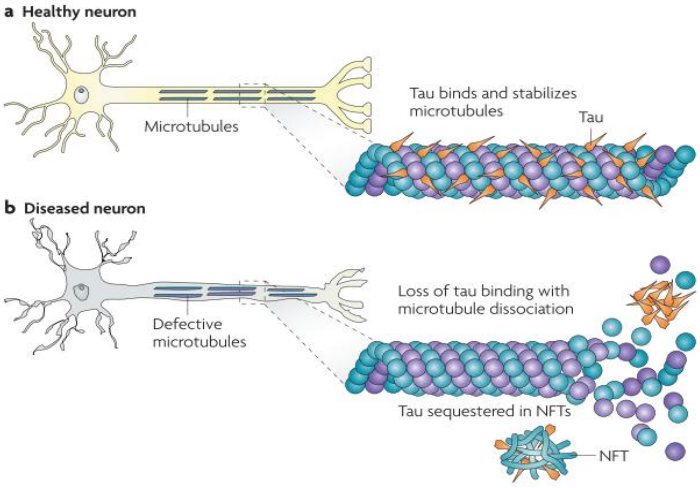

Figure 3.1 a) The stabilising effect of the tau protein on a healthy microtubule, and b) Collapse of a diseased neurons transport system[115]

Studies have shown that NFT contain all six hyperphosphorylated isoforms of the tau protein. A total of 25 serine/threonine sites of abnormal phosphorylation have been identified in AD.[125] It has been observed that almost all of these sites of phosphorylation are also found in non-aggregated tau, but that the tau protein which is found in NFT is phosphorylated to a higher extent.[126]

While there are many factors which contribute to the progression of AD, the loss of function of the tau protein is the main element. Initially, it was thought that the cause of AD progression was either Aβ plaques or NFT formation. After many years of investigation, it appears that there is a definite interplay between these two pathological markers, and that neither is independent of the other. In a study carried out by Roberson *et al*, reduction of endogenous levels of tau protein has prevented the behavioural deficits originally associated with Aβ plaques, but the extent of Aβ plaque formation is not affected.[127] This study, and other evidence, point to a synergistic relationship between tau and Aβ, but also show the central role played by the tau protein in AD.[128, 129] This makes tau an interesting molecular target for treatment of AD, and other tauopathies.

Han *et al* have carried out work which shows the importance of the site of phosphorylation of tau. They found that, by encouraging phosphorylation *in-vitro* at

ser^{202}, of wild-type (WT) tau and four tau mutants, the microtubule assembly-promoting ability of tau was inhibited. This phosphorylated species has been isolated from the brains of AD sufferers. It is suggested that phosphorylation at Ser^{202} is a major event which leads on to NFT development in AD, and also in other tauopathies. Phosphorylation was carried out by the cyclin-dependant protein kinase 5 (CDK-5).[130]

Bramblett *et al* have shown that tau protein isolated from PHF is hyperphosphorylated, it does not bind to microtubules or promote microtubule assembly *in-vitro*. Once this tau protein has been dephosphorylated, it recovers the ability to bind to, and promote, microtubule assembly. They also demonstrate the inhibitory effect that hyperphosphorylation at Ser^{396} of tau has on binding microtubules.[131]

Several other sites of phosphorylation have been implicated in the development of the pathological markers of AD, such as Ser^{262}, Ser^{356}, and Thr^{231}. It is thought that a combination of phosphorylated residues, and not just a specific one, is responsible for the neurotoxic effects of tau.[132] Mutation of 14 sites of phosphorylation in the tau protein to alanine, in place of serine and threonine, resulted in a lack of tau-induced toxicity. When individual residues were mutated to alanine, toxicity was still observed. This study indicated that no particular site was responsible for tau toxicity.[133]

Transgenic mice which have been made to express human tau have shown neurological deficits and neuronal loss, accompanied by the appearance of NFT.[134] It had been assumed that these NFT were responsible for the cytotoxic effects of tau protein, but recent findings, using a mouse model of AD, appear to show that this is not the case. Santacruz *et al* have engineered mice to express a repressible human tau variant. These mice developed progressive age-related NFT, neuronal loss, behavioural impairments and decreased cognitive function. When this human tau was suppressed, the mice recovered cognitive function and neuron numbers stabilised. In older mice models NFT continued to accumulate, but behavioural impairments did not return. This study showed that NFT alone are not enough to cause neuronal loss or behavioural impairments. It is more likely that the loss of normal function of the tau protein, due to hyperphosphorylation, and its aggregation

into soluble oligomers, are the causes of neuronal and cognitive function loss. It also raises the question as to whether the NFT are markers of the disease, or if they are a protective mechanism of the body's, allowing transformation of a neurotoxic species (soluble, hyperphosphorylated tau) into a less toxic form, as seen for the Huntington protein.[135] In some neurodegenerative disease models this aggregation into a less toxic species, followed by elimination from the body by proteasomal activity, or autophagy, has been observed, but this has yet to be proven in AD.[136]

3.5 Current Tau–Focused Strategies for the Treatment of AD

While much work is being carried out which targets Aβ plaques and cholinergic neurons, this discussion will focus on tau-based strategies for the treatment of AD.

3.5.1 Microtubule Stabilising Strategies

The role of the tau protein in the CNS is the stabilisation of microtubules, as mentioned above. When tau becomes hyperphosphorylated and aggregates into NFT this function is lost. Several therapeutics have been investigated to fill this role, and stabilise the neuronal transport system.

The microtubule-stabilising drug, Paclitaxel, was administered to transgenic mice that displayed microtubule and motor deficits. Palitaxel is an antimitotic agent used in the treatment of cancer. An improvement in microtubule density and motor function was noted upon administration of this drug, demonstrating how small-molecule microtubule stabilisers could be a possible treatment in AD. Palitaxel does not readily cross the blood brain barrier, but the effects observed were attributed to uptake at peripheral neuromuscular junctions.[137] Taxane based derivatives which display microtubule-stabilising abilities have been investigated, but, as for Palitaxel, they are often not able to cross the BBB, and would require high doses to illicit the desired effect. It would be desirable to keep the peripheral levels of microtubule-stabilising drugs as low as possible, as they are antimitotic agents and can cause adverse effects in the body. For these reasons, Taxanes are not ideal drug candidates for the treatment of neurological diseases.[115]

An octapeptide, known as NAP, with a sequence of Asn-Ala-Pro-Val-Ser-Ile-Pro-Gln, has been shown to promote microtubule assembly. It has the ability to cross the BBB, and may be a possible candidate for the treatment of neurodegenerative

disorders. In mouse models of AD, a reduction in tau hyperphosphorylation and levels of Aβ plaques was also observed. NAP administration reduced hyperphosphorylation at Thr^{231}, which is a site known to influence microtubule binding.[138]

3.5.2 Reduction of the Level of Hyperphosphorylated Tau in the Brain

Utilising autophagy, one of the mechanisms used by the body to degrade misfolded protein, is another possible tau-based strategy for the treatment of neurodegenerative disease (Fig. 3.2). Misfolded protein is prone to formation of the aggregates associated with diseases like AD. Autophagy is carried out by encapsulation of these proteins by an autophagosome, followed by fusion with a lysosome to degrade the protein aggregates.[139] Chemical inducers of autophagy are of interest in the treatment of neurodegenerative diseases. As mentioned earlier, in the case of AD, the aggregated NFT are not thought to be the toxic species, while non-aggregated, soluble forms of hyperphosphorylated tau may be the cause of tau-toxicity.[132] This approach may enhance elimination of hyperphosphorylated tau.

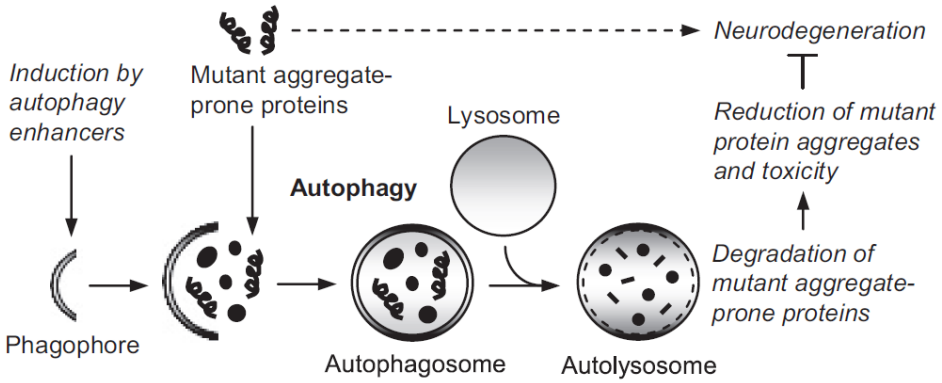

Figure 3.2 Autophagy of aggregated proteins[139]

Several chemical inducers of autophagy are being investigated for the treatment of neurodegenerative diseases. The naturally occurring disaccharide, trehalose, has been shown to increase the removal of abnormal proteins by promotion of autophagy in mouse models (Fig. 3.3). After treatment with trehalose the levels of phosphorylated tau and Aβ plaques were reduced. Trehalose is free of toxic effects at high concentrations, so may be a potential candidate for human trials.[140]

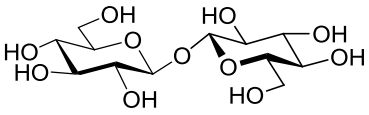

Figure 3.3 Naturally occurring disaccharide Trehalose

Another method of reducing the levels of hyperphosphorylated tau in the brain is by tau immunotherapy. Mice which had been engineered to express tau pathology were immunised with a small, phospho-tau peptide. Three different sequences, each based around known phosphorylated sites of the tau protein, of between 13-18 amino acids, which are phosphorylated at one site, were used in this study. It was observed that the mice produced antibodies that entered the brain, and could reduce tau pathology, as well as improving cognitive impairments.[141]

3.5.3 Inhibition of Tau Oligomer Assembly

When tau becomes hyperphosphorylated it begins to bundle together, and form soluble oligomers. These oligomers aggregate together further, to form the insoluble NFT associated with AD. As discussed above, it is thought that the soluble aggregates of hyperphosphorylated tau are the toxic species (Fig. 3.4). For this reason, inhibiting the formation of these oligomers is an area of interest in the treatment of AD. Decreasing the levels of oligomeric, hyperphosphorylated tau protein could also contribute to microtubule stabilisation by increasing the levels of monomeric tau.[115]

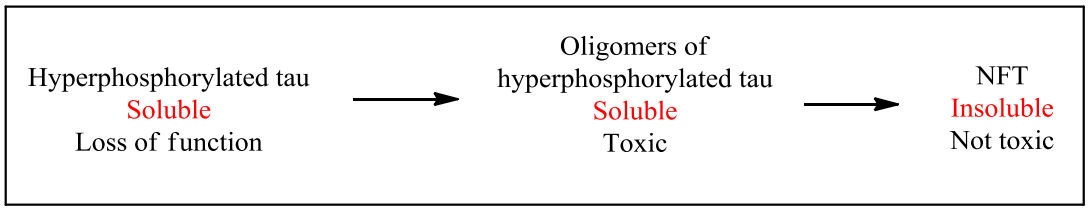

Figure 3.4 The aggregation of hyperphosphorylated tau and the postulated toxicity of each stage

Methylene blue has been used to treat many different diseases, varying from malaria to depression (Fig 3.5). Recently there has been evidence that methylene blue could have potential as a treatment for AD. It has been observed that methylene blue inhibits the aggregation of tau protein, and also Aβ species. Methylene blue has been used for decades for the treatment of other diseases, and so its safety in humans has been well assessed. The drug has undergone some clinical trials, under the trade

name Rember™, and has shown beneficial effects, with reduction of aggregation of both tau and Aβ, along with other aggregation-prone proteins in the body. Rember™ may be available as a registered drug as soon as this year.[142]

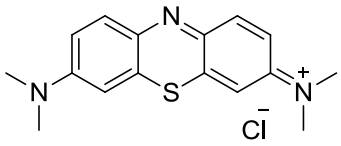

Figure 3.5 The structure of methylene blue

3.5.4 Inhibition of Tau Hyperphosphorylation

A major area of tau-focused strategies in the treatment of AD and other tauopathies is the inhibition or reduction of tau hyperphosphorylation. This is essentially the reason that tau loses the ability to stabilise microtubules, leading to cell death.

The main method which has been investigated is the administration of kinase inhibitors. Kinases are enzymes which catalyse the transfer of a phosphate group (PO_3^-) from a donor molecule, such as the terminal PO_3^- of adenosine-5'-triphosphate (ATP), onto a receiving molecule, such as a protein. Often, the phosphorylated products of these reactions play important roles in cellular processes, and their deregulation contributes to a wide range of pathological conditions.[143]

Many different phosphate kinases are present in the body, but the main kinases which have been associated with AD and tau phosphorylation are the proline directed kinases GSK-3, CDK-5 and ERK-2, and also the non-proline directed kinase microtubule affinity-regulating kinase (MARK). It has been observed that 13 of the phosphorylated sites of the tau protein are followed by proline, and so are potential targets for the proline directed kinases.[119] The microtubule binding region of tau is associated with the Pro-Gly-Gly-Gly motif, as mentioned earlier, and so this region of the tau protein is important for maintaining microtubule integrity. Many known sites of *O*-GlcNAcylation in proteins are also sites which are phosphorylated by proline-directed kinases.[144] For these reasons, inhibition of the proline-directed kinases is interesting in the search for treatments of AD.

Extracellular signal-regulated kinase 2 (ERK-2) is also known as mitogen-activated protein kinase 1 (MAPK-1), and is a serine/threonine kinase. ERK-2 has been found to be upregulated in AD, and in other neurodegenerative diseases, even some that do

not involve tau hyperphosphorylation. Some studies have suggested that ERK-2 may be used as a marker for these diseases, as the levels of this kinase in cerebrospinal-fluid were elevated in patients with neurodegenerative disorders, such as CJD.[145] Inhibition of ERK-2 in mouse models of AD has been shown to have a beneficial effect. Caffeine has an inhibitory effect on ERK-2, which, in turn, has been observed to decrease the levels of Aβ plaques and tau hyperphosphorylation. Caffeine also inhibits other kinases, and so improvements in neuronal survival may be due to a contributory effect.[146]

Inhibitors of cyclin-dependant kinase 5 (CDK-5) have also been investigated. This kinase requires association with a regulatory subunit, either p35 or p39 proteins, to activate it. CDK-5 is essential in neuronal development, but deregulation of this kinase has been observed in AD.[147] The neurodegenerative effects associated with deregulation of CDK-5 appear to be observed when it is associated with a shorter form of p35, which is known as p25. The cleavage of p35 to the truncated form, p25, is mediated by the calcium dependant protease, calpain. The p25 fragment is more stable than p35, and is generally formed under conditions of cell stress or injury. The CDK-5/p25 complex displays aberrant activity, and carries out abnormal phosphorylation of substrates, including the tau protein.[148] Inhibitors of CDK-5 must target the CDK-5/p25 complex. Jain *et al* have synthesised a series of inhibitors, but only one compound displayed acceptable inhibition of the CDK-5/p25 complex (Fig. 3.6). Structural modifications were carried out to investigate the SAR between the inhibitor and CDK-5. It was found that the terminal hydroxyl group, and also the ethyl group, are required for activity. The inhibitor did not show an increased affinity for CDK-5 over other kinases, which may be expected, due to exploitation of binding interactions within the ATP binding pocket, as will be discussed later.[149]

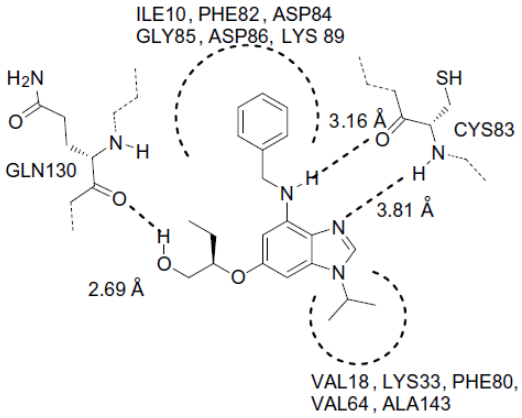

Figure 3.6 Binding interactions between the inhibitor and amino acid residues of CDK-5[149]

One CDK inhibitor which has shown promising results is *R*-roscovitine, which is involved in clinical trials for the treatment of cancer (Fig. 3.7). This compound shows potent inhibition of CDK-5, as well as other kinases in the CDK family. Again, interactions within the ATP binding pocket are utilised.[150]

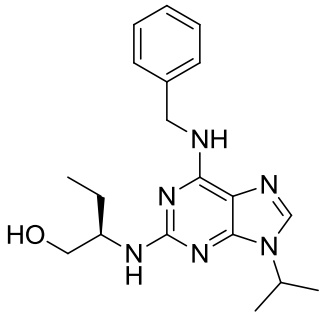

Figure 3.7 The structure of CDK-5/p25 inhibitor, *R*-roscovitine

While inhibition of CDK-5 has shown some success, it may not be an effective target in the treatment of AD. When CDK-5 was inhibited in mouse models of AD, there was a noted decrease in the production of Aβ, but an increase in tau phosphorylation. It was demonstrated that, upon inhibition of CDK-5, an up-regulation of GSK-3 occurs. This indicates that CDK-5 may not be suitable for the treatment of AD, as, even if selective inhibition can be achieved, GSK-3 will carry out phosphorylation in place of CDK-5.[151] Another issue with inhibiting CDK-5 is the central role it plays in neuronal development, as mentioned earlier. Blocking of this function could produce unwanted side-effects, interfering with cell cycle progression.[152]

The evidence leads to the postulation that GSK-3 is the ideal phosphate kinase to inhibit, in order to decrease hyperphosphorylation of the tau protein. In a study carried out by Wang *et al*, the relationship between GSK-3 and *O*-GlcNAcylation of tau was demonstrated. Inhibition of GSK-3 by lithium resulted in an increase in *O*-GlcNAcylation of several sites on tau, while a decrease in *O*-GlcNAcylation has been noted in the brains of people with AD.[144] Most *in-vivo* studies which have been carried using phosphate kinase inhibitors have been targeted at GSK-3 activity, highlighting the importance of this kinase in tau hyperphosphorylation.[115] These results make GSK-3 an interesting target in the treatment of AD. GSK-3, and current inhibitors of this kinase, will be discussed in detail below.

Many different kinase inhibitors have been investigated. These inhibitors have been both ATP competitive and non-competitive. As phosphate kinases use ATP as their source of phosphate, they all possess an ATP binding pocket, and some inhibitors exploit this binding site in their design (Fig. 3.8). These types of inhibitor are known as ATP competitive, such as those discussed above for CDK-5 inhibition (Figs. 3.6 and 3.7).

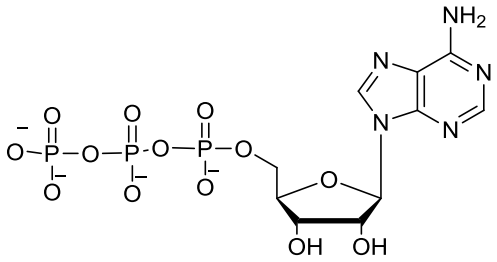

Figure 3.8 The structure of adenosine-5'-triphosphate

In order to make an inhibitor more selective, these molecules may take advantage of residues surrounding the ATP pocket, which are unique to each kinase, to increase their binding affinity.[153] ATP-competitive inhibitors often display poor activity and selectivity *in-vivo*. The high sequence homology among kinase ATP pockets reduces specificity, sometimes producing unwanted side effects. Competition with intracellular levels of ATP also contributes to reduced activity when compared to *in-vitro* studies.[154]

Non-ATP competitive inhibitors have shown some specificity for certain kinases. These compounds do not depend on the ATP binding pocket to increase their

affinity, but use other residues to make binding interactions. Although elucidation of the SAR between other sites on the kinase and the potential inhibitor may be more difficult, this approach is more attractive. It will infer greater kinase specificity on the inhibitor, which, in turn, means that there will be less interference with other ATP mediated processes in the body.

Non-ATP competitive inhibitors generally work by inducing a conformational shift in the kinase, which prevents it from functioning. There are three different approaches to non-ATP competitive inhibitor design. The first involves compounds which bind to the inactive form of the kinase, stopping it from activating, and so preventing it from binding ATP. The second is binding to sites on the kinase other than those surrounding ATP binding cleft, inducing a conformational change in the kinase. The third involves binding to the cysteine residue at the ATP binding cleft, preventing ATP from binding, and so making the kinase inactive. The last approach does not make the inhibitor as selective as the other approaches, unless other sites on the kinase are also utilised for binding.[155]

3.6 Glycogen-Synthase Kinase-3

GSK-3 is a serine/threonine kinase which is involved in many processes in the body, including glucose metabolism, gene expression, structural regulation (microtubules), cell growth, cell survival, cardiac hypertrophy, oncogenesis and apoptosis. GSK-3 is found as two isoforms, GSK-3α and GSK-3β, which are similar in their structure, substrate specificity, and mechanisms of regulation. They share a 98 % sequence homology in their catalytic domains.[156] Deregulation of GSK-3 has been associated with several disorders such as diabetes,[157] some forms of cancer, schizophrenia, and in the development of neurodegenerative diseases like AD. It is highly expressed in the brain, and it has been proven that GSK-3 phosphorylates specific amino acid side chains of the tau protein.[158] This kinase mediates tau hyperphosphorylation and Aβ-induced toxicity.[159] Studies have shown that GSK-3 activity may increase with age, which is in agreement with the age-dependant development of AD. Inhibition of GSK-3 *in-vivo* has resulted in reversal of both tau hyperphosphorylation and behavioural defects in mouse models of AD.[160]

A lot of work has been carried out into the development of GSK-3 inhibitors for the treatment of diseases like AD and diabetes. These inhibitors have been both ATP-competitive, and non-competitive. Elucidation of the crystal structure of GSK-3 has led to a better understanding of the different functions of the kinase. This may also help to design drugs that inhibit specific roles of GSK-3, without interfering with other important processes.[161]

Some of the first non-ATP competitive GSK-3 inhibitors were synthesised by Martinez *et al*. These drugs are small heterocyclic thiadiazolidinones, and display potent inhibition of GSK-3. The most promising compound is shown in Fig. 3.9. They displayed good specificity for GSK-3, and did not show inhibitory activity for other protein kinases tested in this study.[162] Later studies with mouse models have shown neuroprotective and antidepressant effects, with improved cognitive function. This molecule is currently in clinical trials for AD, and can cross the BBB.[163]

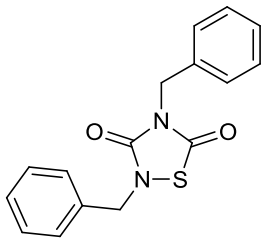

Figure 3.9 Thiadiazolidinone with potent GSK-3 inhibitory properties

Another family of inhibitors are the paullones, the most selective of which, Cazpaullone, is shown below in Fig. 3.10. Members of this group have been shown to decrease tau hyperphosphorylation, and reduce Aβ production *in-vitro*, but *in-vivo* testing has been limited. This type of compound has displayed high specificity for GSK-3 inhibition, even over other proline-directed kinases, like CDK-5.[164, 165] Paullones are ATP-competitive inhibitors, but also take advantage of kinase specific residues at the ATP binding cleft to infer selectivity. Interactions between paullones and Val^{135} of GSK-3 are much stronger than with Cys^{83} of CDK-5, and this increased binding may account for the specificity of these inhibitors.[166]

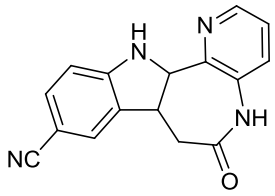

Figure 3.10 Cazpaullone, a selective GSK-3 inhibitor

Lithium has been investigated as a GSK-3 inhibitor. Lithium has been used for decades as a treatment for bipolar disorder, and so has been shown to be safe to administer for prolonged periods. Lithium is a potent GSK-3 inhibitor, acting through competition with magnesium ions, and binding to the kinase. Lithium treatment *in-vivo*, in mice, has displayed a reduction in tau hyperphosphorylation, and decreased Aβ toxicity. These results are promising, but one consideration is that lithium inhibits other enzymes apart from GSK-3, and can be neurotoxic due to alteration of neurotransmitter levels.[167] Lithium treatment of mouse models of AD has demonstrated pathological improvements, but memory deficits were not recovered. Human trials were carried out on a small scale, for 10 weeks, but these trials did not show encouraging results, with no pathological or behavioural improvements.[168]

While many inhibitors of GSK-3 contain aromatic groups in their structure, there has been evidence to suggest that short peptides can selectively inhibit protein kinases. The structure of these peptides can be based on "natural" sequences which are known to be targeted by the kinase, and so make the inhibitor selective.[169] As GSK-3 is essential in many processes in the body, a weak-to-moderate inhibition is desirable. By synthesising a peptide sequence which mimics the natural substrate of GSK-3, there will be competitive binding, resulting in partial inhibition of the kinase. Substrate-competitive inhibitors are more selective than ATP-competitive inhibitors, and so this strategy is attractive for clinical use.[163] As mentioned earlier, the crystal structure of GSK-3 has been obtained. Examination of this structure indicates the presence of a substrate peptide binding site, which is specific for this kinase.[161]

Plotkin *et al* have synthesised a phosphorylated peptide inhibitor of GSK-3, for use in the treatment of diabetes. These peptides are substrate-competitive, and *in-vivo* mouse models of diabetes have shown a marked improvement. The membrane

permeable inhibitor showing the most potential is known as L803-mts. The sequence was derived from a GSK-3 substrate, heat shock factor-1, and contains the GSK-3 recognition motif S^1XXXS^2. S^1 is the site which is known to be phosphorylated by GSK-3, S^2 is the priming site, and X is any amino acid. The sequence of the phospho-peptide, L803-mts, is shown in Fig. 3.11, with S^1 and S^2 underlined. The site of phosphorylation in the natural sequence has been substituted with alanine.[157]

N-Tetradecyl-Gly-Lys-Glu-Ala-Pro-Pro-Ala-Pro-Pro-Gln-Ser(phosphorylated)-Pro

Figure 3.11 Sequence of L803-mts

Structural variations in the peptide revealed that elimination of the phosphate group prevented inhibition, and also that shortening the sequence to just S^1XXXS^2 eliminated the inhibitory capacity.[157] This peptide was found to have neuroprotective effects *in-vitro*.[170] Closer examination revealed that the substrate and inhibitor binding sites were not identical, while both occupied the phosphate binding pocket, the other residues involved in binding were different. The residues are located near to the ATP-binding site, and the phosphate binding pocket which interacts with the phospho-serine of the substrate. The substrate was found to interact with the cavity bordered by Gln^{89} and Asn^{95}, while L803-mts mainly interacted with Phe^{93} and a hydrophobic surface located away from the ATP-binding site. The Pro^8 residue of L803-mts was observed to be involved in the interaction with Phe^{93}. It was thought that this difference in binding was crucial to the inhibitory capacity of the peptide. Alterations in the peptide sequence were later carried out, and resulted in a 3-10 fold increase in GSK-3 inhibition. The increased activity of the inhibitors was attributed to the presence of more hydrophobic groups, and also to increased interaction with Phe^{93}.[171] From this information it is evident that peptides have potential as selective inhibitors of GSK-3. The natural substrates of GSK-3 are proteins, and, by mimicking the sequence of these substrates, a peptide inhibitor could be designed which selectively blocks unwanted functions of GSK-3.

3.7 Solid-Phase Peptide Synthesis

The synthesis of complicated glycopeptides can be hard to achieve in the traditional "solution-phase". These coupling reactions can often be poor yielding, and the

intermediates difficult to purify. The advent of "solid-phase" peptide synthesis (SPPS) was pioneered by Bruce Merrifield in the 1960's as a new approach to peptide synthesis, with the first resin being called Merrifield resin. Many advances have happened in the area of SPPS since then, but the same methodology is in use today.[172] SPPS involves the formation of amide bonds, under standard coupling conditions, where the growing peptide is anchored to a solid support (resin).

SPPS has many advantages over solution phase chemistry. It allows the use of large excesses of reagents, which help to drive these poor yielding reactions almost to completion. The reactions are also faster than the liquid phase chemistry, peptide couplings can be accomplished in less than 30 mins.[173] There is no need for purification at each stage, as the peptide remains on the solid support until the final deprotection step, and excess reagents are simply washed off. SPPS also has the advantage, as with solution phase, of lending itself to the well-established coupling methodologies of TBTU/HOBt. One of the major advantages of SPPS is that it is suitable for automation. Peptide sequences can be programmed into an automated synthesiser, providing non-chemists with access to biologically relevant peptides.[101]

There are two different propagation methods used in SPPS, the Boc/Bzl and Fmoc/tBu strategies. The original resins were designed to be used in conjunction with the Boc/Bzl strategy. As the Boc group is removed under acidic conditions, repeated use of TFA is required in the deprotection steps, which may be too harsh for some peptides, especially glycopeptides.[174] The development of the Fmoc/tBu strategy has allowed SPPS to be carried out using milder chemistry. The Fmoc group is removed under mildly basic conditions, generally by piperidine, but even milder bases have been utilised. Most SPPS today is carried out using the Fmoc/tBu methodology, and has been complimented by the development of suitable resins and side-chain protecting groups.[172]

An important element of SPPS is the choice of resin. As mentioned above, the original Merrifield resin is suitable for the Boc/Bzl strategy, and the finished peptide is cleaved from the resin under basic conditions. Newer resins, such as the Wang or RINK amide resins, contain a linker which is acid-labile. There is a wide variety of resins available, which are composed of a polymeric support, such as polystyrene, to

which a linker is attached. Choice of resin is dependent upon the strategy being used, and also on the nature of the peptide.[175]

SPPS has become an integral part of peptide synthesis, with many advantages. It has made possible the synthesis of complicated structures, which otherwise may not have been accessible. Recent work in the area of SPPS has led to the development of a solid-phase approach to oligosaccharide synthesis, but this is a much more complicated endeavour, and is not suited to all carbohydrate syntheses.[176]

3.8 Aim

The aim of this section was the synthesis of glucosamine based glycopeptides, which have potential kinase inhibitory properties (Fig. 3.12). The kinase which was targeted in the design of this glycopeptide is GSK-3, which has been highly implicated in the development of AD, as discussed earlier.

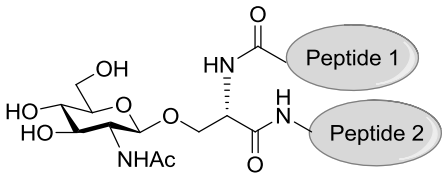

Figure 3.12 General structure of target glycopeptide

It was decided to synthesise a non-ATP competitive inhibitor, in order to infer more selectivity for GSK-3. *O*-Linked-*N*-acetyl glucosamine (GlcNAc) was incorporated into the glycopeptide to investigate the effect that the sugar moiety would have on the affinity of this compound for GSK-3. Glycosylation is biologically carried out on the tau protein, as discussed earlier, and it is postulated that GSK-3 may have a recognition site for GlcNAc. As previously mentioned, peptides are good candidates as specific kinase inhibitors, and some have shown moderate inhibition of GSK-3. The peptide sequence which was synthesised is based on a portion of the repeating sequence identified in the tau protein. Both of the serine moieties in the sequence are known to be involved in the dynamic glycosylation/ GSK-3-mediated phosphorylation of tau.[122] The peptide synthesis was carried out using solid phase methodology, utilising the well-established Fmoc strategy.

3.9 Synthesis of Protected Glycosyl-Serine Building Block 3.5

*3.9.1 Synthesis of N-Fmoc Protected Glycosyl Acceptor **3.2***

The Fmoc protecting strategy was chosen for SPPS. The Fmoc protecting group was used as it is orthogonal to the other protecting groups in the glycopeptide, and can be removed easily in the presence of piperidine. *N*-Fmoc protected serine has also been demonstrated as a good glycosyl acceptor, making it attractive for the synthesis.[177] *N*-Fmoc protected serine was treated with benzyl bromide, in the presence of DIPEA, to selectively alkylate the acid functionality, resulting in **3.2** (Scheme 3.2). This reaction was originally carried out using K_2CO_3 as the base, but yields were not reproducible. The solubility of DIPEA allowed the reaction to proceed at a faster rate, resulting in increased and reproducible yields.

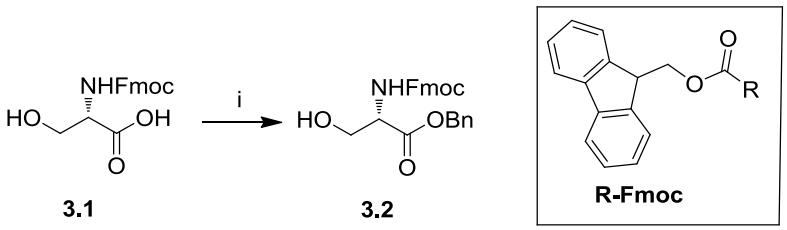

3.1 3.2

Scheme 3.2 Synthesis of *N*-Fmoc protected glycosyl acceptor. Reagents and conditions: i) BnBr, DMF, DIPEA, rt, overnight, 80 %

*3.9.2 Synthesis of Building Block **3.5***

Glycosylation of the protected serine acceptor **3.2** was carried out using the imidate donor **2.34**, discussed in chapter 2. The reaction was carried out using TMSOTf as the promoter to give **3.3**. From this glycosylated serine, removal of the *N*-Troc protecting group was carried out, using freshly activated Zn and acetic anhydride, to give **3.4**. This reaction was initially carried out in the presence of Et_3N. The reaction proceeded, but with poor yields (30 %). The Fmoc group is base labile, and removal of this group accounted for the low yields. The reaction was carried out without Et_3N, and the yields improved greatly, but with a longer reaction time (from 4 h increased to overnight). The next step in the synthesis was the hydrogenolysis of the benzyl ester protecting group, using Pd/C and H_2, to give the free acid **3.5**, which was used as the building block for incorporation into the glycopeptide (Scheme 3.3). This building block is often used in the literature for glycopeptide synthesis.[178]

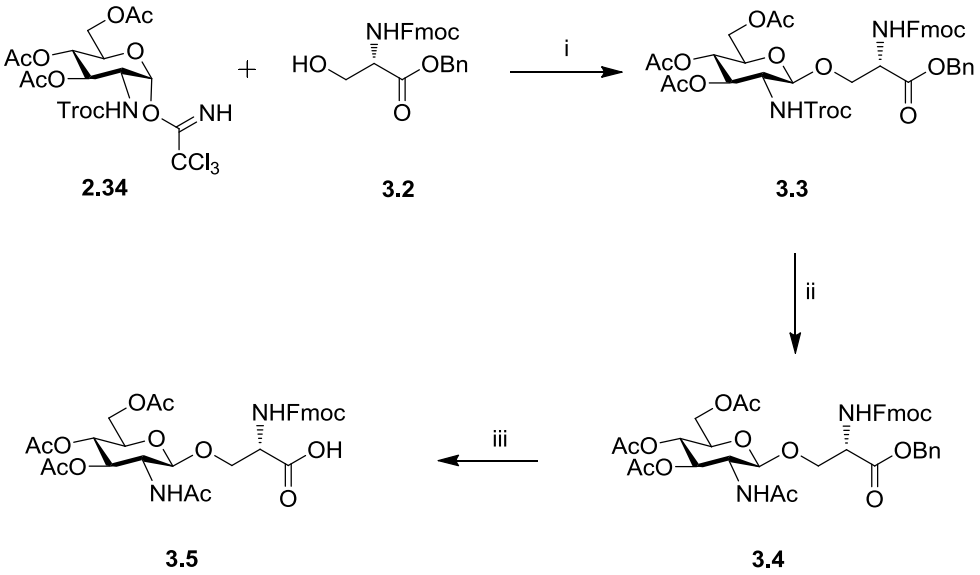

Scheme 3.3 Synthesis of glycosyl building block 3.5. Reagents and conditions: i) TMSOTf, DCM, overnight, rt, 62 %; ii) Zn, Ac_2O, overnight, rt, 80 %; iii) Pd/C, EtOAc, overnight, rt, 70 %

3.10 Synthesis of Glycopeptides

A library of novel peptides was synthesised using solid phase peptide synthesis (SPPS) techniques, following literature procedures.[172]

*3.10.1 Synthesis of Decapeptide **3.6***

HO-Val-Lys-Ser-Lys-Ile-Gly-Ser-Thr-Gly-Asn-NHAc

Figure 3.13 Sequence of decapeptide 3.6

The first target peptide sequence, shown in Fig. 3.13 above, which was synthesised, does not contain any glycosylated amino acid. This was carried out in order to investigate the effect that the sugar moiety would have on the affinity for the GSK-3 kinase.

2-Chlorotrityl chloride (CTC) resin, also known as Barlos resin, was used for the SPPS of our peptides (Fig. 3.14).

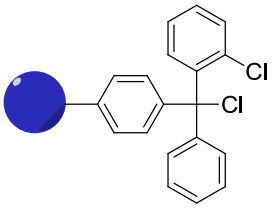

Figure 3.14 2-Chlorotrityl chloride resin

This resin has several advantages over other resins. It is less acid labile than the closely related trityl chloride resin, yet labile enough to allow cleavage of the finished peptide under mild acidic conditions (as low as 1 % TFA in DCM). Racemisation is eliminated as loading of the first amino acid (AA) is carried out by nucleophilic substitution, and so does not necessitate activation of the acid functionality of the AA. A problem encountered with some other resins, such as the Wang resin, is formation of diketopiperazine (DKP), **3.7**, as shown in Scheme 3.4. This usually occurs at the dipeptide stage. The bulky nature of the 2-chlorotrityl group prevents any DKP formation. Another advantage of the CTC resin is that it can be used for both protected and free peptides.[179]

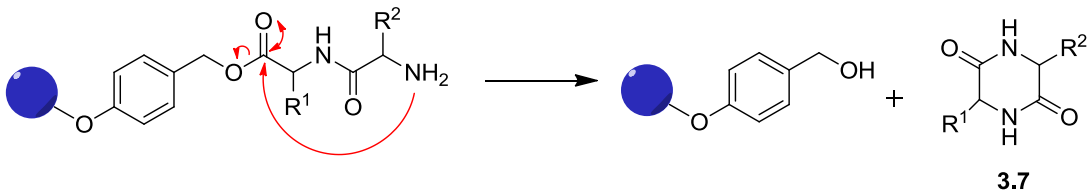

3.7

Scheme 3.4 Diketopiperazine formation

The Fmoc protection strategy was employed for this synthesis. This methodology compliments the use of the CTC resin due to Fmoc removal under basic conditions. Carrying out the synthesis on the solid-phase has many advantages, as discussed earlier, but also poses difficulties not associated with the solution-phase. The main disadvantage is that the product of the reaction is bound to the resin until the final step. This means that traditional monitoring techniques, such as TLC, don't lend themselves to the synthesis. The Kaiser test is a common system used to determine the success of coupling and deprotection steps in SPPS. It is a qualitative test based on the reaction of the amine functionality with ninhydrin, to produce a specific colour change, depending on the structure of the amine involved, for example, a primary amine produces a blue/ purple colour in the Kaiser test. This blue colour

indicates successful deprotection of the Fmoc group, or an incomplete coupling reaction. An amide or carbamate reacts to produce a yellow/clear colour, indicating a successful coupling reaction, or incomplete Fmoc deprotection. It is a useful tool in peptide synthesis as it requires a minimum amount of analyte, and gives a quick result (within 1 min).[172]

Coupling reactions were carried out by pre-activation of the *N*-Fmoc protected amino acid with TBTU, HOBt, and DIPEA for 15 mins. The activated acid was then added to the resin bound free amine, and gently shaken for 1.5 h. The solvent and excess reagents were then easily removed by vacuum filtration, and the resin was washed with DMF and DCM. The Kaiser test was used to indicate complete consumption of the free amino groups. Each of these couplings required one cycle for completion, but a second coupling cycle can be performed, if necessary. This second cycle was avoided by slightly longer reaction times than is needed (the reaction can be complete in 30 mins). This precaution was taken as there are some indications in the literature that this second coupling step can cause elimination of the *N*-Fmoc group. This could result in repetition, with coupling of a second amino acid to the free amine. In SPPS, an excess of reagents is used, and this helps to ensure that the reaction goes to completion. Although the Kaiser test indicated full coupling at each step, the resin was capped by reacting with acetic anhydride. Any remaining free amine groups were so converted into amides at this step, stopping propagation of an incorrect deletion sequence.[172] The *N*-Fmoc protecting group of the terminal amino acid was deprotected at each stage using a 20 % solution of piperidine in DMF. The reactive side chains of the amino acids used were suitably protected, so that the protecting groups were compatible with *N*-Fmoc cleavage conditions. The amino acids used in this synthesis, and their protected side chains, are shown in Fig. 3.15. All amino acids used for this synthesis possess the L configuration.

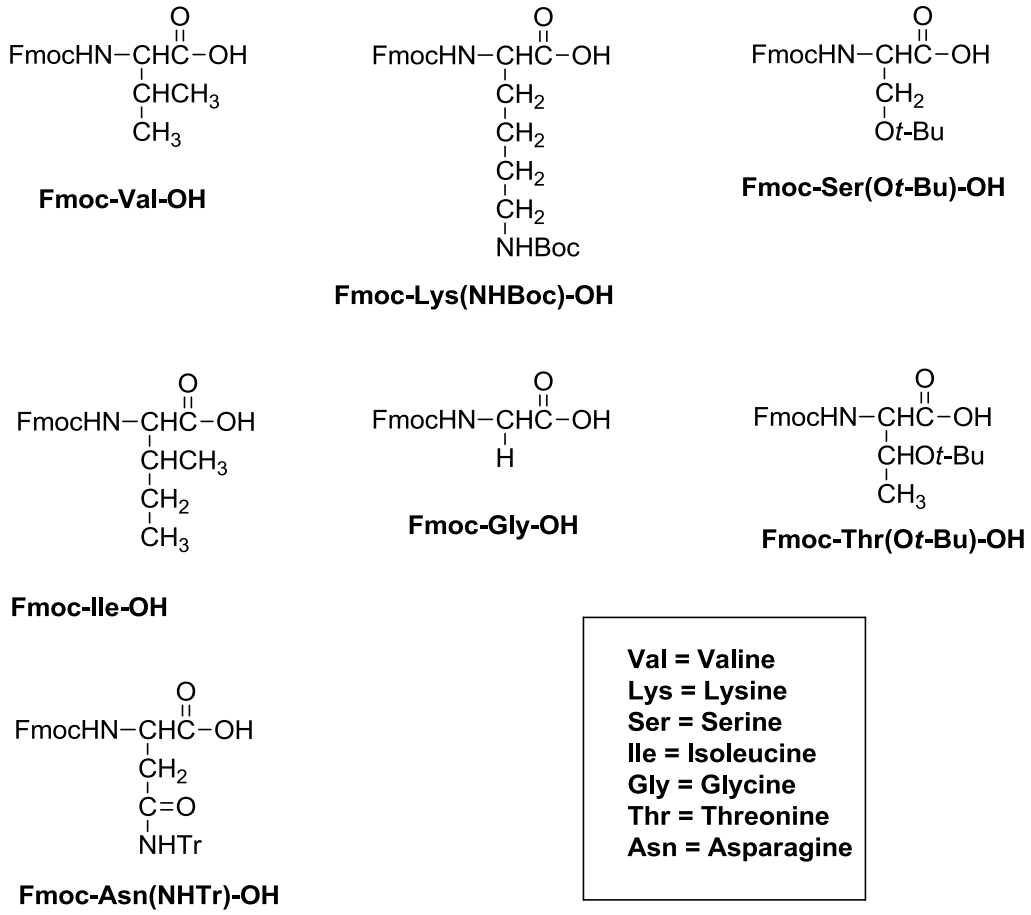

Figure 3.15 L-Amino acid residues used in SPPS, and the abbreviation used to denote them

2-Chlorotrityl-chloride (CTC) resin was selected for the synthesis of the peptides, as discussed earlier. Swelling of the resin is important to allow the reagents to access the reactive site, and DCM is added to the resin before the reaction. This step was also carried out at each stage in which the resin bound peptide had been dried and stored. The first amino acid which was attached to the resin was *N*-Fmoc-Valine-OH. This reaction follows an S_N1 mechanism. The amino acid was added to the resin in the presence of DIPEA, in DCM (Scheme 3.5). DIPEA is used as it is a hindered base, and so does not cause removal of the *N*-Fmoc protecting group. The resin was washed with a solution of MeOH/DCM/DIPEA to cap any unreacted CTC groups on the resin.

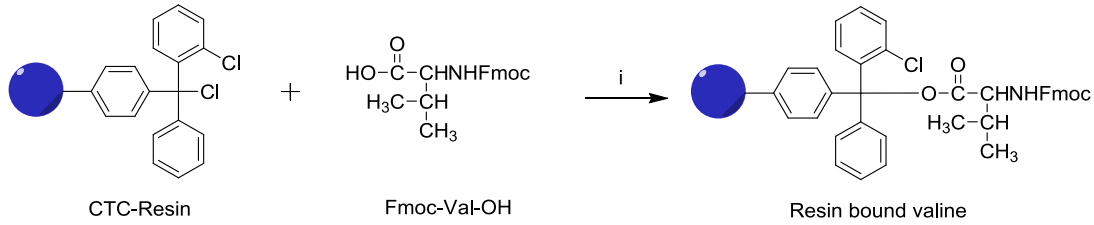

Scheme 3.5 Loading of the first amino acid onto the CTC resin. Reagents and conditions: i) DIPEA, DCM, 2 h, rt

Estimation of the amount of amino acid which had attached to the resin was carried out by UV analysis. A known quantity of the resin-attached *N*-Fmoc-AA was subjected to *N*-Fmoc cleavage conditions of DBU. The level of attachment of the *N*-Fmoc-AA was judged by measurement of the UV absorbance of dibenzofulvene, which is released upon *N*-Fmoc cleavage, at 304 nm. This was found to be 0.72 mmol/g (moles of AA per gram of resin), which was in agreement with literature values of 0.86 mmol/g for CTC resin.[180]

Removal of the *N*-Fmoc group was carried out in the presence of piperidine, followed by removal of reagents by vacuum filtration and rinsing. The success of this reaction was confirmed by the appearance of a blue colour in the Kaiser test. Coupling of the second amino acid, *N*-Fmoc-Lysine-(*N*-Boc)-OH, was carried out by pre-activating the acid in the presence of TBTU, HOBt, and DIPEA for 15 mins, followed by addition to the resin bound free amine (Scheme 3.6). Any unreacted, resin bound free amine was capped by acetylating with Ac_2O in the presence of DIPEA. This step was carried out to reduce the likelihood of deletion sequences. This method of *N*-Fmoc deprotection, coupling of the next amino acid, and capping of any unreacted, resin bound amino peptide was repeated for each consecutive amino acid until the desired decapeptide was synthesised (Fig. 3.13).

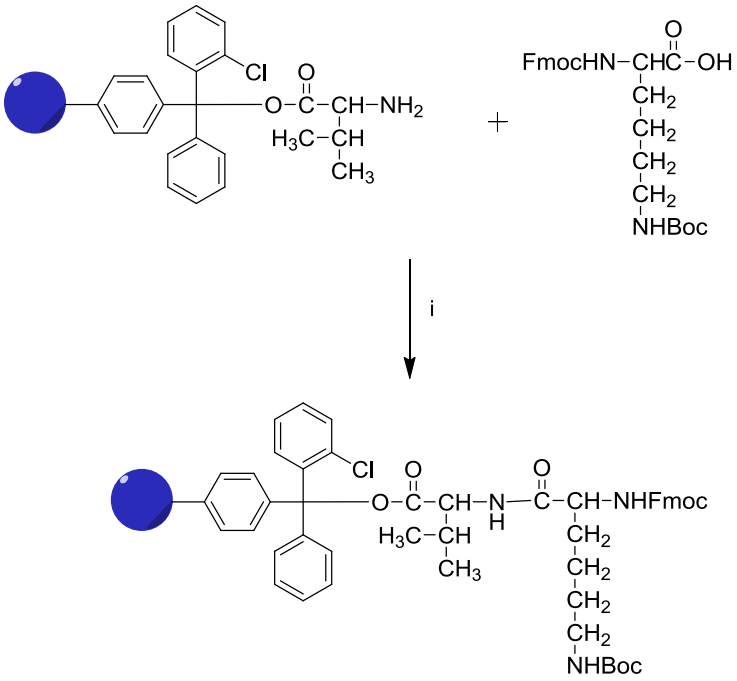

Scheme 3.6 Coupling of the second amino acid. Reagents and conditions: i) TBTU, HOBt, DIPEA, DMF, 1.5 h, rt

One of the main challenges in peptide synthesis is complete characterisation of the peptide intermediate at each step. This is made difficult due to the large number of signals which would appear at the same ppm range in NMR spectra, for example the amide groups connecting each amino acid. The technique used to monitor the presence of the desired peptide intermediates was mass spectrometry (MS). The samples were prepared for analysis by collecting a small amount of the resin bound peptide, and cleaving the peptide from the resin with a 1 % solution of TFA in DCM. This cleavage was first attempted using an aqueous solution of TFA, but was unsuccessful. Water did not encourage swelling of the CTC resin, therefore preventing cleavage of the peptide.

After introduction of the last AA (*N*-Fmoc-Asparagine-(*N*-Tr)-OH), the peptide was subjected to *N*-Fmoc removal, in the presence of piperidine, followed by acetylation of the free amine using Ac_2O, in the presence of DIPEA. Cleavage from the resin was carried out using a 50 % solution (v/v) of TFA in DCM. These conditions also ensured removal of the corresponding side-chain protecting groups. When a more dilute solution of TFA was used, complete removal of the acid-labile side chain protecting groups was not achieved. The synthesis of the desired, deprotected decapeptide **3.6** was confirmed by MS analysis (Calculated for $C_{43}H_{78}N_{13}O_{16}$ (M +

H)$^+$: 1032.5684, found 1032.5662). Purification of peptide **3.6** was carried out using preparative HPLC, with a gradient elution, using H_2O with 0.1 % formic acid, and MeCN with 0.1 % formic acid as the mobile phase. The detector available for our instrument was a UV detector, which made the HPLC analysis difficult due to the lack of a strong UV active group in the peptide. None of the constituent AAs of **3.6** have aromatic groups as their side chains, and so the intensity of the peaks in the chromatogram was rather weak, especially when compared to the background absorption of the mobile phase. The wavelength of maximum absorption for the peptide bond is 190 nm, but measurements are not carried out at this value due to the low output of conventional spectrometers at this wavelength. The side chains of some AA absorb at 205 nm, for example Trp, His, and Cys, but none of these AAs are contained in our peptide sequence.[181] At higher wavelengths the amide bonds should be mildly UV active, and so the analysis was carried out at 214 nm.[182] Fractions were manually collected at 1.5 minute intervals based on the run time, and analysed by MS to determine the fraction which contained the desired product. The time which it would take for the mobile phase to travel from the detector to the collection vessel was estimated at about 50 secs, based on the length and diameter of the tubing. Compound **3.6** was detected in two fractions, 6.5-8 mins, and 8-9.5 mins of run time. These fractions were concentrated, and the material obtained was re-dissolved in H_2O with 0.1 % formic acid. Further HPLC analysis was investigated under several different conditions. Using the gradient elution conditions used previously for purification, a stable baseline was unobtainable. MeCN is UV active at 214 nm also, and so there was a constant shift in the baseline as the concentration of MeCN changed. An isocratic system was also investigated, with a mobile phase of MeOH:H_2O, at various concentrations of MeOH. Unfortunately, due to the lack of a strong chromophore in peptide **3.6**, a UV trace could not be attained to show the time at which the peptide eluted from the column. As mentioned earlier, the peptide bond should be UV active at 214 nm, but measurements at this value are not generally used in analysis of peptides and proteins, due to the complexity of absorbance at this wavelength. Although, there is no other choice for certain sequences. Also, the absorbance at 214 nm is highly dependent on the conformation of the peptide.[182]

To investigate if the acidic content of the mobile phase was necessary to ensure elution of the peptide through the column, an isocratic system of MeCN with 1 %

formic acid:H_2O with 1 % formic acid, at a range of concentrations, was also used. While a much more stable baseline was achieved with the isocratic systems, it was still difficult to associate a peak in the chromatogram with our peptide. MS detection was the only indication of the presence of the peptides. Shown in Fig. 3.16 are the total ion chromatograph (TIC), extracted ion chromatograph (EIC), and UV trace which were produced when compound **3.6** was detected by MS analysis. The ions corresponding to the peptide **3.6** were found to reach the detector at 6.987 mins. Examination of the ions which reached the detector between 7.6-8.9 mins also shows the presence of the desired peptide, in which the deprotection of the AA side chains has not gone to completion. This peptide still has one *t*-butyl group attached ($(M + H)^+$: 1088.6357, and $(M + 2H)^{2+}$: 544.8218).

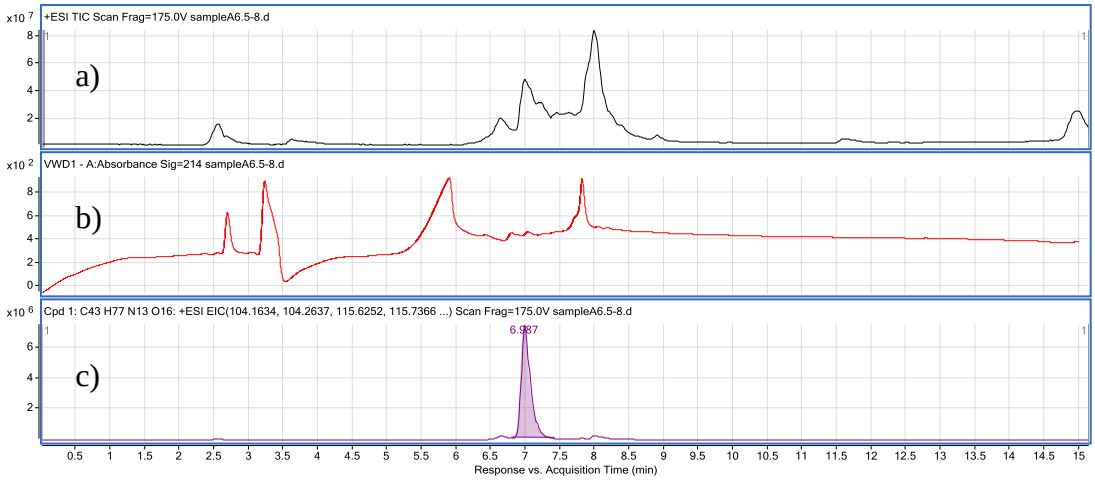

Figure 3.16 a) TIC, b) UV trace, and c) EIC obtained from MS analysis of decapeptide 3.6

*3.10.2 Synthesis of a Library of Glycopeptides, **3.8**, **3.9** and **3.10***

Glycosylation in a specific amino acid in a protein has been shown to affect the glycosylation/phosphorylation at other sites.[18] In order to investigate the effect of glycosylation at a specific site in the desired peptide sequence, glycosylation was carried out on the first serine of the sequence, the second serine of the sequence, or on both. Introduction of *N*-acetyl glucosamine into the peptide sequence was carried out using the SPPS procedures optimised for the decapeptide **3.6**.

The glycopeptide, **3.8**, is glycosylated at the first serine of the sequence (Fig. 3.17). Some discussions in the literature indicate that piperidine may be too basic to use for *N*-Fmoc removal in glycopeptide synthesis, with a weak base like morpholine being

used instead.[183] Others disagree with this theory, and careful use of piperidine was not found to cause β-elimination.[184] Piperidine was used in the first two deprotection steps. Introduction of the glycosylated serine building block **3.5** was carried out using the standard coupling conditions of TBTU/HOBt in the presence of DIPEA, described earlier (Scheme 3.6). The Kaiser test was carried out after 1.5 h, the time allowed for standard peptide couplings, and this indicated that the reaction had not progressed to completion. For all couplings involving a glycosylated AA the reaction was left overnight, and was judged to be complete by the Kaiser test. *N*-Methyl morpholine (*N*-MM) was used to remove the *N*-Fmoc group at this stage, but the reaction was not successful, with failure being indicated by the Kaiser test. The deprotection was then carried out successfully, with careful monitoring of the reaction time, using piperidine. No elimination of the sugar moiety was observed. Subsequent couplings of the remaining AAs led to the synthesis of the complete glycopeptide. The finished glycopeptide was subjected to *N*-Fmoc removal, in the presence of piperidine, followed by acetylation of the free amine using Ac_2O, in the presence of DIPEA. Cleavage from the resin was carried out using a 50 % solution (v/v) of TFA in DCM, as optimised for compound **3.6**, resulting in glycopeptide **3.8** (Fig. 3.17). Purification of crude compound **3.8** was carried out using preparative HPLC. The same type of complications as described earlier for the purification of compound **3.6**, were also encountered for **3.8**. The sugar moiety of the glycopeptide is *O*-acetyl protected, and these groups are not UV active. Neither are the side chains of the other AAs in the sequence of glycopeptide **3.8**. Purification was carried out by manually collecting fractions at 1 minute intervals based on the run time, and analysed by MS to determine the fraction which contained the desired product. The glycopeptide was found in fractions collected at both 6-7 mins, and 7-8 mins of run time. The presence of glycopeptide **3.8** was confirmed by MS (Calculated for $C_{57}H_{98}N_{14}O_{24}$ $(M + 2H)^{+2}$: 681.8448, found 681.8432). The fractions containing the desired product were concentrated, and re-dissolved in MeCN with 1 % TFA. It is interesting to note the difference in physicochemical properties, such as solubility, which were conferred on the peptide by the presence of the sugar moiety. Further HPLC analysis was investigated under each of the elution conditions outlined previously for **3.6**. As mentioned earlier, glycopeptide **3.8** does not contain a strong chromophore, and a UV trace showing the time at which the peptide eluted from the column was not obtained. The TIC, EIC and UV trace obtained by LC-MS analysis

of compound **3.8** are shown in Fig. 3.18. From the EIC, it can be seen that **3.8** reached the MS detector at 7.895 mins. Further analysis of the other ions which reached the detector, as observed in the TIC, show the presence of the desired glycopeptide, in which one acetyl group has been removed ((M + 2H)$^{2+}$: 660.3405).

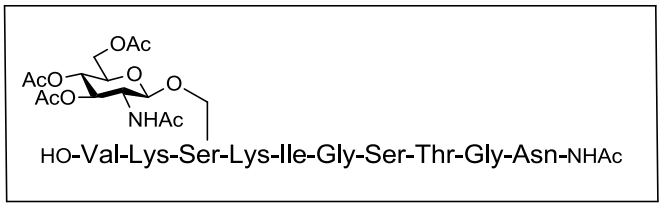

Figure 3.17 The sequence of glycopeptide 3.8

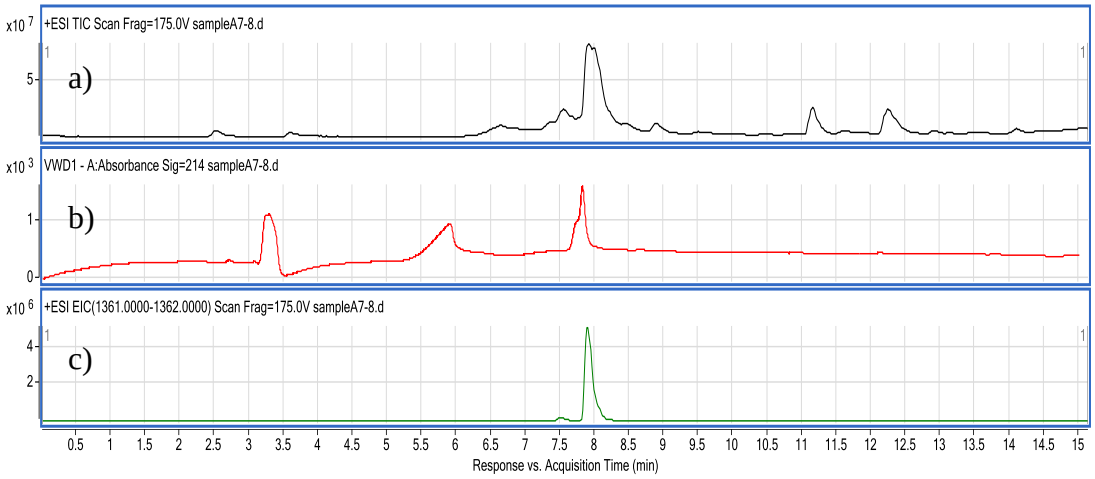

Figure 3.18 a) TIC, b) UV trace, and c) EIC from MS analysis of the purified glycopeptide 3.8

Glycopeptide **3.9** was also synthesised according to the SPPS procedure outlined above. This glycopeptide differs from compound **3.8** in that it is glycosylated on the second serine of the sequence (Fig. 3.19). As for all of the peptides which were synthesised, MS analysis was carried out to confirm the synthesis of the complete, Fmoc protected, sequence, before Fmoc removal. A portion of the resin bound glycopeptide was treated with a 1 % solution of TFA in DCM (v/v). Both *t*-butyl protecting groups, of the Ser and Thr residues, were removed in the resin cleavage stage, while the trityl group on the Asn residue remained attached (MS-ESI/TOF: Calculated for $C_{99}H_{142}N_{16}O_{29}$ (M + 2(NH_4))$^{+2}$: 1010.0074 , found 1010.0096). The peak in the EIC shows compound **3.9** reaching the MS detector at 12.012 mins. Resin-bound glycopeptide **3.9** was subjected to *N*-Fmoc removal, in the presence of piperidine, followed by acetylation of the free amine using Ac_2O, in the presence of

DIPEA. Cleavage from the resin was carried out using a 50 % solution (v/v) of TFA in DCM, as optimised for peptide **3.6**. However, the NHAc protected glycopeptide could not be confirmed by MS, and any partially side-chain deprotected derivatives were also not detected.

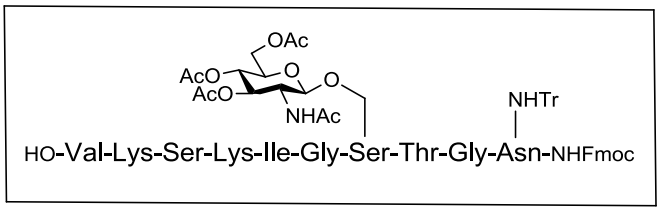

Figure 3.19 The sequence of glycopeptide 3.9

Glycopeptide **3.10** was synthesised according to the procedures outlined above. This glycopeptide is glycosylated on both of the serine moieties in the sequence (Fig. 3.20). The finished glycopeptide was subjected to *N*-Fmoc removal, in the presence of piperidine, followed by acetylation of the free amine using Ac_2O, in the presence of DIPEA. Cleavage from the resin was carried out using a 50 % solution (v/v) of TFA in DCM, resulting in compound **3.10** (Fig. 3.20). Purification of crude **3.10** was carried out using preparative HPLC. The same type of complications as described earlier for the purification of compounds **3.6** and **3.8**, were also encountered for **3.10**. Purification was carried out by manually collecting fractions at 1 minute intervals based on the run time, and analysed by MS to determine the fraction which contained the desired product. The glycopeptide was found in the fractions collected at 7-8 mins, and 8-9 mins of run time. The presence of glycopeptide **3.10** was confirmed by MS (Calculated for $C_{71}H_{117}N_{15}O_{32}$ $(M + 2H)^{+2}$: 846.4004, found 846.3983). The fractions containing the desired product were concentrated, and re-dissolved in MeCN with 1 % TFA. Further HPLC analysis was investigated under each of the elution conditions outlined previously for compound **3.6**. As mentioned earlier, glycopeptide **3.10** does not contain a strong chromophore, and a UV trace showing the time at which the peptide eluted from the column was not obtained. The TIC, EIC and UV trace obtained by LCMS of glycopeptide **3.10** are shown in Fig. 3.21. From the EIC, it can be seen that compound **3.10** reached the MS detector at 7.990 mins. Another major ion which was observed in the TIC of the glycopeptide has a mass of 1596, which corresponds to M - 93 of the desired glycopeptide. The ion with a mass of 798 corresponds to the $(M + 2H)^{2+}$ of this peak. This mass did not

correspond to any obvious incomplete side chain deprotection, or any deletion sequence, and could not be assigned.

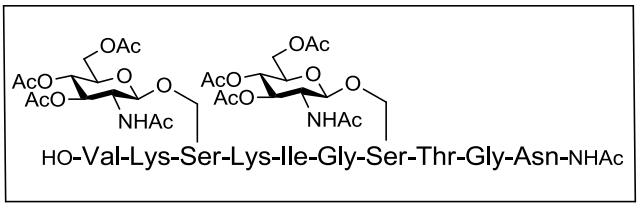

Figure 3.20 The sequence of glycopeptide 3.10

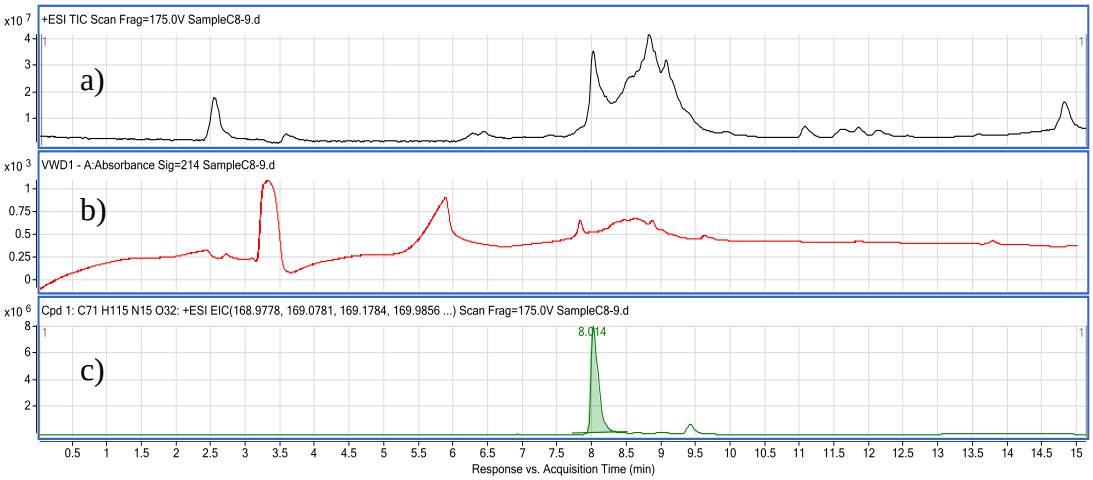

Figure 3.21 a) TIC, b) UV trace, and c) EIC from MS analysis of the purified glycopeptide 3.10

Although we initially envisaged hydrolysis of the *O*-acetyl groups in the sugar moiety of glycopeptides **3.8**-**3.10**, the problems encountered throughout purification limited considerably the amount of material available for further reactions. We did not have enough material to investigate the conditions for the deprotection of the alcohol groups, but it is envisaged that a mild strategy, with careful monitoring of pH, would be required. Nevertheless, acetylated sugars have shown increased absorption through biological membranes, when compared with their deprotected analogues.[185] The acetyl groups on the sugar can then be easily hydrolysed by esterase enzymes inside the cell. Since peptides are naturally rather hydrophilic, the presence of the protected sugar may increase the lipophilicity of these derivatives. This would be a desirable feature for potential drug candidates.

For future work, it would be advisable to carry out deprotection of the alcohol groups, in order to compare the activity of the deprotected sugar with the acetylated derivative.

3.11 Chapter Conclusion

In conclusion, the synthesis of four decapeptides was achieved, including three glycopeptides. The side chains of three of these peptides were deprotected, and the peptides were purified by preparative HPLC analysis. A major problem encountered during this work was the lack of a strong chromophore in any of the peptides, which made the purification difficult. Considering this issue, the peptides were found to be relatively pure by MS analysis. Another difficulty was the small amount of sample which was obtained after cleavage from the resin, preventing further deprotection of the *O*-acetyl groups. If a larger quantity of the peptides had been obtained, it would have been desirable to test these compounds for their affinity for the GSK-3 kinase. Future work could aim to improve the yields of these syntheses, and to send the peptides for biological evaluation.

Further work on this type of glycopeptide should incorporate an AA, for example Tyr, which has a side chain that absorbs strongly in the UV region. Another option is to cleave the peptide from the resin while the Fmoc group is still present, as this is also strongly UV active.

I would also encourage the incorporation of a Pro residue into the glycopeptide, as it is known that GSK-3 is a Pro directed kinase. This may increase the binding affinity of GSK-3 for the peptide.

Chapter 4: Functionalisation at the C-6 Position of Glucosamine-Containing Building Blocks

4.1 Aim

Carbohydrates provide a useful scaffold for the introduction of a variety of different functionalities.[186] The synthesis of such derivatives is complicated by the lack of orthogonality presented by several hydroxyl groups, which possess similar reactivity. At the same time, these groups may allow selective functionalisation at different positions.

The addition of an aromatic group, or a phosphate moiety to the carbohydrate part of the molecule may alter binding interactions between a glycopeptide and its target. This type of derivative may modulate the affinity of the glycopeptide for a kinase, like GSK-3, which was discussed in chapter 3. Also mentioned previously, was the work carried out by Licht-Murava *et al*, indicating the need for a phosphate group in their peptide to illicit an inhibitory effect on GSK-3.[171] For these reasons, the introduction of such a functionalisation into a glucosamine-based derivative was attractive.

Extensive investigation was carried out into conditions for the functionalisation of different sugar moieties at the C-6 position. This was of interest as it was desirable to synthesise an azide containing building block, which could be incorporated into a glycopeptide (Fig 4.1).

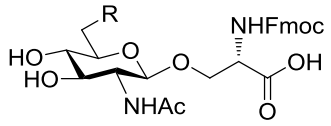

4.26: R = N_3
4.27: R = $OC(O)C_2H_4N_3$

Figure 4.1 Proposed azide functionalised building blocks

Another useful purpose for a glycosyl building block which has been functionalised with an azide group has been exploited by Bertozzi and co-workers. Biological molecules, such as proteins, can be modified experimentally by techniques like

genetics and biosynthesis. In the case of glycans, these methods are often not applicable, as they don't have the genetic template and enzymatic activities which are associated with proteins. Work carried out by Bertozzi and co-workers has utilised bioorthogonal chemistry to incorporate non-natural molecules into living systems, without interfering with the biological functioning of the cell. Azide containing sugars, such as *N*-azidoacetyl mannosamine, were introduced into glycans by treating cells with the azide functionalised derivative of this natural sugar. These were used as tags for visualisation, before flow cytometric analysis was carried out on the cells.[187] Later work by this group has shown the incorporation of *N*-azidoacetyl galactosamine and *N*-azidoacetyl glucosamine into glycoproteins, which allowed identification of proteins that had become *O*-GlcNAcylated. This detection is not an easy task, as discussed in chapter 1, due to the small amount and neutral charge of *O*-GlcNAc in these glycoproteins.[188]

4.2 Functionalisation at the C-6 Position of the Sugar Moiety

*4.2.1 Differential Protection of the C-6 Position of Glycosyl Derivatives **4.1** and **4.7***

Initial attempts to selectively functionalise the hydroxy group at the C-6 position focused on the *N*-Troc protected glucosamine, **4.1**. The first stage in this synthesis involved differentially protecting the C-6 hydroxyl with a group which was orthogonal to the other hydroxyl protecting groups (*O*-acetyl), and also to the *N*-Troc group. A sterically hindered protecting group, such as triphenyl methyl (trityl) ether, or *tert*-butyl dimethylsilyl (TBDMS) ether, would be ideal for this purpose (Scheme 4.1). The trityl group is removed under acidic conditions, which would make it easily deprotected in the presence of the other functionalities. The TBDMS group can be deprotected using strongly acidic conditions, but a more attractive method is using fluoride ions (for example, from TBAF), which would also be compatible with the glycosylated *N*-Fmoc serine benzyl ester **3.4**.

The different reaction conditions investigated in our attempts to directly functionalise **4.1** at the C-6 position are outlined in Table 4.1.

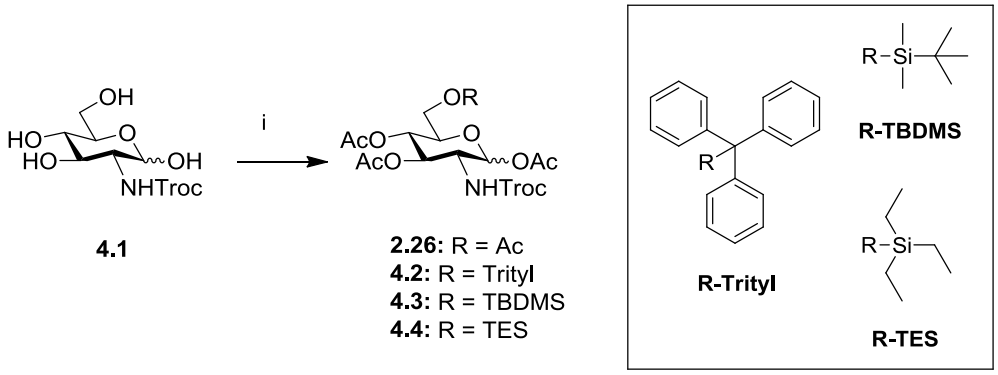

Scheme 4.1 Introduction of an orthogonal group at C-6. Reagents and conditions: i) Listed in Table 4.1

Entry	Reagents	Conditions	Outcome
1	i) TrCl, Et_3N, pyr ii)Ac_2O	i) 4 h, 70 °C, N_2, TrCl (1.2 eq) ii) overnight, rt	Synthesis of **2.26** 5 % yield of **4.2**
2	i) TrCl, DMAP, pyr ii)Ac_2O	i) 3 h, 70 °C, N_2, TrCl (1.2 eq) ii) overnight, rt	Synthesis of **2.26**
3	i) TrCl, DMAP, pyr ii)Ac_2O	i) overnight, 60 °C, N_2, TrCl (1.2 eq) ii) overnight, rt	Synthesis of **2.26**
4*	i) TrCl, Et_3N, pyr ii)TrocCl iii)Ac_2O	i) 3 h, 80 °C, N_2, TrCl (1.2 eq) ii) 2.5 h, rt iii) overnight, rt	Synthesis of **2.26**
5	i) TBDMSCl, imidazole, pyr ii) Ac_2O, pyr	i) overnight, rt, TBDMSCl (1.2 eq) ii) overnight, rt	26 % yield of **4.3** **2.26** produced
6	i) TESCl, Et_3N, pyr ii)Ac_2O	i) 0 °C add base → rt, 4 h, TESCl (1.2 eq) ii) overnight, rt	None recovered
7	i) TrCl, Et_3N, pyr ii) AcCl	i) 3 h, 95 °C, TrCl (5 eq) ii) overnight, 0 °C → rt	39 % yield of **4.2**

Table 4.1 Various reaction conditions for the functionalisation of the C-6 position of 4.1 (*: note that this entry is based on D-glucosamine HCl as the starting material)

For each of these entries, the intermediate compounds were not isolated, as it was desired to carry out a one-pot reaction to achieve the selectively protected product. The progression of the reaction was noted by TLC in each case. For entries **1**-**3** and **5-7** the glycoside **4.1** was obtained from glucosamine hydrochloride, by protection of the amine with TrocCl, in the presence of $NaHCO_3$. Entry **1** details protection of the primary hydroxyl of **4.1** as a trityl ether, using Et_3N as the base. This was followed by acetylation, using Ac_2O. Almost quantitative yield of **2.26** (the per-*O*-acetylated product) resulted, with only a 5 % yield of the desired product **4.2**. Entries **2** and **3** show this reaction carried out in the presence of DMAP, but in this case, there was full conversion to **2.26**. In entry **4** a different reaction sequence was investigated, with protection of the C-6 as the trityl ether, in the presence of Et_3N, followed by protection of the amine using TrocCl, and acetylation of the remaining hydroxy groups. This was carried out to check if the *N*-Troc group was interfering with the reaction, as we had earlier observed the difficulty in removal of the *N*-Cbz group in the presence of *N*-Troc, as discussed in chapter 2. Again there was full conversion to **2.26**. It was postulated that perhaps some acid which was present in the acetylation stage of these reactions may have been able to cleave the trityl group, if it had been attached (Table 4.1). There may also have been some H_2O remaining from the previous reaction, even with careful drying of the starting material.

The TBDMS group is stable in acidic conditions. Entry **5** gives the details of protection using TBDMSCl to form the TBDMS ether, in the presence of imidazole, followed by acetylation of the hydroxy groups. This reaction resulted in a 26 % yield of the desired product, **4.3**, and also formation of **2.26** (Table 4.1). When this selectively protected derivative was treated with dimethylamine in an attempt to form the anomeric hemiacetal, no reaction occurred. This reaction was also carried out in the presence of benzylamine. A change was noted by TLC analysis, but the desired product was not isolated, and instead degradation seemed to have occurred.

As these reactions did not proceed in good yield, it was thought that perhaps the trityl and TBDMS groups were too bulky for introduction into the sugar. Entry **6** shows the reaction carried out using triethyl silyl (TES) chloride, in the presence of Et_3N. This silyl ether is less bulky than TBDMS, although it is removed under acidic conditions, similar to trityl ethers. The reaction did not proceed, with no recovery of a glycosidic product (Table 4.1).

On consideration of the by-products of acetylation with acetic anhydride which were observed for entries **1**-**4**, it was postulated that the acetic acid produced in the reaction may have facilitated cleavage of the trityl group. In order to investigate this, the reaction was carried out in the presence of an excess of TrCl (5 eq), followed by acetylation with acetyl chloride as the acetylating agent (entry **7**, Table 4.1 and Scheme 4.2).

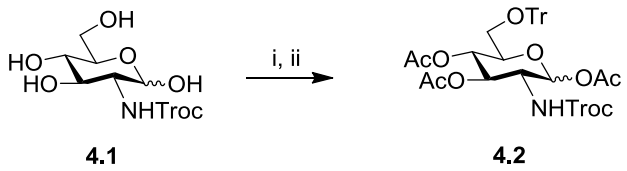

4.1 **4.2**

Scheme 4.2 Acetylation carried out using AcCl. Reagents and conditions: i) TrCl, Et_3N, Pyr, 95 °C, 3 h; ii) AcCl, 0 °C → rt, overnight, 39 %

The reaction was slightly more successful, producing **4.2** in a yield of 39 %, but this was still too low for such an early step in the synthetic scheme, and later attempts at the same reaction did not show good reproducibility. It was decided not to continue with this route, as the trityl group would most likely not withstand the acidic conditions in the later steps of the synthesis, such as the Lewis acid required for glycosylation.

There are very few examples of functionalisation at the C-6 position of glucosamine derivatives, of which the anomeric position is a free hydroxy group, in the literature. In some cases the C-1 position has been protected, and for this reason the glucosamine derivative **4.7** was synthesised, according to literature procedures.[189]

2.26 was prepared as discussed in chapter 2, and was treated with a solution of HBr in acetic acid to form the glycosyl bromide **4.5**. Interestingly, the presence of the *N*-Troc group prevented the formation of an oxazoline-type compound, as was observed earlier, with the *N*-acetyl derivative, **2.32**, this is in agreement with the literature.[190] The glycosyl bromide was activated using $AgCO_3$, and reacted with the glycosyl acceptor, benzyl alcohol, to give **4.6**. The acetyl groups of this glycoside were deprotected, in the presence of 0.1 M aqueous NaOH and MeOH, resulting in the benzyl glycoside, **4.7 (**Scheme 4.3).

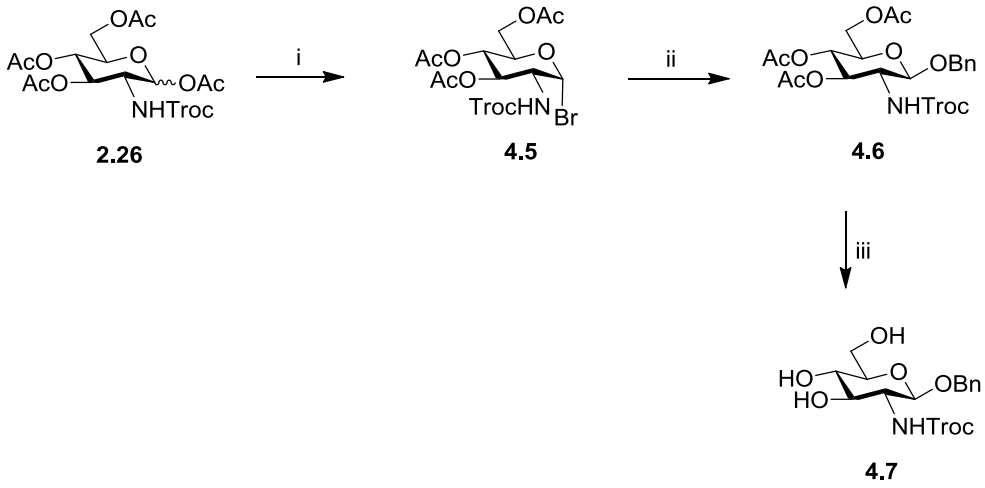

Scheme 4.3 Synthesis of glycosyl derivative 4.7. Reagents and conditions: i) 33 % HBr/AcOH solution, DCM, 3.5 h, 0 °C → rt; ii) $AgCO_3$, DCM, BnOH, overnight, rt, 57 % over 2 steps; iii) 0.1 M $NaOH_{aq}$, MeOH, 1 h, rt, 73 %

The various conditions investigated for functionalisation of the C-6 position of **4.7** are described below in Table 4.2.

Entry	Reagents	Conditions
1	i) TBDMSCl, imidazole, pyr, mol. sieves. ii)Ac_2O	i) rt, 2 days, N_2, TBDMSCl (1.4 eq) ii) overnight, rt
2	i) TMSCl, Et_3N, THF ii)Ac_2O, pyr	i) overnight, rt TMSCl (1.2 eq) ii) overnight, rt
3	i) TESCl, imidazole, DMF ii)Ac_2O, pyr	i) overnight, rt, TESCl (1.2 eq) ii) overnight, rt
4	i) TESCl, imidazole, DMF ii)Ac_2O, pyr	i) overnight, 30 °C, TESCl (1.2 eq), followed by TESCl (2 eq) and imidazole (2 eq) overnight ii) overnight, rt
5	i) FmocCl, pyr ii)Ac_2O	i) N_2, 2 h, 0 °C → rt, 4 h, FmocCl (1.5 eq), followed by FmocCl (1 eq) overnight ii) overnight, rt
6	i) MOMBr, K_2CO_3, acetone ii)Ac_2O, pyr	i) 55 °C overnight, MOMBr (1.5 eq), ii) overnight, rt

Table 4.2 Various conditions for functionalisation of 4.7

Entry **1** shows the reaction of **4.7** with TBDMSCl, in the presence of imidazole and molecular sieves. The desired reaction did not proceed, and none of the acetylated product, **4.6**, was recovered. Several products resulted from this reaction, and on closer examination we were able to isolate and identify one of them as **4.8** (Fig 4.2). This acetylated pyridine derivative is produced by the addition of acetic anhydride to pyridine, and has been reported in the literature.[191] MS analysis confirmed the presence of this unexpected side-product.

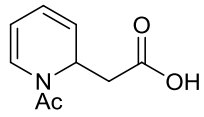

4.8

Figure 4.2 Side-product 4.8

Protection of the C-6 position as a TMS ether was investigated in entry **2**, which was carried out using TMSCl in the presence of Et_3N, followed by acetylation using Ac_2O. This reaction was unsuccessful, but none of the acetylated product **4.6** was recovered either. Entries **3** and **4** detail the reaction to protect the C-6 as a triethyl silyl (TES) ether, which has been shown to be more stable to acid hydrolysis then the TMS ether. The first attempt carried out at rt overnight, and the second was carried out at 30 °C, under a N_2 atmosphere, with further equivalents of TESCl being added in an attempt to push the reaction. Both reaction mixtures were then subjected to acetylation, using Ac_2O. Under both conditions the reaction was unsuccessful, and no recovery of acetylated product was obtained (Table 4.2). The starting material **4.7** is water soluble, and so may have been lost during the work-up.

Some alternative alcohol protecting groups were also investigated. Fmoc protection of alcohols has been successfully utilised in the literature.[192] Entry **5** details the protection of the C-6 position as an Fmoc carbonate. This was carried out using FmocCl, in the presence of pyridine. The desired product was not obtained, but again, the acetylated pyridine side-product, **4.8** was observed. Protection of alcohols as methoxy-methyl (MOM) ethers has been described in the literature.[193] Entry **6** shows this protection which was carried out using MOMBr, in the presence of K_2CO_3, followed by acetylation using Ac_2O. No sugar derivative was isolated after the reaction (Table 4.2).

As will be discussed in chapter 5 in more detail, the deprotected sugar **4.7**, obtained as described in Scheme 4.3, seemed to be unreactive, even with excess amounts of reagents. It is thought that H_2O or hydroxide salts remained from the previous deprotection step, and interfered with the introduction of protecting groups.

4.3 Differential Protection of the C-6 Position of 3.4

The various conditions investigated above for functionalisation of the glycosyl derivatives failed to deliver the desired products. The reactions which produced the desired product were not reproducible, and the yields were very low. The presence of a sterically large group at the C-6 position may compromise the glycosylation step, and also there are several additional synthetic steps, in which the compatibility of the C-6 protecting group would have to be accounted for, in order to reach the desired building block. Optimisation of these reactions would not guarantee that the same conditions would work on the glycosylated serine building block **3.4**. For these reasons it was decided to continue the rest of the investigations on the *N*-Fmoc protected building block **3.4**. Direct functionalisation at the C-6 position of **3.4** was investigated. This strategy is more challenging, as there are several other protecting groups present in the molecule which need to be considered, for example, the base labile *N*-Fmoc group.

*4.3.1 Optimisation of Deprotection Conditions of **3.4***

Selective *O*-deacetylation of **3.4** was attempted under mild conditions of MeOH/H_2O/Et_3N, followed by reaction with TrCl in the presence of DMAP, followed by acetylation with Ac_2O. This reaction was not successful, with no identifiable products isolated. The deprotection was also investigated with slightly harsher conditions of 0.1 M NaOH in MeOH, followed by protection with TBDMSCl in the presence of imidazole, and acetylation using Ac_2O (Scheme 4.4). This reaction did not proceed either, with recovery of some of the acetylated starting material, and again the appearance of the acetylated pyridine side-product **4.8**. This compound has been identified in several of these attempted functionalisation reactions, even with different protecting groups and sugar derivatives. Perhaps this is a reason why, often, even the acetylated product was not isolated.

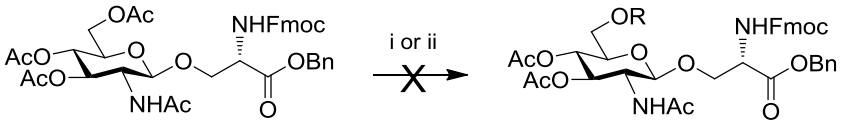

3.4

4.9: R = Trityl
4.10: R = TBDMS

Scheme 4.4 Attempted functionalisation of the C-6 position. Reagents and conditions: i) a) MeOH/H_2O/Et_3N 40 °C, overnight; b) TrCl, DMAP, pyr, rt overnight; c) Ac_2O, rt, overnight; ii) a) 0.1 M NaOH, MeOH, 1 h, rt; b) TBDMSCl, imidazole, pyr, rt, overnight; c) Ac_2O, rt, overnight

It was unclear if the initial deprotection had been carried out, or if the sterically hindered protecting groups could not be incorporated into the glycosylated serine. It was postulated that the problems encountered with the introduction of trityl or TBDMS protection into the C-6 position of **3.4** may have been due to a failure to deprotect the *O*-acetyl groups, without degradation of the glycoside. On review of the results obtained, it was decided to try to isolate the deprotected glycoside to ensure that deprotection of the *O*-acetyl groups was being achieved.

O-Deacetylation of **3.4** was investigated under various different conditions outlined in Tables 4.3 and 4.4 below (Scheme 4.5). A more attractive synthesis would involve selective deprotection of the primary acetyl only (**4.11**), and several methods were also investigated in an attempt to achieve this.

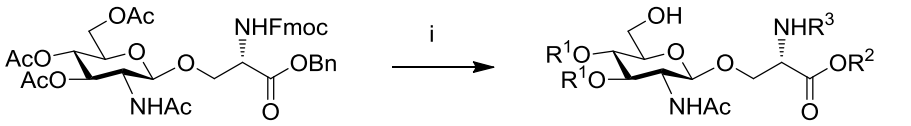

3.4

4.11: R^1 = Ac, R^2 = Bn, R^3 = Fmoc
4.12: R^1 = H, R^2 = Bn, R^3 = Fmoc
4.13: R^1 = H, R^2 = H, R^3 = Fmoc
4.14: R^1 = H, R^2 = Bn, R^3 = H
4.15: R^1 = H, R^2 = H, R^3 = H

Scheme 4.5 Deprotection of 3.4. Reagents and conditions: i) As outlined in Tables 4.3 and 4.4

4.3.2 Enzymatic Deacetylation Methods

Enzymatic methods of deacetylation have shown great success in the literature, and display selective deprotection in the presence of other groups with similar chemical reactivity.[194] The family of enzymes which has demonstrated selectivity for the removal of acetyl groups from sugar derivatives are known as lipases. There are many different kinds of lipase, depending on where they have been isolated from. As

with all enzymes, the catalytic ability of lipases is very dependent upon the structure of the substrate, and, normally, a panel of lipases are tested. A representative sample of two lipases was chosen for this investigation. The enzymes which we used are *Candida antarctica* lipase (CAL B), which is immobilised on a solid support, making purification easier, and *Candida rugosa* lipase (CRL), which is not immobilised. These lipases were selected as they have both shown selective deacetylation of primary acetyls in carbohydrate substrates.[194-196] The desired product of these enzymatic deacetylations is **4.11**, where only the primary acetyl has been deprotected. Table 4.3 shows the enzymatic deacetylation conditions which we investigated.

Entry	Enzyme	Conditions
1	CAL B	THF, n-butanol, 20 →50 °C, 2 days
2	CAL B	Ethanol, n-butanol, 20 →50 °C, 2 days
3	CAL B	Ethanol, PBS (tablet), pH 7, 20 →50 °C, 2 days
4	CAL B	THF, PBS (tablet), pH 7, 20 →50 °C, 2 days
5	CAL B	ACN, phosphate buffer, pH 4.5, 25 °C days → 45 °C 2 days
6	CAL B	Ethanol, phosphate buffer, pH 4.5, 37 °C, overnight
7	CRL	ACN, phosphate buffer, pH 4.5, 25 °C days → 45 °C 2 days
8	CRL	Ethanol, phosphate buffer, pH 4.5, 37 °C, overnight

Table 4.3 Investigation of enzymatic deacetylation

Entries **1** and **2** detail the reaction carried out using *Candida antarctica* lipase, in THF and ethanol, respectively, with the addition of n-butanol. Work carried out by Singh *et al* demonstrated the selective deacetylation of a primary acetyl in the presence of a secondary one under these conditions. The reactions were carried out on nucleosides, and n-butanol is added as an acetyl acceptor.[197] Enzymatic activity is closely related to temperature in many cases, and so a temperature range of 20-50 °C was used. Full recovery of starting material, **3.4**, was achieved. Enzymatic reactions can also be effected by the pH of the environment,[198] and so these reactions were repeated using phosphate buffered saline (PBS), which was made up from a tablet to a specific volume, and was pH 7. The conditions are shown in entries **3** and **4**. The reaction did not proceed, with full recovery of starting material. As pH

plays such an important role in enzymatic reactions, more carefully monitored reactions were carried out, using a freshly made up phosphate buffer, pH adjusted to 4.5. Entries **5** and **6** show these reaction conditions using CAL B, in ACN and ethanol, respectively. The reaction was unsuccessful, with full recovery of starting material. This lipase did not appear to be selective for glycosyl derivative **3.4**, and another lipase, *Candida rugosa* lipase, was investigated. Entries **7** and **8** detail the use of this enzyme, in ACN and ethanol, respectively, over a range of temperatures. This lipase did not show activity with our sugar, and resulted in full recovery of starting material, **3.4**. Neither of the two lipases tested showed specificity for **3.4** (Table 4.3).

4.3.3 Chemical Deacetylation Methods

As the enzymatic methods were unsuccessful, some chemical deacetylation conditions were investigated. Deprotection of **3.4** was carried out using MeOH/Et_3N/H_2O at 40 °C overnight. Examination of the ^1H NMR data did not yield a clear conclusion as to the results of this reaction. TMS-protection of all of the hydroxy groups was attempted from this crude product, but this was not successful, with the NMR data indicating that some kind of degradation had occurred (Scheme 4.6). This degradation had, most likely, occurred at the deacetylation stage, with removal of the base sensitive *N*-Fmoc group.

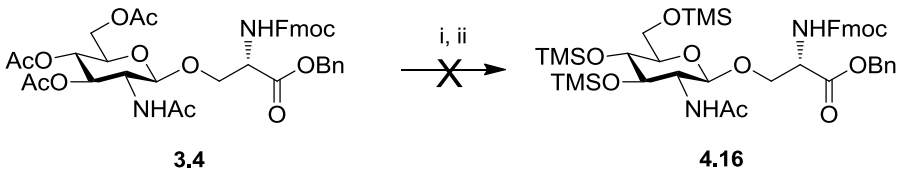

3.4 **4.16**

Scheme 4.6 Attempted deacetylation of 3.4 under mild conditions. Reagents and conditions: i) MeOH/Et_3N/H_2O, 40 °C, overnight; ii) TMSCl, pyr, DIPEA, overnight, rt

In the literature many different methods of chemical deacetylation have been described.[198] Several of these strategies were investigated in the hydrolysis of the acetyl groups of glycoside **3.4**, and these are described in Table 4.4. The structures of the various reaction products have been depicted earlier, in Scheme 4.5.

Entry	Reagents	Conditions	Outcome
1	DIPEA/H_2O/MeOH	Overnight, rt	**4.14**
2	KCN, MeOH	KCN 5 eq, rt, overnight	**4.15**
3	KCN, MeOH	KCN 3 eq, 0 °C, 2 h	Not conclusive from NMR, acetyls still present
4	DBTO, MeOH	DBTO 1 eq, 50 °C, 3 h → rt, overnight → 50 °C, 3 h	Starting material, **3.4**, still present. Presence of **4.13** observed
5	i) Zeolite clay, MeOH, DCM iii) AcCl	i) rt, overnight ii) 50 °C overnight iii) AcCl 0.2 eq	Full recovery of starting material, **3.4**
6	pTsOH, DCM, MeOH	i) pTsOH 1 eq, 3 h, rt ii) pTsOH extra 1 eq, overnight, rt	i) Starting material, **3.4** ii) Starting material, **3.4**. Minor presence of various deacetylation products
7	AcCl, MeOH	i) AcCl 0.1 eq, 3 h, rt ii) AcCl extra 0.1 eq, overnight iii) AcCl extra 0.2 eq, overnight	i) Starting material, **3.4** ii) Starting material, **3.4** iii) Starting material, **3.4**
8	AcCl, MeOH	i) AcCl 0.5 eq, overnight, rt ii) AcCl extra 0.5 eq, overnight, rt	Minor presence of **4.13**. Starting material, **3.4** detected. Various deprotection products observed.
9	AcCl, MeOH	AcCl 5 eq, overnight, rt	**4.13, 4.12**, and various deprotection products observed.

Table 4.4 Various methods investigated for the chemical *O*-deacetylation of 3.4

The basic conditions which have been described previously resulted in a loss of the *N*-Fmoc protecting group, and so alternative strategies were investigated. The *N*-Fmoc group has been demonstrated earlier to be stable to DIPEA, in an overnight reaction during solid phase peptide synthesis. Reaction conditions of DIPEA/MeOH/H_2O were investigated for the *O*-deacetylation of glycoside **3.4** (Entry **1**). *N*-Fmoc deprotection was indicated by a red stain on the TLC in the presence of ninhydrin. The ^{1}H NMR spectrum indicated deprotection of the *O*-acetyl groups, with the benzyl ester protection remaining intact (**4.14**) (Table 4.4).

The use of KCN as a milder method of acetyl hydrolysis has been described.[199] Entries **2** and **3** show the reaction being carried out using KCN and MeOH. The first attempt at this involved 5 eq of KCN, and this appeared to cause hydrolysis of the acetyl groups, and also the benzyl ester and *N*-Fmoc groups. The reaction was repeated at 0 °C, with 3 eq of KCN. The ^{1}H NMR spectrum of this reaction was unclear, but deprotection of the benzyl ester looks to have occurred, indicated by the disappearance of the characteristic aromatic protons at approx. 7.3 ppm, with the Fmoc and acetyl peaks still present (Table 4.4).

Entry **4** shows the conditions for deacetylation using dibutyltin oxide (DBTO). This procedure has been demonstrated in the literature, for deprotection of glucose derivatives.[200] The result of this reaction was partial *O*-deacetylation, and removal of the benzyl ester group. The *N*-Fmoc group remained intact, and some starting material was observed (Table 4.4).

Entry **5** details the use of a zeolite clay for deacetylation. Zeolite is a catalyst which has been used in mild hydrolysis reactions.[201] The type of zeolite which was used in this reaction is called montmorillonite K-10. The reaction was unsuccessful, with full recovery of starting material, glycoside **3.4** (Table 4.4).

Entry **6** details the reaction carried out using *para*-toulenesulfonic acid (pTsOH). The hydrolysis of *O*-acetyl groups by this method has been described in the literature for glucose derivatives.[202] For our sugar, there appeared to be some deprotection, but mainly starting material, glycoside **3.4**, was recovered (Table 4.4).

The cleavage of *O*-acetyl groups of glucosamine derivatives with acetyl chloride (AcCl) and MeOH has been described by Jung *et al*.[203] Entry **7** shows the details of

how this was attempted with our sugar, **3.4**, in the presence of 0.1 eq of AcCl in MeOH. This low equivalence of AcCl was used to investigate if selective deprotection of the primary alcohol could be carried out in the presence of the protected secondary alcohols. The reaction did not proceed after 3 h, and so a further 0.1 eq of AcCl was added, and allowed to stir overnight. No change was observed by TLC, and a further 0.2 eq of AcCl was added (0.4 eq in total). This did not have any effect on the sugar, with the starting material, **3.4**, being recovered in full. On further examination of the literature, it was observed that Yeom *et al* carry out the hydrolysis of *O*-acetyl groups in the presence of benzyl esters, at 0.15 eq of AcCl. In the same work, deacetylation at different positions of glucose and galactose derivatives was carried out, but required a slightly higher equivalence of AcCl, 0.3 eq.[204] Entry **8** details the attempted hydrolysis of the acetyl groups using 0.5 eq of AcCl in MeOH. The reaction was allowed to stir overnight, and TLC analysis indicated partial deprotection had occurred, but still showed the presence of some starting material. An extra 0.5 eq of AcCl was added. This reaction resulted in partial deprotection of the alcohols and removal of the benzyl ester group. In order to investigate if a large excess of AcCl would facilitate deacetylation, 5 eq of AcCl in MeOH was added to the sugar. This is described in entry **9**, which shows that deprotection of the alcohols was successful, leaving the NHAc intact, but also caused the hydrolysis of the benzyl ester protecting group, resulting in what was thought to be glycoside **4.13** (Table 4.4).

4.3.4 Introduction of Azide Functionality at C-6 of Glycosylated Serine Building Block

On review of the above deacetylation reactions, we observed that the selective removal of the acetyl esters, in the presence of the benzyl ester, was difficult to achieve. Therefore, a new scheme was devised. From compound **3.4**, hydrogenolysis of the benzyl ester protecting group was carried out, using Pd/C and H_2, to give the free acid **3.5**, which was earlier used for glycopeptide synthesis. This was carried out to encourage the formation of a single product upon reaction with AcCl, which was the method of deacetylation that had shown the most promising results. The free acid **3.5** was then treated with an excess of AcCl in MeOH. Although, using these conditions, full removal of the *O*-acetyl groups was achieved, the product of this reaction was found to be methyl ester, **4.17**. This product was identified by a distinct

signal in the ^{1}H NMR spectrum which was attributed to the methyl ester CH_3, and confirmed by MS. On review of ^{1}H NMR data from the previous deacetylation reactions involving AcCl, as described in Table 4.4, the mild conditions in entry **8** did not result in formation of the methyl ester. The conditions described in entry **9**, however, did produce the methyl ester **4.17**, among a mixture of products, including the benzyl ester, **4.12**, and the free acid, **4.13**.

Compound **4.17** was then selectively tosylated at the C-6 position of the sugar moiety, by reaction with tosyl chloride at 0 °C, to give glycoside **4.18**. The next stage in the synthesis was the conversion of the tosyl group to an azide functionality, using NaN_3 in DMF (Scheme 4.7). These conditions have been shown in the literature to be compatible with functionalised GlcNAc derivatives.[205, 206] For our sugar, this reaction was not successful, and several degradation products were observed. The main product of this reaction had undergone Fmoc cleavage under these standard reaction conditions, but otherwise still contained the sugar and serine moieties, with the NHAc and OMe groups still intact. Further analysis of this compound by IR revealed an absorbance band at 2101 cm^{-1} which indicated that the azide had indeed replaced the tosyl group.[207] The conditions required to introduce an azide into the C-6 position proved to be too harsh in the presence of the Fmoc protecting group. The Fmoc protection is needed if this building block is to be suitable for introduction into a glycopeptide, using SPPS methodologies.

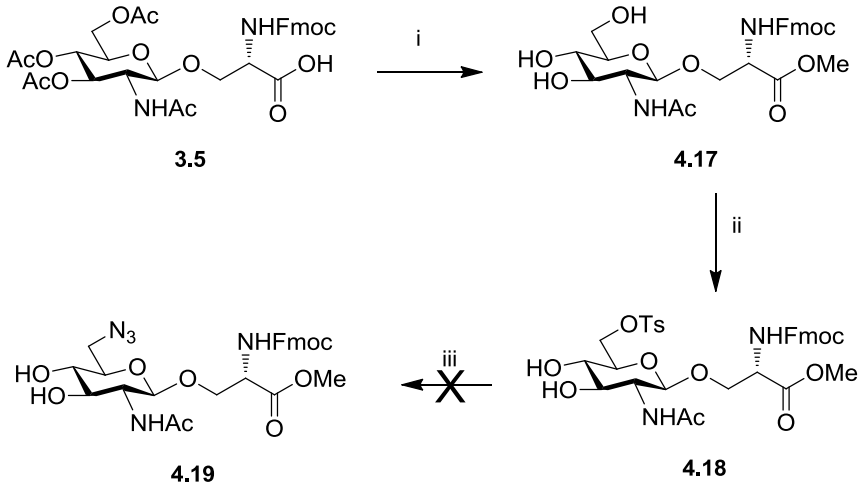

Scheme 4.7 Attempted introduction of an azide functionality at the C-6 position. Reagents and conditions: i) AcCl, MeOH, overnight, rt, 89 %; ii) TsCl, pyr, 0 °C → rt, overnight, 24 %; iii) NaN_3, DMF, 75 °C, 2.5 h

There is precedence of a linker attached azide being incorporated into a peptide molecule for use in biological systems, and so this approach was considered.[208] The linker attached azide used in this synthesis was 3-azido-propionic acid, **4.21**. This was synthesised, following literature procedures, via a substitution reaction from 3-bromopropionic acid, **4.20**, using an excess of NaN_3 (Scheme 4.8).[209]

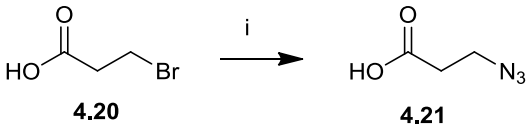

4.20 **4.21**

Scheme 4.8 Synthesis of linker attached azide 4.21. Reagents and conditions: i) NaN_3, MeCN, reflux, 3 h, 36 %

In order to introduce this azide linker into the sugar moiety, the free hydroxy groups at the C-3 and C-4 positions needed to be protected to prevent unwanted coupling reactions. Fernández *et al* have shown that trimethyl silyl (TMS) ether protection at the C-6 position can be selectively removed in the presence of other TMS groups in glucose. This strategy would be compatible for the introduction of the azide functionality.[210]

The hydroxy groups of **4.17** were TMS protected, using TMSCl in the presence of HMDS, resulting in **4.22**. The primary TMS group at the C-6 position of the sugar was selectively deprotected, using AcOH, to give **4.23**. Using standard coupling conditions of TBTU/HOBt in the presence of DIPEA, introduction of the linker attached azide, **4.21**, into the C-6 position of **4.23** was attempted. However, this experiment was not successful, with recovery of **4.17** as the main product (Scheme 4.9), with no evidence of compounds **4.22** or **4.23**.

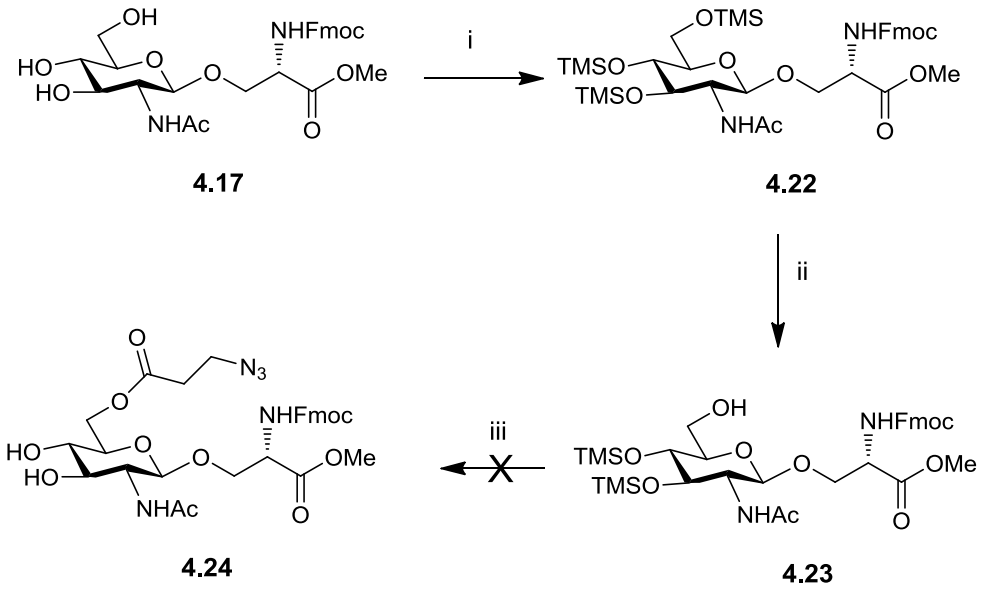

4.17 **4.22** **4.24** **4.23**

Scheme 4.9 Attempted synthesis of C-6 functionalised 4.24. Reagents and conditions: i) TMSCl, HMDS, pyr, 0 °C → rt, overnight, 90 %; ii) AcOH, acetone:MeOH, 0 °C → rt, 7 h, 67 %; iii) TBTU, HOBt, DIPEA, **4.21**, overnight, 0 °C → rt

Introduction of the azide functionality was also investigated with alternative conditions, using DCC as the coupling reagent, in the presence of DMAP (Scheme 4.10). The product of this reaction was a complicated mixture of products, due to the presence of the labile TMS ethers. Some of the desired product, **4.25**, was isolated from the reaction mixture, with the major product found to be **4.23**. The yield of this reaction could be greatly improved by increasing the reaction time, for this investigation a reaction time of 5 h was allowed, due to the base sensitivity of the Fmoc group. No product was found in which the Fmoc group had been deprotected during this reaction, and so the DCC mediated coupling seems to be more suitable for the formation of **4.24**.

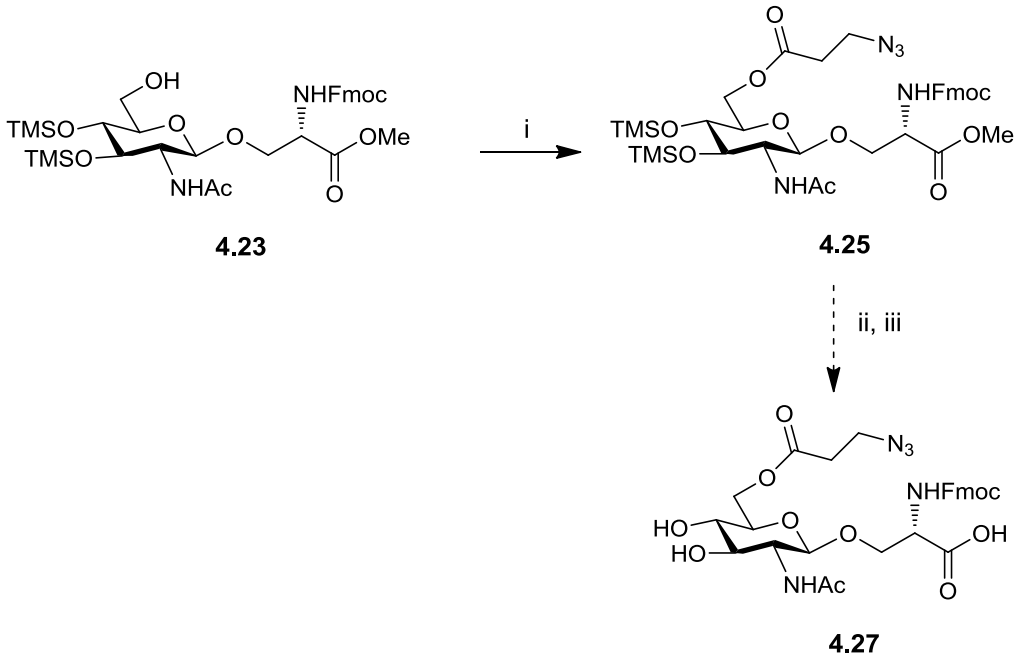

Scheme 4.10 Introduction of the linker attached azide under DCC coupling conditions.
Reagents and conditions: i) DCC, DMAP, DCM, **4.21**, 0 °C → rt, 5 h, 9 %; ii) 2 % TFA in DCM; iii) LiI

From **4.25**, the remaining TMS ethers can be removed with a 2 % solution of TFA in DCM. Following this, the acid could be deprotected, using LiI.[211] LiI is anticipated to be selective for the methyl ester, and should not hydrolyse the ester bond linking the azide to the sugar. These mild deprotection conditions are also suited to the presence of the sensitive glycosidic bond. This acid should be ready for introduction into a glycopeptide, using SPPS techniques. This functionalised carbohydrate derivative would present the opportunity to introduce many different biologically relevant moieties into the C-6 position, such as phosphates or aromatic group. This may modulate the activity of compounds containing this building block. This type of functionalisation may be beneficial in the case of GSK-3. It is known that GSK-3 has a binding site for ATP, and many aromatic compounds take advantage of this to increase their affinity for the kinase. GSK-3 also has a binding pocket for the phosphate portion of ATP, and introduction of a phosphate, or phosphonate, would also have the potential to increase the binding affinity of the glycopeptide for GSK-3. As ATP-competitive inhibitors are often not as kinase selective as those which are non-competitive, a combination of a peptide, substrate based sequence, which also contains the added binding affinity of the ATP site, may be a successful candidate.

4.4 Chapter Conclusion

Important progress towards the synthesis of building block **4.27** was achieved. Selectively functionalised glycoside, **4.27**, could be incorporated into a glycopeptide using standard SPPS conditions. Many problems were encountered throughout this synthesis. The first difficulty was met when attempting to introduce a selective orthogonal protecting group into the C-6 position of compound **4.1**. This was mostly unsuccessful, and, when the desired product was produced, the results were not reproducible.

These problems were not overcome when using the benzyl glycoside, **4.7**. Side products, such as acetyl pyridinium derivative **4.8**, were obtained and identified from these attempts. When working with the serine-glycosylated derivative, **3.4**, incomplete hydrolysis of the *O*-acetyl groups presented some difficulty. Several different deacetylation reactions were investigated, with the use of AcCl in the presence of MeOH found to be the most successful method. From the deprotected glycoside, **4.16**, it was attempted to introduce an azide functionality into the C-6 position. This did not prove successful, with removal of the Fmoc group occurring. Finally, a linker attached azide was investigated. Standard coupling conditions of TBTU/HOBt were not found to be suitable for this reaction, with none of the desired product being isolated. Alternative coupling conditions of DCC did produce the TMS protected building block, **4.25**. The yield of this reaction could be improved with longer reaction times.

For future work, this azide containing glycoside can be incorporated into a glycopeptide sequence, and the affinity of a kinase, like GSK-3, for this glycopeptide can be compared to that of the non-functionalised derivative.

From work carried out in chapter 5, on a glycosyl-dopamine prodrug, it is thought that perhaps a similar approach would be best for introducing an azide into the C-6 position. Building from a TMS protected glycoside, which has not been functionalised with Fmoc protected serine, may allow for introduction of the azide under harsher conditions.

Chapter 5: The Synthesis of a Glycosylated-Dopamine Prodrug

5.1 Introduction: Prodrugs

5.1.1 What is a Prodrug

A prodrug is a drug which does not have any biological effect, but, once administered, will be transformed into a biologically active molecule by metabolic reactions in the body. It has been defined as a bioreversible derivative of a drug molecule, which will undergo enzymatic or chemical transformation *in-vivo* to give the active drug.[212] Several therapeutically important substances are degraded too quickly by the body, or are not delivered to the area where they are needed. Disguising these substances in the form of a prodrug can reverse these drawbacks. The use of prodrugs has become widespread in the pharmaceutical community, including many drugs which are currently on the market. A prodrug must possess specific properties: it should not display activity against any pharmaceutical target, have high aqueous solubility, be resistant to hydrolysis during the absorption phase, be converted into the active drug once it has reached the target location, and any groups which are cleaved must be non-toxic.[213] For these reasons, glycosylation has become the modification of choice for many products. Examples of glycosylated prodrugs are Fabrazyme®, which is a treatment for Fabry disease, and also Rebif® which is used in the treatment of multiple sclerosis.[214]

5.1.2 Improving the Pharmacokinetic Properties of a Drug

Several advancements have been made in the discovery of new drug treatments. The disadvantage is that some of these drugs, especially those which are peptides or proteins, display a poor pharmacokinetic profile. Potential drug candidates will display good pharmacodynamic properties, but this is not enough to ensure the desired response. The pharmacokinetic properties of a compound are an important consideration in drug design. This refers to processes like absorption, distribution, metabolism, and excretion. Many therapeutics can undergo elimination from the body, even before they have had any benefit. This elimination is facilitated by

processes such as enzymatic degradation, renal filtration, and liver clearance. Accumulation within tissues can also remove the drug from the bloodstream.[215]

One example of a modification carried out on peptide drugs is PEGylation (Fig. 5.1). Poly-ethylene-glycol (PEG) has been shown to alter the pharmacokinetic and biodistribution properties of protein conjugates. It appears to prolong the life of the drug in the body, and to enhance localisation of the drug to specific disease sites. It does this in a number of ways, such as size enlargement of the molecule, disguising the peptide from glycosylation or other surface modifications which would ordinarily occur, and by charge modification. Size enlargement has been demonstrated to slow down kidney filtration, allowing the drug more time to reach the target area. The prevention of chemical transformations, such as glycosylation, can alter targeting of the drug by the immune system, also allowing the drug to have a longer half-life.[216]

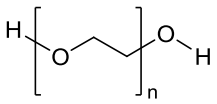

Figure 5.1 Poly-ethylene-glycol

Khondee *et al* have shown that complexation of Keratinocyte Growth Factor-2 (KGF-2) with PEGylated polyanions has a stabilising effect. KGF-2 is a heparin-binding protein which has potent regenerative properties. The disadvantage of using KGF-2 as a therapeutic is that it unfolds and aggregates at approximately 37 °C. It was observed that once KGF-2 had been complexed with the PEGylated polyanions, dextrin sulphate or pentosan polysulphate, the melting temperature of the protein was increased by 9-17 °C.[217]

5.2 Glycosylation can Enhance Pharmacological Profile of Drugs

5.2.1 Glycosyl Prodrugs

Glycosylation has been shown to alter the pharmacokinetic and pharmacodynamic profiles of drugs. Attachment of a sugar moiety can increase the amount of drug that reaches the target area, for example, via transporters such as the glucose transporter (GLUT 1-4). It can also reduce the toxicity of some drugs, allowing a higher dose to be administered.[218] Glycosylation of drugs has allowed for targeted delivery to the desired site, for example in the treatment of lysosomal diseases, like Gaucher and

Fabry disease. The active drug is transported, via receptor-mediated endocytosis, to the lysosome, after targeting specific mannose-6-phosphate receptors. This targeting is achieved by glyco-engineering of the active proteins to express either mannose or mannose-6-phosphate at their termini. While not strictly a prodrug, this illustrates how glycosylation could be used to enhance a drugs pharmacological profile.[214]

Larrosa *et al* have synthesised several glycosyl prodrugs based on the naturally occurring polyphenol, reservatol (Fig. 5.2). Reservatol has shown anti-inflammatory activity, and has become of interest in the treatment of inflammatory bowel diseases (IBD). While reservatol shows promise as a therapeutic due to its pharmacodynamic properties, the pharmacokinetic profile is not as attractive. Reservatol is rapidly metabolised in the body, lessening its efficacy in the colon. It was found that, by conjugating a sugar moiety, this rapid metabolism was prevented, allowing the reservatol prodrug to reach its target site, the colon. An added effect of glycosylation was a reduction in mucosal barrier imbalance, preventing diarrhea in the subjects, again increasing the amount of active drug which could act on the colon tissue.[219]

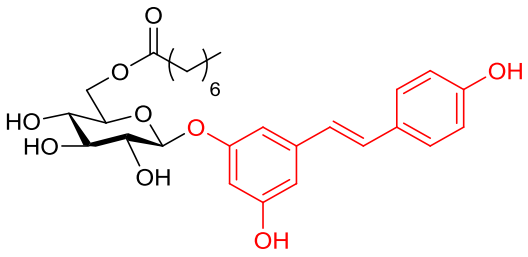

Figure 5.2 Glycosyl reservatol prodrug (Reservatol portion shown in red)

Glycosyl prodrugs have also been developed for the selective treatment of cancer. Duocarmycin is an antibiotic chemotherapeutic, but cannot be administered in high enough doses to be effective, without adverse side-effects. Tietz *et al* have developed glucosylated duocarmycin prodrugs which are effectively delivered to the cancer tissue through an antibody-directed enzyme prodrug therapy (ADEPT) approach. The conjugation of the sugar moiety allowed for localisation of the prodrug in the tumor tissues, where the active drug was released through enzymatic hydrolysis of the glycosidic bond. The duocarmycin exhibited cytotoxic effects on the cancer cells.[220]

5.2.2 Barriers to the Treatment of CNS Disorders

The uptake of solutes into the brain is controlled by the BBB. It separates the central nervous system (CNS) from the rest of the systemic circulation, and is the "gate-keeper" of the brain. The BBB plays a vital role in maintaining homeostasis, allowing nutrients into the brain, and protecting the brain from harmful substances.[221] The blood capillaries which feed the brain are lined with tight-fitting cells, which, unlike other capillaries in the body, do not contain any pores. In addition, these cells are covered with a fatty layer, formed by nearby cells. Together, this results in the BBB being an effective barrier to substances which may be harmful to the brain. In order to enter the brain drugs must be able to pass through the fatty cells coating the capillaries, and also though their poreless cell membrane.[222]

The treatment of many brain related diseases has been hampered by the inability of substances, known to alleviate symptoms, to cross the BBB. It has been estimated that 98 % of small-molecular weight drugs, and 100 % of large-molecular weight drugs, which have been developed for the treatment of CNS diseases do not readily cross the BBB.[223] Many drugs which have shown CNS activity have been discarded in the early trial stages, due to their inability to reach their target.[224]

The BBB allows nutrients to enter the brain through transport channels, for example the large neutral amino acid transporter (LAT-1) and glucose transporters (GLUT 1-4) carriers, or by receptor-mediated transport, like insulin. By administering the active substance as a prodrug, these transport mechanisms can be exploited to deliver the drug into the brain, where the prodrug is broken down into the active substance, and a harmless by-product, for example a sugar (Fig. 5.3).[212]

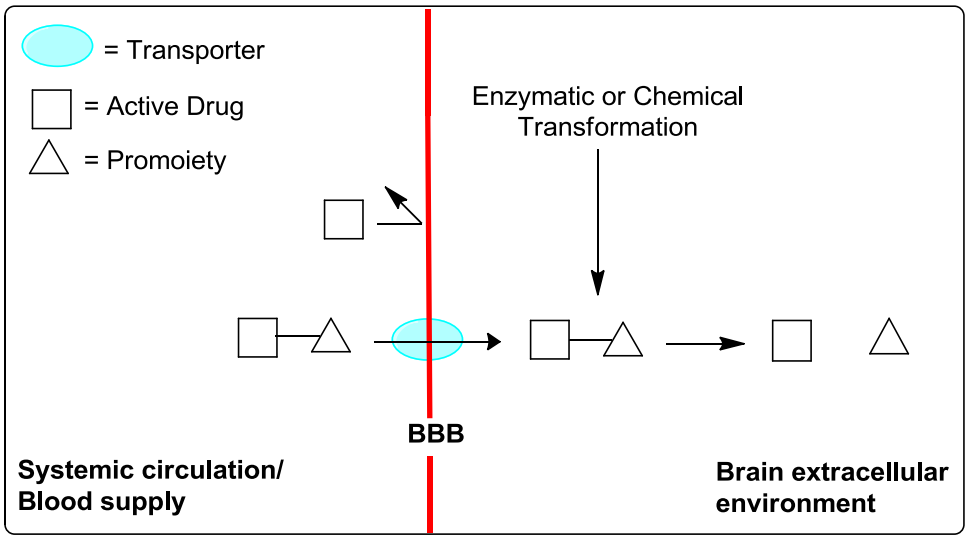

Figure 5.3 Illustration of prodrug transport across the BBB

5.2.3 GLUT Transporter

One mechanism of glucose delivery across membranes is via the GLUT carrier, and there are several different sub-types of this transporter (GLUT 1-4). The transporter which has been associated with glycosyl dopamine prodrugs is GLUT-1, which carries glucose and other hexoses through the BBB into the brain. The large energy demand of the brain is primarily satisfied by glucose, but, in the mammalian brain, the cells do not keep a large storage of glycogen. In order to maintain healthy brain function there must be a mechanism to take in glucose across the BBB. Cellular diffusion of glucose does not occur at any of the membranes in the body, and, as the BBB is no exception, a carrier is required to deliver it to the brain. This process is carried out by the GLUT-1 transport protein, in a regulated manner. The uptake of glucose is very close to the amount of glucose utilised in maintaining brain function. GLUT-1 has the highest transport capacity of all the carrier-mediated transporters at the BBB.[225] The GLUT transporter generally associated with glucosamine is the GLUT-2 carrier.[226] There has also been evidence to demonstrate that a decrease in GLUT-1 and GLUT-3 in the BBB is associated with AD and diabetes. This has been shown to correlate to a decrease in the level of *O*-GlcNAcylation of proteins in the brain.[227]

This well characterised transporter has been investigated for the delivery of CNS active compounds across the BBB.

5.2.4 Glycosylated Prodrugs for CNS Targeting

Work carried out by Gynther *et al* investigated the ability of glyco-conjugates to cross the BBB via GLUT-1. The drugs which they studied were Ketoprofen and Indomethacin, which were modified with D-glucose using a bioreversible ester linkage (Fig. 5.4). They found that the glyco-conjugates did bind to GLUT-1, and also that the prodrug was detected in brain tissue. To further prove that the method of delivery to the brain was through GLUT-1 transport, glucose was added to the perfusion medium. It was found that this decreased the amount of prodrug which was detected in the brain tissue, showing that both D-glucose and the glyco-conjugate shared a transport mechanism. These prodrugs were shown to be susceptible to hydrolysis by rat brain homogenate, to give glucose and the active substance.[228]

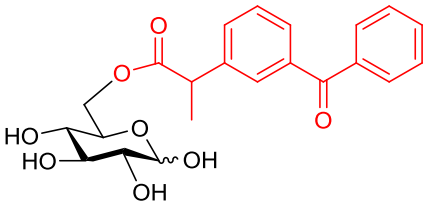

Figure 5.4 Ketoprofen glyco-conjugate (Ketoprofen portion shown in red)

Some studies have shown that GLUT-1 is a bidirectional transporter, mediating both blood to brain, and brain to blood transportation of hexoses. This may limit the effectiveness of some prodrugs, with elimination from the brain before hydrolysis and release of the active drug can occur.[229] In order to investigate if a complex kind of linkage would prevent this bidirectional transport from occurring, Fan *et al* synthesised an array of glucosyl thiamine disulfide prodrugs of naproxen (Fig. 5.5). The thiamine disulfide moiety is quickly reduced by the abundant disulfide reductase, and ring-closed to a thiazolium once it has entered the brain. This thiazolium locks the prodrug into the brain, and renders the GLUT-1 transporter unidirectional for this substance. The ester linkage then becomes hydrolysed at a slower pace, resulting in a sustained release of the active naproxen. The prodrugs synthesised and tested in this study were transported across the BBB, and high levels of naproxen were measured in the brain.[230]

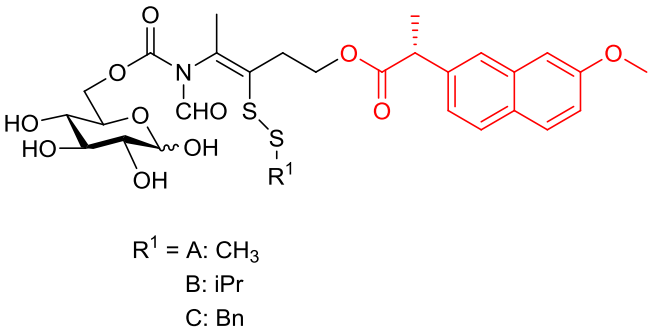

Figure 5.5 Thiamine disulfide derivatives of naproxen (Naproxen portion shown in red)

5.3 Dopamine

5.3.1 The Neurotransmitter Dopamine

Dopamine is a catecholamine neurotransmitter, which plays many roles in the CNS. It is derived from the amino acid tyrosine (Scheme 5.1). Dopamine is involved in many processes, including movement, learning, and motivation. Dopamine is a precursor in the biosynthesis of norepinephrine and epinephrine (Scheme 5.1). It plays a part in the regulation of complex processes such as mood, attentiveness and emotion.[231]

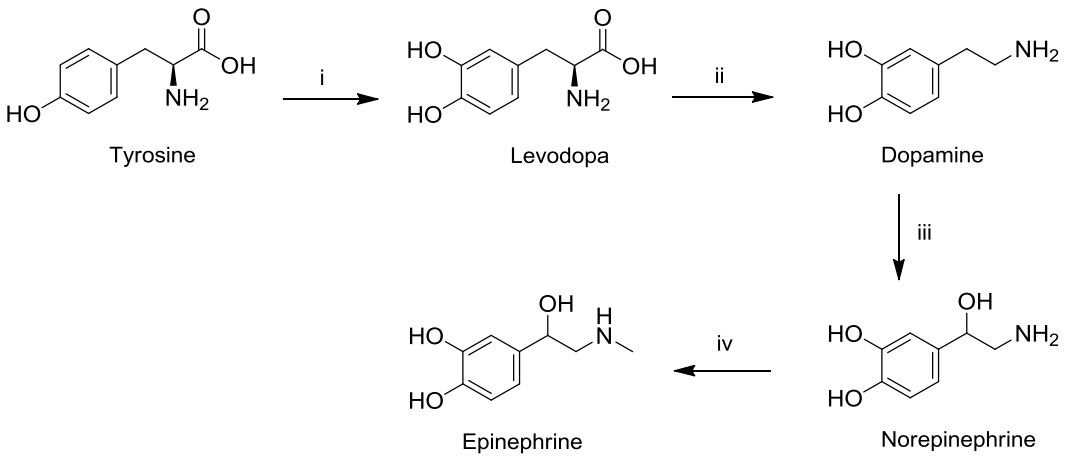

Scheme 5.1 Catecholamine biosynthetic pathway. i) Tyrosine hydroxylase; ii) Aromatic L-amino acid decarboxylase; iii) Dopamine β-hydroxylase; iv) Phenylethanolamine *N*-methyltransferase

There are two main projections in the brain associated with dopamine; the mesolimbic pathway, which can also be activated by most psychoactive substances, and the nigrostriatal pathway. Degradation of dopaminergic neurons in the nigrostriatal pathway is related to Parkinson's disease.[232] Five different dopamine

receptors are known in the body; D_1 – D_5. D_2 appears to be the main receptor involved with Parkinson's disease. Parkinson's disease is characterised by a large reduction in dopamine levels in the basal ganglia, which occurs as a result of this degradation. Dysregulation of dopaminergic activity has also been implicated in schizophrenia, with an excessive release of dopamine in the striatum.[233]

Parkinson's disease is a progressive neurodegenerative disorder, which is characterised by a reduction in the levels of dopamine in the brain, as discussed above. Symptoms of this disease include tremors, rigidity, slow movement and poor balance. As dopamine stimulates the motor neurons involved in muscle movement, sufferers of Parkinson's disease become unable to control movement and coordination.[234] Much research has gone into the use of dopamine to treat diseases such as Parkinson's. Dopamine cannot cross the BBB, because of its hydrophilicity and the lack of a specific transport system, and so treatment directly with this neurotransmitter is not possible, without using intrusive methods.[235]

L-Dopa or Levodopa (L-3,4-dihydroxyphenyl alanine) is the natural precursor of dopamine, as illustrated earlier (Scheme 5.1). This has become the prodrug of choice in the treatment of the motor impairments of Parkinson's disease. L-Dopa has the ability to cross the BBB though the LAT-1 carrier, and is converted to dopamine in the brain. Prolonged treatment with L-Dopa has unwanted side-effects, such as the appearance of abnormal involuntary movements (dyskinesia). This has been attributed to overstimulation of dopaminergic receptors in the substantia nigra.[236] Also, L-Dopa can be converted to dopamine in the peripheral tissues, causing unwanted side-effects, and reducing the amount of dopamine which reaches the brain.[237] New treatments are, therefore, vital to the quality of life of Parkinson's disease sufferers.

5.3.2 Glycosylation as a Transport Mechanism for Dopamine Delivery

Fernández *et al* have synthesised several glycosyl dopamine derivatives as antiparkinsonian agents (Fig. 5.6). These prodrugs consist of the active neurotransmitter, dopamine, linked to D-glucose through a succinyl linker. The compounds contain ester, amide and glycosidic linkages, which can be cleaved by enzymes in the brain tissue. The synthesised prodrugs were tested for activity on the dopamine D_2 receptor, to check if they would be pharmacologically active before

enzymatic release of the dopamine molecule. They did not show any binding affinity, as expected. This demonstrates that both the amino and phenol groups are required for dopamine binding to the D_2 receptor. Stability studies were carried out to investigate the enzymatic degradation of the ester, amide and glycosidic bonds in brain tissue. It was found that the ester bond is cleaved via esterase-catalysed hydrolysis, and that the amide bond is then cleaved by amidase or protease activation to release dopamine. Glycosidic bonds were broken by glycosidase activity. The prodrugs synthesised did not have the desired effect when tested on mouse models of Parkinson's disease. It was thought that either the compounds were not able to cross the BBB, or that the bioconversion into dopamine, by enzymatic degradation, was occurring too slowly.[210]

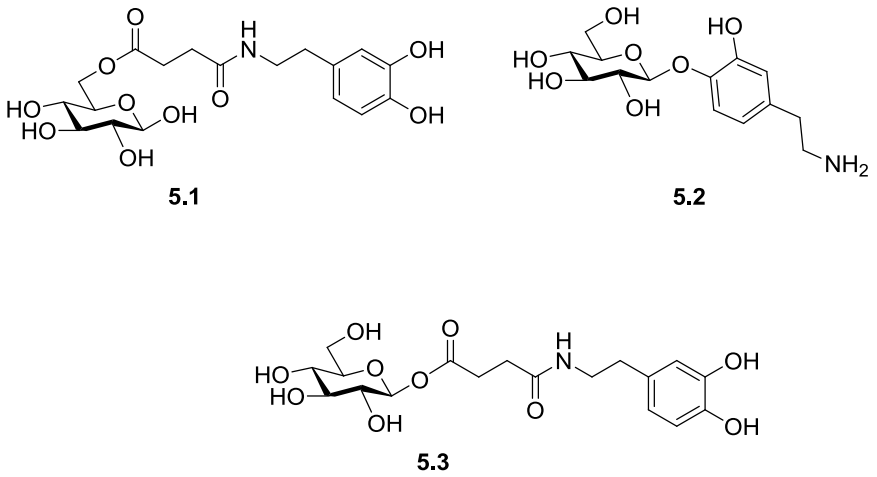

Figure 5.6 Glucosyl-dopamine prodrugs synthesised by Fernández *et al*[210]

The same group later synthesised more glycosyl-dopamine prodrugs (Fig. 5.7), which also showed affinity for the GLUT-1 carrier. They explored the effects of different linkers, or attachment at different positions of the sugar moiety. The compound **5.4**, containing a carbamate bond, was found not to release dopamine when exposed to rat brain tissue. It was thought that perhaps oxidation of the catechol ring was happening faster than hydrolysis of the carbamate bond, and so the free dopamine molecule was not formed. Glycoside **5.5** exhibited the properties of a desired prodrug, in that the dopamine was released upon hydrolysis of the glycosidic bond, but did not show affinity for the GLUT-1 carrier. Carbamate **5.6** was the best candidate from this study, with a high affinity for GLUT-1, and efficient hydrolysis to release dopamine.[238]

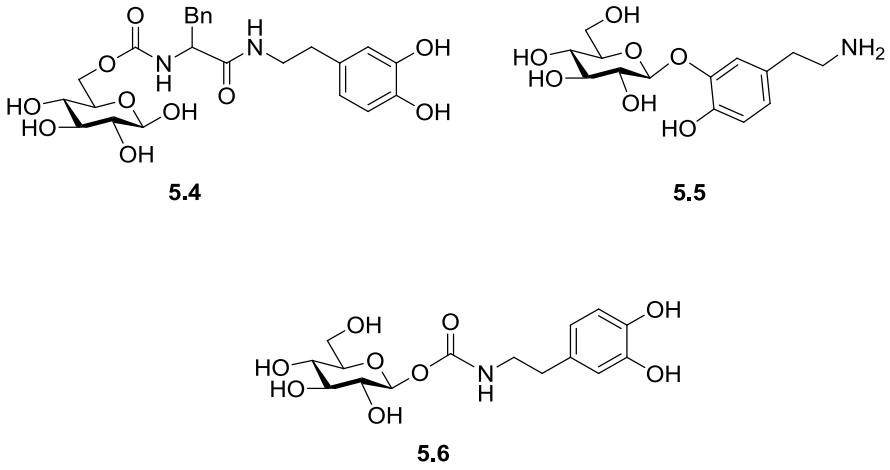

Figure 5.7 Second generation of glycosyl-dopamine prodrugs synthesised by Fernández *et al*[238]

Dalpiaz *et al* have tested the affinity of glucosyl-dopamine, linked at the C-3 position, for the GLUT-1 transporter (Fig. 5.8). They found that this analogue had a greater level of binding to GLUT-1 than some other analogues.[234]

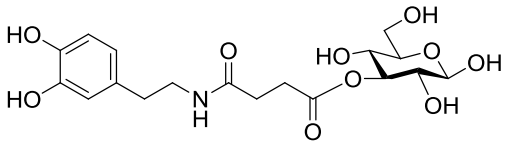

Figure 5.8 Glucose-dopamine linked at C-3

Bonnina *et al* synthesised some of the same derivatives as Fernández *et al*, but via a different synthetic scheme. They also synthesised the L-Dopa derivatives. It was observed that the galactose-dopamine prodrug, **5.7**, and the glucose-L-Dopa analogue, **5.8**, were the best candidates (Fig. 5.9). They were shown to be transported across the BBB, utilizing the GLUT-1 carrier, and were hydrolysed in brain tissue to release dopamine or L-Dopa. They were active in reducing morphine induced locomotion in the mouse model of Parkinson's.[239]

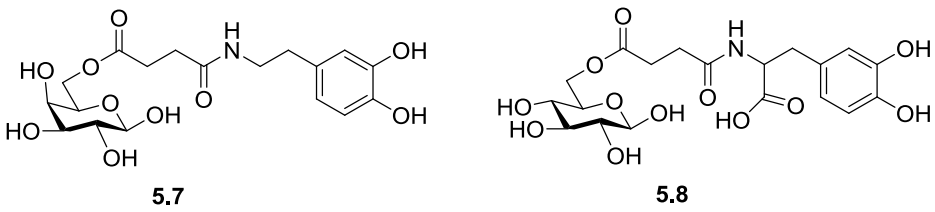

Figure 5.9 Glycosyl-dopamine derivatives synthesised by Bonina *et al*[239]

Yoon *et al* have synthesised α-glycosyl-dopamine and α-glycosyl-L-Dopa derivatives via enzymatic transglycosylation reactions (Fig. 5.10). The stability profile of these compounds under physiological conditions was assessed. It was found that the α-derivatives were less susceptible to non-enzymatic oxidation than L-Dopa. It was postulated that, while the β-anomeric prodrugs synthesised by Fernández *et al* did not induce a strong enough response to be used as therapeutics in Parkinson's disease, the α-anomer might be broken down quicker once it reached the brain. The reasoning behind this is that there are more α-glucosidases in the body than β-glucosidases, and so more dopamine would be released in the brain, over a shorter period, than with a β-glycoside. These compounds were not tested for their affinity for GLUT-1 in this this study, or their ability to cross the BBB.[240]

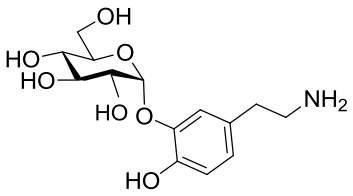

Figure 5.10 α-Glucosyl-dopamine derivative

5.3.3 Non-Glycosidic Dopamine Prodrug Approaches

Alternative approaches utilising other transport mechanisms of the brain have also been investigated.

Trapani *et al* have used chitosan nanoparticles to encapsulate dopamine. These biodegradable carriers have been tested and used to transport anticancer drugs to the brain, and so have been shown to be safe. The surface of the chitosan nanoparticle is positively charged, and it was hypothesised that this would result in transport across the BBB via adsorptive-mediated transcytosis (AMT). This transport mechanism is used to allow cationic substances through the BBB. *In-vivo* experiments on rats showed an increase in the levels of dopamine detected in the brain after administration of the chitosan/dopamine nanoparticle.[241]

Work carried out by Carafa *et al* investigated the use of prodrug-loaded liposomes as a delivery method. It has been shown that condensation of dopamine with neutral amino acids could utilise the LAT-1 transporter to carry the prodrug across the BBB. The dopamine prodrug 2-amino-*N*-[2-(3,4-dihydroxyphenyl)-ethyl]-3-phenyl-

propionamide (DOPH) employs such a strategy. The downside of DOPH is its low bioavailability; it is sensitive to photodegradation, and also to enzymatic degradation. DOPH was encapsulated into a liposome made of dimiristoylphosphatidylcholine (CMPC). It was found that this process did infer protection against photodegradation, and also increased the half-life of DOPH in the blood, *in-vitro*.[242] It is uncertain whether an amino acid linked molecule would be able to cross the BBB in patients suffering from Parkinson's. Ohtsuki *et al* have carried out research into the effect that Parkinson's has on the BBB transport mechanisms. In their mouse model it was observed that the level of substances transported via the LAT-1 carrier was severely decreased, while no significant decrease was observed in other carriers such as GLUT-1. It was postulated that this could be the reason for the low activity of the antiparkinsonian drug levodopa.[243]

5.4 Aim

The aim of this section was the synthesis and biological evaluation of a novel glucosamine-based prodrug, which has potential to improve the pharmacokinetic properties of dopamine. This compound includes a succinyl linker bridging the dopamine and glucosamine molecules. The target compound **5.9** is shown below (Fig 5.11).

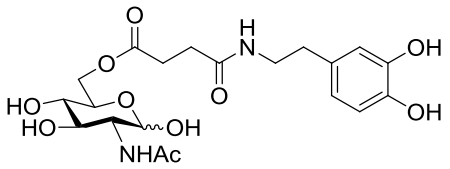

5.9

Figure 5.11 Glucosamine-based dopamine prodrug

There were several reasons for selecting GlcNAc as the sugar moiety. Similar compounds have been synthesised utilising glucose and galactose to transport the dopamine molecule across the BBB, these have been detailed earlier in this chapter. We wanted to investigate if a GlcNAc derivative would display an increased affinity for the GLUT-1 carrier. Some synthetic carbohydrate receptors have been designed by Davis and co-workers, which show an increased affinity for GlcNAc over some other sugars, such as glucose.[244] It was postulated that natural receptors may follow this trend, perhaps increasing the amount of prodrug, and therefore dopamine, which

is transported across the BBB. GlcNAc may also have an alternative mechanism of crossing the BBB, which would be more efficient. As mentioned previously, other GLUT transporters, including GLUT-2 and -3, have been associated with GlcNAc and GlcN. Syntheses of a prodrug involving GlcNAc may therefore be rewarding, albeit more challenging.

5.5 The Synthesis of Glucosamine-Based Dopamine Prodrug 5.9

5.5.1 The Synthesis of Linker-Attached Dopamine

Dopamine was attached to a succinic acid linker, following literature procedures.[210] A succinic linker was chosen as the ester bond between the linker and sugar will be easily hydrolysed by enzymes in the brain. The amide bond between the linker and dopamine molecules should also be labile, and cleaved in the brain by a protease or amidase, as discussed earlier.[210] The first step in this synthesis was the protection of the hydroxy groups on the dopamine aromatic ring. Dopamine hydrochloride, **5.10**, was *N*-Boc protected using Boc anhydride, in the presence of Et_3N. This was carried out to prevent the reactive amine from becoming alkylated in the next step. The hydroxy groups of the dopamine molecule were then benzylated, by treatment with benzyl bromide, in the presence of K_2CO_3 to give protected dopamine **5.11**. The acid labile *N*-Boc group was removed with a 5 % solution of TFA in DCM, resulting in the free amine **5.12**. This benzyl protected dopamine **5.12** could then carry out nucleophilic attack on the carbonyl carbon of succinic anhydride, to give free acid **5.13** (Scheme 5.2).

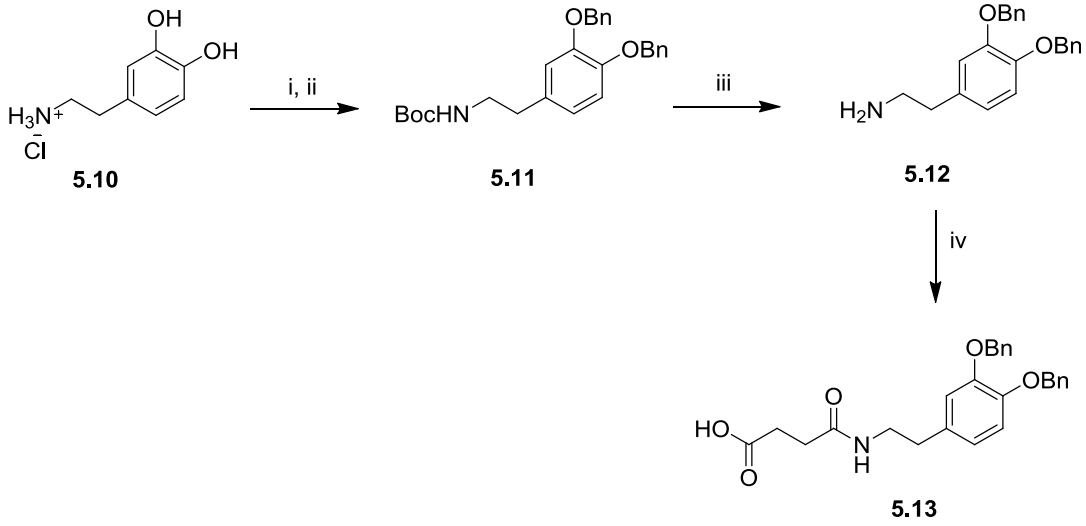

Scheme 5.2 The synthesis of linker attached dopamine 5.13. Reagents and conditions: i) MeOH:Et_3N (9:1), Boc anhydride, 1 h, 50 °C; ii) K_2CO_3, DMF, BnBr, overnight, rt, 43 % over two steps; iii) 5 % TFA, DCM, 6 h, rt, 87 %; iv) Succinic anhydride, pyr, 3 h, rt, 82 %

*5.5.2 The Synthesis of Sugar Moiety **5.18***

As mentioned in chapter 4, Fernández *et al* have used TMS ether protection to selectively introduce the succinic acid dopamine derivative, **5.13**, into the C-6 position of glucose and galactose derivatives.[210] According to work by Gervay-Hague and co-workers, this transformation worked well with most sugars, but, when this selective deprotection was carried out on glucosamine, the TMS group at C-1 was also removed (Scheme 5.3).[245]

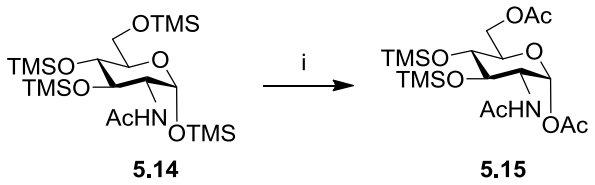

Scheme 5.3 Selective TMS protection demonstrated by Gervais-Hague and co-workers. Reagents and conditions: i) AcOH, Ac_2O, pyr, rt, 48 h

To avoid unwanted coupling of the dopamine-linker to a free hydroxyl at C-1, it was decided to differentially protect the C-1 hydroxy as a benzyl ether. D-Glucosamine hydrochloride was *N*-Troc protected at the amine functionality, by reacting with TrocCl, in the presence of $NaHCO_3$, as discussed earlier in chapter 2. This was followed by acetylation of the hydroxy groups with acetic anhydride, in the presence of pyridine, to give the anomeric mixture of **2.26**. The protected glucosamine **2.26**

was converted into α-glycosyl halide **4.5** by treatment with HBr in AcOH. This bromide donor was activated with Ag_2CO_3, and glycosylation of benzyl alcohol, to give **4.6**, was carried out. Once the C-1 hydroxy had been orthogonally protected, hydrolysis of the acetyl groups was carried out using an aqueous solution of NaOH and MeOH, following literature procedures, resulting in **4.7**.[189] The deprotected glycoside was then TMS protected, using TMSCl in the presence of DIPEA, to give **5.17**. Selective removal of the C-6 trimethyl silyl ether was carried out using AcOH, resulting in **5.18** (Scheme 5.4).

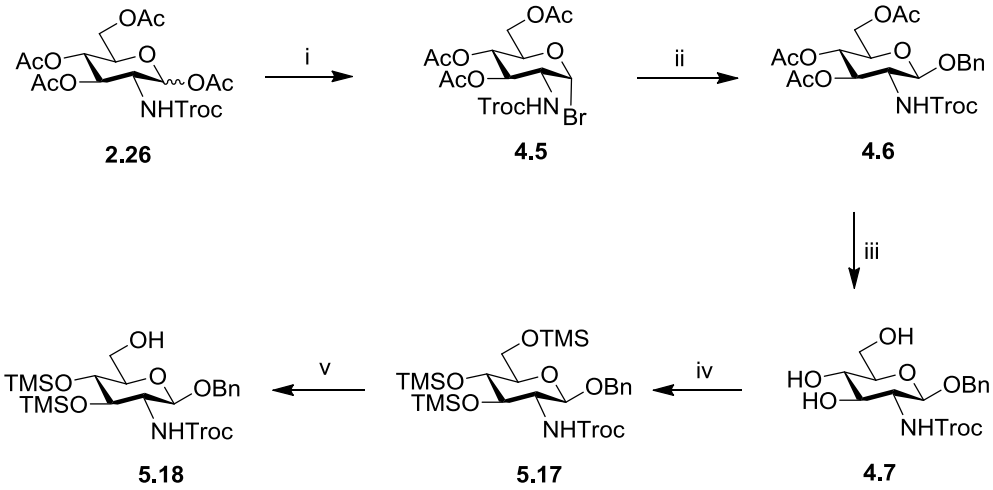

Scheme 5.4 Synthetic scheme for glycoside 5.18. Reagents and conditions: i) 33 % HBr/AcOH solution, DCM, 3.5 h, 0 °C → rt; ii) $AgCO_3$, DCM, BnOH, overnight, rt, 57 % over 2 steps; iii) 0.1 M $NaOH_{aq}$, MeOH, 1 h, rt, 73 %; iv) TMSCl, pyr, DIPEA, overnight, 0 °C → rt, 35 %; v) AcOH, $(CH_3)_2CO$, MeOH, 2 h, 0 °C, 72 %

*5.5.3 Synthesis of Glucosyl-Dopamine Prodrug **5.9***

Coupling of the succinic acid dopamine derivative **5.13** to the sugar moiety **5.18** was carried out using DCC coupling conditions, resulting in **5.24** (Scheme 5.6). Dicyclohexylcarbodiimide (DCC) is a carbodiimide reagent which is often used to activate carboxylic acids, especially in peptide coupling.[246, 247] The initial step of the coupling reaction is the deprotonation of the acid by a base. This is followed by attack on the DCC reagent, **5.20**, by this carboxylate, **5.19**, to form an activated ester, **5.21**. The activated ester is called an *O*-acylisourea, and its formation is rapid. The carbonyl carbon of **5.21** then undergoes nucleophilic attack by the amine/alcohol molecule, to form the amide/ester bond, with elimination of dicyclohexylurea, **5.23**, as the side product (Scheme 5.5). This side product is insoluble in most solvents, and

so purification of the desired product is simple. When used in peptide chemistry, for the formation of an amide bond, an additive such as HOBt is generally used to help prevent racemisation during the reaction.[248] In our case we are not concerned about racemisation, and so HOBt was not required. When this coupling reaction is carried out in the presence of DMAP it is known as a Steglich esterification.

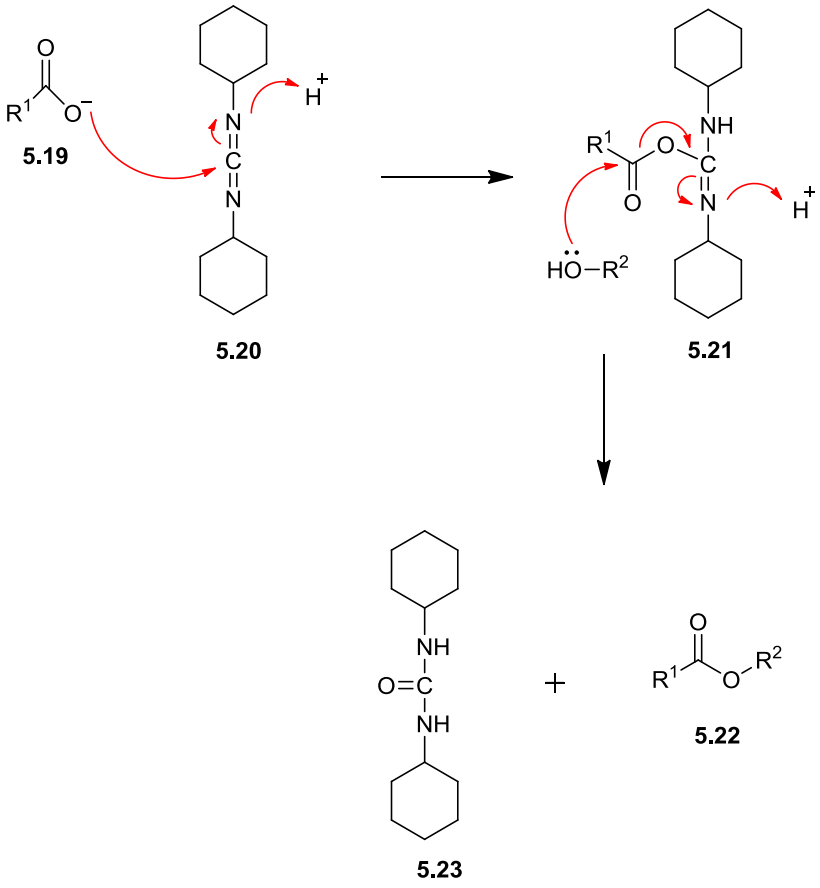

Scheme 5.5 Mechanism of ester formation using DCC as the coupling reagent

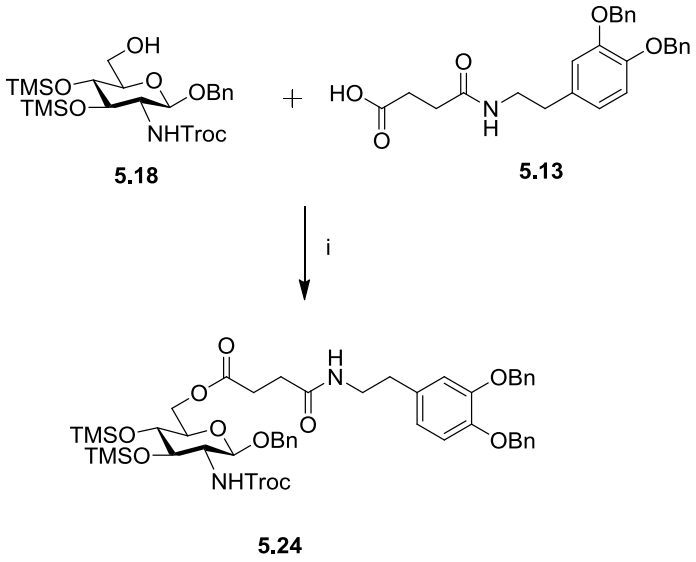

Scheme 5.6 DCC mediated coupling reaction. Reagents and conditions: i) DCC, DMAP, DCM, 3 h, rt, 60 %

Following formation of the ester bond to give **5.24**, deprotection of the remaining TMS groups was carried out by treating with a 2 % solution of TFA in DCM to give **5.25**. The removal of the *N*-Troc protecting group was then accomplished using the standard conditions of Zn in acetic anhydride. The *N*-Troc group was successfully reduced, but, as well as the amine functionality becoming acetylated, as was desired, partial acetylation of the hydroxyl groups was observed (Scheme 5.7).

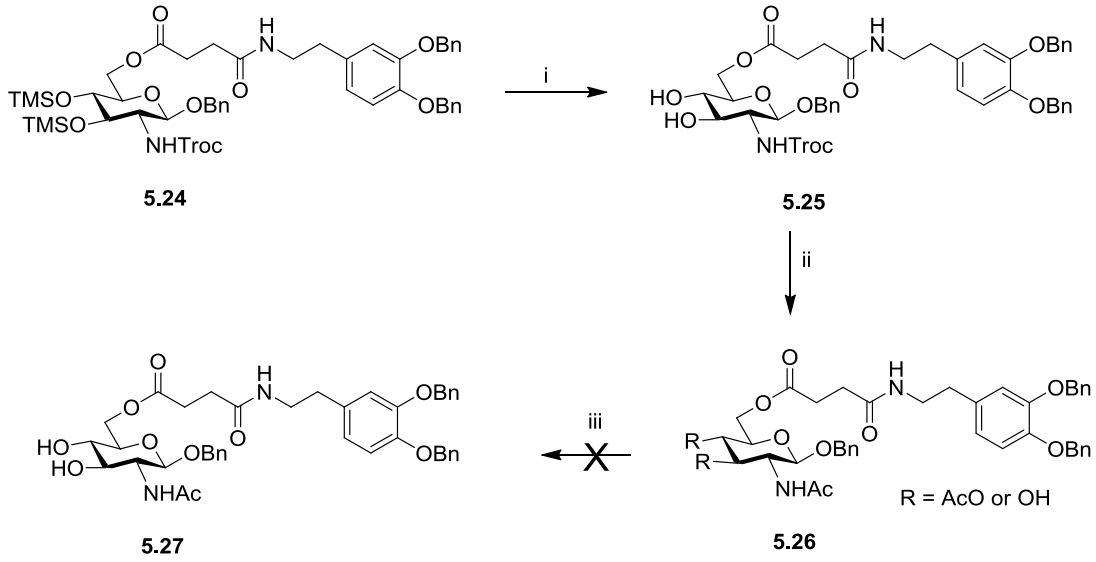

Scheme 5.7 TMS removal, followed by *N*-Troc reduction. Reagents and conditions: i) 2 % TFA in DCM solution, 0 °C, 1 h, 98 %; ii) Zn, Ac_2O, overnight, rt; iii) MeOH/H_2O/Et_3N, 45 °C, overnight

Hydrolysis of the *O*-acetyls from **5.26** was attempted using mild conditions of MeOH/H_2O/Et_3N at 45 °C overnight, but no reaction occurred, with full recovery of starting material. Mild conditions were required due to the presence of the ester bond between the sugar and the succinic linker, which prevented the use of most standard deacetylation procedures.

As this deprotection was posing a problem, removal of the *N*-Troc group was carried out prior to removal of the TMS hydroxy protecting groups (Scheme 5.8). The *N*-Troc deprotection was carried out in the presence of Et_3N, in an attempt to neutralise the Lewis acidic $ZnCl_2$ produced during this reaction, which may have caused removal of the TMS groups. Under these conditions, elimination of the TMS groups and full acetylation of the free hydroxyl groups was observed, resulting in **5.28**.

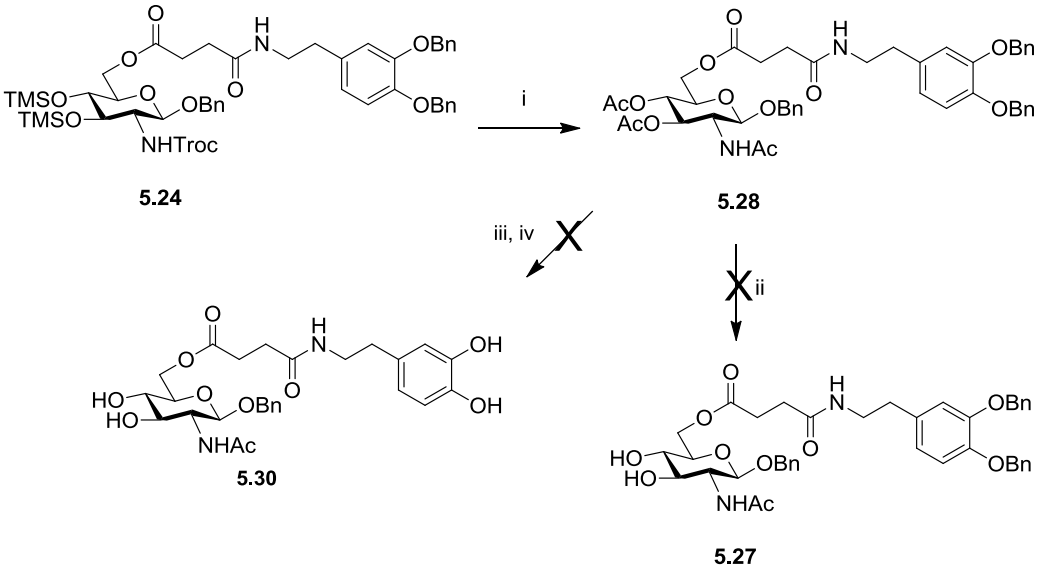

Scheme 5.8 *N*-Troc deprotection. Reagents and conditions: i) Zn, Et_3N, Ac_2O, rt, 3 h, 40 %; ii) Conditions in Table 5.1; iii) H_2, EtOAc/MeOH, overnight, rt, 82 % of **5.29**; iv) MeOH/H_2O/Et_3N, overnight, 45 °C

Selective *O*-deacetylation was attempted under various different conditions, summarised in Table 5.1, but was unsuccessful. Deacetylation carried out using mild basic methods of MeOH/H_2O/Et_3N, shown in entry **1**, resulted in recovery of starting material. Entries **2** and **3** show the conditions for deacetylation using NaOMe over a range of temperatures. Work by Xia *et al* shows acetyl removal in the presence of a pivaloyl ester, at low temperatures using NaOMe,[249] but this did not work for our compound. When carried out at very low temperatures of -20 → -15 °C no reaction occurred, being confirmed by NMR analysis. When the experiment was carried out at higher temperatures of 0 °C, in addition to *O*-deacetylation of the sugar moiety, hydrolysis of the labile ester linkage was observed. Compound **5.34** was isolated from the reaction mixture. Entry **4** details this reaction carried out in the presence of aqueous NaOH and MeOH, again resulting in hydrolysis of the ester linkage.

Enzymatic methods of deprotection have been discussed earlier, in chapter 3. They are highly dependent on the structure of the substrate, and usually several different enzymes are tested for each compound.[195] Two enzymes were investigated for this deacetylation, shown in entries **5** and **6**, using *Candida rugosa* lipase (CRL) and *Candida antarctica* lipase (CAL B) respectively. Neither enzyme had any effect, with recovery of starting material.

Mild acidic conditions were also investigated, as discussed previously in chapter 3. Acetyl chloride has been used for the removal of acetyl groups.[204] When the reaction was carried out in the presence of AcCl (entry **7**), this resulted in hydrolysis of the labile ester linkage, with recovery of deprotected glycoside **5.34**.

Entry	Conditions	Result
1	MeOH/H_2O/Et_3N, 45 °C, overnight	Recovery of starting material, **5.28**
2	NaOMe, -20 → -15 °C	Recovery of starting material, **5.28**
3	NaOMe, 0 °C	Hydrolysis of the ester linkage
4	$NaOH_{aq}$, MeOH, 0 °C	Hydrolysis of the ester linkage
5	CRL, phosphate buffer, pH 7.4, ACN, 25 → 45 °C	Recovery of starting material, **5.28**
6	CAL B, ethanol, 45 °C	Recovery of starting material, **5.28**
7	AcCl, MeOH, rt, 2 days	Hydrolysis of the ester linkage

Table 5.1 Conditions investigated for deacetylation

As an alternative strategy, removal of the benzyl ester protecting groups, under standard conditions of Pd/C in EtOAc/MeOH was carried out on **5.28**. The benzyl protection was easily removed from the hydroxyl groups of the dopamine moiety, but the C-1 benzyl protection was not removed under these conditions, resulting in **5.29**. Acetyl deprotection was attempted on this compound using standard conditions of MeOH/Et_3N/H_2O at 45 °C, which had no effect on **5.28**. The result was degradation of **5.29**, with recovery of deprotected glycoside **5.34** (Scheme 5.8).

As it did not appear to be possible to remove the acetyl groups selectively in the presence of the succinate ester linkage, another strategy was considered. From compound **5.25**, protection of the hydroxy groups with a less labile group than the TMS ethers was attempted. The first protecting group investigated was triethyl silyl (TES) ether, which is 10-100 times more stable to acid hydrolysis or nucleophilic attack than TMS,[250] but this reaction did not proceed, with recovery of starting material. Protection as chloro-acetyls was also attempted, but again no reaction occurred with recovery of starting material (Scheme 5.9).

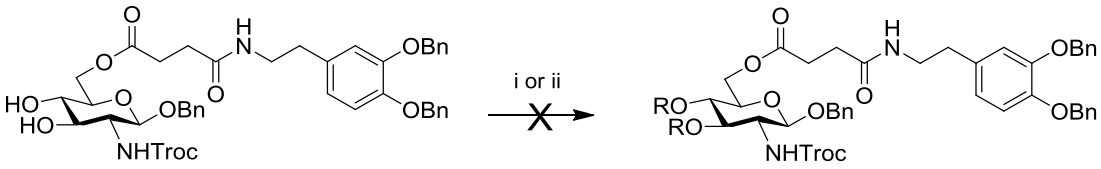

5.25 **5.31:** R = TES **5.32:** R = AcCl

Scheme 5.9 Protection of hydroxy groups. Reagents and conditions: i) TESCl, imidazole, DMF, rt, overnight; ii) $AcCl_2$, pyr, 0 °C → rt, overnight

N-Troc deprotection at a later stage in the synthesis had proven problematic, and so an alternative strategy was devised. Removal of the *N*-Troc group was carried out at a much earlier stage, before introducing the succinic acid dopamine derivative **5.13**. *N*-Troc deprotection from **4.6** was carried out, as before, using Zn and acetic anhydride, to give **5.33**. Deacetylation was carried out in the presence of aqueous NaOH and MeOH, to give the deprotected sugar **5.34**, which was used as a crude. TMS protection of the free hydroxyl groups was attempted, as described earlier, for the *N*-Troc protected sugar (Scheme 5.10). This reaction did not proceed, with recovery of starting material in the aqueous layer of the wash. The experiment was repeated with more equivalents of TMSCl, but was still unsuccessful. Imidazole is a common base used in silyl ether protections.[250] The experiment was then carried out in the presence of imidazole, but again, the starting glycoside **5.34** was recovered.

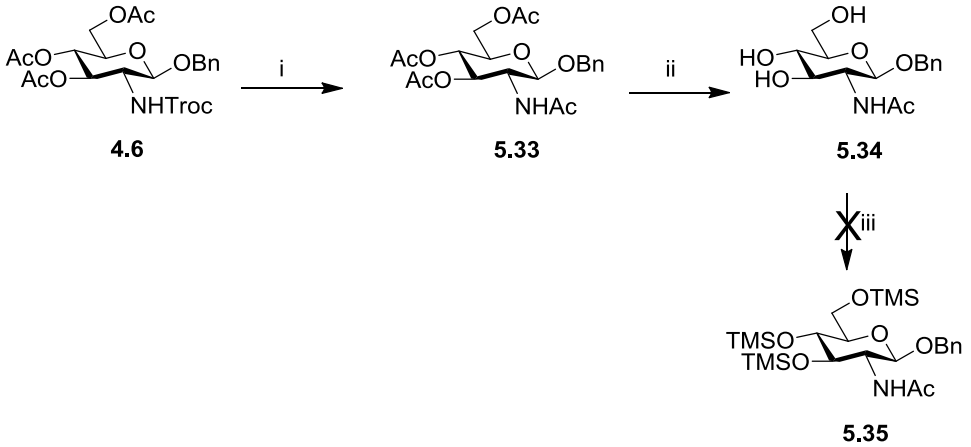

4.6 **5.33** **5.34** **5.35**

Scheme 5.10 Synthesis of TMS protected glycoside 5.35. Reagents and conditions: i) Ac_2O, Zn, Et_3N, 5 h, rt, 71 %; ii) 0.1 M NaOH, MeOH, 1 h, rt, 80 %; iii) TMSCl, DIPEA, pyr, overnight, 0 °C → rt

The lack of reactivity of **5.34** was surprising as this compound appears in the literature, and is involved in reactions at the hydroxyl groups.[251] The difficulty

experienced may have been due to hydroxide salts still present from the deacetylation step, which were interfering with the reactions.

An alternative preparation of **5.34** was followed, according to literature procedures, starting with *N*-acetyl glucosamine **5.36**.[46] From this compound, **5.36**, the anomeric position was selectively protected as the benzyl ether, using 1.2 equivalence of BnBr in the presence of NaH, to give **5.34.** TMS protection of the free hydroxyl groups was then achieved using TMSCl, in the presence of DIPEA in pyridine, to give **5.35**. This reaction was also carried out using hexamethyldisilazane (HMDS) as the base, which resulted in improved yields (44 → 74 %). Selective removal of the TMS ether at C-6 was carried out in the presence of AcOH, resulting in an anomeric mixture of **5.37** (Scheme 5.12).

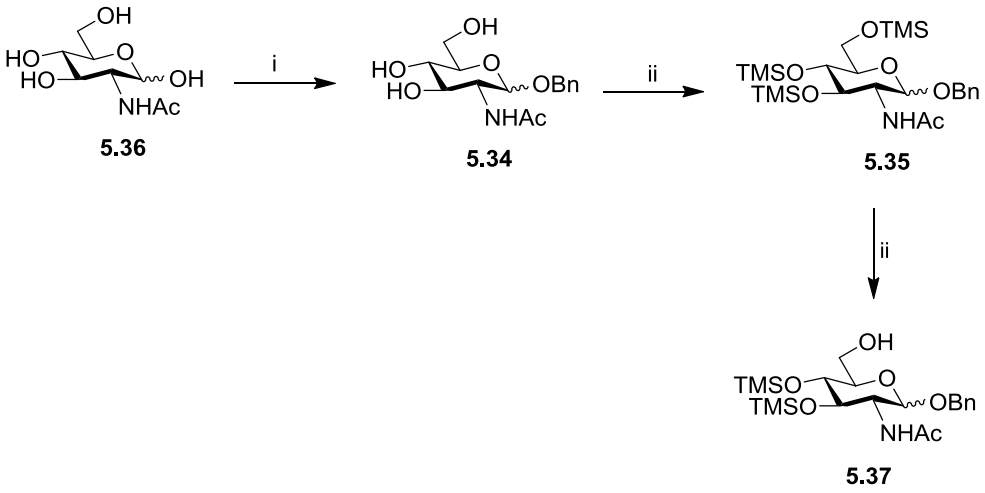

Scheme 5.12 Synthesis of glycoside 5.37. Reagents and conditions: i) BnBr, NaH, 4 h, 0 °C, 78 %; ii) TMSCl, HMDS, pyr, overnight, 0 °C → rt, 74 %; iii) AcOH, MeOH, $(CH_3)_2CO$, 0 °C, 2 h, 86 %

The glycoside **5.37** was then coupled to the dopamine succinyl linker, **5.13**, using DCC in the presence of DMAP, resulting in **5.38**. This was then treated with a 2 % solution of TFA in DCM to remove the remaining TMS ether groups, to give **5.39**. Hydrogenolysis was carried out on **5.39**, using Pd/C in a H_2 atmosphere, to give the deprotected glycoside **5.9**, which will serve as the potential glycosyl dopamine prodrug (Scheme 5.13). Benzyl deprotection at the dopamine hydroxy groups was easily achieved using this method, but the anomeric benzyl ether required a greater amount of Pd/C, with H_2 bubbled through the reaction mixture, to go to completion. Care had to be taken during this step, as, in an earlier trial reaction, using a large

excess of Pd/C and longer reaction times, hydrolysis of the amide bond linking the dopamine also occurred.

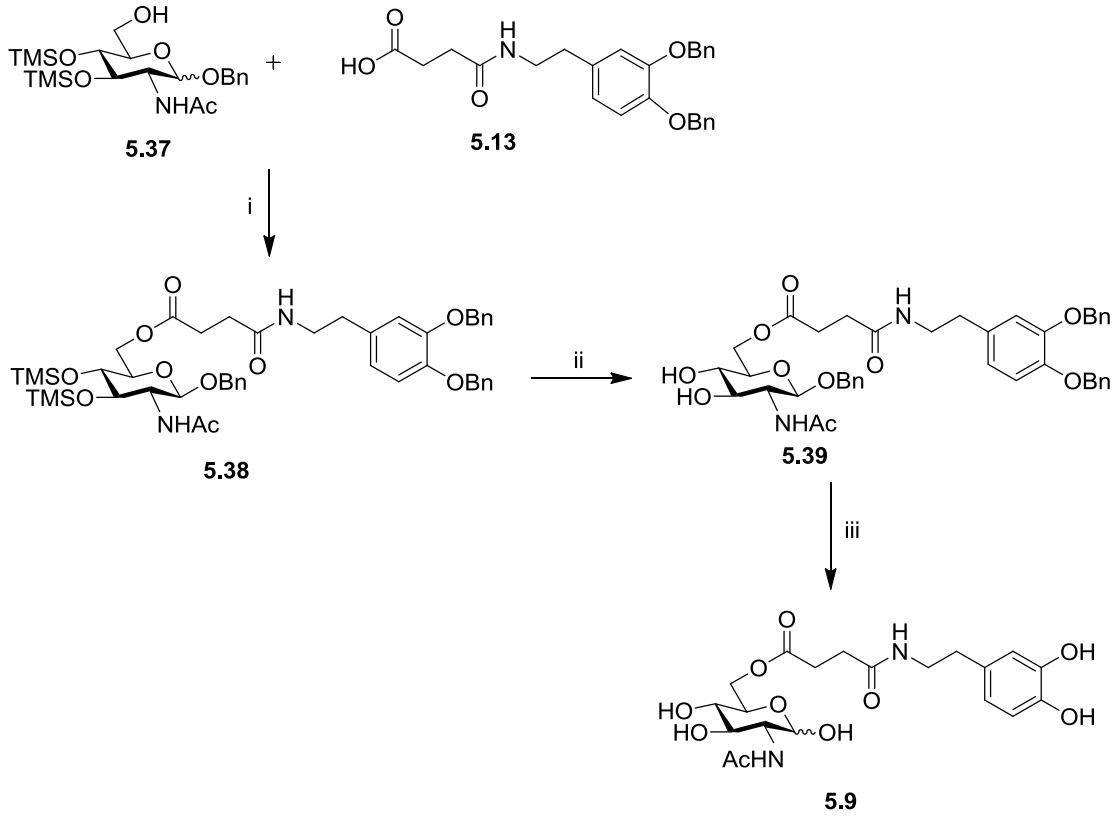

Scheme 5.13 Synthesis of glycosyl dopamine prodrug 5.9. Reagents and conditions: i) DCC, DMAP, DCM, rt, 4 h, 52 %; ii) 2 % solution of TFA in DCM, 0 °C, 1 h, 50 %; iii) Pd/C, H_2, MeOH, rt, 4 h, 56 %

The ^{1}H NMR spectrum of the deprotected glycosyl prodrug **5.9** is shown in Fig. 5.12. It is noteworthy that the configuration of the deprotected final product is predominantly α. While the anomeric position was protected as a benzyl glycoside, in compounds **5.38** and **5.39**, the β-anomer was the only one observed.

Compound **5.9** will be tested for its ability to cross the BBB in mice, and, if successful, further studies can be carried out into the mechanism of transport into the brain capillaries, the affinity of the molecule for glucose transporters, and the subsequent release of the dopamine molecule.

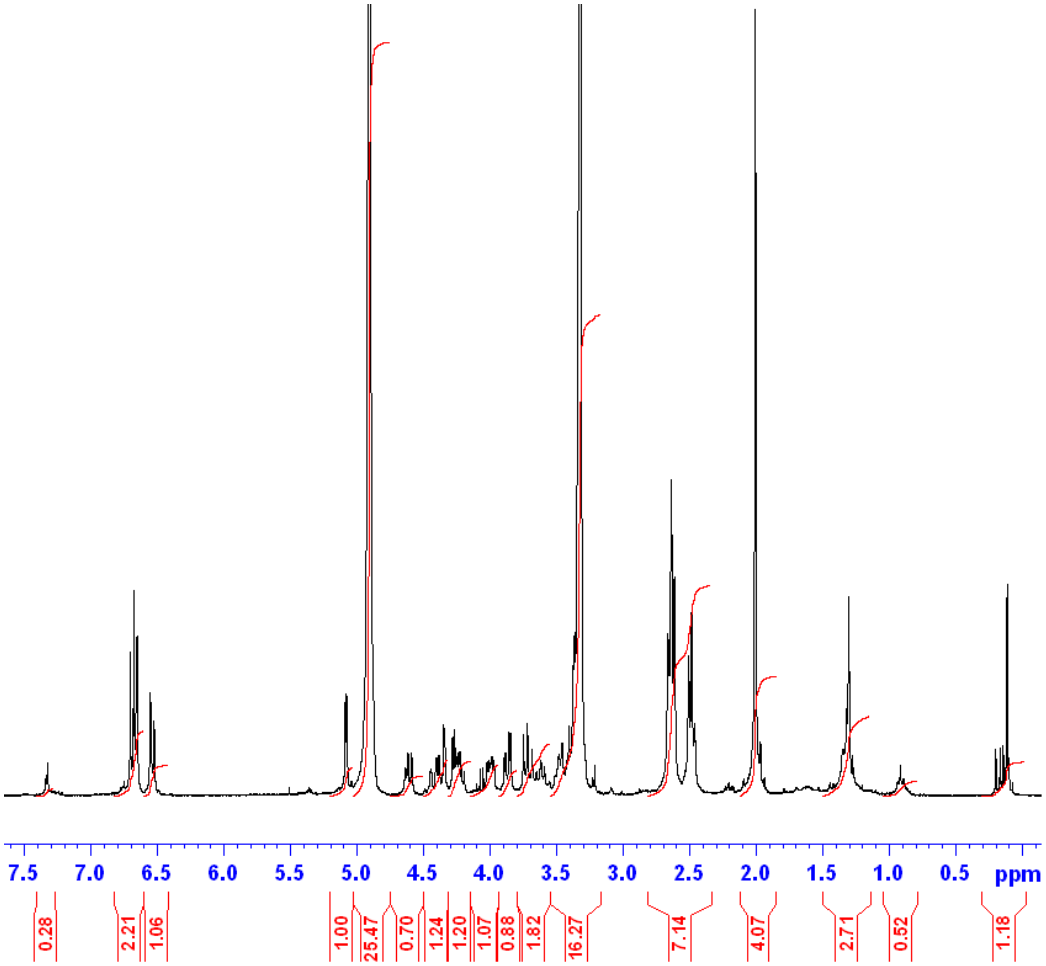

Figure 5.12 ^{1}H NMR spectrum of 5.9 carried out in CD_3OD

5.6 Chapter Conclusions

The glycosylated dopamine prodrug, **5.9**, was successfully synthesised. Some problems encountered during the synthesis include the difficulty presented by the undesired acetylation of the hydroxy groups during the *N*-Troc deprotection step. The removal of these *O*-acetyl groups was complicated by the presence of the ester bond linking the dopamine to the C-6 of the sugar. No method was found which was suitable to selectively deprotect the *O*-acetyl groups, while leaving the ester linker intact. An alternative route was devised, which involved coupling of the dopamine succinate to a sugar moiety in which the amine was protected as an NHAc instead of NHTroc. This synthesis presented its own problems, with the sugar produced from a deprotection step proving unreactive. It was found that some side-product of the deprotection reaction was preventing the TMS protection of hydroxy groups. Again, another route was conceived, synthesising the *O*-TMS protected sugar moiety, **5.35**,

from a different starting material, **5.36**. This method proved successful, resulting in the synthesis of the desired glycosylated dopamine prodrug.

Future work could involve investigation of a different linker to the succinamide one used in this synthesis. Also, testing of **5.9** for its ability to cross the BBB, and an investigation into the mechanism of transport into the brain capilliaries, should be carried out.

Chapter 6: Experimental Details

6.1 General Procedures

6.1.1 Reagents

Reagents used in the experiments were purchased from Sigma Aldrich, Fluka, or Novabiochem and used without further purification. All solvents for synthesis, extraction and column chromatography were distilled and dried before use, if necessary, or bought as anhydrous solvents or reagents, e.g.: DMF, pyridine, and Et_3N from Sigma Aldrich. Solvents were dried as follows: DCM was distilled over calcium hydride, and THF was distilled from sodium wire and benzophenone.

6.1.2 Equipment

^1H NMR and ^{13}C NMR spectra were recorded on a Bruker Avance 300 MHz spectrometer operated at 300 MHz for ^1H and 75 MHz for ^{13}C at 298 K, or on Bruker Avance II 600 NMR operated at 600 MHz for ^1H NMR spectroscopy in Trinity College Dublin. NMR spectra were obtained by using $CDCl_3$, CD_3OD, C_6D_5N, or $(CD_3)_2SO$ as the deuterated solvent; chemical shifts are expressed as δ units (ppm) relative to respective residual solvent peaks[252]. The abbreviations s, d, dd, t, q, m and bs refer to singlet, doublet, doublet of doublets, triplet, quartet, multiplet and broad singlet signal, respectively, in ^1H NMR spectroscopic data. In ^{13}C NMR data s, d, t, and q refer to quaternary C, CH, CH_2, and CH_3, respectively. COSY (Correlation Spectroscopy), HSQC (Heteronuclear Single Quantum Correlation), NOESY (Nuclear Overhauser Effect Spectroscopy), and Dept 135 (Distortionless Enhancement by Polarization Transfer) were used to aid assignation of ^1H and ^{13}C NMR spectra. Mass spectrometry was carried out on samples using a Liquid chromatography/Time of flight-mass spectrometer. The LC was a model 1200 Series (Agilent Corp, Santa Clara, CA). Standard injection volumes were 1 µL, with a mobile phase of A = ACN with 0.1 % formic acid and B = 0.1 % formic acid in water (A:B, 0:100 to 50:50 to 100:0 to 50:50 to 0:100 over 20 mins). The spectrometer was a model 6210 Time-Of-Flight LC/MS (Agilent Corp, Santa Clara, CA) with an electrospray source both positive and negative (ESI+/-), capillary 3,500 V, nebuliser spray 30 psig, drying gas 5 L/min, source temperature 325 °C. The

fragmentor voltage was used at 175 V. Reference masses (Agilent Solution) were 121.050873, 149.02332, 322.048121, 922.009798, 1221.990633, 1521.971475 and 2421.91399 m/z. Optical rotations were measured on an ADP410 polarimeter (sensitivity one millidegree) at room temperature. The light source was a light emitting diode with interface filter (589 nm). The concentrations of solutions prepared for $[\alpha]_D$ measurements are given in g/ 100 mL of corresponding solvent. Column chromatography was performed using Merck silica gel 60 (particle size 0.040- 0.063 mm). Reactions were monitored by thin layer chromatography (TLC) using Merck silica gel 60, $F_{254.}$ Sample spots were visualized by staining with a suitable dye followed by charring (either 5 % sulphuric acid in ethanol or 0.5 % ninhydrin in ethanol). Infrared spectra were obtained, either as a film on a NaCl plate or as a solid in a KBr disc, in the region 4000–400 cm^{-1} on a Nicolet Impact 400 D spectrophotometer. Melting points of recrystallised compounds were obtained using a Stuart Scientific Melting Point SMP1, and are uncorrected. Temperatures given for experiments requiring heating of the reaction mixture are given in ˚C of the silicon oil bath. All air and moisture sensitive reactions were carried out under a nitrogen atmosphere.

6.2 Experimental Details

N^{α}-[(1,1-Dimethylethoxy)carbonyl]-*O*-[(2-deoxy-2-acetamino-3,4,6-tri-*O*-acetyl)-β-D-glucopyranosyl]-L-serine-phenylmethyl ester (2.21)[87]

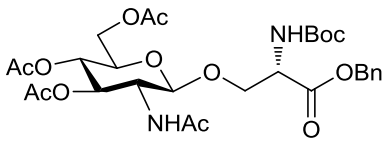

Protected glycoside **2.22** (92 mg, 0.12 mmol) was dissolved in acetic anhydride (3 mL, 31.8 mmol). Freshly activated zinc powder (171 mg, 2.63 mmol) (activated by rinsing twice with 2 M HCl, followed by H_2O, acetone, and diethyl ether) and Et_3N (0.04 mL, 0.26 mmol) were added to the reaction mixture, and this was allowed to stir at rt for 4 h. The reaction mixture was filtered through celite to remove the zinc salts. The solvent was co-evaporated with toluene under reduced pressure, then the remaining residue was dissolved in DCM and washed twice with sat. $NaHCO_3$ solution, followed by brine, then dried ($MgSO_4$), and filtered. The organic layer was concentrated under reduced pressure, and the crude product was purified by column chromatography (Hex:EtOAc, 2:1 to 1:1 to MeOH) to give the *N*-acetyl protected glycoside **2.21** as a white solid (70 mg, 86 %). Spectroscopic data was in agreement with reported values.

R_f: 0.2 (Hex:EtOAc, 1:1); ^{1}H NMR: ($CDCl_3$, 300 MHz) δ = 7.40-7.33 (m, 5 H, Ph-*H*), 5.69 (d, 1 H, N*H*C(O)CH_3, *J* = 12 Hz), 5.44 (d, 1 H, N*H*C(O)OC$(CH_3)_3$, *J* = 9 Hz), 5.23-5.20 (m, 1 H, *H*-3), 5.17-5.08 (m, 2 H, Ph-CH_2), 5.03 (t, 1 H, *H*-4, *J* = 9 Hz), 4.71 (d, 1 H, *H*-1, *J* = 9 Hz), 4.46-4.45 (m, 1 H, α-*H*), 4.28-4.21 (m, 2 H, overlapping β-H_a and *H*-6_a), 4.11-4.06 (m, 1 H, *H*-6_b), 3.86-3.81 (dd, 1 H, β-H_b, *J* = 3 Hz, 12 Hz), 3.79-3.75 (m, 1 H, *H*-2), 3.67-3.63 (m, 1 H, *H*-5), 2.06, 2.02, 2.01 (each s, 9 H, OC(O)CH_3), 1.93 (s, 3 H, NHC(O)CH_3), 1.43 (s, 9 H, C(C$H_3)_3$); (Lit[87]: ^{1}H NMR: ($CDCl_3$, 300 MHz) δ = 7.36-7.28, 5.53, 5.43, 5.24, 5.18, 5.12, 5.00, 4.68, 4.45, 4.25-4.18, 4.06, 3.79, 3.72, 3.60, 2.03, 2.00, 1.99, 1.91, 1.41);^{13}C NMR: ($CDCl_3$, 75 MHz) δ = 170.8, 170.7, 170.6 (each s, O*C*(O)CH_3), 169.4 (s, NH*C*(O)CH_3), 166.4 (d, *C*(O)OBn) 155.4 (NH*C*(O)OC$(CH_3)_3$), 135.4 (s, Ph-*C*), 128.5, 128.4, 128.2 (d, Ph-*C*H), 100.8 (d, *C*-1), 80.1 (s, *C*$(CH_3)_3$), 72.0 (d, *C*-3), 71.9 (d, *C*-5), 69.4 (t, β-*C*), 68.5 (d, *C*-4), 67.3 (t, Ph-*C*H_2), 62.0 (t, *C*-6), 54.6 (d, *C*-2), 54.0 (d, α-*C*), 28.3 (q, C(*C*$H_3)_3$), 22.2 (q, NHC(O)CH_3), 20.7, 20.7, 20.6 (each q, OC(O)CH_3); IR: (DCM

film on NaCl plate) 3288, 3066, 2978, 1748, 1500, 1231 cm^{-1}; MS-ESI/TOF: Calculated for $C_{29}H_{41}N_2O_{13}$ $(M + H)^+$: 635.2603, found 625.2600.

N^{α}-[(1,1-Dimethylethoxy)carbonyl]-*O*-[(2-deoxy-2-[(2,2,2-trichloroethoxy carbonyl)amino]-3,4,6-tri-*O*-acetyl)-β-D-glucopyranosyl]-L-serine-phenylmethyl ester (2.22)[87]

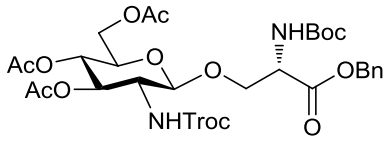

Imidate donor **2.34** (1.28 g, 2.06 mmol) and protected serine acceptor **2.24** (490 mg, 1.72 mmol) were placed under N_2, in the presence of 4Å molecular sieves, and dissolved in dry DCM (2 mL). A freshly made solution of TMSOTf in dry DCM (0.04 M, 4.3 mL, 0.17 mmol) was added, and the reaction was left to stir at rt overnight. The reaction was quenched by adding solid $NaHCO_3$ (100 mg) to the reaction mixture and allowed to stir for 5 mins. H_2O (50 mL) was added to the flask. The product was extracted twice with DCM. The organic layers were combined and washed with H_2O, then dried ($MgSO_4$), and filtered. The organic layer was concentrated under reduced pressure, and the remaining residue was purified by column chromatography (Hex:EtOAc, 1:1) to give glycoside **2.22** as a yellow oil (640 mg, 49 %). Spectroscopic data was in agreement with reported values.

R_f: 0.8 (Hex:EtOAc, 1:1); ^{1}H NMR: ($CDCl_3$, 300 MHz) δ = 7.37-7.34 (m, 5 H, Ph-*H*), 5.28-5.13 (m, 5 H, overlapping *H*-3, Ph-CH_2, N*H*C(O)OCH_2, and N*H*C(O)OC$(CH_3)_3$) , 5.00 (t, 1 H, *H*-4, *J* = 9 Hz), 4.82-4.77 (m, 1 H, NHC(O)OCH_{2a}), 4.67-4.61 (m, 2 H, overlapping NHC(O)OCH_{2b} and *H*-1), 4.32-4.31 (m, 1 H, α-*H*), 4.28-4.13 (m, 2 H, overlapping β-H_a and *H*-6_a), 4.10-4.06 (m, 1 H, *H*-6_b), 3.84-3.80 (dd, 1 H, β-H_b, *J* = 3 Hz, 9 Hz), 3.65-3.61 (m, 1 H, *H*-5), 3.58-3.51 (m, 1 H, *H*-2), 2.08, 2.04, 2.02 (each s, 9 H, OC(O)CH_3), 1.45 (s, 9 H, C(CH_3)$_3$); (Lit[87]: ^{1}H NMR: ($CDCl_3$, 250 MHz) δ = 7.35-7.30, 5.40, 5.22, 5.18, 5.12, 5.00, 4.77, 4.64, 4.61, 4.45, 4.28, 4.22, 4.06, 3.79, 3.60, 3.50, 2.00, 1.97, 1.42); ^{13}C NMR: ($CDCl_3$, 75 MHz) δ = 170.6 (s, CH*C*(O)OBn), 169.9, 169.8, 169.5 (each s, O*C*(O)CH_3), 155.5 (s, NH*C*(O)OC$(CH_3)_3$), 154.0 (s, NH*C*(O)OCH_2), 135.4 (s, Ph-*C*), 128.6, 128.4, 128.3 (each d, Ph-*C*H), 100.8 (d, *C*-1), 95.3 (s, *C*Cl_3), 80.3 (s, *C*$(CH_3)_3$), 74.5 (t, NHC(O)O*C*H_2), 72.1 (d, *C*-3), 69.7 (t, β-*C*), 68.5 (d, *C*-5), 68.0 (d,

C-4), 67.1 (t, Ph-*C*H_2), 62.0 (t, *C*-6), 56.2 (d, *C*-2), 54.7 (d, α-*C*), 28.3 (q, C(*C*H_3)$_3$), 21.1, 20.7, 20.6 (each q, OC(O)*C*H_3); IR: (DCM film on NaCl plate) 3350, 2978, 1751, 1234 cm^{-1}; MS-ESI/TOF: Calculated for $C_{30}H_{40}Cl_3N_2O_{14}$ $(M + H)^+$: 757.1540, found 757.1567.

N^{α}-[(1,1-Dimethylethoxy)carbonyl]-L-serine-phenylmethyl ester (2.24)[88, 253]

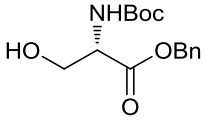

L-Serine-N^{α}-[(1,1dimethylethoxy)carbonyl] (1.50 g, 7.3 mmol) and K_2CO_3 (1.49 g, 10 mmol) were placed under N_2. Anhydrous DMF (30 mL) was added and the resulting suspension was stirred for 5 mins. Benzyl bromide (1.1 mL, 9.3 mmol) was added slowly. The reaction mixture was stirred at rt overnight. The solvent was evaporated under reduced pressure. The organic layer was concentrated under reduced pressure, and the remaining residue was dissolved in DCM, then washed with H_2O, and brine. The organic phase was then dried ($MgSO_4$), and filtered. The solvent was evaporated under reduced pressure to give protected serine derivative **2.24** as a white solid (1.46 g, 68 %). Spectroscopic data was in agreement with reported values.

R_f: 0.5 (Hex:EtOAc, 2:1); ^{1}H-NMR: **(**$CDCl_3$, 300 MHz): δ = 7.34 (s, 5 H, Ph-*H*), 5.57 (d, 1 H, N*H*, *J* = 6 Hz), 5.21 (d, 2 H, Ph-CH_2, *J* = 3 Hz), 4.41-4.39 (m, 1 H, α-*H*), 3.99-3.88 (m, 2 H, β-*H*), 2.90 (t, 1 H, O*H*, *J* = 6 Hz), 1.43 (s, 9 H, C(CH_3)$_3$); (Lit[253]: ^{1}H-NMR: **(**$CDCl_3$, 300 MHz): δ = 7.35, 5.47, 5.21, 4.42, 3.98-3.88, 2.34, 2.04); ^{13}C-NMR: ($CDCl_3$, 75 MHz): δ = 170.8 (s, O*C*(O)NH), 155.7 (s, O*C*(O)CH), 135.3 (s, *C*(CH_3)$_3$), 128.5, 128.3, 128.0 (each d, Ph-*C*), 80.0 (s, Ph-*C*), 67.2 (t, Ph-*C*H_2), 63.2 (t, β-*C*), 55.9 (d, α-*C*), 34.6, 28.2, 20.9 (each q, C(*C*H_3)$_3$); IR: (KBr disc) 3421, 3366, 2980, 1761, 1670, 1527 cm $^{-1}$; MS-ESI/TOF: Calculated for $C_{15}H_{22}NO_5$ $(M + H)^+$: 296.1492, found 296.1480.

(2-Deoxy-2-[(2,2,2-trichloroethoxycarbonyl)amino]-1,3,4,6-tetra-*O*-acetyl)-α/β-D-glucopyranoside (2.26)[89, 254]

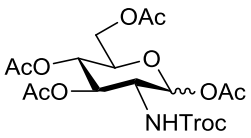

D (+) -Glucosamine hydrochloride (2.00 g, 9.0 mmol) and $NaHCO_3$ (2.27 g, 27 mmol) were suspended/ dissolved in H_2O (20 mL). The resulting suspension was stirred for 5 mins at rt. Trichloroethoxy carbonyl chloride (TrocCl) (1.45 mL, 10.8 mmol) was added dropwise. The reaction mixture was stirred at rt for 2 h, then neutralized (1 M HCl). The solvent was evaporated under reduced pressure, and the remaining residue was dissolved in pyridine (8.9 mL). Acetic anhydride (4.5 mL, 47 mmol) was added dropwise at 0 ˚C. The reaction mixture was allowed to reach rt, and stir overnight. The solvent was evaporated using a rotary evaporator, and the remaining residue was dissolved in DCM, and washed with sat. $NaHCO_3$ solution, and brine, then dried ($MgSO_4$), and filtered. The organic layer was concentrated under reduced pressure, and the remaining residue was purified by column chromatography (Hex:EtOAc, 4:1 to 3:1 to 2:1 to 1:1) to leave the protected sugar **2.26** as an off-white solid (4.08 g, 87 %). Spectroscopic data was in agreement with reported values. **2.26** was an anomeric mixture α:β in the ratio of 1:0.3.

R_f: 0.7 (Hex:EtOAc, 1:1); ^{1}H NMR: ($CDCl_3$, 300 MHz) δ = 6.25 (d, 1 H, *H*-1 (α-anomer), *J* = 3 Hz), 5.81-5.76 (m, 2 H, overlapping N*H*C(O)OCH$_2$ and *H*-1 (β-anomer)), 5.35-5.26 (m, 1 H, *H*-3), 5.22-5.11 (m, 1 H, *H*-4), 4.86-4.60 (m, 2 H, NHC(O)C*H*$_2$), 4.30-4.19 (m, 2 H, overlapping *H*-2 and *H*-6$_a$), 4.09-4.01 (m, 2 H, overlapping *H*-6$_b$ and *H*-5), 2.15, 2.10, 2.07, 2.04 (each s, 12 H, OC(O)C*H*$_3$); (Lit[254]: ^{1}H NMR for β-anomer: ($CDCl_3$, 300 MHz) δ = 5.73, 5.22, 5.11, 5.14, 4.72, 4.29, 4.10, 3.93, 3.81, 2.10, 2.08, 2.03; Lit[255]: ^{1}H NMR for α-anomer: ($CDCl_3$) δ = 6.25, 5.28, 4.64, 4.30, 4.22, 4.07, 4.03, 2.22, 2.12, 2.06); ^{13}C NMR: ($CDCl_3$, 75 MHz) δ = 170.6, 170.4, 169.1, 168.6 (each s, O*C*(O)CH$_3$), 154.2 (s, NH*C*(O)OCH$_2$), 95.3 (s, *C*Cl$_3$), 92.2 (d, *C*-1 (β-anomer)), 90.4 (d, *C*-1 (α-anomer)), 74.5 (t, NHC(O)O*C*H$_2$), 70.4 (d, *C*-3), 69.6 (d, *C*-5), 67.7 (d, *C*-4), 61.5 (t, *C*-6), 53.1 (d, *C*-2), 20.9, 20.7, 20.5, 20.4 (each q, OC(O)*C*H$_3$); IR: (film on NaCl) 3327, 2959, 1755,

1226 cm^{-1}; MS-ESI/TOF: Calculated for $C_{17}H_{26}Cl_3N_2O_{11}$ $(M + NH_4)^+$: 539.0597, found 539.0621.

(2-Deoxy-2-acetamido-1,3,4,6-tetra-*O*-acetyl)-α/β-D-glucopyranoside (2.30)[256]

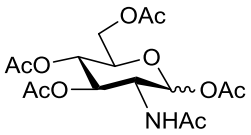

D (+) -Glucosamine hydrochloride (3.00 g, 1.4 mmol) was suspended in pyridine (30 mL). To this suspension, acetic anhydride (4.2 mL, 44.7 mmol) was added slowly at 0 ˚C. The reaction mixture was allowed to reach rt and stirred for 48 h. The solvent was evaporated under reduced pressure. The resulting residue was dissolved in DCM, and washed with 0.5 M HCl, and twice with sat. $NaHCO_3$ solution, followed by H_2O, dried ($MgSO_4$), and filtered. The solvent was evaporated using a rotary evaporator, and the crude product was crystallized (Hex and EtOAc) to give peracetylated derivative **2.30** as a white solid (1.82 g, 34 %). Spectroscopic data was in agreement with reported values.

R_f: 0.2 (Hex:EtOAc, 1:2); ^{1}H-NMR: ($CDCl_3$, 300 MHz): δ = 6.18 (d, 1 H, *H*-1, *J* = 3 Hz), 5.53 (d, 1 H, N-*H*, *J* = 9 Hz), 5.24-5.20 (m, 2 H, overlapping *H*-3 and *H*-4), 4.52-4.46 (m, 1 H, *H*-2), 4.28-4.22 (dd, 1 H, H-6_a, *J* = 6 Hz, 12 Hz), 4.09-4.04 (dd, 1 H, H-6_b, *J* = 3 Hz, 12 Hz), 4.01-3.98 (m, 1 H, *H*-5), 2.19, 2.09, 2.05, 2.04, 1.94 (each s, 15 H, NHC(O)CH_3 and OC(O)CH_3); (Lit[256]: ^{1}H-NMR: ($CDCl_3$, 400 MHz): δ = 6.31, 5.70, 5.45, 5.24, 5.15-5.06, 4.27, 4.11-4.06, 3.83, 2.16, 2.10, 2.07, 2.02, 2.01, 2.00); ^{13}C-NMR: ($CDCl_3$, 75 MHz): δ = 171.7, 170.7, 169.9, 169.1, 168.6 (each s, NH*C*(O)CH_3 and O*C*(O)CH_3), 90.7 (d, *C*-1), 70.7 (d, *C*-4), 69.7 (d, *C*-5), 67.5 (d, *C*-3), 61.5 (t, *C*-6), 51.1 (d, *C*-2), 23.1, 20.9, 20.7, 20.7, 20.6 (each q, C(O)*C*H_3); m.p.: 134-136 ˚C; IR: (KBr disc) 3439, 2953, 1741, 1674, 1519, 1241 cm^{-1}; MS-ESI/TOF: Calculated for $C_{16}H_{27}N_2O_{10}$ $(M + NH_4)^+$: 407.1660, found 407.1676.

(2-Deoxy-1-(*O*:2-*N*,*N*-ethylidyne)-3,4,6-tri-*O*-acetyl)-α-D-glucopyranoside (2.32)[94]

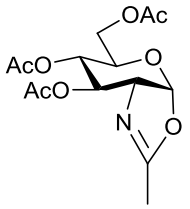

Peracetylated glucosamine **2.30** (800 mg, 2.1 mmol) was dissolved in dry DCM (4 mL). HBr (33 % solution in AcOH) (4.0 mL, 70 mmol) was added to the reaction mixture at 0 ˚C. The reaction mixture was allowed to reach rt, and stirred overnight. The solvent was co-evaporated with toluene under reduced pressure, and the remaining residue was dissolved in DCM, and washed with sat. $NaHCO_3$ solution, followed by brine, then dried ($MgSO_4$), and filtered. The organic layer was concentrated under reduced pressure, and the crude product was purified by column chromatography (Hex:EtOAc, 1:2) to give compound **2.32** as a yellow oil (300 mg, 44 %). Spectroscopic data was in agreement with reported values.

R_f: 0.1 (Hex:EtOAc, 1:2); ^{1}H NMR: ($CDCl_3$, 300 MHz) δ = 5.98 (d, 1 H, *H*-1, *J* = 9 Hz), 5.26 (t, 1 H, *H*-3, *J* = 6 Hz), 4.95-4.91 (m, 1 H, *H*-4), 4.18-4.08 (m, 3 H, overlapping *H*-2 and *H*-6), 3.64-3.58 (m, 1 H, *H*-5), 2.11, 2.10, 2.09, 2.08 (each s, 12 H, N(C)CH_3 and OC(O)CH_3); (Lit[94]: ^{1}H NMR: ($CDCl_3$, 60 MHz) δ = 5.9, 5.2, 4.9, 4.2, 4.1, 3.6, 2.1); IR: (DCM film on NaCl plate) 3340, 2959, 1747, 1660, 1543, 1230 cm^{-1}; MS-ESI/TOF: Calculated for $C_{14}H_{20}NO_8$ $(M + H)^+$: 330.1183, found 330.1192.

(2-Deoxy-2-[(2,2,2-trichloroethoxycarbonyl)amino]-3,4,6-tri-*O*-acetyl)-α/β-D-glucopyranose (2.33)[89]

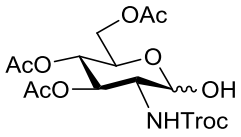

Method A

To a solution of protected glycoside **2.26** (2.46 g, 4.7 mmol) in THF (15 mL) benzylamine (0.62 mL, 5.6 mmol) was added. The reaction mixture was allowed to

stir at 50 ˚C overnight. The solvent was evaporated under reduced pressure to leave a brown oil. This residue was dissolved in DCM, then washed with 0.5 M HCl and brine, then dried ($MgSO_4$), and filtered. The organic layer was concentrated under reduced pressure, and the remaining residue was then purified by column chromatography (Hex:EtOAc, 1:1) to give hemiacetal **2.33** as a white solid (1.98 g, 88 %). Spectroscopic data was in agreement with reported values.

Method B

To a solution of protected glycoside **2.26** (5.00 g, 9.5 mmol) in THF (60 mL) dimethylamine (2 M solution in THF, 9.5 mL, 19.1 mmol) was added. The reaction mixture was allowed to stir at 80 ˚C overnight. The solvent was evaporated under reduced pressure to leave a brown oil. This residue was dissolved in DCM, and washed with 1.0 M HCl, followed by brine, then dried ($MgSO_4$), and filtered. The organic layer was concentrated under reduced pressure, and the remaining residue was purified by column chromatography (Hex:EtOAc, 1:1) to give hemiacetal **2.33** as a white solid (3.69 g, 81 %). Spectroscopic data was in agreement with reported values.

Method C

Protected glycoside **2.26** (2.66 g, 5.1 mmol) and hydrazine acetate (550 mg, 6.0 mmol) were dissolved in anhydrous DMF, under N_2. The reaction mixture was stirred at rt for 2 h, then further hydrazine acetate (230 mg, 2.6 mmol) was added. This was allowed to stir at rt for 2.5 h. The reaction mixture was diluted with EtOAc (20 mL), and this was washed twice with H_2O. The organic layer was dried ($MgSO_4$), and filtered, then concentrated under reduced pressure to give hemiacetal **2.33** as a white solid (2.40 g crude, 98 %), which was used without further purification. Spectroscopic data was in agreement with reported values.

R_f: 0.4 and 0.5 (α and β anomers respectively, Hex:EtOAc, 1:1); ^{1}H NMR: ($CDCl_3$, 300 MHz) δ = 5.66 (d, 1 H, N*H*C(O)OCH_2, *J* = 9 Hz), 5.37-5.30 (m, 2 H, overlapping *H*-1 and *H*-3), 5.12 (t, 1 H, *H*-4, *J* = 9 Hz), 4.83 (d, 1 H, NHC(O)OCH_{2a}, *J* = 12 Hz), 4.63 (d, 1 H, NHC(O)OCH_{2b}, *J* = 12 Hz), 4.26-4.01 (m, 4 H, overlapping *H*-2, *H*-5, and *H*-6), 2.10, 2.04, 2.01 (each s, 9 H, OC(O)CH_3); (Lit[89]: ^{1}H NMR: ($CDCl_3$, 250 MHz) δ = 5.48-5.09, 4.83-4.61, 4.29-4.01, 3.65, 2.21-2.01); ^{13}C NMR:

($CDCl_3$, 75 MHz) δ = 171.6, 171.1, 169.6 (each s, O*C*(O)CH_3), 154.3 (s, NH*C*(O)OCH_2), 95.4 (s, *C*Cl_3), 91.6 (d, *C*-1), 74.5 (t, NHC(O)O*C*H_2), 70.8 (d, *C*-5), 68.3 (d, *C*-3), 67.6 (d, *C*-4), 62.0 (t, *C*-6), 54.2 (d, *C*-2), 21.0, 20.7, 20.6 (each t, OC(O)*C*H_3); IR: (KBr disc) 3583, 3338, 2958, 1747, 1235 cm^{-1}; MS-ESI/TOF: Calculated for $C_{15}H_{24}Cl_3N_2O_{10}$ $(M + NH_4)^+$: 497.0491, found 497.0509.

(2-Deoxy-2-[(2,2,2-trichloroethoxycarbonyl)amino]-3,4,6-tri-*O*-acetyl-1-trichloroacetimido)-α-D-glucopyranoside (2.34)[257]

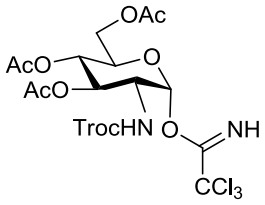

Method A

Hemiacetal **2.33** (1.60 g, 3.3 mmol) was placed under N_2, in the presence of 4 Å molecular sieves, and dissolved in dry DCM (15 mL). Cl_3CCN (2.34 mL, 2.33 mmol) was added dropwise. NaH (60 % in mineral oil) (66 mg, 1.6 mmol) was carefully added to the reaction mixture, which was allowed to stir under N_2, at rt for 1 h. The reaction mixture was filtered through celite (prewashed with wet DCM). The solvent was evaporated under reduced pressure to leave a brown oil, which was purified by column chromatography (Hex:EtOAc, 2:1) to give imidate derivative **2.34** as a yellow oil (1.77 g, 86 %). Spectroscopic data was in agreement with reported values.

Method B

Hemiacetal **2.33** (3.37 g, 7.03 mmol) was placed under N_2, in the presence of 4Å molecular sieves, and dissolved in dry DCM (40 mL). Cl_3CCN (5.03 mL, 49 mmol) was added dropwise, followed by addition of DBU (0.26 mL, 1.75 mmol). The reaction mixture was allowed to stir at rt for 4 h. The reaction was filtered to remove the molecular sieves, and the solvent was evaporated under reduced pressure. The remaining residue was purified by column chromatography (Hex:EtOAc, 2:1 to 1:1) to give imidate derivative **2.34** as a yellow oil (2.73 g, 72 %). Spectroscopic data was in agreement with reported values.

R_f: 0.6 (Hex:EtOAc, 2:1); ^{1}H NMR: ($CDCl_3$, 300 MHz) δ = 8.81 (s, 1 H, C(N*H*)), 6.43 (d, 1 H, *H*-1, *J* = 3 Hz), 5.39-5.21 (m, 3 H, overlapping *H*-3, *H*-4, and N*H* C(O)OCH_2), 4.72 (d, 2 H, NHC(O)OCH_2, *J* = 3 Hz), 4.31-4.25 (m, 2 H, overlapping *H*-2 and *H*-6_a), 4.10-4.16 (m, 2 H, overlapping *H*-5 and *H*-6_b), 2.08, 2.06, 2.04 (each s, 9 H, OC(O)CH_3); (Lit[257]: ^{1}H NMR: ($CDCl_3$, 400 MHz) δ = 8.80, 6.42, 5.35, 5.25, 5.19, 4.73, 4.70, 4.29, 4.28, 4.12, 2.08, 2.06); ^{13}C NMR: ($CDCl_3$, 75 MHz) δ = 170.6 (s, *C*(NH)), 169.3 (s, NH*C*(O)OCH_2), 160.4, 160.4, 154.1 (each s, O*C*(O)CH_3), 95.2 (s, *C*Cl_3), 94.5 (d, *C*-1), 90.6 (s, *C*Cl_3), 74.6 (t, NHC(O)OCH_2), 70.3, 70.3 (each s, *C*-5 and *C*-3), 67.4 (s, *C*-4), 61.4 (t, *C*-6), 53.9 (s, *C*-2), 21.0, 20.7, 20.6 (each q, OC(O)*C*H_3); IR: (DCM film on a NaCl plate) 3336, 3000, 1728, 1235 cm^{-1}; MS-ESI/TOF: Calculated for $C_{17}H_{20}Cl_6N_2NaO_{10}$ $(M + Na)^+$: 644.9141, found 644.9163.

N^{α}-[(1,1-Dimethylethoxy)carbonyl]-*O*-[(2-deoxy-2-[(2,2,2-trichloroethoxy carbonyl)amino]-3,4,6-tri-*O*-acetyl)-β-D-glucopyranosyl]-L-serine (2.38)

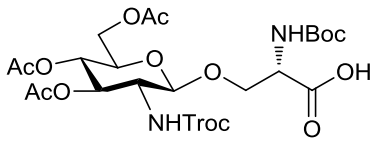

Glycoside **2.22** (100 mg, 0.13 mmol) was dissolved in distilled EtOAc (5 mL) and placed under N_2. 10 % Pd/C (w/w) (10 mg) was added to the reaction mixture, and the flask was placed under H_2. The reaction mixture was allowed to stir at rt for 1.5 h. The Pd/C was filtered off over celite. The solvent was evaporated under reduced pressure, and the remaining residue was dissolved in DCM and washed twice with H_2O, then dried ($MgSO_4$), and filtered to give the free acid **2.38** as a white foam (70 mg, 75 %).

R_f: 0.3 (DCM:MeOH, 9:1); ^{1}H NMR: ($CDCl_3$, 300 MHz) δ = 5.72 (s, 1 H, N*H*C(O)OCH_2), 5.52 (s, 1 H, N*H*C(O)OC$(CH_3)_3$), 5.32-5.25 (m, 1 H, *H*-3), 5.06 (t, 1 H, *H*-4, *J* = 9 Hz), 4.81 (d, 1 H, NHC(O)OCH_{2a}, *J* = 12 Hz), 4.73-4.66 (m, 2 H, overlapping NHC(O)OCH_{2b} and *H*-1), 4.46 (s, 1 H, α-*H*), 4.26-4.08 (m, 3 H, overlapping β-H_a, and *H*-6), 3.92 (d, 1 H, β-H_b, *J* = 9 Hz), 3.73-3.65 (m, 2 H, overlapping *H*-5 and *H*-2), 2.10, 2.04, 2.03 (each s, 9 H, OC(O)CH_3), 1.46 (s, 9 H, C(C$H_3)_3$); ^{13}C NMR: ($CDCl_3$, 75 MHz) δ = 173.2 (s, *C*(O)OH), 171.1, 170.7, 169.6 (each s, O*C*(O)CH_3), 155.9 (s, NH*C*(O)OCH_2), 154.4 (s, NH*C*(O)OC$(CH_3)_3$), 101.1 (d, *C*-1), 95.5 (s, *C*Cl_3), 80.6 (s, *C*$(CH_3)_3$), 74.5 (t, NHC(O)OCH_2), 71.9 (d,

overlapping *C*-5 and *C*-3), 69.6 (t, β-*C*), 68.6 (d, *C*-4), 62.0 (t, *C*-6), 55.9 (d, *C*-2), 53.7 (d, α-*C*), 28.3 (q, C(*C*H_3)$_3$), 20.8, 20.6, 19.2 (each q, OC(O)*C*H_3); IR: (DCM film on NaCl plate) 3410, 2980, 2127, 1652, 1250 cm^{-1}; $[\alpha]_D$: + 9.3 (*c* 1.5, CH_2Cl_2); MS-ESI/TOF: Calculated for $C_{46}H_{67}Cl_6N_4O_{28}$ $(2M + H)^+$: 1333.2068, found 1333.2131.

N^{α}-[(1,1-Dimethylethoxy)carbonyl]-*O*-[(2-deoxy-2-[(2,2,2-trichloroethoxy carbonyl)amino]-3,4,6-tri-*O*-acetyl)-β-D-glucopyranosyl]-L-serine-tetradecylamide (2.39)

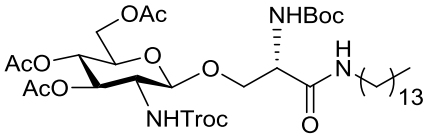

Free acid **2.38** (73 mg, 0.11 mmol) was placed under N_2, and dissolved in anhydrous DMF (2 mL). To this solution, HOBt (16 mg, 0.12 mmol) and TBTU (38 mg, 0.12 mmol) were added and allowed to stir for 5 mins. Tetradecylamine (25 mg, 0.12 mmol) and Et_3N (0.02 mL, 0.13 mmol) were added to the reaction mixture. This was allowed to stir at rt overnight. The solvent was evaporated under reduced pressure, and the remaining residue was dissolved in DCM. The organic layer was washed with 0.5 M HCl, followed by brine, then dried ($MgSO_4$), and filtered. The organic layer was concentrated under reduced pressure, and the crude product was purified by column chromatography (Hex:EtOAc, 1:2) to give the tetradecyl derivative **2.39** as a clear oil (72 mg, 77 %).

R_f: 0.3 (Pet. Ether: EtOAc, 1:1); ^{1}H NMR: ($CDCl_3$, 300 MHz) δ = 6.52 (s, 1 H, C(O)N*H*CH_2), 5.67 (d, 1 H, N*H*C(O)OCH_2, *J* = 9 Hz), 5.45 (s, 1 H, N*H*C(O)OC$(CH_3)_3$), 5.25 (t, 1 H, *H*-3, *J* = 9 Hz), 5.04 (t, 1 H, *H*-4, *J* = 9 Hz), 4.82 (d, 1 H, NHC(O)OCH_{2a}, *J* = 12 Hz), 4.70 (d, 1 H, *H*-1, *J* = 9 Hz), 4.63 (d, 1 H, NHC(O)OCH_{2b}, *J* = 12 Hz), 4.28-4.16 (m, 3 H, overlapping α-*H* and *H*-6) 4.05-4.02 (m, 1 H, β-H_a), 3.80-3.69 (m, 3 H, overlapping β-H_b, *H*-5 and *H*-2), 3.24 (d, 2 H, C(O)NHCH_2, *J* = 9 Hz), 2.09, 2.04, 2.02 (each s, 9 H, OC(O)CH_3), 1.44 (s, 9 H, C(CH_3)$_3$), 1.25 (m, 24 H, (CH_2)$_{12}$), 0.87 (t, 3 H, CH_2CH_3, *J* = 6 Hz); ^{13}C NMR: ($CDCl_3$, 75 MHz) δ = 170.7, 169.6, 169.5 (each s, O*C*(O)CH_3 and *C*(O)NHCH_2), 155.4 (s, NH*C*(O)OCH_2), 154.4 (s, NH*C*(O)OC$(CH_3)_3$), 102.1 (d, *C*-1), 95.5 (s, *C*Cl_3), 80.3 (s, O*C*$(CH_3)_3$), 74.5 (t, NHC(O)O*C*H_2), 72.0 (d, overlapping *C*-3 and *C*-

5), 70.4 (t, β-*C*), 68.4 (d, *C*-4), 61.8 (t, *C*-6), 56.1 (d, *C*-2), 53.6 (d, α-*C*), 38.7, 31.9, 29.7, 29.7, 29.6, 29.4, 29.3, 29.3, 26.9, 23.7, 23.0, 22.7 (each t, CH_2), 28.3 (q, $C(CH_3)_3$), 20.7, 20.6 (each q, $OC(O)CH_3$), 14.1 (q, CH_2CH_3); IR: (DCM film on NaCl plate) 3329, 2925, 1749, 1654, 1552, 1235 cm^{-1}; $[\alpha]_D$: + 10 (*c* 0.6, CH_2Cl_2); MS-ESI/TOF: Calculated for $C_{37}H_{63}Cl_3N_3O_{13}$ $(M + H)^+$: 862.3421, found 862.3434.

N^{α}-[(1,1-Dimethylethoxy)carbonyl]-*O*-[(2-deoxy-2-[(2,2,2-trichloroethoxy carbonyl)amino]-3,4,6-tri-*O*-acetyl)-β-D-glucopyranosyl]-L-serine-propylamide (2.50)

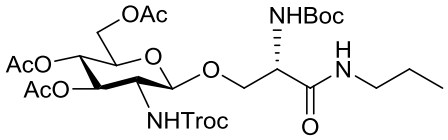

Free acid **2.38** (124 mg, 0.19 mmol) was placed under N_2, and dissolved in anhydrous DCM (10 mL). To this solution, HOBt (27 mg, 0.20 mmol) and TBTU (65 mg, 0.20 mmol) were added and allowed to stir for 5 mins. Propylamine (0.02 mL, 0.20 mmol) and Et_3N (0.03 mL, 0.22 mmol) were added to the reaction mixture, and this was allowed to stir at rt overnight. The solvent was evaporated, and the remaining residue was dissolved in DCM. The organic layer was washed with 0.5 M HCl, followed by brine, then dried ($MgSO_4$), and filtered. The organic layer was concentrated under reduced pressure, and the remaining residue was purified by column chromatography (Hex:EtOAc, 1:2) to give the propyl derivative **2.50** as a white paste (70 mg, 87 %).

R_f: 0.5 (Hex:EtOAc, 1:2); ^{1}H NMR: ($CDCl_3$, 300 MHz) δ = 6.52 (bs, 1 H, $C(O)NHCH_2$), 5.58-5.41 (m, 2 H, overlapping peaks $NHC(O)OCH_2$ and $NHC(O)OC(CH_3)_3$), 5.30-5.20 (m, 1 H, *H*-3), 5.10-5.01 (m, 1 H, *H*-4), 4.83- 4.58 (m, 3 H, overlapping $NHC(O)OCH_2$ and *H*-1), 4.30-4.08 (m, 3 H, overlapping α-*H* and *H*-6), 4.01-3.90 (m, 1 H, β-H_a), 3.76-3.64 (m, 3 H, overlapping β-H_b, *H*-5, and *H*-2), 3.28-3.20 (m, 2 H, $NHCH_2$), 2.09, 2.04, 2.02 (each s, 9 H, $OC(O)CH_3$), 1.58-1.49 (m, 2 H, $NHCH_2CH_2$), 1.44 (s, 9 H, $C(CH_3)_3$), 0.94 (t, 3 H, CH_2CH_3, *J* = 6 Hz); ^{13}C NMR: ($CDCl_3$, 75 MHz) δ = 170.8, 170.7, 169.7, 169.5 (each s, $OC(O)CH_3$ and $C(O)NHCH_2$), 154.4 (s, $NHC(O)OCH_2$), 154.4 (s, $NHC(O)OC(CH_3)_3$), 102.1 (d, *C*-1), 95.4 (s, CCl_3), 80.4 (s, $OC(CH_3)_3$), 74.5 (t, $NHC(O)OCH_2$), 72.1 (t, β-*C*), 72.0, 71.9 (each d, *C*-3 and *C*-5), 68.4 (d, *C*-4), 61.9 (t, *C*-6), 56.2 (d, *C*-2), 52.9 (d, α-*C*),

41.5 (t, C(O)NH*C*H_2), 28.5 (q, C(*C*H_3)$_3$), 22.6 (t, C(O)NHCH$_2$*C*H_2), 20.8, 20.7, 20.7 (each q, OC(O)*C*H_3), 11.3 (q, CH_2*C*H_3); IR: (DCM film on NaCl plate) 3326, 2967, 1749, 1654, 1538, 1235 cm^{-1}; $[\alpha]_D$: - 2.7 (*c* 0.75, CH_2Cl_2); MS-ESI/TOF: Calculated for $C_{26}H_{41}Cl_3N_3O_{13}$ $(M + H)^+$: 712.1657, found 712.1689.

_O_-[(2-Deoxy-2-[(2,2,2-trichloroethoxycarbonyl)amino]-3,4,6-tri-_O_-acetyl)-β-D-glucopyranosyl]-L-serine-propylamide (2.51)

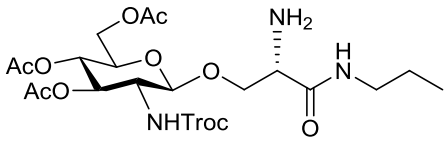

Propyl derivative **2.50** (13 mg, 0.02 mmol) was dissolved in DCM (2 mL) and cooled to 0 °C. A 50 % (v/v) solution of TFA in DCM (0.03 mL, 1.42 mmol) was added to the reaction mixture, and this was allowed to return to rt, then stirred at rt overnight. The reaction mixture was washed with a sat. solution of $NaHCO_3$, followed by brine. The organic layer was dried ($MgSO_4$), filtered, and concentrated under reduced pressure. The remaining residue was purified by column chromatography (Hex:EtOAc, 1:1 to 1:3) to give the free amine **2.51** as a clear oil (9 mg, 97 %).

R_f: 0.53 (DCM:MeOH, 9:1); ^{1}H NMR: ($CDCl_3$, 300 MHz) δ = 7.51-7.42 (m, 1 H, C(O)N*H*CH_2), 5.48 (d, 1H, N*H*C(O)CH_2, *J* = 9 Hz), 5.24 (t, 1 H, *H*-3, *J* = 6 Hz), 5.07 (t, 1 H, *H*-4, *J* = 9 Hz), 4.84-4.59 (m, 3 H, overlapping NHC(O)*C*H_2 and *H*-1), 4.30-4.23 (dd, 1 H, *H*-6$_a$, *J* = 6 Hz, 15 Hz), 4.16-4.11 (m, 1 H, *H*-6$_b$), 4.06-3.92 (m, 2 H, β-*H*), 3.70-3.62 (m, 2 H, overlapping *H*-2 and *H*-5), 3.52-3.49 (m, 1 H, α-*H*), 3.22-3.10 (m, 2 H, C(O)NHC*H*$_2$), 2.09, 2.03 (each s, 9 H, OC(O)C*H*$_3$), 1.91 (bs, 2 H, N*H*$_2$), 1.57-1.50 (m, 2 H, NHCH$_2$C*H*$_2$), 0.93 (t, 3 H, CH_2C*H*$_3$, *J* = 9 Hz); ^{13}C NMR: ($CDCl_3$, 75 MHz) δ = 169.7, 168.4, 100.1, 94.4, 73.5, 70.9, 67.6, 60.9, 58.0, 55.1, 53.9, 40.1, 29.9, 21.7, 19.7, 19.6, 10.4; $[\alpha]_D$: - 4.4 (*c* 0.45, CH_2Cl_2); MS-ESI/TOF: Calculated for $C_{42}H_{64}Cl_6N_6NaO_{22}$ $(2M + Na)^+$: 1237.2097, found 1237.2160.

_O_-[(2-Deoxy-2-[(2,2,2-trichloroethoxycarbonyl)amino]-3,4,6-tri-_O_-acetyl)-β-D-glucopyranosyl]-L-serine-phenylmethyl ester (2.52)

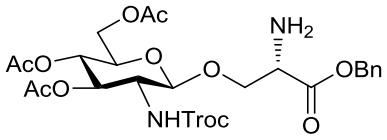

Protected glycoside **2.22** (200 mg, 0.26 mmol) was placed under N_2, and dissolved in dry DCM (5 mL). A 50 % (v/v) solution of TFA in DCM (0.4 mL, 2.63 mmol) was added to the reaction at 0 ˚C, and allowed to stir for 1 h. The solvent was evaporated under reduced pressure to leave a yellow oil. The reaction mixture was purified by column chromatography (Hex:EtOAc, 2:1 to 1:1 to MeOH) to give free amine **2.52** as a yellow oil (160 mg, 90 %).

R_f: 0.53 (DCM:MeOH, 9:1); ^{1}H NMR: (CD_3OD, 300 MHz) δ = 7.43-7.39 (m, 5 H, Ph-*H*), 5.32 (s, 2 H, Ph-C*H*$_2$), 5.24 (t, 1 H, *H*-3, *J* = 9 Hz), 4.98 (t, 1 H, *H*-4, *J* = 9 Hz), 4.92-4.82 (Overlapped by H_2O peak: N*H*$_2$, N*H*C(O)OCH$_2$ and NHC(O)OC*H*$_{2a}$), 4.75 (d, 1 H, *H*-1, *J* = 9 Hz), 4.66 (d, 1 H, NHC(O)OC*H*$_{2b}$, *J* = 12 Hz), 4.36-4.35 (m, 1 H, α-*H*), 4.30-4.28 (m, 1 H, β-*H*$_a$), 4.25-4.24 (m, 1 H, *H*-6$_a$), 4.16-4.15 (m, 1 H, *H*-6$_b$), 4.12-4.11 (m, 1 H, β-*H*$_b$), 3.76-3.73 (m, 1 H, *H*-5), 3.68-3.62 (m, 1 H, *H*-2), 2.02 (s, 6 H, OC(O)C*H*$_3$), 1.99 (s, 3 H, OC(O)C*H*$_3$); ^{13}C NMR: (CD_3OD, 75 MHz) δ = 170.9, 170.2, 169.6 (each s, O*C*(O)CH$_3$), 166.6 (s, *C*(O)OBn), 155.5 (s, NH*C*(O)OCH$_2$), 134.9 (s, Ph-*C*), 128.4, 128.3, 128.2 (each d, Ph-*C*H), 100.1 (d, *C*-1), 95.6 (s, *C*Cl$_3$), 74.1 (t, NHC(O)O*C*H$_2$), 72.3 (d, *C*-3), 71.7 (d, *C*-5), 68.5 (d, *C*-4), 68.0 (t, Ph-*C*H$_2$), 66.0 (t, β-*C*), 61.6 (t, *C*-6), 55.4 (d, *C*-2), 52.9 (d, α-*C*), 19.3, 19.2, 19.2 (each q, OC(O)*C*H$_3$); IR (DCM film on NaCl plate): 2917, 1750, 1677, 1206 cm^{-1}; $[\alpha]_D$: - 2.4 (*c* 0.83, CH_2Cl_2); MS-ESI/TOF: Calculated for $C_{25}H_{32}Cl_3N_2O_{12}$ $(M + H)^+$: 657.1015, found 657.1026.

N^{α}-(1-Oxodecyl)-*O*-[(2-deoxy-2-[(2,2,2-trichloroethoxycarbonyl)amino]-3,4,6-tri-*O*-acetyl)-β-D-glucopyranosyl]-L-serine-phenylmethyl ester (2.53)

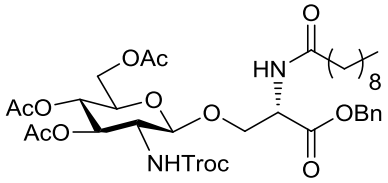

Decanoic acid (20 mg, 0.13 mmol), TBTU (40 mg, 0.13 mmol), and HOBt (20 mg, 0.13 mmol) were dissolved in dry DCM (7 mL) under N_2, in the presence of 4Å molecular sieves. Et_3N (0.05 mL, 0.36 mmol) was added to the reaction mixture. This was allowed to stir at rt for 15 mins. A solution of free amine **2.52** (80 mg, 0.19 mmol) in dry DCM (10 mL), and THF (1 mL for solubility) was then added to the reaction mixture. This was allowed to stir at rt overnight. The solution was filtered to remove the molecular sieves, then washed with a sat. $NaHCO_3$ solution, and 1.0 M HCl. The organic layer was dried ($MgSO_4$), and filtered. The organic layer was concentrated under reduced pressure, and the remaining residue was purified by column chromatography (Hex:EtOAc, 1:1) to give the oxodecyl derivative **2.53** as a clear oil (80 mg, 88 %).

R_f: 0.4 (Hex:EtOAc, 1:1); ^{1}H NMR: ($CDCl_3$, 300 MHz) δ = 7.40-7.31 (m, 5 H, Ph-*H*), 6.49 (d, 1 H, N*H*C(O)CH_2, *J* = 6 Hz), 5.43 (d, 1 H, N*H*C(O)OCH_2, *J* = 9 Hz), 5.24-5.13 (m, 3 H, overlapping *H*-3 and Ph-CH_2), 5.02 (t, 1 H, *H*-4, *J* = 9 Hz), 4.84-4.64 (m, 4 H, overlapping NHC(O)OCH_2, *H*-1, and α-*H*), 4.26-4.20 (m, 2 H, overlapping *H*-6_a and β-H_a), 4.13-4.07 (m, 1 H, *H*-6_b), 3.92-3.87 (dd, 1 H, β-H_b, *J* = 3 Hz, 9 Hz), 3.62-3.52 (m, 2 H, overlapping *H*-5 and *H*-2), 2.25 (t, 2 H, NHC(O)CH_2, *J* = 6 Hz), 2.05-2.01 (m, 9 H, OC(O)CH_3), 1.61 (t, 2 H, C(O)CH_2CH_2, *J* = 9 Hz), 1.26-1.37 (m, 12 H, (CH_2)$_6$), 0.87 (t, 3 H, CH_2CH_3, *J* = 9 Hz); ^{13}C NMR: ($CDCl_3$, 75 MHz) δ = 173.5 (s, NH*C*(O)CH_2), 171.2 (s, *C*(O)OBn), 170.6, 169.7, 169.4 (each s, O*C*(O)CH_3), 154.3 (s, NH*C*(O)OCH_2), 135.2 (s, Ph-*C*), 128.6, 128.5, 128.3 (each d, Ph-*C*), 100.3 (d, *C*-1), 95.4 (s, *C*Cl_3), 74.5 (t, NHC(O)O*C*H_2), 71.9 (d, *C*-3), 71.8 (d, *C*-5), 69.1 (t, β-*C*), 68.4 (d, *C*-4), 67.5 (t, *C*H_2Ph), 61.9 (t, *C*-6), 56.2 (d, *C*-2), 52.3 (d, α-*C*), 36.4 (t, NHC(O)*C*H_2), 33.8, 31.9, 29.5, 29.4, 29.3, 29.3, 22.6 (each t, *C*H_2), 25.5 (t, NHC(O)CH_2*C*H_2), 20.7, 20.6 (each q, OC(O)*C*H_3), 14.1 (q, CH_2*C*H_3); IR: (DCM film on NaCl plate) 3308, 2927, 2855, 1752, 1655, 1536, 1234

cm^{-1}; $[\alpha]_D$: -1.1 (*c* 1.85, CH_2Cl_2); MS-ESI/TOF: Calculated for $C_{35}H_{49}Cl_3KN_2O_{13}$ $(M + K)^+$: 849.1932, found 849.1934.

N^{α}-(1-Oxodecyl)-*O*-[(2-deoxy-2-[(2,2,2-trichloroethoxycarbonyl)amino]-3,4,6-tri-*O*-acetyl)-β-D-glucopyranosyl]-L-serine (2.54)

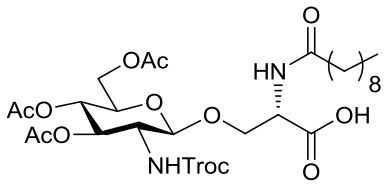

The oxodecyl derivative **2.53** (514 mg, 0.63 mmol) was dissolved in distilled EtOAc (15 mL) and placed under N_2. 10 % Pd/C (w/w) (100 mg) was added to the reaction mixture, and the flask was placed under H_2. The reaction mixture was allowed to stir at rt for 3 h. The reaction mixture was filtered through celite, and the solvent was evaporated under reduced pressure to give the free acid **2.54** as a clear oil (449 mg, 98 %).

R_f: 0.26 (DCM:MeOH, 9:1); ^{1}H NMR: ($CDCl_3$, 300 MHz) δ = 6.80 (s, 1 H, N*H*C(O)CH_2), 6.04 (s, 1 H, N*H*C(O)OCH_2), 5.25 (t, 1 H, *H*-3, *J* = 9 Hz), 5.07 (t, 1 H, *H*-4, *J* = 9 Hz), 4.85-4.65 (m, 4 H, overlapping NHC(O)OCH_2, *H*-1 and α-*H*), 4.25-4.22 (m, 3 H, overlapping *H*-6 and β-H_a), 3.99-3.97 (m, 1 H, β-H_b), 3.75-3.69 (m, 2 H, overlapping *H*-5 and *H*-2), 2.27-2.25 (m, 2 H, NHC(O)CH_2), 2.05-2.01 (m, 9 H, OC(O)CH_3), 1.61 (bs, 2 H, NHC(O)CH_2CH_2), 1.26 (m, 12 H, $(CH_2)_6$), 0.87 (t, 3 H, CH_2CH_3, *J* = 6 Hz); ^{13}C NMR: ($CDCl_3$, 75 MHz) δ = 183.6 (s, *C*(O)OH), 170.7, 169.5 (each s, O*C*(O)CH_3 and NH*C*(O)CH_2), 152.6 (s, NH*C*(O)OCH_2), 100.7 (d, *C*-1), 95.4 (s, *C*Cl_3), 74.6 (t, NHC(O)O*C*H_2), 71.9 (d, *C*-3 and *C*-5), 68.5 (d, *C*-4), 68.3 (t, β-*C*), 62.0 (t, *C*-6), 56.4 (d, *C*-2), 53.3 (d, α-*C*), 36.3 (t, NHC(O)*C*H_2), 31.9, 29.5, 29.4, 29.3, 22.6 (each t, *C*H_2), 25.4 (t, NHC(O)CH_2*C*H_2), 20.8, 20.6 (each q, OC(O)*C*H_3), 14.3 (q, CH_2*C*H_3); IR: (DCM film on NaCl plate) 3408, 2927, 2856, 1750, 1649, 1547, 1236 cm^{-1}; $[\alpha]_D$: - 4 (*c* 1.0, CH_2Cl_2); MS-ESI/TOF: Calculated for $C_{28}H_{44}Cl_3N_2O_{13}$ $(M + H)^+$: 721.1903, found 721.1933.

N^{α}-(1-Oxodecyl)-*O*-[(2-deoxy-2-[(2,2,2-trichloroethoxycarbonyl)amino]-3,4,6-tri-*O*-acetyl)-β-D-glucopyranosyl]-L-serine-tetradecylamide (2.55)

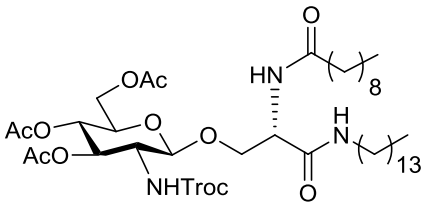

Free acid **2.54** (40 mg, 0.06 mmol), TBTU (20 mg, 0.06 mmol), and HOBt (8 mg, 0.06 mmol) were dissolved in anhydrous DCM (5 mL) under N_2, in the presence of 3Å molecular sieves. The reaction mixture was allowed to stir at rt for 15 mins. A solution of tetradecylamine (13 mg, 0.06 mmol) in anhydrous DCM (3 mL) was then added, and the reaction mixture was allowed to stir at rt overnight. The solvent was evaporated under reduced pressure, and the remaining residue was washed with 1.0 M HCl, dried ($MgSO_4$), and filtered. The organic layer was concentrated using a rotary evaporator, and the crude product was purified by column chromatography (Hex:EtOAc, 1:1) to give glycolipid derivative **2.55** as a cream solid (16 mg, 13 %).

N^{α}-(1-Oxodecyl)-β-dehydroxy-(β,β-dibromo)-L-dehydroserine (2.58)

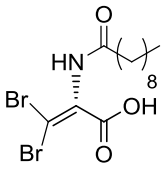

The free acid **2.54** (40 mg, 0.05 mmol) was dissolved in anhydrous DCM (3 mL). To this was added HOBt (7.4 mg, 0.06 mmol), TBTU (17 mg, 0.06 mmol), Et_3N (0.01 mL, 0.06 mmol) and NBS (19 mg, 0.11 mmol). The reaction mixture was allowed to stir at rt for 2 h, then washed with H_2O. The organic layer was reduced using a rotary evaporator, to leave the crude dibrominated product **2.58** and hemiacetal **2.33**.

N^{α}-(N^{α}-[(1,1-Dimethylethoxy)carbonyl]-L-leucine-)-*O*-[(2-deoxy-2-[(2,2,2-trichloroethoxycarbonyl)amino]-3,4,6-tri-*O*-acetyl)-β-D-glucopyranosyl]-L-serine (2.59)

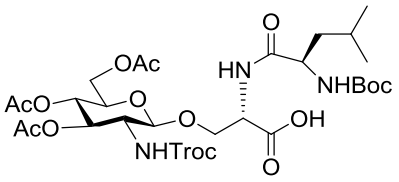

N^{α}-[(1,1-Dimethylethoxy)carbonyl]-L-leucine (38 mg, 0.17 mmol), TBTU (53 mg, 0.17 mmol), and HOBt (22 mg, 0.17 mmol) were dissolved in dry DCM (10 mL) under N_2, in the presence of 4 Å molecular sieves. Et_3N (0.06 mL, 0.45 mmol) was added to the reaction mixture. This was allowed to stir at rt for 15 mins. A solution of free amine **2.52** (89 mg, 0.13 mmol) in dry DCM (5 mL), and THF (1 mL to aid solubility) was then added to the reaction mixture. This was allowed to stir at rt overnight. The solution was filtered to remove the molecular sieves, then washed with a sat. $NaHCO_3$ solution, followed by 1.0 M HCl. The organic layer was dried ($MgSO_4$), and filtered. The organic layer was concentrated under reduced pressure, and the remaining residue was purified by column chromatography (Hex:EtOAc, 1:1) to give the benzylated glycoside as a clear oil (64 mg, 56 %).

R_f: 0.8 (Pet. Ether:EtOAc, 1:1); ^{1}H NMR: ($CDCl_3$, 300 MHz) δ = 7.36-7.34 (m, 5 H, Ar-*H*), 7.13, 6.78 (each d, 1 H, N-*H*, *J* = 6 Hz), 7.01, 6.70 (each d, 1 H, N-*H*, *J* = 9 Hz), 5.03-4.96 (m, 7 H, overlapping including ph-CH_2, *H*-3, *H*-4, N-*H*, and β-H_a), 4.62-4.58 (m, 2 H, overlapping α-*H* and β-H_b), 4.50-4.47 (m, 1 H, *H*-6_a), 4.41-4.21 (m, 5 H, overlapping *H*-1, NHC(O)CH_{2a}, β-H_a (Leu), α-*H* (Leu), and *H*-6_b), 4.08-4.00 (m, 3 H, overlapping including β-H_b (Leu) and NHC(O)CH_{2b}), 3.87-3.77 (m, 1 H, *H*-5), 3.57-3.49 (m, 1 H, *H*-2), 2.04, 2.02, 1.99 (each s, 9 H, OC(O)CH_3), 1.71-1.67 (m, 1 H, C*H*(CH_3)$_2$), 1.48 (s, 9 H, C(CH_3)$_3$), 0.96-0.83 (m, 6 H, CH(CH_3)$_2$); ^{13}C NMR: ($CDCl_3$, 75 MHz) δ = 170.7, 169.1, 134.9, 128.7, 128.4, 128.0, 103.3, 95.5, 80.7, 74.7, 72.2, 71.9, 68.7, 67.7, 62.0, 53.7, 83.4, 41.2, 31.5, 29.0, 28.4, 26.9, 24.8, 22.6, 20.8, 20.1, 18.8, 14.1; IR: (DCM film on NaCl plate) 3367, 2926, 1751, 1677, 1527, 1232 cm^{-1}; $[\alpha]_D$: + 6.7 (*c* 0.3, CH_2Cl_2); MS-ESI/TOF: Calculated for $C_{36}H_{50}Cl_3N_3NaO_{15}$ $(M + Na)^+$: 892.2200, found 892.2241.

The benzylated glycoside (58 mg, 0.07 mmol) was dissolved in EtOAc (8 mL) and 10 % Pd/C (w/w) (20 mg) was added. The reaction vessel was placed under a H_2 atmosphere, and the reaction mixture was stirred at rt for 3 h, then filtered over celite. The solvent was evaporated under reduced pressure, and the remaining residue was purified by column chromatography (EtOAc:Hex, 1:1 to MeOH). **2.59** was obtained as a white oily solid (30 mg, 60 %).

N^{α}-[(1,1-Dimethylethoxy)carbonyl]-L-serine-tetradecylamide (2.61)[258]

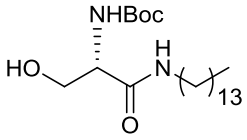

N^{α}-[(1,1-Dimethylethoxy)carbonyl]-L-serine (300 mg, 1.46 mmol) and TBTU (510 mg, 1.60 mmol) were dissolved in dry DCM (10 mL) under N_2, in the presence of 4Å molecular sieves. Et_3N (0.41 mL, 2.9 mmol) was added to the reaction mixture. This was allowed to stir at rt for 15 mins. A solution of tetradecylamine (342 mg, 1.6 mmol) in dry DCM (5 mL) was then added to the reaction mixture. This was allowed to stir at rt overnight. The solution was filtered to remove the molecular sieves, and washed with 1.0 M HCl, then dried ($MgSO_4$), and filtered. The organic layer was concentrated under reduced pressure, and the remaining residue was purified by column chromatography (Hex: EtOAc, 1:1) to give tetradecyl derivative **2.61** as a white solid (436 mg, 75 %). Spectroscopic data was in agreement with reported values.

R_f: 0.48 (Hex:EtOAc, 1:1); ^{1}H NMR: ($CDCl_3$, 300 MHz) δ = 6.82 (s, 1 H, C(O)N*H*CH_2), 5.68 (s, 1 H, N*H*C(O)OC$(CH_3)_3$), 4.13-4.06 (m, 2 H, overlapping α-*H* and β-H_a), 3.66-3.61 (m, 1 H, β-H_b), 3.33-3.12 (m, 3 H, overlapping NHCH_2 and CH_2O*H*), 1.49-1.46 (m, 11 H, overlapping NHCH$_2$CH_2 and C(C$H_3)_3$), 1.25 (m, 22 H, (C$H_2)_{11}$), 0.88 (t, 3 H, CH_2CH_3, J = 6 Hz); (Lit[258]: ^{1}H NMR: (DMSO-d_6, 60 MHz) δ = 7.70, 6.50, 4.76, 3.88, 3.52, 3.07, 1.40, 1.58-0.74); ^{13}C NMR: ($CDCl_3$, 75 MHz) δ = 169.6 (s, *C*(O)NHCH$_2$), 154.9 (s, NH*C*(O)OCH$_2$), 66.7 (t, β-*C*), 58.4 (d, α-*C*), 43.3 (t, C(O)NH*C*H$_2$), 35.7, 33.4, 33.4, 33.3, 33.2, 33.1, 33.0, 30.6, 26.4 (each t, *C*H$_2$), 32.1 (q, CH$_2$*C*H$_3$); IR: (DCM film on NaCl plate) 3403, 2921, 2851, 2112, 1653, 1529, cm^{-1}.

L-Serine-tetradecylamide (2.62)[258]

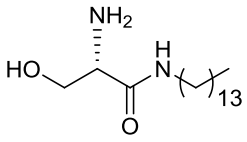

The Boc protected serine derivative **2.61** (436 mg, 1.09 mmol) was placed under N_2, and dissolved in dry DCM (10 mL). A 50 % solution (v/v) of TFA in DCM (1.68 mL, 10 mmol) was added to the reaction at 0 ˚C, and allowed to stir at rt for 5 h. The solvent was evaporated under reduced pressure, and the remaining residue was purified through a silica plug (Hex:EtOAc, 1:2 to MeOH) to give the free amine **2.62** as a white solid (300 mg, 91 %).

R_f: 0.1 (DCM:MeOH, 9:1); ^{1}H NMR: ($(CD_3)_2SO$, 300 MHz) δ = 8.32 (t, 1 H, C(O)N*H*CH_2, *J* = 6 Hz), 8.07 (s, 2 H, N*H*$_2$), 5.48 (s, 1 H, O*H*), 3.74-3.63 (m, 3 H, overlapping β-*H* and α-*H*), 3.13-3.07 (m, 2 H, C(O)NHC*H*$_2$), 1.41-1.39 (m, 2 H, C(O)NHCH$_2$C*H*$_2$), 1.24 (m, 22 H, (C*H*$_2$)$_{11}$), 0.86 (t, 3 H, CH$_2$C*H*$_3$, *J* = 6 Hz); (Lit[258]: ^{1}H NMR: ($(CD_3)_2SO$, 60 MHz) δ = 8.35, 8.11, 4.58, 3.71, 3.09, 1.53-0.67); ^{13}C NMR: ($(CD_3)_2SO$, 75 MHz) δ = 166.3 (s, *C*(O)NHCH$_2$), 60.2 (t, β-*C*), 54.2 (d, α-*C*), 31.1, 30.6, 28.8, 28.7, 28.5, 26.1, 21.9 (each t, *C*H$_2$), 13.8 (q, CH$_2$*C*H$_3$); MS-ESI/TOF: Calculated for $C_{16}H_{36}N_2O_2$ $(M + H)^+$: 301.285, found 301.286.

N^{α}-(1-Oxodecyl)-L-serine-tetradecylamide (2.63)[105]

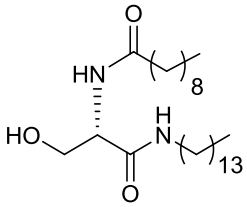

Decanoic acid (139 mg, 1.1 mmol) and TBTU (353 mg, 1.1 mmol) were dissolved in anhydrous DMF (7 mL), under N_2, in the presence of 4Å molecular sieves. Et_3N (0.27 mL, 2.0 mmol) was added to the reaction mixture. This was allowed to stir at rt for 15 mins. A solution of the free acid **2.62** (300 mg, 1.0 mmol) in anhydrous DMF (10 mL) was then added to the reaction mixture. This was allowed to stir at rt overnight. The molecular sieves were removed by filtration. The organic layer was concentrated under reduced pressure. The remaining residue was dissolved in DCM,

and washed with sat. $NaHCO_3$ solution, followed by brine, then dried ($MgSO_4$), and filtered. The organic layer was concentrated under reduced pressure, and the crude product was purified by column chromatography (Hex:EtOAc, 1:1) to give the lipid derivative **2.63** as a white solid (144 mg, 32 %). Spectroscopic data was in agreement with reported values.

R_f: 0.2 (Hex:EtOAc, 1:1); ^{1}H NMR: ($CDCl_3$, 300 MHz) δ = 6.87 (bs, 1 H, C(O)N*H*CH_2), 6.66 (d, 1 H, N*H*C(O)CH_2, *J* = 6 Hz), 4.42-4.36 (m, 2 H, overlapping CH_2O*H* and α-*H*), 4.14 (d, 1 H, β-H_a, *J* = 12 Hz), 3.61-3.56 (dd, 1 H, β-H_b, *J* = 3 Hz, 12 Hz), 3.30-3.19 (m, 2 H, C(O)NHCH_2), 2.33-2.25 (m, 2 H, NHC(O)CH_2), 1.76-1.61 (m, 2 H, NHC(O)CH_2CH_2), 1.48-1.44 (m, 2 H, NHCH_2CH_2), 1.25 (m, 34 H, CH_2 x 17), 0.88 (t, 6 H, CH_2CH_3); (Lit[105]: ^{1}H NMR: ($CDCl_3$, 250 MHz) δ = 6.83, 6.64, 4.45-4.30, 4.20-4.10, 3.70-3.50, 3.30-3.15, 2.30-2.15, 1.75-1.40, 1.40-1.15, 0.88); ^{13}C NMR: ($CDCl_3$, 75 MHz) δ = 174.5, 173.0 (each s, NH*C*(O)CH_2 and *C*(O)NHCH_2), 63.3 (t, β-*C*), 53.3 (d, α-*C*), 39.5 (t, C(O)NH*C*H_2), 36.4, 31.9, 31.9, 29.7, 29.6, 29.5, 29.4, 29.4, 29.3, 29.2, 26.9, 25.6, 22.7 (each t, *C*H_2), 14.1 (q, CH_2*C*H_3); MS-ESI/TOF: Calculated for $C_{27}H_{54}N_2O_3K_2$ $(M + 2K)^{+2}$ 266.1699, found 266.1683.

N^{α}-(Benzyloxycarbonyl)-L-serine-tetradecylamide (2.65)[43]

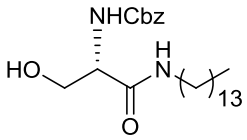

N^{α}-(Benzyloxycarbonyl)-L-serine (500 mg, 2.09 mmol), TBTU (738 mg, 2.29 mmol) and HOBt (309 mg, 2.29 mmol) were dissolved in dry DCM (25 mL), under N_2, in the presence of 4Å molecular sieves. Et_3N (0.58 mL, 4.18 mmol) was added to the reaction mixture. This was allowed to stir at room temp for 15 mins. A solution of tetradecylamine (488 mg, 2.29 mmol) in dry DCM (5 mL) was then added to the reaction mixture, and allowed to stir at rt overnight. The solution was filtered to remove the molecular sieves, then dissolved in DCM. The organic layer was washed with 1.0 M HCl, followed by brine, then dried ($MgSO_4$), and filtered. The organic layer was concentrated under reduced pressure, and the crude product was purified by column chromatography (Hex:EtOAc, 2:1 to 1:1) to give the tetradecyl derivative

2.65 as an off-white solid (500 g, 55 %). Spectroscopic data was in agreement with reported values.

R_f: 0.4 (Hex:EtOAc, 1:1); ^{1}H NMR: ($CDCl_3$, 300 MHz) δ = 7.37-7.31 (m, 5 H, Ph-*H*), 6.70 (s, 1 H, C(O)N*H*CH_2), 5.99 (d, 1 H, N*H*C(O)OBn, *J* = 6 Hz), 5.10 (s, 2 H, Ph-CH_2), 4.22-4.16 (m, 1 H, α-*H*), 4.07-4.03 (dd, 1 H, β-H_a, *J* = 3 Hz, 9 Hz), 3.77-3.63 (m, 2 H, overlapping β-H_b and CH_2O*H*), 3.24-3.17 (m, 2 H, NHCH_2), 1.44 (s, 2 H, NHCH_2CH_2), 1.25 (m, 22 H, (CH_2)$_{11}$), 0.87 (t, 3 H, CH_2CH_3, *J* = 12 Hz); (Lit[43]: ^{1}H NMR: ($CDCl_3$, 270 MHz) δ = 7.36, 5.14, 4.15, 3.65, 3.23, 1.47, 1.25, 0.88); ^{13}C NMR: ($CDCl_3$, 75 MHz) δ = 170.8 (s, *C*(O)NHCH_2), 156.8 (s, NH*C*(O)OBn), 135.9 (s, Ph-*C*), 128.6, 128.3, 128.0 (each d, Ph-*C*H), 67.3 (t, Ph-*C*H_2), 62.8 (t, β-*C*), 55.5 (d, α-*C*), 39.7 (t, C(O)NH*C*H_2), 31.9 (t, NHCH_2*C*H_2), 29.7, 29.6, 29.6, 29.5, 29.4, 29.3, 29.3, 26.8, 22.7 (each t, *C*H_2), 14.1 (q, CH_2*C*H_3); IR: (KBr disc) 3294, 2919, 2850, 1694, 1650, 1546, 1240 cm^{-1}; MS-ESI/TOF: Calculated for $C_{25}H_{43}N_2O_4$ (M + H)$^+$: 437.3278, found 437.3265.

N^{α}-(Benzyloxycarbonyl)-*O*-[(2-deoxy-2-[(2,2,2-trichloroethoxycarbonyl)amino]-3,4,6-tri-*O*-acetyl)-β-D-glucopyranosyl]-L-serine-tetradecylamide (2.67)

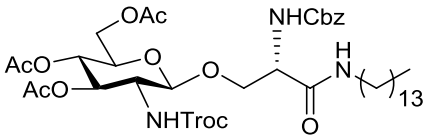

Imidate donor **2.34** (425 mg, 0.68 mmol) and protected serine derivative **2.65** (248 mg, 0.57 mmol) were placed under N_2, and dissolved in dry DCM (30 mL), in the presence of 3Å molecular sieves. A freshly made solution of 0.04 M TMSOTf (1.42 mL, 0.06 mmol) was added. The reaction was left to stir at rt overnight. The reaction was quenched by adding solid $NaHCO_3$ (100 mg) to the reaction mixture and allowed to stir for 5 mins. H_2O (50 mL) was added to the flask. The product was extracted twice with DCM. The organic layers were combined and washed with H_2O, dried ($MgSO_4$), and filtered to leave a brown, foamy oil. The crude product was purified by column chromatography (Hex:EtOAc, 2:1 to 1:1) to give glycoside **2.67** as an off-white solid (450 mg, 88 %).

R_f: 0.6 (Hex:EtOAc, 1:1); ^{1}H NMR: ($CDCl_3$, 300 MHz) δ = 7.39-7.31 (m, 5 H, Ph-*H*), 6.44 (s, 1 H, C(O)N*H*CH_2), 5.76 (s, 1 H, N*H*C(O)OBn), 5.46 (s, 1 H,

N*H*C(O)OCH_2), 5.25-5.00 (m, 4 H, overlapping *H*-3, *H*-4, and Ph-CH_2), 4.84-4.47 (m, 3 H, overlapping NHC(O)OCH_2 and *H*-1), 4.37-4.36 (m, 1 H, α-*H*), 4.25-4.01 (m, 3 H, overlapping *H*-6 and β-H_a), 3.84-3.64 (m, 3 H, overlapping β-H_b, *H*-5, and *H*-2), 3.28-3.19 (m, 2 H, C(O)NHCH_2), 2.05, 2.03, 2.02 (each s, 9 H, OC(O)CH_3), 1.49 (bs, 2 H, NHCH$_2$CH_2), 1.25 (m, 22 H, (CH_2)$_{11}$), 0.88 (t, 3 H, CH$_2$CH_3, J = 6 Hz); ^{13}C NMR: ($CDCl_3$, 75 MHz) δ = 170.7 (s, *C*(O)NHCH$_2$), 169.4, 169.1 (each s, O*C*(O)CH$_3$), 154.4 (s, NH*C*(O)OCH$_2$), 154.4 (s, NH*C*(O)OBn), 136.1 (s, Ph-*C*), 101.9 (d, *C*-1), 95.4 (s, *C*Cl$_3$), 74.5 (t, NHC(O)O*C*H$_2$), 72.1 (d, *C*-5), 71.8 (d, *C*-3), 70.2 (t, β-*C*), 68.3 (d, *C*-4), 67.2 (t, Ph-*C*H$_2$), 61.8 (t, *C*-6), 56.1 (d, *C*-2), 53.9 (d, α-*C*), 39.8 (t, C(O)NH*C*H$_2$), 31.9, 29.7, 29.7, 29.6, 29.4, 29.3, 29.3, 26.9, 22.7 (each t, *C*H$_2$), 20.7, 20.6 (each q, OC(O)*C*H$_3$), 14.1 (q, CH$_2$*C*H$_3$); m.p.: 116-120 ˚C; IR: (DCM film on NaCl plate) 3375, 2928, 1748, 1652, 1535, 1233 cm^{-1}; $[\alpha]_D$: + 8 (*c* 1.0, CH_2Cl_2); MS-ESI/TOF: Calculated for $C_{40}H_{60}Cl_3KN_3O_{13}$ $(M + K)^+$: 935.2856, found 935.2859.

N^{α}-(Benzyloxycarbonyl)-*O*-[(2-deoxy-2-acetamido-3,4,6-tri-*O*-acetyl)-β-D-glucopyranosyl]-L-serine-tetradecylamide (2.68)

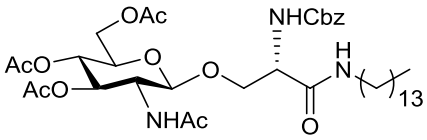

Glycoside **2.67** (225 mg, 0.25 mmol) and freshly activated zinc powder (activated by rinsing three times with 2 M HCl, followed by H_2O, then acetone, and ether) (330 mg, 5.0 mmol) were dissolved/ suspended in acetic anhydride (8 mL, 84 mmol) and THF (2 mL) was added to aid solubility. Et_3N (0.1 mL, 0.70 mmol) was added to the reaction mixture. The reaction mixture was allowed to stir at rt for 2 h, and then filtered through celite to remove zinc salts. The solvent was evaporated under reduced pressure, and the remaining residue was dissolved in DCM. This was washed with brine, then dried ($MgSO_4$), and filtered. The organic layer was concentrated under reduced pressure, and the crude product was purified by column chromatography (Hex:EtOAc, 1:1 to MeOH) to give *N*-acetyl protected glycoside **2.68** as an off-white solid (132 mg, 69 %).

R_f: 0.6 (DCM:MeOH, 9:1); ^{1}H NMR: ($CDCl_3$, 300 MHz) δ = 7.34 (s, 5 H, Ph-*H*), 6.56 (s, 1 H, C(O)N*H*CH$_2$), 6.03 (d, 1 H, N*H*C(O)CH$_3$, J = 9 Hz), 5.87 (s, 1 H,

N*H*C(O)OBn), 5.19-5.01 (m, 4 H, overlapping *H*-3, Ph-CH_2, and *H*-4), 4.62 (d, 1 H, *H*-1, *J* = 6 Hz), 4.36 (s, 1 H, α-*H*), 4.24-4.11 (m, 2 H, *H*-6), 4.07-3.96 (m, 2 H, overlapping β-H_a and *H*-2), 3.79-3.73 (m, 2 H, overlapping β-H_b and *H*-5), 3.21 (t, 2 H, C(O)NHCH_2, *J* = 6 Hz), 2.05, 2.02, 1.89 (each s, 12 H, OC(O)CH_3 and NHC(O)CH_3), 1.48 (s, 2 H, NHCH$_2$CH_2), 1.30 (m, 22 H, (CH_2)$_{11}$), 0.87 (t, 3 H, CH$_2$CH_3, *J* = 6 Hz); ^{13}C NMR: ($CDCl_3$, 75 MHz) δ = 171.1 (s, NH*C*(O)CH$_3$), 170.7 (s, *C*(O)NHCH$_2$), 169.3, 169.2 (each s, O*C*(O)CH$_3$), 156.3 (s, NH*C*(O)OBn), 136.1 (s, Ph-*C*), 128.5, 128.3, 128.1 (each d, Ph-*C*H), 101.8 (d, *C*-1), 72.4 (d, *C*-5), 72.0 (d, *C*-3), 69.6 (t, β-*C*), 68.3 (d, *C*-4), 67.1 (t, Ph-*C*H$_2$), 61.9 (t, *C*-6), 54.1 (d, overlapping α-*C* and *C*-2), 39.8 (t, C(O)NH*C*H$_2$), 31.9, 29.7, 29.6, 29.6, 29.4, 29.3, 26.9, 22.7 (each t, *C*H$_2$), 23.2 (q, NHC(O)*C*H$_3$), 20.7, 20.6 (each q, OC(O)*C*H$_3$), 14.1 (q, CH$_2$*C*H$_3$); m.p.: 156-160 ˚C; IR: (DCM film on NaCl plate) 3431, 2923, 2107, 1742, 1650, 1239 cm^{-1}; $[\alpha]_D$: - 10 (*c* 0.20 , CH_2Cl_2); MS-ESI/TOF: Calculated for $C_{39}H_{65}N_4O_{12}$ (M + NH_4)$^+$: 781.4593, found 781.4556.

_O_-[(2-Deoxy-2-acetamido-3,4,6-tri-_O_-acetyl)-β-D-glucopyranosyl]-L-serine-tetradecylamide (2.69)[83]

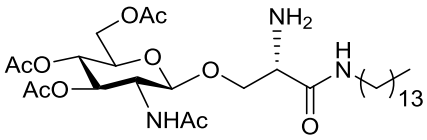

Protected glycoside **2.68** (100 mg, 0.13 mmol) was dissolved in EtOAc (25 mL) and placed under N_2. 10 % Pd/C (w/w) (50 mg) was added to the reaction mixture, and the flask was placed under H_2. The reaction mixture was allowed to stir at rt for 5 h. The reaction mixture was filtered through celite, and the solvent was evaporated under reduced pressure to leave free amine **2.69** as a white solid (80 mg, 98 %). Spectroscopic data was in agreement with reported values.

^{1}H NMR: (CD_3OD, 300 MHz) δ = 5.23 (t, 1 H, *H*-3, *J* = 9 Hz), 4.99 (t, 1 H, *H*-4, *J* = 9 Hz), 4.73 (d, 1 H, *H*-1, *J* = 9 Hz), 4.34-4.28 (dd, 1 H, *H*-6$_a$, *J* = 6 Hz, 12 Hz), 4.18-4.14 (m, 1 H, *H*-6$_b$), 3.94-3.84 (m, 4 H, overlapping *H*-2, *H*-5, and β-*H*), 3.23-3.15 (m, 2 H, C(O)NHCH_2), 2.07 (s, 3 H, NHC(O)CH_3), 2.02, 1.99, 1.94 (each s, 9 H, OC(O)CH_3), 1.55-1.51 (m, 2 H, NHCH$_2$CH_2), 1.17 (m, 22 H, (CH_2)$_{11}$), 0.91 (t, 3 H, CH$_2$CH_3, *J* = 6 Hz); (Lit[83]: ^{1}H NMR: ($CDCl_3$, 270 MHz) δ = 5.71, 5.17, 5.07, 4.59, 4.25, 4.13, 3.98, 3.90, 3.82, 3.70-3.64, 3.54, 3.26-3.18, 2.09, 2.03, 1.95, 1.50, 1.26,

0.88); ^{13}C NMR: (CD_3OD, 75 MHz) δ = 170.9 (s, NH*C*(O)CH_3), 170.4 (s, *C*(O)NHCH_2), 169.0 (s, O*C*(O)CH_3), 100.7 (d, *C*-1), 72.7 (d, *C*-5), 71.6 (d, *C*-3), 69.7 (t, β-*C*), 68.7 (d, *C*-4), 61.8 (t, *C*-6), 53.9 (d, overlapping α-*C* and *C*-2), 39.1 (t, C(O)NH*C*H_2), 31.7, 29.4, 29.1, 26.6, 22.3 (each t, *C*H_2), 21.5 (q, NHC(O)*C*H_3), 19.3, 19.2 (each q, OC(O)*C*H_3), 13.1 (q, CH_2CH_3); MS-ESI/TOF: Calculated for $C_{62}H_{114}N_7O_{20}$ $(2M + NH_4)^+$: 1276.8113, found 1276.8155.

N^{α}-(1-Oxodecyl)-*O*-[(2-deoxy-2-acetamido-3,4,6-tri-*O*-acetyl)-β-D-glucopyranosyl]-L-serine-tetradecylamide (2.70)

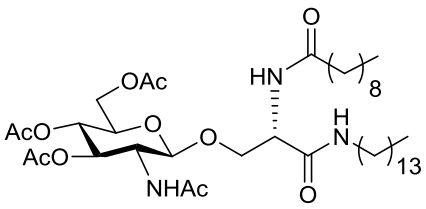

Decanoic acid (30 mg, 0.19 mmol), TBTU (60 mg, 0.19 mmol), and HOBt (30 mg, 0.19 mmol) were dissolved in anhydrous DMF (20 mL) under N_2, in the presence of 3Å molecular sieves. Anhydrous Et_3N (0.05 mL, 0.34 mmol) was added to the reaction mixture. This was allowed to stir at rt for 15 mins. A solution of free amine **2.69** (106 mg, 0.16 mmol) in anhydrous DMF (5 mL) was then added to the reaction mixture, and allowed to stir at rt overnight. The solvent was evaporated under reduced pressure, and the remaining residue was washed with 1.0 M HCl, dried ($MgSO_4$), and filtered. The organic layer was concentrated using a rotary evaporator, and the crude product was purified by column chromatography (Hex:EtOAc, 1:2 to DCM:MeOH, 9:1) to give glycolipid derivative **2.70** as a cream solid (96 mg, 72 %).

R_f: 0.4 (DCM:MeOH, 9:1); ^{1}H NMR: ($CDCl_3$, 300 MHz) δ = 6.64-6.60 (m, 2 H, overlapping C(O)N*H*CH_2 and N*H*C(O)CH_2), 5.99 (d, 1 H, N*H*C(O)C*H*$_3$, *J* = 9 Hz), 5.17 (t, 1 H, *H*-3, *J* = 9 Hz), 5.06 (t, 1 H, *H*-4, *J* = 9 Hz), 4.69 (d, 1 H, *H*-1, *J* = 9 Hz), 4.63-4.57 (m, 1 H, α-*H*), 4.29-4.23 (dd, 1 H, *H*-6_a, *J* = 6 Hz, 12 Hz), 4.18-4.14 (m, 1 H, *H*-6_b), 4.03-3.98 (m, 2 H, overlapping β-H_a and *H*-2), 3.77-3.71 (m, 2 H, overlapping β-H_b and *H*-5), 3.28-3.15 (m, 2 H, C(O)NHC*H*$_2$), 2.22 (t, 2 H, NHC(O)C*H*$_2$, *J* = 6 Hz), 2.08, 2.03, 1.94 (s, 12 H, OC(O)C*H*$_3$ and NHC(O)C*H*$_3$), 1.61 (s, 2 H, NHC(O)CH_2C*H*$_2$), 1.49 (s, 2 H, NHCH_2C*H*$_2$), 1.30 (m, 34 H, C*H*$_2$ x 17), 0.87 (t, 6 H, CH_2C*H*$_3$, *J* = 6 Hz); ^{13}C NMR: ($CDCl_3$, 75 MHz) δ = 172.7 (s,

overlapping *C*(O)NHCH$_2$ and NH*C*(O)CH$_2$), 170.0 (s, NH*C*(O)CH$_3$), 169.6, 169.5, 168.3 (each s, O*C*(O)CH$_3$), 101.1 (d, *C*-1), 71.5 (d, *C*-5), 71.1 (d, *C*-3), 68.5 (t, β-*C*), 67.2 (d, *C*-4), 60.9 (t, *C*-6), 53.1 (d, *C*-2), 51.1(d, α-*C*), 38.8 (t, C(O)NH*C*H$_2$), 35.4 (t, NHC(O)*C*H$_2$), 30.9 (t, NHCH$_2$*C*H$_2$), 30.8, 28.7, 28.6, 28.6, 28.4, 28.4, 28.3, 25.9, 24.6, 21.7 (each t, *C*H$_2$), 22.3 (q, NHC(O)*C*H$_3$), 19.7, 19.6 (each q, OC(O)*C*H$_3$), 13.0 (q, CH$_2$*C*H$_3$); m.p.: 162-168 ˚C; IR: (DCM film on NaCl plate) 3419, 2091, 1641 cm^{-1}; $[\alpha]_D$: - 20 (*c* 0.1, CH$_2$Cl$_2$); MS-ESI/TOF: Calculated for $C_{41}H_{74}N_3O_{11}$ (M + H)$^+$: 784.5318, found 784.5316.

N^{α}-(1-Oxodecyl)-*O*-[(2-deoxy-2-acetamido)-β-D-glucopyranosyl]-L-serine-tetradecylamide (2.71)

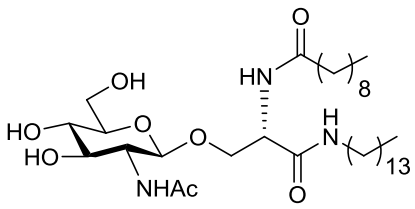

Protected glycolipid **2.70** (48 mg, 0.06 mmol) was dissolved in MeOH (5 mL). H$_2$O (2.5 mL) was added, followed by Et$_3$N (0.10 mL). THF (2 mL) was added to aid solubility. The reaction mixture was stirred at 40 ˚C overnight. A white precipitate crashed out of solution. The solvent was evaporated under reduced pressure to leave a yellow oil and a white solid, which were triturated with MeOH (3 x 5 mL) to give the deprotected glycolipid **2.71** as a white solid (insoluble in MeOH) (16 mg, 41 %).

R$_f$: 0.23 (DCM:MeOH, 9:1); ^{1}H NMR: (C$_5$D$_5$N, 600 MHz) δ = 9.00 (d, 1 H, N*H*C(O)CH$_3$, *J* = 6 Hz), 8.68-8.67 (m, 2 H, overlapping C(O)N*H*CH$_2$ and N*H*C(O)CH$_2$), 5.36 (d, 1 H, α-*H*, *J* = 6 Hz), 5.09 (d, 1 H, *H*-1, *J* = 12 Hz), 4.57-4.53 (m, 1 H, *H*-2), 4.51-4.48 (m, 2 H, overlapping *H*-6$_a$ and β-*H*$_a$), 4.34-4.31 (m, 1 H, β-*H*$_b$), 4.29-4.25 (m, 2 H, overlapping *H*-3 and *H*-6$_b$), 4.13 (t, 1 H, *H*-4, *J* = 6 Hz), 3.87-3.84 (m, 1 H, *H*-5), 3.61-3.41 (m, 2 H, C(O)NHC*H*$_2$), 2.47 (t, 2 H, NHC(O)C*H*$_2$, *J* = 6 Hz), 2.16 (s, 3 H, NHC(O)C*H*$_3$), 1.80-1.77 (m, 2 H, NHC(O)CH$_2$C*H*$_2$), 1.64-1.61 (m, 2 H, NHCH$_2$C*H*$_2$), 1.33-1.17 (m, 34 H, C*H*$_2$ x 17), 0.88-0.83 (m, 6 H, CH$_2$C*H*$_3$); ^{13}C NMR: (C$_5$D$_5$N, 150 MHz) δ = 174.4, 172.2, 171.6 (each s, *C*(O)NHCH$_2$, NH*C*(O)CH$_2$, and NH*C*(O)CH$_3$), 103.3(d, *C*-1), 80.1 (d, *C*-5), 77.2 (d, *C*-3), 73.0 (d, *C*-4), 70.2 (t, β-*C*), 63.3 (t, *C*-6), 57.9 (d, *C*-2), 55.8 (d, α-*C*),

40.7 (t, C(O)NH*C*H_2), 37.2 (t, NHC(O)*C*H_2), 32.8, 32.7, 30.7, 30.6, 30.4, 30.3, 30.2, 28.0, 26.8, 23.7, 23.6 (each t, *C*H_2), 24.3 (q, NHC(O)*C*H_3), 15.0 (q, CH_2CH_3); MS-ESI/TOF: Calculated for $C_{35}H_{68}N_3O_8$ $(M + H)^+$: 658.5001, found 658.4972.

N^{α}-(1-Oxotetracosanoyl)-*O*-[(2-deoxy-2-acetamido-3,4,6-tri-*O*-acetyl)-β-D-glucopyranosyl]-L-serine-tetradecylamide (2.73)

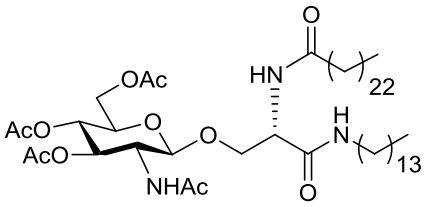

Tetracosanoic acid (182 mg, 0.45 mmol), TBTU (159 mg, 0.49 mmol), and HOBt (67 mg, 0.49 mmol) were dissolved in anhydrous DMF (15 mL) under N_2, in the presence of 4Å molecular sieves. Anhydrous Et_3N (0.13 mL, 0.9 mmol) was added to the reaction mixture. This was allowed to stir at rt for 15 mins. A solution of free amine **2.69** (283 mg, 0.45 mmol) in anhydrous DMF (5 mL) was added to the reaction mixture, and allowed to stir at rt for 5 h. The solvent was evaporated under reduced pressure. The remaining residue was dissolved in DCM and washed with 1.0 M HCl, then dried ($MgSO_4$), and filtered. The organic layer was concentrated under reduced pressure, and the crude product was purified by column chromatography (DCM:MeOH, 12:1) to give glycolipid derivative **2.73** as a white solid (63 mg, 17 %).

R_f: 0.47 (DCM:MeOH, 12:1); ^{1}H NMR: ($CDCl_3$, 300 MHz) δ = 6.58-6.56 (m, 2 H, overlapping C(O)N*H*CH_2 and N*H*C(O)CH_2), 5.80 (d, 1 H, N*H*C(O)CH_3, *J* = 9 Hz), 5.14-5.07 (m, 2 H, overlapping *H*-3 and *H*-4), 4.68 (d, 1 H, *H*-1, *J* = 9 Hz), 4.64-4.60 (m, 1 H, α-*H*), 4.27-4.14 (m, 2 H, *H*-6), 4.05-3.98 (m, 2 H, overlapping β-H_a and *H*-2), 3.77-3.71 (m, 2 H, overlapping β-H_b and *H*-5), 3.24-3.20 (m, 2 H, C(O)NHCH_2), 2.24-2.18 (m, 2 H, NHC(O)CH_2), 2.08, 2.04, 1.95 (each s, 12 H, OC(O)CH_3 and NHC(O)CH_3), 1.61 (bs, 2 H, NHC(O)CH_2CH_2), 1.49 (bs, 2 H, NHCH_2CH_2), 1.25 (m, 62 H, CH_2 x 31), 0.87 (t, 6 H, CH_2CH_3, *J* = 6 Hz); ^{13}C NMR: ($CDCl_3$, 75 MHz) δ = 173.6, 171.2, 170.7, 170.5, 169.4, 169.3 (each s, *C*(O)NHCH_2, NH*C*(O)CH_2, NH*C*(O)CH_3, and O*C*(O)CH_3), 102.1 (d, *C*-1), 72.4 (d, *C*-3), 72.2 (d, *C*-5), 69.6 (t, β-*C*), 68.0 (d, *C*-4), 61.8 (t, *C*-6), 54.2 (d, *C*-2), 52.0 (d, α-*C*), 39.8 (t, C(O)N*HCH*$_2$),

36.5 (t, NHC(O)CH_2CH_2), 32.0, 29.7, 29.6, 29.4, 29.3, 26.9, 25.6, 22.7 (each t, CH_2), 23.4 (q, NHC(O)CH_3), 20.8, 20.7, 20.7 (each q, OC(O)CH_3), 14.0 (q, CH_2CH_3); m.p.: 164-168 ˚C; $[\alpha]_D$: - 23 (*c* 0.26, CH_2Cl_2); IR: (DCM film on NaCl plate) 3293, 2919, 2850, 1745, 1667, 1643, 1554, 1260 cm^{-1}; MS-ESI/TOF: Calculated for $C_{55}H_{102}N_3O_{11}$ $(M + H)^+$: 980.7509, found 980.7513.

N^{α}-(1-Oxotetracosanoyl)-*O*-[(2-deoxy-2-acetamido)-β-D-glucopyranosyl]-L-serine-tetradecylamide (2.74)

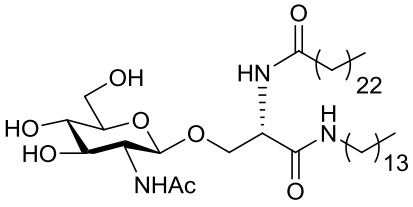

Protected glycolipid **2.73** (22 mg, 0.02 mmol) was dissolved in warm DCM. MeOH (3 mL) and H_2O (1.5 mL) were added to the reaction mixture, followed by Et_3N (0.10 mL). The reaction mixture was stirred at 45 ˚C overnight. The solvent was evaporated under reduced pressure to leave a yellow oil and a white solid, which was triturated with MeOH (3 x 5 mL) to give deprotected glycolipid **2.74** as a white solid (insoluble in MeOH) (11 mg, 57 %).

R_f: 0.18 (DCM: MeOH, 12:1); ^{1}H NMR: (C_5D_5N, 600 MHz) δ = 9.03 (d, 1 H, N*H*C(O)CH_3, *J* = 6 Hz), 8.67 (m, 2 H, overlapping N*H*CH_2 and N*H*C(O)CH_2, partially overlapped by solvent peak), 5.39-5.35 (m, 1 H, α-*H*), 5.12-5.11 (m, 1 H, *H*-1, overlapped by H_2O peak), 4.56-4.35 (m, 3 H, overlapping *H*-2, *H*-6_a, and β-H_a), 4.33-4.27 (m, 3 H, overlapping β-H_b, *H*-3, and *H*-6_b), 4.15 (t, 1 H, *H*-4, *J* = 6 Hz), 3.87-3.84 (m, 1 H, *H*-5), 3.47-3.43 (m, 2 H, C(O)NHCH_2), 2.50 (t, 2 H, NHC(O)CH_2, *J* = 6 Hz), 2.18 (s, 3 H, NHC(O)CH_3), 1.82-1.77 (m, 2 H, NHC(O)CH_2CH_2), 1.65-1.61 (m, 2 H, NHCH_2CH_2), 1.41-1.21 (m, 62 H, CH_2 x 31), 0.98-0.86 (m, 6 H, CH_2CH_3); ^{13}C NMR: (C_5D_5N, 150 MHz) δ = 174.4, 172.2, 171.6 (each s, *C*(O)NHCH_2, NH*C*(O)CH_2, and NH*C*(O)CH_3), 103.4 (d, *C*-1), 79.4 (d, *C*-5), 77.3 (d, *C*-3), 73.1 (d, *C*-4), 70.2 (t, β-*C*), 63.3 (t, *C*-6), 58.1 (d, *C*-2), 54.8 (d, α-*C*), 40.7 (t, C(O)NH*C*H_2), 37.2 (t, NHC(O)*C*H_2), 32.9, 30.7, 28.1, 26.9, 23.7 (each t, *C*H_2), 24.2 (q, NHC(O)*C*H_3), 15.1 (q, CH_2*C*H_3); MS-MALDI-TOF: Calculated for $C_{49}H_{95}N_3O_8Na$ $(M + Na)^+$: 876.7017, found 876.7047.

N$^{\alpha}$-(9-Fluorenylmethoxycarbonyl)-L-serine-phenylmethyl ester (3.2)[259]

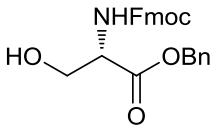

Method A

N$^{\alpha}$-(9-Fluorenylmethoxycarbonyl)-L-serine (800 mg, 2.4 mmol) and K_2CO_3 (500 mg, 3.6 mmol) were dissolved/suspended in anhydrous DMF (5 mL). Benzyl bromide (0.38 mL, 3.17 mmol) was then added to the reaction, and it was allowed to stir at rt overnight. The solvent was concentrated under reduced pressure, and the remaining residue washed with 1.0 M HCl and brine, then dried ($MgSO_4$), and filtered. The organic layer was concentrated under reduced pressure, and the remaining residue was purified by column chromatography (Hex:EtOAc, 2:1 to 1:1) to give benzyl protected **3.2** as a white syrup (822 mg, 81 %). Spectroscopic data is in agreement with literature values.

Method B

N$^{\alpha}$-(9-Fluorenylmethoxycarbonyl)-L-serine (800 mg, 2.4 mmol) and K_2CO_3 (500 mg, 3.6 mmol) were dissolved/suspended in anhydrous DMF (5 mL), under N_2. Tetrabutylammonium iodide (90 mg, 0.24 mmol) was added to the reaction mixture, and this was allowed to stir for 10 mins at rt. Benzyl bromide (0.84 mL, 7.32 mmol) was then added to the reaction, and it was allowed to stir at rt for 7 h. The solvent was concentrated under reduced pressure. The remaining residue was dissolved in EtOAc, and washed twice with sat. $NaHCO_3$ solution, then dried ($MgSO_4$), and filtered. The organic layer was concentrated under reduced pressure, and the remaining residue was purified by column chromatography (Hex:EtOAc, 2:1 to 1:1) to give benzyl protected **3.2** as a white syrup (842 mg, 82 %). Spectroscopic data is in agreement with literature values.

Method C

N$^{\alpha}$-(9-Fluorenylmethoxycarbonyl)-L-serine (680 mg, 2.0 mmol) and DIPEA (0.25 mL, 3.0 mmol) were dissolved in anhydrous DMF (6 mL). Benzyl bromide (0.32 mL, 2.7 mmol) was then added to the reaction, and it was allowed to stir at rt

overnight. The solvent was concentrated under reduced pressure, and the remaining residue was dissolved in DCM, and washed with 1.0 M HCl and brine, then dried ($MgSO_4$), and filtered. The organic layer was concentrated under reduced pressure, and the remaining residue was purified by column chromatography (Hex:EtOAc, 1:1) to give benzyl protected **3.2** as a white syrup (722 mg, 85 %). Spectroscopic data is in agreement with literature values.

R_f: 0.6 (Hex:EtOAc, 1:1); ^{1}H NMR: ($CDCl_3$, 300 MHz) δ = 7.79 (d, 2 H, Fmoc-*H*, *J* = 9 Hz), 7.63 (d, 2 H, Fmoc-*H*, *J* = 6 Hz), 7.42-7.28 (m, 9 H, overlapping Fmoc-*H* and Ph-*H*), 6.01 (d, 1 H, N*H*-Fmoc, *J* = 6 Hz), 5.23 (s, 2 H, Ph-CH_2), 4.52-4.37 (m, 3 H, overlapping α-*H* and Fmoc-CH_2), 4.25-4.13 (m, 1 H, Fmoc-C*H*), 4.02 (bs, 1 H, β-H_a), 3.94 (bs, 1 H, β-H_b), 2.84 (bs, 1 H, CH_2OH); (Lit[259]: ^{1}H NMR: ($CDCl_3$, 300 MHz) δ = 7.77, 7.60, 7.43-7.26, 5.75, 5.23, 4.50-4.20, 4.22, 4.07, 2.15); ^{13}C NMR: ($CDCl_3$, 75 MHz) δ = 170.6 (s, *C*(O)OBn), 156.4 (s, Fmoc-*C*(O)), 143.8, 143.7, 141.4, 141.3 (each s, Fmoc-*C*), 135.2 (s, Ph-*C*), 128.6, 128.5, 128.3, 128.2, 127.7, 127.2 (each d, Fmoc-*C*H and Ph-*C*H), 125.1, 120.4 (each d, Fmoc-*C*H), 67.5 (t, Ph-*C*H_2), 67.3 (t, Fmoc-*C*H_2), 63.2 (t, β-*C*), 56.3 (d, α-*C*), 47.1 (d, Fmoc-*C*H); IR: (DCM film on NaCl plate) 3375, 3065, 2950, 1719, 1520, 1450, 1195 cm^{-1}; MS-ESI/TOF: Calculated for $C_{25}H_{24}NO_5$ $(M + H)^+$: 418.1649, found 418.1654.

N^{α}-(9-Fluorenylmethoxycarbonyl)-*O*-[(2-deoxy-2-[(2,2,2-trichloroethoxycarbonyl)amino]-3,4,6-tri-*O*-acetyl)-β-D-glucopyranosyl]-L-serine-phenylmethyl ester (3.3)[178]

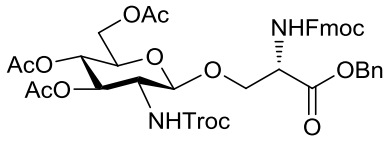

Fmoc protected serine derivative **3.2** (411 mg, 0.97 mmol) and imidate **2.34** (666 mg, 1.07 mmol) were dissolved in dry DCM, under N_2. A freshly made solution of 0.04 N TMSOTf in dry DCM (2.42 mL, 0.10 mmol) was then added to the reaction mixture. This was stirred at rt overnight. The reaction mixture was washed with sat. $NaHCO_3$ solution, followed by brine, then the organic layer was dried ($MgSO_4$), and filtered. The organic layer was concentrated under reduced pressure, and the crude product was purified by column chromatography (Hex:EtOAc, 2:1 to 1:1) to yield

glycoside **3.3** as a yellow oil (540 mg, 62 %). Spectroscopic data was in agreement with reported values.

R_f: 0.67 (Hex:EtOAc, 1:1); ^{1}H NMR: ($CDCl_3$, 300 MHz) δ = 7.77 (d, 2 H, Fmoc-*H*, *J* = 9 Hz), 7.61 (d, 2 H, Fmoc-*H*, *J* = 6 Hz), 7.42-7.32 (m, 9 H, overlapping Fmoc-*H* and Ph-*H*), 5.80 (d, 1 H, N*H*-Fmoc, *J* = 6 Hz), 5.29-5.18 (m, 4 H, overlapping *H*-3, N*H*C(O)OCH$_2$ and Ph-C*H*$_2$), 5.03 (t, 1 H, *H*-4, *J* = 9 Hz), 4.79-4.72 (m, 1 H, NHC(O)OC*H*$_{2a}$), 4.62-4.50 (m, 4 H, overlapping α-*H*, *H*-1, Fmoc-C*H*$_{2a}$ and NHC(O)OC*H*$_{2b}$), 4.26-4.20 (m, 4 H, overlapping Fmoc-C*H*, β-*H*$_a$, *H*-6$_a$ and Fmoc-C*H*$_{2b}$), 4.09 (d, 1 H, *H*-6$_b$, *J* = 9 Hz), 3.92-3.89 (m, 1 H, β-*H*$_b$), 3.62-3.51 (m, 2 H, overlapping *H*-2 and *H*-5), 2.03 (s, 9 H, OC(O)C*H*$_3$); (Lit[178]: ^{1}H NMR: ($CDCl_3$, 400 MHz) δ = 7.76, 7.61, 7.42-7.27, 5.81, 5.31-5.17, 5.02, 4.81-4.58, 4.53-4.39, 4.23, 4.10, 3.92, 3.59, 2.07, 2.03, 2.02); ^{13}C NMR: ($CDCl_3$, 75 MHz) δ = 170.6, 170.5, 169.4 (each s, O*C*(O)CH$_3$ and *C*(O)OBn), 156.1 (s, NH*C*(O)OCH$_2$), 154.1 (s, Fmoc-*C*(O)), 143.9, 143.6, 141.3 (each s, Fmoc-*C*), 135.2 (s, Ph-*C*), 128.6, 128.5, 128.3, 127.8, 127.2 (each d, Fmoc-*C*H and Ph-*C*H), 125.2, 125.1, 120.0 (each d, Fmoc-*C*H), 95.3 (d, *C*-1), 83.2 (s, *C*Cl$_3$), 74.5 (t, NHC(O)O*C*H$_2$), 71.9 (d, *C*-5), 71.7 (d, *C*-3), 69.7 (t, β-*C*), 68.5 (d, *C*-4), 67.6 (t, Fmoc-*C*H$_2$), 67.4 (t, Ph-*C*H$_2$), 61.9 (t, *C*-6), 56.4 (d, *C*-2), 56.1 (d, α-*C*), 47.1 (d, Fmoc-*C*H), 20.7, 20.6 (each q, OC(O)*C*H$_3$); m.p.: 46-50 ˚C; IR: (DCM film on NaCl plate) 3342, 3066, 2957, 1750, 1531, 1233 cm^{-1}; MS-ESI/TOF: Calculated for $C_{40}H_{42}Cl_3N_2O_{14}$ $(M + H)^+$: 879.1696, found 879.1678.

N$^{\alpha}$-(9-Fluorenylmethoxycarbonyl)-*O*-[(2-deoxy-2-acetamido-3,4,6-tri-*O*-acetyl)-β-D-glucopyranosyl]-L-serine-phenylmethyl ester (3.4)[178]

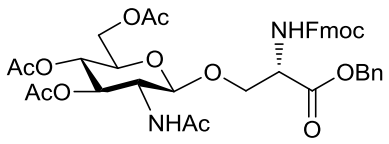

Protected glycoside **3.3** (135 mg, 0.15 mmol) was dissolved in Ac_2O (6 mL) and freshly activated zinc dust (Activated by rinsing twice with 2 M HCl, followed by H_2O, then acetone, and ether) (197 mg, 3.0 mmol) was added. The reaction mixture was stirred at rt overnight, then filtered over celite to remove the zinc salts. The solvent was concentrated under reduced pressure, and the remaining residue was purified by column chromatography (Hex:EtOAc, 2:1 to 1:2) to give the *N*-acetyl

derivative **3.4** as a white solid (91 mg, 80 %). Spectroscopic data was in agreement with reported values.

R_f: 0.24 (Hex:EtOAc, 1:2); ^{1}H NMR: ($CDCl_3$, 300 MHz) δ = 7.76 (d, 2 H, Fmoc-*H*, *J* = 9 Hz), 7.63 (d, 2 H, Fmoc-*H*, *J* = 9 Hz), 7.41-7.32 (m, 9 H, overlapping Fmoc-*H* and Ph-*H*), 6.00-5.94 (m, 2 H, overlapping N*H*C(O)CH_3 and N*H*-Fmoc), 5.29-5.17 (m, 3 H, overlapping *H*-3 and Ph-CH_2), 5.02 (t, 1 H, *H*-4, *J* = 9.6 Hz), 4.67 (d, 1 H, *H*-1, *J* = 9 Hz), 4.52-4.34 (m, 3 H, overlapping α-*H* and Fmoc-CH_2), 4.20-4.05 (m, 4 H, overlapping Fmoc-C*H*, β-H_a, and *H*-6), 3.86-3.63 (m, 3 H, overlapping β-H_b, *H*-2 and *H*-5), 2.00 (s, 9 H, OC(O)CH_3), 1.85 (s, 3 H, NHC(O)CH_3); (Lit[178]: ^{1}H NMR: ($CDCl_3$, 400 MHz) δ = 7.77, 7.63, 7.42-7.30, 5.81, 5.37, 5.25, 5.19, 5.02, 4.67, 4.53, 4.45, 4.23, 4.08, 3.86, 3.70, 3.62, 2.07, 2.04, 2.03, 1.82); ^{13}C NMR: ($CDCl_3$, 75 MHz) δ = 169.9, 169.7, 169.6, 168.6, 168.4 (each s, O*C*(O)CH_3, NH*C*(O)CH_3, and *C*(O)OBn), 155.1 (s, Fmoc-*C*(O)), 142.8, 140.2 (each s, Fmoc-*C*), 134.2 (s, Ph-*C*), 127.5, 127.4, 127.1, 126.7, 126.1 (each d, Fmoc-*C*H and Ph-*C*H), 124.1, 118.9 (each d, Fmoc-*C*H), 99.6 (d, *C*-1), 71.0 (d, *C*-3), 70.8 (d, *C*-5), 67.9 (t, β-*C*), 67.5 (d, *C*-4), 66.4 (t, Fmoc-*C*H_2), 65.9 (t, Ph-*C*H_2), 61.0 (t, *C*-6), 53.4 (d, α-*C*), 53.3 (d, *C*-2), 46.1 (d, Fmoc-*C*H), 22.0 (q, NHC(O)*C*H_3), 19.6, 19.5 (each q, OC(O)*C*H_3); IR: (DCM film on NaCl plate) 3307, 3065, 2954, 1748, 1663, 1532, 1232 cm^{-1}; MS-ESI/TOF: Calculated for $C_{39}H_{43}N_2O_{13}$ $(M + H)^+$: 747.2760, found 747.2788.

N$^{\alpha}$-(9-Fluorenylmethoxycarbonyl)-*O*-[(2-deoxy-2-acetamido-3,4,6-tri-*O*-acetyl)-β-D-glucopyranosyl]-L-serine (3.5)[178]

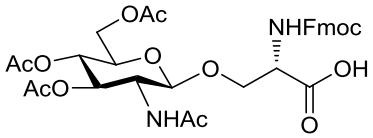

Protected glycoside **3.4** (402 mg, 0.53 mmol) was placed under N_2, and dissolved in DCM (4 mL). EtOAc (15 mL) was added, followed by 10 % Pd/C (w/w) (20 mg) and the flask placed under H_2. The reaction was stirred at rt overnight. The Pd/C was removed by filtration over celite, and the solvent was evaporated under reduced pressure to give free acid **3.5** as a white solid (252 mg, 70 %). Spectroscopic data was in agreement with reported values.

R_f: 0.2 (DCM:MeOH, 10:1); ^{1}H NMR: (CD_3OD, 300 MHz) δ = 7.82 (d, 2 H, Fmoc-*H*, *J* = 9 Hz), 7.70 (d, 2 H, Fmoc-*H*, *J* = 9 Hz), 7.43-7.31 (m, 4 H, Fmoc-*H*), 5.27-5.20 (m, 1 H, *H*-3), 4.99 (t, 1 H, *H*-4, *J* = 9 Hz), 4.74 (d, 1 H, *H*-1, *J* = 9 Hz), 4.47-4.35 (m, 3 H, overlapping α-*H* and Fmoc-CH_2), 4.29-4.23 (m, 2 H, overlapping Fmoc-C*H* and *H*-6_a), 4.16-4.10 (m, 2 H, overlapping β-H_a and *H*-6_b), 3.96-3.91 (dd, 1 H, β-H_b, *J* = 6 Hz, 12 Hz), 3.85-3.76 (m, 2 H, overlapping *H*-2 and *H*-5), 2.04, 2.01, 1.99 (each s, 9 H, OC(O)CH_3), 1.87 (s, 3 H, NHC(O)CH_3); (Lit[178]: ^{1}H NMR: (CD_3OD, 400 MHz) δ = 7.94, 7.82, 7.54, 7.47, 5.36, 5.11, 4.83, 4.55, 4.49, 4.43-4.36, 4.33-4.21, 4.18, 4.04-3.91, 2.17, 2.15, 2.11, 2.00); IR: (DCM film on NaCl plate) 3427, 2096, 1649 cm^{-1}; MS-ESI/TOF: Calculated for $C_{25}H_{24}NO_5$ $(M + H)^+$ 657.2290, found 657.2299.

(2-Deoxy-2-[(2,2,2-trichloroethoxycarbonyl)amino]-1,3,4-tri-*O*-acetyl-6-*O*-(triphenylmethyl))-α/β-D-glucopyranoside (4.2)

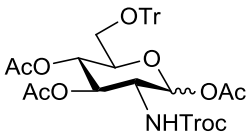

D (+) -Glucosamine hydrochloride (2.00 g, 9.0 mmol) and solid $NaHCO_3$ (2.27 g, 27 mmol) were dissolved in H_2O (20 mL). The reaction mixture was stirred for 5 mins at rt. TrocCl (1.45 mL, 10.8 mmol) was added dropwise. The reaction mixture was stirred at rt for 2 h, then neutralized (1 M HCl). The solvent was evaporated under reduced pressure. The NH-Troc protected glucosamine was obtained as a cream solid which was used without further purification. A portion of this intermediate (150 mg, 0.46 mmol) was dissolved in dry pyridine (10 mL). Et_3N (0.02 mL, 0.12 mmol) and TrCl (640 mg, 2.3 mmol) was added to the reaction mixture. This was stirred at 95 °C for 3 h. The reaction mixture was cooled to 0 °C, then acetyl chloride (0.19 mL, 2.76 mmol) was added slowly. The reaction mixture was allowed to return to rt, then stirred at rt overnight. The solvent was evaporated under reduced pressure, and the remaining residue was dissolved in DCM, and washed with brine. The organic layer was dried ($MgSO_4$), and filtered, then concentrated under reduced pressure. The crude product was purified by column chromatography (Hex:EtOAc, 2:1) to give protected glucosamine derivative **4.2** as a clear oil (132 mg, 39 %) (Anomeric mixture of α:β in the ratio 1:0.4).

R_f: 0.53 (Pet. Ether: EtOAc, 2:1); ^{1}H NMR: ($CDCl_3$, 300 MHz) δ = 7.44-7.19 (m, 15 H, Ph-*H*), 6.35 (d, 1 H, *H*-1 (α-anomer), *J* = 3 Hz), 5.72 (d, 1 H, *H*-1 (β-anomer), *J* = 9 Hz), 5.35 (t, 1 H, *H*-4, *J* = 9 Hz), 5.24-5.15 (m, 1 H, *H*-3), 5.11 (d, 1 H, N*H*C(O)OCH$_2$, *J* = 9 Hz), 4.83 (d, 1 H, NHC(O)OCH_{2a} (α-anomer), *J* = 12 Hz), 4.73 (s, 2 H, NHC(O)OCH_2 (β-anomer)), 4.63 (d, 1 H, NHC(O)OCH_{2b} (α-anomer), *J* = 12 Hz), 4.27-4.13 (m, 1 H, *H*-2 (α-anomer)), 4.03-3.97 (m, 1 H, *H*-2 (β-anomer)), 3.93-3.86 (m, 1 H, *H*-5 (α-anomer)), 3.68-3.63 (m, 1 H, *H*-5 (β-anomer)), 3.35-3.27 (m, 2 H, *H*-6$_a$ (both anomers)), 3.10-3.01 (m, 2 H, *H*-6$_b$ (both anomers)), 2.17-2.01 (m, 18 H, OC(O)CH_3 (both anomers)); ^{13}C NMR: ($CDCl_3$, 75 MHz) δ = 171.5, 169.3, 168.7 (each s, O*C*(O)CH$_3$), 154.1 (s, NH*C*(O)OCH$_2$), 143.5 (s, Ph-*C*), 128.7, 127.9, 127.8, 127.3, 127.0 (each d, Ph-*H*), 95.3 (s, *C*Cl$_3$), 92.6 (s, *C*(ph)$_3$), 90.7 (d, *C*-1), 74.7 (t, NHC(O)O*C*H$_2$), 71.2 (d, *C*-5), 71.0 (d, *C*-3), 67.8 (d, *C*-4), 61.4 (t, *C*-6), 53.4 (d, *C*-2), 21.0, 20.7, 20.4 (each q, OC(O)*C*H$_3$); $[\alpha]_D$: + 41.6 (*c* 1.2, CH_2Cl_2); IR: (DCM film on NaCl plate) 3421, 3059, 1753, 1647, 1219 cm^{-1}; MS-ESI/TOF: Calculated for $C_{15}H_{20}Cl_3NNaO_{10}$ (M (-Tr) + Na)$^+$ (Tr removed by formic acid in the mobile phase): 502.0045, found 502.0061.

(2-Deoxy-2-[(2,2,2-trichloroethoxycarbonyl)amino]-1,3,4-tri-*O*-acetyl-6-*O*-(*tert*-butyldimethylsilyl))-α/β-D-glucopyranoside (4.3)

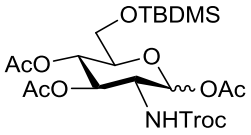

D (+) -Glucosamine hydrochloride (2.00 g, 9.0 mmol) and solid $NaHCO_3$ (2.27 g, 27 mmol) were dissolved in H_2O (20 mL). The reaction mixture was stirred for 5 mins at rt. TrocCl (1.45 mL, 10.8 mmol) was added dropwise. The reaction mixture was stirred at rt for 2 h, then neutralized (1 M HCl). The solvent was evaporated under reduced pressure. The NH-Troc protected glucosamine was obtained as a cream solid which was used without further purification. This intermediate (307 mg, 0.85 mmol) was dissolved in dry pyridine (3 mL) under N_2, in the presence of 3Å molecular sieves. Imidazole (63 mg, 0.94 mmol) and TBDMSCl (154 mg, 1.02 mmol) were added to the reaction mixture. This was stirred at rt overnight. Acetic anhydride (0.48 mL, 5.1 mmol) was added, and the reaction was left to stir at rt overnight. The solvent was evaporated under reduced pressure, and the remaining residue was

dissolved in DCM, and washed twice with water. The organic layer was dried ($MgSO_4$), and filtered, then concentrated under reduced pressure. The crude product was purified by column chromatography (Hex:EtOAc, 4:3) to give the protected glucosamine derivative **4.3** as a yellow oil (131 mg, 26 %) (Anomeric mixture of α:β in the ratio 3:1).

R_f: 0.9 (Hex:EtOAc, 4:1); ^{1}H NMR: ($CDCl_3$, 300 MHz) δ = 6.20 (d, 1 H, *H*-1 (α-anomer), *J* = 3 Hz), 5.68 (d, 1 H, *H*-1 (β-anomer), *J* = 9 Hz), 5.44 (d, 1 H, N*H*C(O)OCH$_2$ (β-anomer), *J* = 9 Hz), 5.27-5.12 (m, 4 H, overlapping *H*-3, N*H*C(O)OCH$_2$, and *H*-4 (α-anomer), and *H*-3 (β-anomer)), 5.12-5.06 (m, 1 H, *H*-4 (β-anomer)), 4.78 (d, 1 H, NHC(O)OCH_{2a} (α-anomer), *J* = 12 Hz), 4.72-4.69 (m, 2 H, NHC(O)OCH_2 (β-anomer)), 4.59 (d, 1 H, NHC(O)OCH_{2b} (α-anomer), *J* = 12 Hz), 4.15-4.07 (m, 2 H, overlapping *H*-2 (α-anomer) and *H*-6$_a$ (β-anomer)) 3.83-3.78 (m, 2 H, overlapping *H*-5 (α-anomer) and *H*-2 (β-anomer)), 3.64-3.60 (m, 4 H, overlapping *H*-5 and *H*-6$_b$ (β-anomer), and *H*-6 (α-anomer)), 2.14-2.00 (m, 18 H, OC(O)CH_3 (both anomers)), 0.84 (s, 18 H, SiC(CH_3)$_3$ (both anomers)), 0.03- -0.01 (m, 12 H, SiCH_3 (both anomers)); ^{13}C NMR: ($CDCl_3$, 75 MHz) δ = 170.4, 169.9, 168.3, 168.0, 167.7 (each s, O*C*(O)CH$_3$), 153.1 (s, NH*C*(O)OCH$_2$), 94.5, 94.3 (each s, *C*Cl$_3$ (both anomers)), 91.3 (d, *C*-1 (β-anomer)), 89.5 (d, *C*-1 (α-anomer)), 73.9 (t, NHC(O)O*C*H$_2$ (β-anomer)), 73.4 (t, NHC(O)O*C*H$_2$ (α-anomer)), 71.5 (d, *C*-5), 69.9 (d, *C*-3), 67.5 (d, *C*-4 (β-anomer)), 67.0 (d, *C*-4 (α-anomer)), 61.07, 60.8 (each t, *C*-6 (both anomers)), 52.3 (d, *C*-2), 24.8, 24.5 (each q, SiC(*C*H$_3$)$_3$), 19.9, 19.8, 19.7, 19.6 (each q, OC(O)*C*H$_3$), -6.41 (q, Si*C*H$_3$); IR: (as a DCM film on NaCl plate) 3327, 2957, 1755, 1538, 1368, 1219 cm^{-1}.

(2-Deoxy-2-[(2,2,2-trichloroethoxycarbonyl)amino]-3,4,6-tri-*O*-acetyl-1-*O*-phenylmethyl)-β-D-glucopyranoside (4.6)[189, 260]

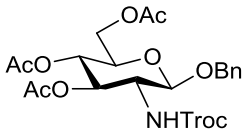

Acetylated derivative **2.26** (1.32 g, 2.5 mmol) was dissolved in DCM (10 mL), and cooled to 0 ˚C. To this a 33 % solution (v/v) of HBr in AcOH (2.4 mL) was added, and the reaction mixture was stirred for 45 mins. The reaction mixture was allowed to reach rt, and stirred for 45 mins. A further portion of HBr solution (1.2 mL) was

added to the reaction, and this was allowed to stir at rt for 2 h. DCM was added to the reaction mixture, and the round bottomed flask was placed on ice. Sat. $NaHCO_3$ solution was added to the flask. The product was extracted by washing twice with DCM. The organic layer was then washed with brine, dried ($MgSO_4$), and filtered. The solvent was removed under reduced pressure to give the α-bromide product, which was used without further purification.

This material was placed into a round bottomed flask, which was covered with tinfoil. $AgCO_3$ (870 mg, 3.1 mmol) was added, in the presence of 3 Å molecular sieves, then the reaction flask was placed under N_2, and dry DCM (10 mL) was added. To this, benzyl alcohol (0.52 mL, 5.0 mmol) was added, and allowed to stir at rt overnight. The silver salts were filtered off over celite, and the filtrate concentrated under reduced pressure, and the remaining residue was purified by column chromatography (Hex:EtOAc, 3:1 to 2:1) to give benzyl glycoside **4.6** as a white solid (800 mg, 57 %). Spectroscopic date is in agreement with literature values.

R_f: 0.65 (Hex:EtOAc, 1:1); ^{1}H NMR ($CDCl_3$, 300 MHz): δ = 7.38-7.29 (m, 5 H, Ph-*H*), 5.23 (t, 1 H, *H*-3, *J* = 9 Hz), 5.09 (t, 1 H, *H*-4, *J* = 9 Hz), 4.97 (ab d, 1 H, CH_2-Ph_a, *J* = 9 Hz), 4.17 (s, 2 H, NHC(O)OCH_2), 4.63-4.59 (m, 2 H, overlapping *H*-1 and CH_2-Ph_b), 4.32-4.26 (dd, 1 H, *H*-6_a, *J* = 6 Hz, 12 Hz), 4.19-4.14 (dd, 1 H, *H*-6_b, *J* = 3 Hz, 12 Hz), 3.77-3.63 (m, 2 H, overlapping *H*-5 and *H*-2), 2.11 (s, 3 H, OC(O)CH_3), 2.02 (s, 6 H, OC(O)CH_3); (Lit[260]: ^{1}H NMR ($CDCl_3$, 500 MHz): δ = 7.36-7.30, 5.23, 5.09, 5.03, 4.92, 4.71, 4.62, 4.30, 4.17, 3.73, 3.66, 2.11, 2.02); IR: (KBr disc) 3360, 2955, 2886, 1752, 1720, 1542, 1230 cm^{-1}; MS-ESI/TOF: Calculated for $C_{44}H_{52}Cl_6N_2NaO_{20}$ $(2M + Na)^+$: 1163.1114, found 1163.1128.

N^{α}-(9-Fluorenylmethoxycarbonyl)-*O*-[(2-deoxy-2-acetamido)-β-D-glucopyranosyl]-L-serine-methyl ester (4.17)

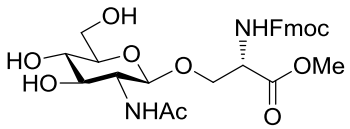

Protected glycoside **3.5** (271 mg, 0.41 mmol) was dissolved in MeOH (15 mL), and AcCl (0.18 mL, 2.47 mmol) was added to the reaction mixture. The reaction was allowed to stir overnight at rt. Upon consumption of the starting material, as

indicated by TLC, the solvent was evaporated under reduced pressure, and the remaining residue was purified by column chromatography (DCM:MeOH, 9:1 to 7:1) to give glycoside **4.17** as a white solid (198 mg, 89 %).

R_f: 0.2 (DCM:MeOH, 7:1); ^{1}H MNR (CD_3OD (a drop of D_2O to improve solubility) 300 MHz): δ = 7.83 (d, 2 H, Ph-*H*, *J* = 6 Hz), 7.69 (d, 2 H, Ph-*H*, *J* = 9 Hz), 7.46-7.34 (m, 4 H, Ph-*H*), 4.49-4.38 (m, 4 H, overlapping *H*-1, Fmoc-CH_2, and α-*H*), 4.25 (t, 1 H, Fmoc-C*H*, *J* = 6 Hz), 4.18-4.13 (dd, 1 H, β-H_a, *J* = 6 Hz, 9 Hz), 3.91-3.83 (m, 2 H, overlapping β-H_b and *H*-6_a), 3.75 (s, 3 H, C(O)OCH_3), 3.73-3.61 (m, 2 H, overlapping *H*-2 and *H*-6_b), 3.51-3.45 (m, 1 H, *H*-3), 3.35-3.30 (m, 2 H, (overlapped by MeOH peak) overlapping *H*-5 and *H*-4), 1.94 (s, 3 H, NHC(O)CH_3); ^{13}C NMR: (CD_3OD (a drop of D_2O to improve solubility), 75 MHz) δ = 173.3, 167.5 (each s, *C*(O)OCH_3 and NH*C*(O)CH_3), 143.6, 141.1 (each s, Fmoc-*C*(O) and Ph-*C*), 127.7, 127.1, 124.8, 119.7 (each d, Fmoc-*C*H and Ph-*C*H), 101.2 (d, *C*-1), 76.4, 74.1, 70.2, 66.8, 55.8, 54.3, 52.3, 29.7 (not assigned due to poor solubility of sample), 21.9 (q, NHC(O)*C*H_3); IR: (KBr disc) 3319, 2952, 1748, 1690, 1654, 1535 cm^{-1}; $[\alpha]_D$: - 1.7 (*c* 1.3, CH_3OH); MS-ESI/TOF: Calculated for $C_{27}H_{33}N_2O_{10}$ $(M + H)^+$: 546.2162, found 546.2184.

N^{α}-(9-Fluorenylmethoxycarbonyl)-*O*-[(2-deoxy-2-acetamido-6-*O*-*p*-tosyl)-β-D-glucopyranosyl]-L-serine-methyl ester (4.18)

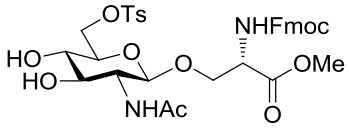

Glycoside **4.17** (60 mg, 0.11 mmol) was placed under N_2 and dissolved in anhydrous pyridine (2 mL). The reaction mixture was cooled to 0 °C, and a solution of TsCl (100 mg, 0.52 mmol) in anhydrous pyridine (2 mL) was added. The reaction was stirred at 0 °C for 1 h, allowed to return to rt, and stirred at rt overnight. The solvent was co-evaporated with toluene under reduced pressure, and the remaining residue was purified by column chromatography (DCM:MeOH, 15:1 to 10:1) to give the tosylated glycoside **4.18** as a clear oil (19 mg, 24 %).

R_f: 0.5 (DCM:MeOH, 7:1); ^{1}H MNR ($CDCl_3$, 300 MHz): δ = 7.74 (t, 4 H, Ph-*H*, *J* = 6 Hz), 7.57 (d, 2 H, Ph-*H*, *J* = 6 Hz), 7.37 (t, 2 H, Ph-*H*, *J* = 6 Hz), 7.29-7.23 (m, 4

H, Ph-*H*), 6.91 (bs, 1 H, N*H*C(O)CH_3), 5.99 (d, 1 H, N*H*C(O)OCH_2, *J* = 9 Hz), 4.50-4.36 (m, 2 H, overlapping *H*-1 and α-*H*), 4.27-4.14 (m, 5 H, overlapping *H*-6, Fmoc-C*H*, and Fmoc-CH_2), 4.05-4.00 (dd, 1 H, β-H_a, *J* = 6 Hz, 9 Hz), 3.86-3.83 (m, 1 H, β-H_b), 3.72 (s, 3 H, C(O)OCH_3), 3.65-3.39 (m, 4 H, overlapping *H*-2, *H*-3, *H*-4, and *H*-5), 2.36 (s, 3 H, Ph-CH_3), 1.95 (s, 3 H, NHC(O)CH_3); ^{13}C NMR: ($CDCl_3$, 75 MHz) δ = 173.2, 170.4 (each s, *C*(O)OCH_3 and NH*C*(O)CH_3), 156.4 (s, Fmoc-*C*(O)), 145.1, 143.7, 143.6, 141.23, 132.48 (each s, Ph-*C*), 129.9, 127.9, 127.8, 127.1, 125.1, 120.0 (each d, Fmoc-*C*H and Ph-*C*H), 100.3 (d, *C*-1), 74.9, 73.5, 70.3 (each d, *C*-2, *C*-3, *C*-4, and *C*-5), 69.1, 37.2 (each t, *C*-6, Fmoc-*C*H_2, and β-*C*), 53.9 (d, α-*C*), 52.89 (q, C(O)O*C*H_3), 23.2 (q, NHC(O)*C*H_3), 21.61 (q, Ph-*C*H_3); IR: (DCM film on NaCl plate) 3349, 2984, 1723, 1655, 1548, 1176 cm^{-1}; $[\alpha]_D$: - 2.8 (*c* 0.85, CH_2Cl_2); MS-ESI/TOF: Calculated for $C_{34}H_{39}N_2O_{12}S$ $(M + H)^+$: 700.2250, found 700.2268.

3-Azido-propionic acid (4.21)[209]

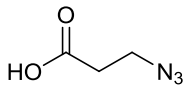

3-Bromopropionic acid (1.50 g, 9.8 mmol) was dissolved in MeCN (4 mL). NaN_3 (956 mg, 14.7 mmol) was added and the reaction mixture, and heated at reflux (85 °C) for 3 h. The reaction was allowed to return to rt, then carefully washed with 0.1 M HCl, dried ($MgSO_4$) and filtered. The solvent was evaporated to almost dryness under reduced pressure, with care taken that the water bath was not heated. The remaining orange oil was used without further purification (400 mg, 36 % crude yield).

^{1}H NMR: ($CDCl_3$, 300 MHz) δ = 9.87 (bs, 1 H, O-*H*), 3.58 (t, 2 H, CH_2N_3, *J* = 6 Hz), 2.63 (t, 2 H, OC(O)CH_2, *J* = 6 Hz); (Lit[209]: ^{1}H NMR: ($CDCl_3$, 400 MHz) δ = 11.00, 3.60, 2.65); IR: (Liquid IR in $CDCl_3$) 3165, 2941, 2104, 1718 cm^{-1}.

N^{α}-(9-Fluorenylmethoxycarbonyl)-*O*-(2-deoxy-2-acetamido-3,4-di-*O*-trimethylsilyl-6-[3-Azido-propionic ester]-β-D-glucopyranosyl)-L-serine methyl ester (4.25)

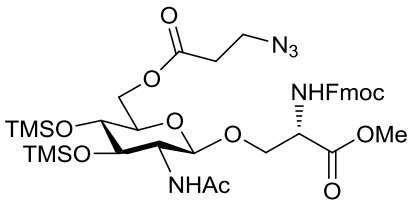

Glycoside **4.17** (60 mg, 0.11 mmol) was dissolved in anhydrous pyridine (4 mL), under N_2, and cooled to 0 °C. To this, a solution of HMDS (0.06 mL, 0.28 mmol) and TMSCl (0.09 mL, 0.71 mmol) was added. The reaction mixture was allowed to return to rt, and stirred overnight. The solvent was co-evaporated with toluene using a rotary evaporator, then the remaining residue was dissolved in DCM and washed with H_2O. The organic layer was dried ($MgSO_4$) and filtered, then evaporated under reduced pressure to give the TMS protected product, **4.22**, as a yellow oil, which was used without further purification (75 mg, 90%).

The crude product, **4.22** (75 mg, 0.09 mmol) was dissolved in an acetone:MeOH mixture (1:0.8 mL), and this solution was cooled to 0 °C. AcOH (0.025 mL, 0.2 mmol) was added to the reaction mixture, and this was stirred at 0 °C for 1 h. As no major change was noted by TLC the reaction was allowed to return to rt, and stirred for 4 h. A further portion of AcOH (0.025 mL, 0.2 mmol) was added to the reaction mixture, and this was allowed to stir at rt for 2 h. When most of the starting material had been consumed, as indicated by TLC, the reaction mixture was diluted with DCM, and washed with $NaHCO_3$, followed by H_2O. The organic layer was dried ($MgSO_4$) and filtered, and then concentrated under reduced pressure to give the C-6 deprotected derivative **4.23** as a clear oil, which was used without further purification (45 mg, 67 %).

Azido propionic acid **4.21** (120 mg, which still contained some MeCN) was dissolved in anhydrous DCM under N_2, and cooled to 0 °C. DCC (26 mg, 0.13 mmol) and DMAP (1.5 mg, 0.13 mmol) were added, and the reaction mixture was allowed to stir for 5 mins. A solution of the crude TMS protected glycoside, **4.23** (45 mg, 0.06 mmol) in anhydrous DCM was added slowly to the reaction mixture. This was stirred at 0 °C for 20 mins, and then allowed to return to rt. The reaction mixture

was stirred at rt for 5 h, and then washed with H_2O. The organic layer was dried ($MgSO_4$) and filtered, and then concentrated under reduced pressure to almost dryness. The remaining oil was purified by column chromatography (Pet. Ether: EtOAc, 1:1 →1:2) to give the functionalised glycoside **4.25** as a clear oil (5 mg, 9 %).

R_f: 0.7 (Pet. Ether:EtOAc, 1:3); ^{1}H NMR ($CDCl_3$, 300 MHz): δ = 7.77 (d, 2 H, Ph-*H*, *J* = 6 Hz), 7.69-7.65 (m, 2 H, Ph-*H*), 7.43-7.30 (m, 4 H, Ph-*H*), 5.91 (d, 1 H, N*H*C(O)OCH$_2$, *J* = 6 Hz), 5.86 (d, 1 H, N*H*Ac, *J* = 9 Hz), 4.88 (d, 1 H, *H*-1, *J* = 6 Hz), 4.52-4.43 (m, 3 H, overlapping α-*H*, β-H_a, and *H*-6$_a$), 4.38-4.32 (m 1 H, β-H_b), 4.28-4.13 (m, 3 H, overlapping *H*-6$_b$ and Fmoc-CH_2), 3.89 (t, 1 H, *H*-3, *J* = 6 Hz), 3.82-3.77 (m, 1 H, Fmoc-C*H*), 3.75 (s, 3 H, C(O)OCH_3), 3.60-3.49 (m, 4 H, overlapping *H*-4, *H*-5, and CH_2N$_3$), 3.45-3.37 (m, 1 H, *H*-2), 2.64-2.58 (m, 2 H, OC(O)CH_2), 1.97 (s, 3 H, NHC(O)CH_3), 0.17, 0.16 (each s, 18 H, Si(CH_3)$_3$); ^{13}C NMR ($CDCl_3$, 75 MHz): δ = 155.2, 151.3, 126.7, 126.1, 124.2, 118.9, 99.1, 71.1, 66.1, 54.9, 53.2, 51.5, 30.1, 28.7, 22.7, -0.3, -0.4; IR: (Liquid IR in $CDCl_3$) 3155, 2962, 2104, 1816, 1712, 1563, 1249 cm^{-1}; $[\alpha]_D$: + 8 (*c* 0.25, CH_2Cl_2); MS-ESI/TOF: Calculated for $C_{33}H_{44}N_5O_{11}Si$ (M (-TMS) + H)$^+$: 714.2801, found 714.2818 (1 X TMS removed by formic acid in the mobile phase).

(2-Deoxy-2-acetamido-6-*O*-[*N*-(3,4-hydoxyphenylethyl)-succinamide])-α/β-D-glucopyranose (5.9)

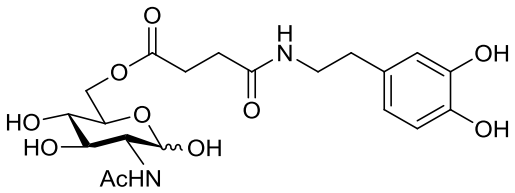

Glycosyl derivative **5.39** (40 mg, 0.06 mmol) was dissolved in MeOH (5 mL), and 10 % Pd/C (w/w) (40 mg) was added. The reaction was carried out by bubbling H_2 through the reaction mixture, at rt for 4 h. The reaction mixture was filtered through celite, and the solvent was removed under reduced pressure. The remaining residue was purified by column chromatography (EtOAc:MeOH, 4:1) to give the deprotected glycosyl dopamine derivative **5.9** as a white oily solid (14 mg, 56 %). (Anomeric ratio 1:0.6, α:β)

R_f: 0.3 (EtOAc:AcOH:H_2O, 4:1:1); ^{1}H NMR (CD_3OD, 300 MHz): δ = 6.76-6.66 (m, 2 H, Ar-*H*), 6.54 (d, 1 H, Ar-*H*, *J* = 6 Hz), 5.09 (d, 1 H, *H*-1 (α-anomer), *J* = 3 Hz), 4.61 (d, 1 H, *H*-1 (β-anomer), *J* = 9 Hz), 4.45-4.35 (m, 1 H, *H*-6_a), 4.29-4.20 (m, 1 H, *H*-6_b), 4.08-3.98 (m, 1 H, *H*-5), 3.89-3.84 (dd, 1 H, *H*-2, *J* = 3 Hz, 12 Hz), 3.74-3.68 (m, 1 H, *H*-3) 3.38-3.30 (m, 3 H, overlapped by CD_3OD peak, *H*-4 and CH_2-Ar), 2.66-2.62 (m, 4 H, overlapping NHCH_2 and C(O)CH_2), 2.49 (t, 2 H, C(O)CH_2, *J* = 6 Hz), 2.01 (s, 3 H, NHC(O)CH_3); ^{13}C NMR ($CDCl_3$, 75 MHz): δ = 172.9, 172.8 (each s, NH*C*(O)CH_3 and *C*(O)CH_2), 145.0, 143.3, 130.7 (each s, Ar-*C*), 119.7, 115.5, 114.9 (each d, Ar-*C*H), 91.2 (d, *C*-1), 73.9, 71.1 (each d, *C*-3 and *C*-5), 69.3 (d, *C*-4), 63.7 (t, *C*-6), 54.4 (d, *C*-2), 40.9 (t, *C*H_2NH), 34.5 (t, C(O)*C*H_2), 30.1 (t, C(O)*C*H_2), 29.1 (t, *C*H_2-Ar), 21.2 (q, NHC(O)*C*H_3); IR: (DCM film on NaCl plate) 3390, 1702, 1635, 1557, 1259 cm^{-1}; $[\alpha]_D$: + 40 (*c* 0.2, CH_3OH); MS-ESI/TOF: Calculated for $C_{20}H_{28}O_{10}N_2$ $(M + H)^+$: 457.1817, found 457.1835.

_N_-[(1,1-Dimethylethoxy)carbonyl]-3,4-Dibenzyloxyphenylethylamine (5.11)[210]

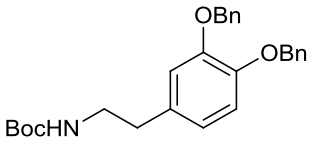

Dopamine hydrochloride (2.50 g, 0.13 mmol) was dissolved in MeOH:Et_3N (9:1 ratio, 71.5 mL). Boc anhydride (3.17 g, 14.5 mmol) was added to the reaction mixture, which was allowed to stir at 50 ˚C for 1 h. The solvent was evaporated, then ice-cold 1 M HCl was added to the residue, and allowed to stir for 10 mins. The product was extracted by washing twice with EtOAc. The organic layer was dried ($MgSO_4$), and filtered, then concentrated under reduced pressure. The crude product was purified by column chromatography (Hex:EtOAc:MeOH, 4:1:0.5 to 2:1:0.5), to yield *N*-Boc protected dopamine. Solid K_2CO_3 (11.00 g, 79 mmol) was added to this intermediate, and the flask placed under N_2. Anhydrous DMF (20 mL) was added, followed by benzyl bromide (3.6 mL, 30 mmol). The reaction mixture was stirred at rt overnight, then filtered through celite. The celite was rinsed twice with ether. The filtrate and combined ether rinses were washed with ice water, followed by 1 M HCl and brine. The organic layer was dried ($MgSO_4$), and filtered. The solvent was removed under reduced pressure. The resulting white solid was purified by column chromatography (Hex:EtOAc, 7:1 to 3:1) to give the protected dopamine derivative

5.11 as a white solid (2.50 g, 43 %). Spectroscopic data was in agreement with reported values.

R_f: 0.4 (Hex:EtOAc, 3:1); ^{1}H NMR ($CDCl_3$, 300 MHz): δ = 7.37-7.29 (m, 10 H, Ar-*H*), 6.87 (d, 1 H, Ar-*H*, *J* = 6 Hz), 6.78 (bs, 1 H, Ar-*H*), 6.71-6.68 (dd, 1 H, Ar-*H*, *J* = 3 Hz, 9 Hz), 5.14, 5.13 (each s, 2 H, CH_2-Ph), 4.48 (bs, 1 H, N*H*CH_2), 3.34-3.27 (m, 2 H, NHCH_2), 2.68 (t, 2 H, CH_2-Ar, *J* = 9 Hz), 1.43 (s, 9 H, C(CH_3)$_3$); (Lit[210]: ^{1}H NMR ($CDCl_3$, 200 MHz): δ = 7.39, 6.89, 6.71, 5.15, 4.45, 3.32, 2.7, 1.45); ^{13}C NMR ($CDCl_3$, 75 MHz): δ = 155.8, 149.0, 147.7, 137.5, 137.3, 132.4 (each s, Ar-*C* and NH*C*(O)OC$(CH_3)_3$), 128.5, 127.8, 127.7, 127.4, 127.3, 121.7, 115.9, 115.4 (each d, Ar-*C*H), 71.5, 71.4 (each t, O*C*H_2-Ph), 41.8 (t, NH_2*C*H_2), 35.6 (t, *C*H_2-Ph), 28.4 (q, C(*C*H_3)$_3$); IR: (KBr disc) 3380, 3003, 2970, 1681, 1592, 1519, 1277, 1240 cm^{-1}; MS-ESI/TOF: Calculated for $C_{54}H_{63}N_2O_8$ $(2M + H)^+$: 867.4579, found 867.4606.

3,4-Dibenzyloxyphenylethylamine (5.12)[210]

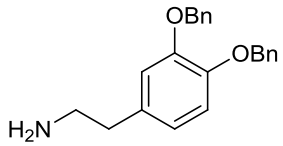

A 5 % solution of TFA in DCM (v/v) (40 ml) was added to Boc protected dopamine derivative **5.11** (1.50 g, 3.4 mmol). The reaction mixture was allowed to stir for 6 h at rt, then the solvent was co-evaporated with toluene. The remaining solid was recrystallised (EtOAc/Hex). The free amine **5.12** was obtained as a white solid (1.00 g, 87 %). Spectroscopic data was in agreement with reported values.

R_f: 0.4 (DCM:MeOH, 9:1); ^{1}H NMR (CD_3OD, 300 MHz): δ = 7.47-7.29 (m, 10 H, Ar-*H*), 7.02-6.96 (m, 2 H, Ar-*H*), 6.83-6.80 (dd, 1 H, Ar-*H*, *J* = 3 Hz, 6 Hz), 5.14, 5.12 (each s, 2 H, Ph-CH_2), 3.12 (t, 2 H, NH_2CH_2, *J* = 6 Hz), 2.87 (t, 2 H, CH_2-Ar, *J* = 6 Hz); (Lit[210]: ^{1}H NMR (CD_3OD, 300 MHz): δ = 7.65-7.47, 7.20, 7.14, 7.00, 5.32, 5.30, 3.30, 3.04); ^{13}C NMR (CD_3OD, 75 MHz,): δ = 149.2, 148.2 (each s, Ar-*C*), 137.4, 137.3 (each s, Ar-*C*) 130.0 (s, Ar-*C*), 128.1, 127.5, 127.3, 127.2, 121,6, 115.7, 115.5 (each d, Ar-*C*H), 71.1 (t, Ph-*C*H_2), 40.6 (t, NH_2*C*H_2), 32.7 (t, *C*H_2-Ar); IR: (DCM film on NaCl plate) 3438, 3033, 1680, 1514, 1204 cm^{-1}; MS-ESI/TOF: Calculated for $C_{22}H_{24}NO_2$ $(M + H)^+$: 335.1835, found 335.1829.

N-(3,4-Dibenzyloxyphenylethyl)-succinamic acid (5.13)[210]

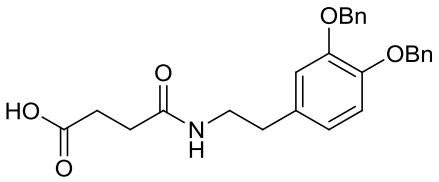

The free amine **5.12** (1.00 g, 2.99 mmol) was dissolved in pyridine (2 mL), and succinic anhydride (0.54 g, 5.41 mmol) was added to the reaction mixture. This was allowed to stir at rt for 3 h. The solvent was co-evaporated with toluene under reduced pressure, and the remaining residue was purified by column chromatography (DCM:MeOH, 15:1 to 10:1) to give succinyl-dopamine derivative **5.13** as a white solid (1.06 g, 82 %). Spectroscopic data was in agreement with reported values.

R_f: 0.5 (DCM:MeOH, 9:1); ^{1}H NMR ($CDCl_3$, 300 MHz): δ = 7.43-7.28 (m, 10 H, Ar-*H*), 6.86 (d, 1 H, Ar-*H*, *J* = 9 Hz), 6.76 (d, 1 H, Ar-*H*, *J* = 3 Hz), 6.68-6.65 (m, 1 H, Ar-*H*), 5.71 (bs, 1 H, N*H*CH_2), 5.12, 5.11 (each s, 2 H, Ph-CH_2), 3.45-3.39 (m, 2 H, NHCH_2), 2.68 (t, 2 H, CH_2-Ar, *J* = 6 Hz), 2.61 (t, 2 H, C(O)CH_2, *J* = 6 Hz), 2.37 (t, 2 H, C(O)CH_2, *J* = 6 Hz); (Lit[210]: ^{1}H NMR ($CDCl_3$, 200 MHz): δ = 7.39, 6.89, 6.80, 6.71, 5.55, 5.17, 5.15, 3.45, 2.70, 2.65, 2.38); ^{13}C NMR ($CDCl_3$, 75 MHz): δ = 149.0, 147.8 (each s, CH_2*C*(O)), 137.3, 131.9 (each s, Ar-*C*), 128.5, 127.8, 127.4, 127.3, 121.7, 115.9, 115.2 (each d, Ar-*C*H), 40.85 (t, NH*C*H_2), 34.7, 31.7 (each t, *C*H_2C(O)), 30.2 (t, *C*H_2-Ph); IR: (KBr disc) 3324, 3035, 2927, 1694, 1640, 1523, 1266 cm^{-1}.

(2-Deoxy-2-[(2,2,2-trichloroethoxycarbonyl)amino]-3,4,6-tri-*O*-trimethylsilyl-1-*O*-phenylmethyl ether)-β-D-glucopyranoside (5.17)

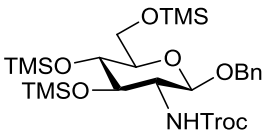

Benzyl glycoside **4.6** (1.04 g, 2.2 mmol) was dissolved in distilled MeOH (18 mL), and 0.1 M $NaOH_{(aq)}$ (18 mL) was added. The reaction mixture was stirred at rt for 1 h, then neutralized with AcOH (10 mL). The organic solvent was evaporated using a rotary evaporator, and the remaining aqueous solution was extracted with EtOAc. The organic layer was washed twice with sat. $NaHCO_3$ solution, then dried ($MgSO_4$),

and filtered. The organic layer was concentrated under reduced pressure, and the crude product was purified by column chromatography (EtOAc:MeOH, 4:1) to give the deprotected glycoside as a white solid (717 mg, 73 %).

The deprotected glycoside (717 mg, 1.61 mmol) was dissolved in dry pyridine (30 mL) under N_2. The solution was cooled to 0 ˚C, then a solution of TMSCl (1.23 mL, 9.66 mmol) and DIPEA (0.56 mL, 3.2 mmol) was added. The reaction was allowed to reach rt, then stirred overnight. The solvent was co-evaporated with toluene, and the remaining residue was dissolved in DCM. The organic layer was washed with H_2O, then dried ($MgSO_4$), and filtered. The crude product was purified by column chromatography (Pet. Ether:EtOAc, 4:1) to leave TMS protected glycoside **5.17** as a white solid (0.37 g, 35 %).

R_f: 0.75 (Pet. Ether: EtOAc, 4:1); ^{1}H NMR ($CDCl_3$, 300 MHz): δ = 7.31 (s, 5 H, Ph-*H*), 5.01 (d, 1 H, N*H*C(O)OCH$_2$, *J* = 9 Hz), 4.85 (d, 1 H, Ph-CH_{2a}, *J* = 12 Hz), 4.72-4.54 (m, 4 H, overlapping *H*-1, NHC(O)OCH_2, and Ph-CH_{2b}), 3.88-3.60 (m, 4 H, overlapping H_6, *H*-3 and *H*-4), 3.45-3.34 (m, 1 H, *H*-2), 3.26-3.20 (m, 1 H, *H*-5), 0.17, 0.13 (each s, 27 H, SiC(CH_3)$_3$); ^{13}C NMR ($CDCl_3$, 75 MHz): δ = 153.3 (s, NH*C*(O)OCH$_2$), 136.8 (s, Ph-*C*), 127.7, 127.3, 127.1 (each d, Ph-*C*H), 98.3 (d, *C*-1), 94.7 (s, *C*Cl$_3$), 76.1 (d, *C*-5), 74.7 (d, *C*-3), 74.0 (t, NHC(O)O*C*H$_2$), 71.1 (d, *C*-4), 69.5 (t, Ph-*C*H$_2$), 61.3 (t, *C*-6), 57.8 (d, *C*-2), 0.1, 0.0, -0.8 (each q, SiC(*C*H$_3$)$_3$); m.p.: 74-78 ˚C ; IR: (DCM film on NaCl plate) 3324, 2955, 1712, 1551, 1250 cm^{-1}; $[\alpha]_D$: -15.9 (*c* 3.15, CH_2Cl_2); MS-ESI/TOF: Calculated for $C_{25}H_{48}Cl_3N_2O_7Si_3$ $(M + NH_4)^+$: 677.1829, found 677.1849.

(2-Deoxy-2-[(2,2,2-trichloroethoxycarbonyl)amino]-3,4-di-*O*-trimethylsilyl-1-*O*-phenylmethyl ether)-β-D-glucopyranoside (5.18)

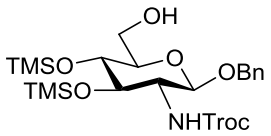

TMS protected glycoside **5.17** (483 mg, 0.7 mmol) was dissolved in an acetone:MeOH mixture (3:4 mL). The reaction mixture was cooled to 0 ˚C, then AcOH (0.08 mL, 1.46 mmol) was added, and this was stirred for 2 h. Solid $NaHCO_3$ was added to the reaction mixture, and stirred for 10 mins. The reaction mixture was

diluted with DCM (20 mL), and the solid $NaHCO_3$ was removed by filtration. The filtrate was concentrated under reduced pressure, and the remaining residue was purified by column chromatography (Hex:EtOAc, 9:1 to 3:1) to give the selectively deprotected glycoside **5.18** as a white solid (298 mg, 72 %).

R_f: 0.32 (Pet. Ether: EtOAc, 4:1); ^{1}H NMR ($CDCl_3$, 300 MHz): δ = 7.31-7.26 (m, 5 H, Ph-*H*), 5.14 (bs, 1 H, N*H*C(O)OCH_2), 4.85 (d, 1 H, Ph-CH_{2a}, *J* = 12 Hz), 4.69-4.66 (m, 3 H, overlapping *H*-1 and NHC(O)OCH_2), 4.59 (d, 1 H, Ph-CH_{2b}, *J* = 12 Hz), 3.86-3.65 (m, 3 H, overlapping H_{6a}, *H*-3 and *H*-4), 3.56 (t, 1 H, H_{6b}, *J* = 9 Hz), 3.41-3.29 (m, 2 H, overlapping *H*-2 and *H*-5), 0.17, 0.13 (each s, 18 H, SiC(CH_3)$_3$); ^{13}C NMR ($CDCl_3$, 75 MHz): δ = 153.4 (s, NH*C*(O)OCH_2), 136.4 (s, Ph-*C*), 127.7, 127.2, 127.1 (each d, Ph-*C*H), 98.8 (d, *C*-1), 94.5 (s, *C*Cl_3), 75.4 (d, *C*-5), 74.5 (d, *C*-3), 74.0 (t, NHC(O)O*C*H_2), 71.5 (d, *C*-4), 70.3 (t, Ph-*C*H_2), 61.2 (t, *C*-6), 58.1 (d, *C*-2), 0.12, 0.00 (each q, SiC(*C*H_3)$_3$); m.p.: 70- 74 ˚C; $[\alpha]_D$: - 7.3 (*c* 0.55, CH_2Cl_2); IR: (DCM film on NaCl plate) 3351, 2098, 1642, 1546, 1251 cm^{-1}; MS-ESI/TOF: Calculated for $C_{22}H_{40}Cl_3N_2O_7Si_2$ $(M + NH_4)^+$: 607.1409, found 607.1417.

(2-Deoxy-2-[(2,2,2-trichloroethoxycarbonyl)amino]-3,4-di-*O*-trimethylsilyl-6-*O*-[*N*-(3,4-dibenzyloxyphenylethyl)-succinamyl]-1-*O*-phenylmethyl)-β-D-glucopyranoside (5.24)

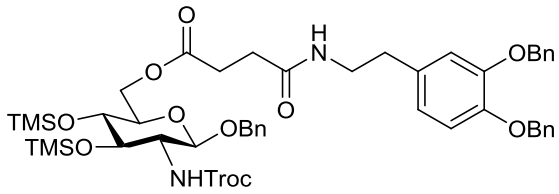

Benzyl glycoside **5.18** (298 mg, 0.51 mmol) was dissolved in dry DCM (10 mL), under N_2, and DCC (120 mg, 0.58 mmol) was added. This was then added to a solution of the succinyl-dopamine derivative **5.13** (242 mg, 0.56 mmol) in dry DCM (25 mL) under N_2. DMAP (4.3 mg, 0.03 mmol) was added to the reaction mixture, and this was allowed to stir at rt for 3 h. The reaction mixture was filtered through celite. The filtrate was diluted with DCM (20 mL) and washed with an aqueous solution of 5 % AcOH, followed by H_2O. The organic layer was dried ($MgSO_4$), and filtered. The crude product was purified by column chromatography (Pet. Ether:EtOAc, 4:1 to 2:1) to give the protected glycoside **5.24** as a clear syrup (306 mg, 60 %).

R_f: 0.6 (Pet. Ether: EtOAc, 1:1); ^{1}H NMR ($CDCl_3$, 300 MHz): δ = 7.45-7.25 (m, 15 H, Ar-*H*), 6.87 (d, 1 H, Ar-*H*, *J* = 9 Hz), 6.79-6.78 (m, 1 H, Ar-*H*), 6.70-6.66 (dd, 1 H, Ar-*H*, *J* = 3 Hz, 9 Hz), 5.60 (bs, 1 H, N*H*C(O)CH_2), 5.14-5.12 (m, 5 H, overlapping Ph-CH_2 and N*H*C(O)OCH_2), 4.85 (d, 1 H, Ph-CH_{2a}, *J* = 12 Hz), 4.67-4.48 (m, 5 H, overlapping *H*-1, Ph-CH_{2b}, NHC(O)OCH_2 and *H*-6_a), 4.15-4.09 (dd, 1 H, *H*-6_b, *J* = 6 Hz, 12 Hz), 3.73 (t, 1 H, *H*-3, *J* = 9 Hz), 3.57 (t, 1 H, *H*-4, *J* = 9 Hz), 3.49-3.34 (m, 4 H, overlapping *H*-5, *H*-2 and CH_2-Ar), 2.73-2.66 (m, 4 H, overlapping NHCH_2 and C(O)CH_2), 2.39-2.35 (m, 2 H, C(O)CH_2), 0.15, 0.13 (each s, 18 H, SiC(CH_3)$_3$) ; ^{13}C NMR ($CDCl_3$, 75 MHz): δ = 171.9, 170.3 (each s, *C*(O)CH_2), 153.2 (s, NH*C*(O)OCH_2), 148.3, 146.9, 136.7, 136.5, 136.4, 131.6 (each s, Ar-*C*), 127.7, 127.6, 127.5, 127.2, 127.1, 127.0, 126.6, 126.5, 120.9, 115.0, 114.7 (each d, Ar-*C*H), 98.4 (d, *C*-1), 94.5 (s, *C*Cl_3), 74.2 (d, *C*-3), 73.9 (t, NHC(O)O*C*H_2), 73.2, 57.5 (each d, *C*-2 and *C*-5), 71.7 (d, *C*-4), 70.7, 70.5 (each t, Ph-*C*H_2), 69.8 (t, Ph-*C*H_2), 63.0 (t, *C*-6), 40.0 (t, *C*H_2NH), 34.4, 30.2 (each t, C(O)*C*H_2), 28.7 (t, *C*H_2-Ph), 0.1, 0.0 (each q, SiC(*C*H_3)$_3$; IR: (DCM film on NaCl plate) 3368, 3065, 2956, 1737, 1650, 1512, 1252 cm^{-1}; $[\alpha]_D$: - 7.3 (*c* 1.9, CH_2Cl_2); MS-ESI/TOF: Calculated for $C_{42}H_{45}Cl_3KN_2O_{11}$ (M + K[– 2 x TMS])$^+$: 897.1721, found 897.1766.

(2-Deoxy-2-[(2,2,2-trichloroethoxycarbonyl)amino]-6-*O*-[*N*-(3,4-dibenzyloxy phenylethyl)-succinamyl]-1-*O*-phenylmethyl)-β-D-glucopyranoside (5.25)

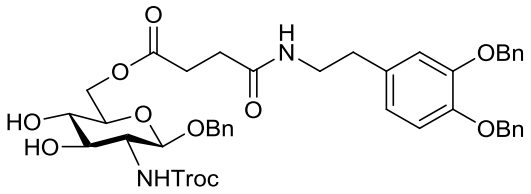

A 2 % solution of TFA in DCM (v/v) (12.25 mL, 3.18 mmol) was added to the protected glycoside **5.24** (200 mg, 0.19 mmol) at 0 ˚C, and this was allowed to stir for 1 h. To the reaction mixture solid $NaHCO_3$ (400 mg) was added, and stirred for 2 mins. The solid was removed by gravity filtration, and the filtrate was concentrated under reduced pressure. The remaining residue was purified by column chromatography (DCM:MeOH, 50:1 to 30:1) to give glycoside **5.25** as a white solid (160 mg, 98 %)

R_f: 0.55 (DCM:MeOH, 9:1); ^{1}H NMR ($CDCl_3$, 300 MHz): δ = 7.44-7.17 (m, 15 H, Ar-*H*), 6.86 (d, 1 H, Ar-*H*, *J* = 9 Hz), 6.78 (d, 1 H, Ar-*H*, *J* = 1.8 Hz), 6.68-6.65 (dd,

1 H, Ar-*H*, *J* = 3 Hz, 9 Hz), 5.74 (t, 1 H, N*H*C(O)CH_2, *J* = 6 Hz), 5.52 (d, 1 H, N*H*C(O)OCH_2, *J* = 9 Hz), 4.90 (d, 1 H, NHC(O)OCH_{2a}, *J* = 15 Hz), 4.68-4.50 (m, 5 H, overlapping *H*-1, Ph-CH_2, NHC(O)OCH_{2b}, and *H*-6_a), 4.27-4.23 (m, 1 H, *H*-6_b),3.95 (bs, 1 H, O*H*), 3.66-3.60 (m, 1 H, *H*-3), 3.52-3.36 (m, 5 H, overlapping *H*-2, *H*-4, *H*-5, and CH_2NH), 2.70-2.59 (m, 4 H, overlapping CH_2-Ar and C(O)CH_2), 2.38 (t, 2 H, C(O)CH_2, *J* = 6 Hz); ^{13}C NMR ($CDCl_3$, 75 MHz): δ = 173.3, 171.7, 154.9, 149.0, 147.7, 137.3, 137.2, 137.0, 132.2 (each s, Ar-*C*), 128.5, 127.9, 127.8, 127.4, 127.4, 121.7, 115.9, 115.5 (each d, Ar-C*H*), 99.8 (d, *C*-1), 95.5 (s, *C*Cl_3), 74.7 (t, NHC(O)O*C*H_2), 73.9, 73.7 (each d, *C*-3 and *C*-4), 71.5, 71.3 (each t, Ph-*C*H_2), 70.8, 70.5 (each d, *C*-2 and *C*-5), 63.4 (t, *C*-6), 40.8 (t, *C*H_2NH), 34.9, 30.9 (each t, C(O)*C*H_2), 29.5 (t, *C*H_2-Ar); m.p.: 152-154 ˚C; IR: (KBr disc) 3380, 3320, 2962, 1718, 1638, 1261; $[\alpha]_D$: -30 (*c* 0.65, $CHCl_3$); MS-ESI/TOF: Calculated for $C_{42}H_{45}Cl_3N_2NaO_{11}$ $(M + Na)^+$: 883.1963, found 883.1978.

(2-Deoxy-2-acetamido-3,4-di-*O*-trimethylsilyl-6-*O*-[*N*-(3,4-dibenzyloxy phenylethyl)-succinamyl]-1-*O*-phenylmethyl)-β-D-glucopyranoside (5.28)

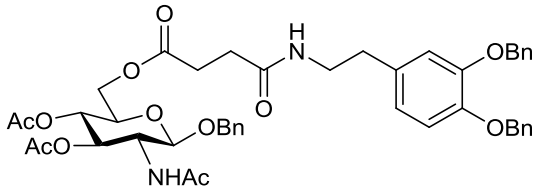

N-Troc protected glycoside **5.24** (268 mg, 0.27 mmol) and freshly activated zinc powder (activated by rinsing twice with 2 M HCl, followed by H_2O, then acetone and ether) (171 mg, 2.6 mmol) were dissolved/suspended in Ac_2O (15 mL) and DCM (3 mL). Et_3N (0.1 mL, 0.75 mmol) was added to the reaction mixture, and this was allowed to stir for 3 h at rt. The reaction mixture was filtered through celite to remove the zinc salts, then the solvent was removed by co-evaporation with toluene under reduced pressure. The remaining residue was dissolved in DCM, then washed with brine, dried ($MgSO_4$), and filtered. The crude product was purified by column chromatography (Pet. Ether:EtOAc, 1:3 to 1:4) to give the *N*-acetyl derivative **5.28** as a white solid (88 mg, 40 %).

R_f: 0.44 (DCM:MeOH, 9:1); ^{1}H NMR ($CDCl_3$, 300 MHz): δ = 7.45-7.27 (m, 15 H, Ar-*H*), 6.88 (d, 1 H, Ar-C*H*, *J* = 9 Hz), 6.80 (d, 1 H, Ar-C*H*, *J* = 3 Hz), 6.71-6.67 (dd, 1 H, Ar-C*H*, *J* = 3 Hz, 9 Hz), 5.63 (t, 1 H, N*H*C(O)CH_2, *J* = 6 Hz), 5.46 (d, 1 H,

N*H*C(O)CH_3, *J* = 9 Hz), 5.21-5.12 (m, 5 H, overlapping *H*-3 and Ph-CH_2), 5.04 (t, 1 H, *H*-4, *J* = 9 Hz), 4.87 (d, 1 H, Ph-CH_{2a}, *J* = 12 Hz), 4.62-4.55 (m, 2 H, overlapping *H*-1 and PhCH_{2b}), 4.20-4.12 (m, 2 H, *H*-6), 4.01-3.91 (m, 1 H, *H*-2), 3.68-3.62 (m, 1 H, *H*-5), 3.46-3.39 (m, 2 H, NHCH_2), 2.71-2.67 (m, 4 H, overlapping C(O)CH_2 and CH_2-Ar), 2.41-2.33 (m, 2 H, C(O)CH_2), 1.99, 1.98 (each s, 6 H, OC(O)CH_3), 1.88 (s, 3 H, NHC(O)CH_3); ^{13}C NMR ($CDCl_3$, 75 MHz): δ = 172.5, 171.1, 170.9, 170.1, 169.48 (each s, *C*(O)CH_2, NH*C*(O)CH_3, and O*C*(O)CH_3), 149.0, 147.7, 137.4, 137.3, 136.9, 132.4 (each s, Ar-*C*), 128.5, 128.0, 127.8, 127.7, 127.4, 127.3, 121.6, 116.6, 115.8, 115.5 (each d, Ar-*C*H), 99.5 (d, *C*-1), 72.5 (d, *C*-3), 71.8, 71.5 (each t, Ph-*C*H_2), 70.7 (d, *C*-5), 68.7 (d, *C*-4), 62.4 (t, Ph-*C*H_2), 54.5 (d, *C*-2), 40.8 (t, NH*C*H_2), 35.1 (t, C(O)*C*H_2), 30.9 (t, C(O)*C*H_2), 29.4 (t, *C*H_2-Ph), 23.3 (q, NHC(O)*C*H_3), 20.7, 20.6 (each q, OC(O)*C*H_3); m.p.: 120-124 ˚C; IR: (DCM film on NaCl plate) 3431, 2100, 1650, 1237 cm^{-1}; $[\alpha]_D$: -16.5 (*c* 1.7, CH_2Cl_2); MS-ESI/TOF: Calculated for $C_{45}H_{52}N_2O_{12}$ $(M + 2H)^{+2}$: 406.1755, found 406.1739 .

(2-Deoxy-2-acetamido-3,4,6-tri-*O*-acetyl-1-*O*-phenylmethyl)-β-D-glucopyranoside (5.33)[251, 261]

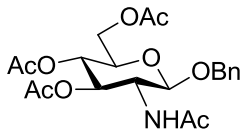

N-Troc protected glycoside **3.18** (736 mg, 1.29 mmol) and freshly activated zinc dust (activated by rinsing twice with 2 M HCl, then H_2O, followed by acetone and ether) (1.26 g, 19 mmol) were dissolved/suspended in Ac_2O (20 mL). Et_3N (0.35 mL, 2.58 mmol) was added to the reaction mixture, and this was allowed to stir at rt for 5 h. The solvent was evaporated, and the remaining residue was purified by column chromatography (Hex: EtOAc, 1:1 to EtOAc flush) to give the *N*-acetyl derivative **5.33** as a white solid (400 mg, 71 %). Spectroscopic data was in agreement with reported values.

R_f: 0.67 (DCM:MeOH, 9:1); ^{1}H NMR ($CDCl_3$, 300 MHz): δ = 7.38-7.29 (m, 5 H, Ar-*H*), 5.39 (d, 1 H, N*H*C(O)CH_3, *J* = 9 Hz), 5.20 (t, 1 H, *H*-3, *J* = 9 Hz), 5.09 (t, 1 H, *H*-4, *J* = 9 Hz), 4.89 (d, 1 H, Ph-CH_{2a}, *J* = 12 Hz), 4.64-4.58 (m, 2 H, overlapping Ph-CH_{2b} and *H*-1), 4.30-25 (dd, 1 H, *H*-6_a, *J* = 4.8 Hz, 12 Hz), 4.19-4.14 (dd, 1 H, *H*-6_b, *J* = 3 Hz, 12 Hz), 4.02-3.92 (m, 1 H, *H*-2), 3.70-3.64 (m, 1 H, *H*-5), 2.10, 2.01

(each s, 9 H, OC(O)CH_3), 1.90 (s, 3 H, NHC(O)CH_3); (Lit[251]: ^{1}H NMR ($CDCl_3$, 200 MHz): δ = 7.28-7.26, 5.78, 5.21, 5.04, 4.85, 4.64, 4.56, 4.24, 4.12, 3.92, 3.66, 2.05, 1.97, 1.85); ^{13}C NMR ($CDCl_3$, 75 MHz): δ = 170.9, 170.8, 170.3, 169.4 (each s, O*C*(O)CH_3 and NH*C*(O)CH_3), 136.9 (s, Ar-*C*), 128.6, 128.5, 128.3, 128.0 (each d, Ar-*C*H), 99.5 (d, *C*-1), 72.5 (d, *C*-3), 71.9 (d, *C*-5), 70.7 (t, Ph-*C*H_2), 68.7 (d, *C*-4), 62.2 (t, *C*-6), 54.5 (d, *C*-2), 23.3 (q, NHC(O)*C*H_3), 20.8, 20.7, 20.6 (each q, OC(O)*C*H_3); MS-ESI/TOF: Calculated for $C_{21}H_{28}NO_9$ $(M + H)^+$: 439.1792, found 439.1807.

(2-Deoxy-2-acetamido-1-*O*-phenylmethyl)-α/β-D-glucopyranoside (5.34)[261, 262]

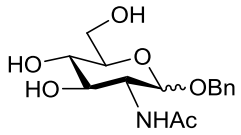

Method A

Acetylated derivative **5.33** (140 mg, 0.32 mmol) was dissolved in distilled MeOH (10 mL), and H_2O (5 mL) was added. The reaction mixture was stirred at 45 °C overnight. The organic solvent was evaporated using a rotary evaporator, and the remaining aqueous solution was extracted with EtOAc. The organic layer was then washed twice with sat. $NaHCO_3$ solution, then dried ($MgSO_4$), and filtered. The organic layer was concentrated under reduced pressure, to give the crude deprotected product, **5.34**, as a white oily solid (80 mg, 80 %). Following this method only the β-anomer is obtained.

Method B

(2-Deoxy-2-acetamido)-β-D-glucopyranose (500 mg, 2.26 mmol) was dissolved in anhydrous DMF (5 mL) and placed under N_2 at 0 °C. BnBr (0.57 mL, 4.79 mmol) and NaH (120 mg, 5.0 mmol) was added to the reaction in four portions, over 2 h, then the reaction was allowed to stir at 0 °C for a further 2 h. The reaction mixture was filtered through celite. The celite was rinsed with DMF, and the filtrate was reduced using a rotary evaporator. The remaining residue was dissolved in H_2O and washed three times with DCM. The aqueous layer was co-evaporated with toluene under reduced pressure to give an anomeric mixture of the benzyl glycoside **5.34** as a

white oily solid (547 mg, 78 %). Spectroscopic data is in agreement with literature values. (Anomeric ratio 0.5:1, α:β)

^{1}H NMR (D_2O, 300 MHz): δ = 7.58-7.38 (m, 5 H, Ph-C*H*), 4.96 (d, 1 H, *H*-1 (α-anomer), *J* = 3 Hz), 4.91 (d, 1 H, Ph-CH_{2a}, *J* = 12 Hz), 4.70 (d, 1 H, Ph-CH_{2b}, *J* = 12 Hz), 4.59-4.54 (m, 2 H, overlapping *H*-1 (β-anomer) and Ph-CH_{2b} (α-anomer)), 3.99-3.47 (m, 12 H, overlapping *H*-3, *H*-4, *H*-5, *H*-6, and *H*-2 (both anomers)), 1.99, 1.95 (each s, 3 H, NHC(O)CH_3 (both anomers)); (Lit[262]: ^{1}H NMR (D_2O, 300 MHz): δ = 7.46-7.37, 4.89, 4.68, 4.54, 3.95, 3.76, 3.70-3.46, 1.94); ^{13}C NMR (D_2O, 75 MHz): δ = 174.5, 174.3 (each s, NH*C*(O)CH_3 (both anomers)), 137.0, 136.8 (each s, Ph-*C* (both anomers)), 129.2, 128.7, 128.6, 128.5, 128.4, 128.4 (each d, Ph-*C*H), 99.9 (d, *C*-1 (β-anomer)), 95.8 (d, *C*-1 (α-anomer)), (75.9, 73.7, 72.1, 71.6, 71.4, 70.8, 70.1, 69.9, 60.8, 60.6, 60.5, 55.53, 53.7), 22.1, 21.8 (each q, NHC(O)*C*H_3 (both anomers)); IR: (KBr disc) 3291, 2870, 2419, 1651, 1553, 1080 cm^{-1}; MS-ESI/TOF: Calculated for $C_{15}H_{22}NO_6$ $(M + H)^+$: 312.1442, found 312.1449.

(2-Deoxy-2-acetamido-3,4,6-tri-*O*-trimethylsilyl-1-*O*-phenylmethyl)-α/β-D-glucopyranoside (5.35)

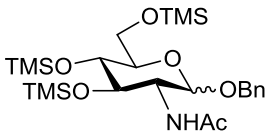

Method A

Glycoside **5.34** (268 mg, 0.64 mmol) was dissolved in dry pyridine (6 mL). The solution was cooled to 0 ˚C, then a solution of TMSCl (0.49 mL, 3.84 mmol) and DIPEA (0.30 mL, 1.28 mmol) was added. The reaction was allowed to reach rt, then stirred overnight at rt. The solvent was co-evaporated with toluene, and the remaining residue was dissolved in DCM. The organic layer was washed with H_2O, then dried ($MgSO_4$), and filtered. The crude product was purified by column chromatography (Pet. Ether:EtOAc, 1:1) to give an anomeric mixture of TMS protected glycoside **5.35** as a white solid (150 mg, 44 %).

Method B

Glycoside **5.34** (268 mg, 0.64 mmol) was dissolved in dry pyridine (6 mL). The solution was cooled to 0 ˚C, then a solution of TMSCl (0.49 mL, 3.84 mmol) and hexamethyldisilazane (0.27 mL, 1.28 mmol) was added. The reaction was allowed to reach rt, then stirred overnight at rt. The solvent was co-evaporated with toluene, and the remaining residue was dissolved in DCM. The organic layer was washed with H_2O, then dried ($MgSO_4$), and filtered. The crude product was purified by column chromatography (Pet. Ether:EtOAc, 1:1) to give an anomeric mixture of the TMS protected glycoside **5.35** as a white solid (250 mg, 74 %). (Anomeric ratio 0.5:1, α:β)

R_f: 0.8 (Pet. Ether: EtOAc, 1:2); ^{1}H NMR ($CDCl_3$, 300 MHz): δ = 7.35-7.26 (m, 10 H, Ph-*H* (both anomers)), 5.61 (d, 1 H, N*H*C(O)CH_3 (β-anomer), *J* = 9 Hz), 5.44 (d, 1 H, N*H*C(O)CH_3 (α-anomer), *J* = 9 Hz), 5.05 (d, 1 H, *H*-1 (α-anomer), *J* = 3 Hz), 4.82 (d, 1 H, Ph-CH_{2a} (β-anomer), *J* = 12 Hz), 4.71-4.65 (m, 2 H, overlapping *H*-1 (β-anomer) and Ph-CH_{2a} (α-anomer)), 4.54 (d, 1 H, Ph-CH_{2b} (β-anomer), *J* = 12 Hz), 4.43 (d, 1 H, Ph-CH_{2b} (α-anomer), *J* = 12 Hz), 4.14-3.99 (m, 2 H, overlapping *H*-2 (both anomers)), 3.98-3.54 (m, 8 H, overlapping *H*-6, *H*-3 and *H*-4 (both anomers)), 3.34-3.23 (m, 2 H, *H*-5 (both anomers)), 1.93, 1.92 (each s, 6 H, NHC(O)CH_3 (both anomers)) 0.16, 0.14, 0.13, 0.12, 0.01, 0.09 (each s, 54 H, SiC(CH_3)$_3$ (both anomers)); ^{13}C NMR ($CDCl_3$, 75 MHz): δ = 170.0, 169.9 (each s, NH*C*(O)CH_3 (both anomers)), 138.1, 137.6 (each s, Ph-*C* (both anomers)), 128.7, 128.6, 128.5, 128.4, 128.2, 128.0, 127.7 (each d, Ph-*C*H (both anomers)), 99.4 (d, *C*-1 (β-anomer)), 92.8 (d, *C*-1 (α-anomer)), 76.9 (d, *C*-5), 75.1, 74.5, 73.1, 71.9 (each d, *C*-3 and *C*-4 (both anomers)), 70.2, 69.5 (each t, Ph-*C*H_2 (both anomers)), 62.3, 61.9 (each t, *C*-6 (both anomers)), 54.8 (d, *C*-2 (α-anomer)), 53.9 (d, *C*-2 (β-anomer)), 1.3, 1.2, 1.1, 1.0, 0.9, 0.8 (each q, SiC(*C*H_3)$_3$ (both anomers)); IR: (DCM film on NaCl plate) 3288, 2956, 1655, 1562, 1250 cm^{-1}; $[\alpha]_D$: + 10 (*c* 1.0, CH_2Cl_2); MS-ESI/TOF: Calculated for $C_{21}H_{36}NO_6Si_2$ (M (-TMS) – H)$^-$ (1 x TMS removed by formic acid in mobile phase): 454.2087, found 454.2089.

(2-Deoxy-2-acetamido-3,4-di-*O*-trimethylsilyl-1-*O*-phenylmethyl)-α/β-D-glucopyranoside (5.37)

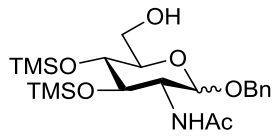

TMS protected glycoside **5.35** (51 mg, 0.10 mmol) was dissolved in an acetone:MeOH mixture (0.8:0.6 mL). The reaction mixture was cooled to 0 ˚C, then AcOH (0.01 mL, 0.2 mmol) was added, and this was stirred for 2 h at 0 ˚C. Solid $NaHCO_3$ (10 mg) was added and stirred for 10 mins. The reaction mixture was diluted with DCM (20 mL), and the solid $NaHCO_3$ was removed by filtration. The filtrate was washed with a sat. solution of $NaHCO_3$, then dried ($MgSO_4$) and filtered. The organic layer was concentrated under reduced pressure, and the remaining residue was purified by column chromatography (Pet. Ether:EtOAc, 1:1) to give the selectively deprotected derivative **5.37** as a clear oil (38 mg, 86 %). (Anomeric ratio 0.6:1, α:β)

R_f: 0.6 (Pet. Ether: EtOAc, 1:2); ^{1}H NMR ($CDCl_3$, 300 MHz): δ = 7.35-7.30 (m, 10 H, Ph-*H* (both anomers)), 5.50 (d, 1 H, N*H*C(O)CH_3 (β-anomer), *J* = 9 Hz), 5.31 (d, 1 H, N*H*C(O)CH_3 (α-anomer), *J* = 6 Hz), 5.09 (d, 1 H, *H*-1 (α-anomer), *J* = 3 Hz), 4.89-4.82 (m, 2 H, overlapping *H*-1 (β-anomer) and Ph-CH_{2a}), 4.59 (d, 1 H, Ph-CH_{2b}, *J* = 12 Hz), 4.06-3.99 (td, 1 H, *H*-2 (α-anomer), *J* = 9 Hz, 15 Hz), 3.96-3.89 (dd, 1 H, *H*-3 (β-anomer), *J* = 9 Hz, 12 Hz), 3.85-3.80 (dd, 1 H, *H*-6_a (β-anomer), *J* = 3 Hz, 9 Hz),), 3.73-3.59 (m, 5 H, overlapping *H*-6_b (β-anomer), *H*-3, *H*-4 and *H*-6 (α-anomer)), 3.53 (t, 1 H, *H*-4 (β-anomer), *J* = 9 Hz), 3.44-3.32 (m, 2 H, overlapping *H*-2 and *H*-5 (β-anomer)), 1.99, 1.94 (each s, 6 H, NHC(O)CH_3 (both anomers)), 0.18, 0.16, 0.13, 0.10 (each s, 36 H, SiC(CH_3)$_3$ (both anomers)); ^{13}C NMR ($CDCl_3$, 75 MHz): δ = 169.5, 168.9 (each s, NH*C*(O)CH_3 (both anomers)), 136.8 (s, Ph-*C*), 127.7, 127.2, 127.1 (each d, Ph-*C*H), 98.7 (d, *C*-1 (β-anomer)), 91.8 (d, *C*-1 (α-anomer)), 75.4 (d, *C*-5), 74.0 (d, *C*-3), 71.6 (d, *C*-4), 70.4 (t, Ph-*C*H_2), 61.4, 60.9 (each t, *C*-6 (both anomers)), 57.3 (d, *C*-2 (β-anomer)), 53.8 (d, *C*-2 (α-anomer)), 23.2, 22.9 (each q, NHC(O)*C*H_3 (both anomers)), 0.3, 0.2, 0.1, -0.9 (each q, SiC(*C*H-$_3$)$_3$ (both anomers)); IR: (DCM film on NaCl plate) 3431, 2925, 1625, 1243 cm^{-1}; $[\alpha]_D$: - 9.4 (*c* 0.85, CH_3OH); MS-ESI/TOF: Calculated for $C_{15}H_{20}NO_6$ (M (-2 x

TMS) - H)$^-$ (TMS removed by formic acid mobile phase): 310.1296, found 310.1310.

(2-Deoxy-2-acetamido-6-*O*-[*N*-(3,4-dibenzyloxyphenylethyl)-succinamyl]-1-*O*-phenylmethyl)-β-D-glucopyranoside (5.39)

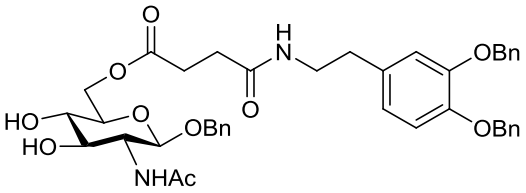

Glycoside **5.37** (100 mg, 0.21 mmol) was dissolved in dry DCM (4 mL), under N_2, and DCC (52 mg, 0.25 mmol) was added. This was then added to a solution of **5.13** (104 mg, 0.24 mmol) in dry DCM (2 mL) under N_2. DMAP (1.8 mg, 0.001 mmol) was then added to the reaction mixture, and this was allowed to stir at rt for 4 h. The reaction mixture was filtered through celite. The filtrate was diluted with DCM and washed with an aqueous solution of 5 % AcOH (v/v), followed by H_2O. The organic layer was dried ($MgSO_4$), and filtered. The crude product was purified by column chromatography (Pet. Ether:EtOAc, 1:1) to give glycosyl-dopamine derivative **5.38** as a clear syrup (100 mg, 52 %).

This glycosyl-dopamine derivative **5.38** (100 mg, 0.11 mmol) was dissolved in a 2 % solution of TFA (v/v) in DCM (7.5 mL) at 0 °C. The reaction mixture was allowed to stir at 0 °C for 1 h, then solid $NaHCO_3$ (50 mg) was added, and stirred for 5 mins. The reaction mixture was diluted with DCM, then filtered by gravity to remove the $NaHCO_3$. The filtrate was concentrated under reduced pressure, and purified by column chromatography (DCM:MeOH, 30:1 to 20:1 to 9:1) to give glycoside **5.39** as a clear oil (44 mg, 50 %).

R_f: 0.5 (DCM:MeOH, 9:1); ^{1}H NMR ($CDCl_3$ with a drop of CD_3OD, 300 MHz): δ = 7.46-7.25 (m, 15 H, Ar-*H*), 6.87 (d, 1 H, Ar-*H*, *J* = 6 Hz), 6.81 (d, 1 H, Ar-*H*, *J* = 2.1 Hz), 6.71-6.68 (dd, 1 H, Ar-*H*, *J* = 3 Hz, 6 Hz), 5.14, 5.11 (each s, 4 H, Ph-CH_2), 4.86 (d, 1 H, Ph-CH_{2a}, *J* = 15 Hz), 4.56 (d, 1 H, Ph-CH_{2b}, *J* = 15 Hz), 4.48 (d, 1 H, *H*-1, *J* = 9 Hz), 4.44 (bs, 2 H, *H*-6), 3.66 (t, 1 H, *H*-2, *J* = 9 Hz), 3.52-3.35 (m, 5 H, overlapping *H*-4, *H*-5, *H*-3 and CH_2-Ar), 2.70-2.65 (m, 4 H, overlapping NHCH_2 and C(O)CH_2), 2.41 (t, 2 H, C(O)CH_2, *J* = 6 Hz), 1.95 (s, 3 H, NHC(O)CH_3); ^{13}C NMR

($CDCl_3$, 75 MHz): δ = 173.2 (s, NH*C*(O)CH_3) 172.4, 172.1 (each s, *C*(O)CH_2), 148.9, 147.6, 137.3, 137.2, 132.5 (each s, Ar-*C*), 128.5, 128.4, 128.0, 127.9, 127.9, 127.5, 127.4, 121.7, 115.8, 115.5 (each d, Ar-*C*H), 99.8 (d, *C*-1), 74.4 (d, *C*-3), 73.8 (d, *C*-5), 71.5, 71.4 (each t, Ph-*C*H_2), 70.7 (t, Ph-*C*H_2), 70.4 (d, *C*-4), 63.5 (t, *C*-6), 56.3 (d, *C*-2), 40.9 (t, *C*H_2NH), 35.0 (t, C(O)*C*H_2), 30.6 (t, C(O)*C*H_2), 29.4 (t, *C*H_2-Ar), 23.0 (q, NHC(O)*C*H_3); IR: (DCM film on NaCl plate) 3299, 2984, 1736, 1641, 1554, 1260 cm^{-1}; $[\alpha]_D$: - 21.5 (*c* 0.65, CH_3OH).

6.3 General Procedures for Solid Phase Peptide Synthesis (SPPS)[172]

6.3.1 Swelling of the Resin

2-Chlorotrityl chloride (CTC) resin (300 mg) was placed into SPPS apparatus. Dry DCM (3 mL) was added, and the vessel was gently shaken for 15 mins. The solvent was removed by vacuum filtration. This was repeated twice.

6.3.2 Introduction of the First Amino Acid (AA)

The recommended loading of CTC resin is 1.0-1.6 mmol AA/g of resin. The first NHFmoc-AA (0.42 mmol) was dissolved in dry DCM (3 mL), and DIPEA (0.28 mL, 4 eq to carboxylic acid, 1.68 mmol) was added. This solution was gently syringed onto the swollen resin, and stirred for 1.75 h. The liquid was then removed by vacuum filtration.

6.3.3 Capping of the First AA

The resin was washed with 3 x DCM/ MeOH/ DIPEA (17:2:1 mL), followed by 3 x DCM (2 mL), 2 x DMF (2 mL), 2 x DCM (2 mL), then dried by vacuum filtration.

6.3.4 Estimation of Loading of the First AA[180]

The resin (50 mg) was weighed into a 100 mL beaker, DMF (20 mL) was added. This suspension was stirred for 30 min, then DBU (0.4 mL) was added. (This gave a 2 % DBU/DMF soln.) The mixture was stirred for 30 mins then diluted to 100 mL with acetonitrile. 2 mL of this solution was transferred to a 25 mL beaker and diluted with acetonitrile to 25 mL. A reference solution was prepared in the same way, without addition of the resin. The sample and reference solutions were measured by UV in quartz cuvettes at 294 and 304 nm, and the absorbance resulting from the

dibenzofulvene released upon Fmoc cleavage was used to calculate the level of loading of the first AA (Fig. 6.1).

$$\text{Loading (mmol/g)}_{304\ nm} = \frac{\text{absorbance} \times 163.96}{\text{mg of resin bound AA}}$$

Figure 6.1 Equation for the calculation of the level of attachment of the first AA

The literature value for CTC resin loading is 0.86 mmol/g.

6.3.5 Removal of Fmoc Protecting Group

Swelling of the resin was carried out, as described above. A 20 % piperidine solution in DMF (v/v) (1.5 mL) was added to the resin, and gently shaken for 1 min. The liquid was removed by vacuum filtration, and a further 1.5 mL of this solution was added. The resin was gently shaken for 10 mins, then the liquid removed. The resin was washed with DMF x 7 (2 mL).

6.3.6 Monitoring Fmoc Removal/ Coupling of AA – The Kaiser Test:

Reagents:
A) 500 mg ninhydrin in 10 mL EtOH
B) 0.4 mL of a 0.001 M KCN_{aq} solution in 20 mL pyridine

Figure 6.2 Reagents required for the Kaiser test

A few beads were transferred to a glass vial and washed three times with EtOH (EtOH added, swirled, then decanted). Each of the above solutions (0.10 mL of A and 0.10 mL of B) was added to the beads, and the vial was heated with a heat gun for 2 mins (Fig. 6.2). The colour change of the beads was noted (Fig. 6.3). It is important to take note of the colour of the resin, and not the liquid. This test can be carried out with pyridine and reagent A, but the colour change may be different.

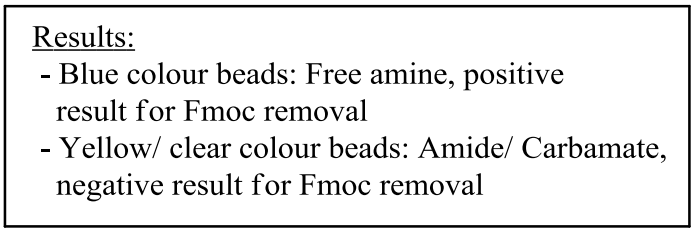

Figure 6.3 Colour changes in the Kaiser test

The Kaiser test was also used to monitor the success of coupling reactions, as denoted by a colour change to clear or yellow. The Kaiser test became less useful for glycopeptides with colour changes of red being observed at certain stages.

6.3.7 Coupling of the Second, and Each Consecutive AA

NHFmoc-AA (0.42 mmol), TBTU (148 mg, 1.1 eq, 0.46 mmol), and HOBt (62 mg, 1.1 eq) were dissolved in DMF (3 mL). DIPEA (0.15 mL, 2 eq) was added to the mixture. This was allowed to react for 10 mins, then added to the pre-swelled resin. The resin was gently shaken for 1.5 h, then filtered. The liquid was removed from the resin by vacuum filtration, and the resin was washed with DMF (2 mL x 7 times), followed by DCM (3 mL x 3 times). (Wash with DCM ensures removal of DMF which may cause unwanted Fmoc removal over time).

6.3.8 Capping of the Second, and Consecutive AA After Coupling

Capping of any unreacted free amines was carried out after each coupling. The resin was swelled, then DMF (1.4 mL), DIPEA (0.2 mL), and Ac_2O (0.2 mL) were added. The resin was gently shaken for 15 mins, then filtered. The resin was washed with DMF (2 mL x 7 times).

6.3.9 Cleavage from the Resin for Mass Spectrometry and for Final Peptide

Monitoring of the intermediates of each stage in the synthesis was carried out by removing a few beads from the reaction vessel. These were washed with EtOH x 3 times. A 1 % TFA solution (v/v) in DCM (3 mL) was added to the resin and left to react at rt for 10 mins. The liquid was removed (filtered through cotton wool to remove the beads) and concentrated under reduced pressure. The resulting oil was dissolved in DMF or DCM and sent for analysis.

The cleavage of the final glycopeptide was carried out with 50 % TFA (v/v) in DCM, for 1 h. Purification of the final glycopeptides was carried out by HPLC.

Peptide 3.6:

The bulk of the peptide was cleaved from the resin as described above, to give a mixture of crude products. The solvent was evaporated under reduced pressure, and the remaining residue was triturated with a 10 % solution of TFA in DCM (4 x 5 mL). The combined DCM/TFA extracts were concentrated under reduced pressure to give a clear oil (12 mg, 16 % crude yield). This oil was redissolved in a 10 % solution of TFA in DCM, and purified by RP-HPLC. Preparative HPLC was carried out using an Agilent Zorbex Eclipse XDB-C18 column, using a mobile phase of A = H_2O with 0.1 % formic acid, and B = MeCN with 0.1 % formic acid, gradient elution was used (A:B, 100:0 to 50:50 to 0:100 to 50:50 to 100:0 over 20 mins). The presence of the peptide, **3.6**, was confirmed by MS analysis in fractions collected at 6.5-8 and 8-9.5 mins run time.

Glycopeptide 3.8:

The bulk of the peptide was cleaved from the resin as described above, to give a crude mixture of products. The solvent was evaporated under reduced pressure, and the remaining residue was triturated with a 10 % solution of TFA in DCM (4 x 5 mL). The combined DCM/TFA extracts were concentrated under reduced pressure to give a yellow oil (12 mg, 30 % crude yield). This oil was redissolved in a 10 % solution of TFA in DCM, and purified by RP-HPLC. Preparative HPLC was carried out using an Agilent Zorbex Eclipse XDB-C18 column, using a mobile phase of A = H_2O with 0.1 % formic acid, and B = MeCN with 0.1 % formic acid, gradient elution was used (A:B, 100:0 to 50:50 to 0:100 to 50:50 to 100:0 over 20 mins). The presence of the peptide, **3.8**, was confirmed by MS analysis in fractions collected at 6-7 and 7-8 mins run time.

Glycopeptide 3.10:

The bulk of the peptide was cleaved from the resin as described above, to give a crude mixture of products. The solvent was evaporated under reduced pressure, and the remaining residue was triturated with a 10 % solution of TFA in DCM (4 x 5 mL). The combined DCM/TFA extracts were concentrated under reduced pressure to give a yellow oil (13 mg, 26 % crude yield). This oil was redissolved in a 10 % solution of TFA in DCM, and purified by RP-HPLC. Preparative HPLC was carried

out using an Agilent Zorbex Eclipse XDB-C18 column, using a mobile phase of A = H_2O with 0.1 % formic acid, and B = MeCN with 0.1 % formic acid, gradient elution was used (A:B, 100:0 to 50:50 to 0:100 to 50:50 to 100:0 over 20 mins). The presence of the peptide, **3.10**, was confirmed by MS analysis in fractions collected at 7-8 and 8-9 mins run time.

Chapter 7: Appendices

7.1 Appendix 1: Assignation of ^{1}H NMR data for Glycoside 5.37

^{1}H NMR spectral data for glycoside **5.37** was assigned with the aid of the 2 D techniques HSQC and COSY. The ^{1}H NMR spectrum for this compound is shown in Fig 7.1, with the COSY in Fig 7.2 and the HSQC displayed in Fig. 7.3. This compound was obtained as a mixture of anomers, in the ratio of 0.6:1, α:β.

The first step in the analysis of this spectral data was the assignation of the H-1 proton signal. For sugars, the carbon which is attached to this proton resonates at ≈ 90-105 ppm.[263] By examining the HSQC data (Fig. 7.3), there are two signals in this region, at 98.65 and 91.80 ppm. The signal resulting from the β-anomer will resonate at a slightly higher ppm than the corresponding α-anomer in the ^{13}C NMR. Following these two signals on the HSQC shows interaction with two peaks on the ^{1}H NMR. The signal at 98.65 ppm is associated with a proton resonance at ≈ 4.85 ppm. In the ^{1}H NMR spectrum, the H-1 of the β-anomer will resonate at a slightly lower ppm than the α-anomer, and will also have a larger *J* value. In this spectrum it is difficult to ascertain the *J* value, due to overlapping of the signals for H-1 and the CH_2 of the benzyl group. The other C-1 signal in the HSQC shows an interation with a resonance at 5.09 ppm. The *J* value for the H-1 signal at 5.09 is 3 Hz, which is a relatively small value, and this signal corresponds to the α-anomer. Now that the signals for H-1 have been assigned, the data from the COSY can be examined. Looking at the H-1 signal from the α-anomer, for example, it can be seen that there is one crosspeak, representing interactions between the H-1 and the neighbouring proton, H-2. Following this crosspeak it can be deduced that H-2 (α-anomer) resonates at 4.03 ppm. H-2 shows crosspeak interactions with 3 protons, H-1, H-3, and the amide proton from NHAc. The amide proton should be a doublet, while the H-3 proton should be a dd, and so the amide proton can be assigned to the signal at 5.31 ppm. The signal representing H-3 is found in the multiplet at 3.73-3.59 ppm. The COSY is followed in this manner to assign all of the sugar protons. A signal at 7.35-7.30 ppm is indicative of aromatic protons, and it is observed that this signal integrates for 10 H. This is assigned as the aromatic protons from the benzyl group of both anomers. The protons belonging to the TMS ether protection have been

assigned to the singlets at 0.18-0.10 ppm. Due to the presence of the electropositive Si atom these protons are very shielded, and so resonate at almost 0 ppm. The acetyl CH_3 are assigned to the singlets at 1.99 and 1.94 ppm (both anomers). CH_3 signals typically appear at a slightly lower ppm, but due to the presence of the electronegative oxygen of the acetyl group these protons resonate further downfield.

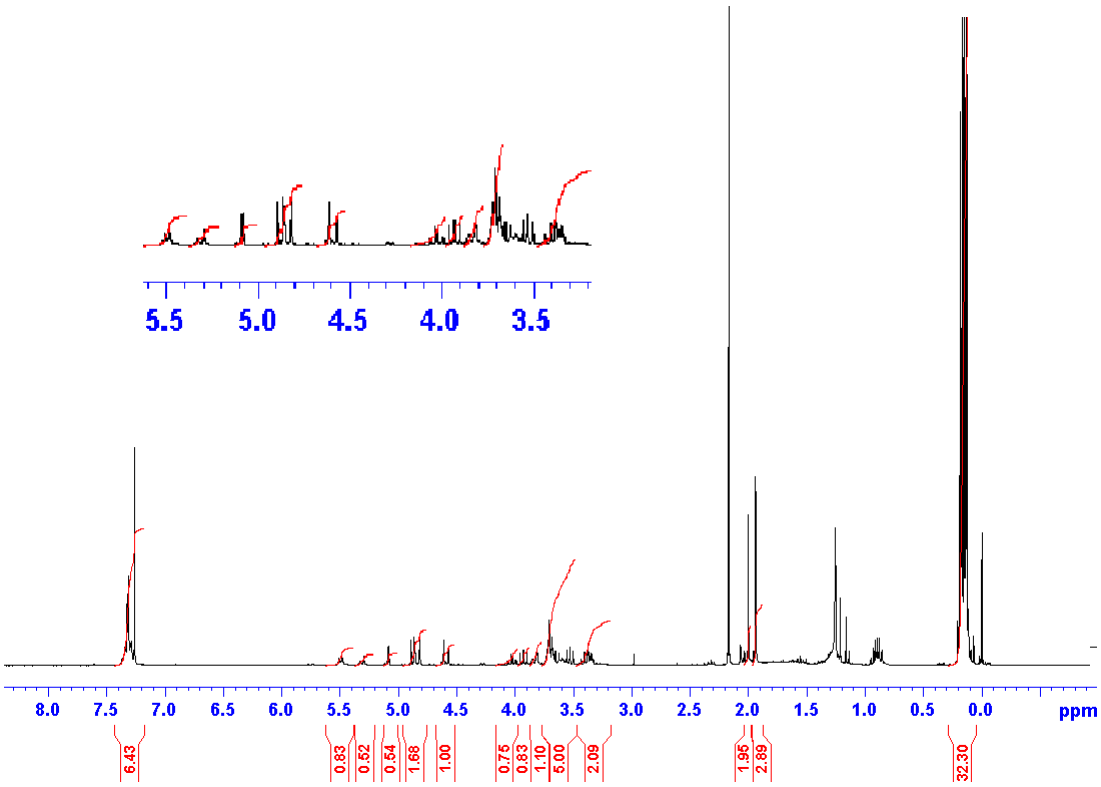

Figure 7.1[1] H NMR spectrum for glycoside 5.37

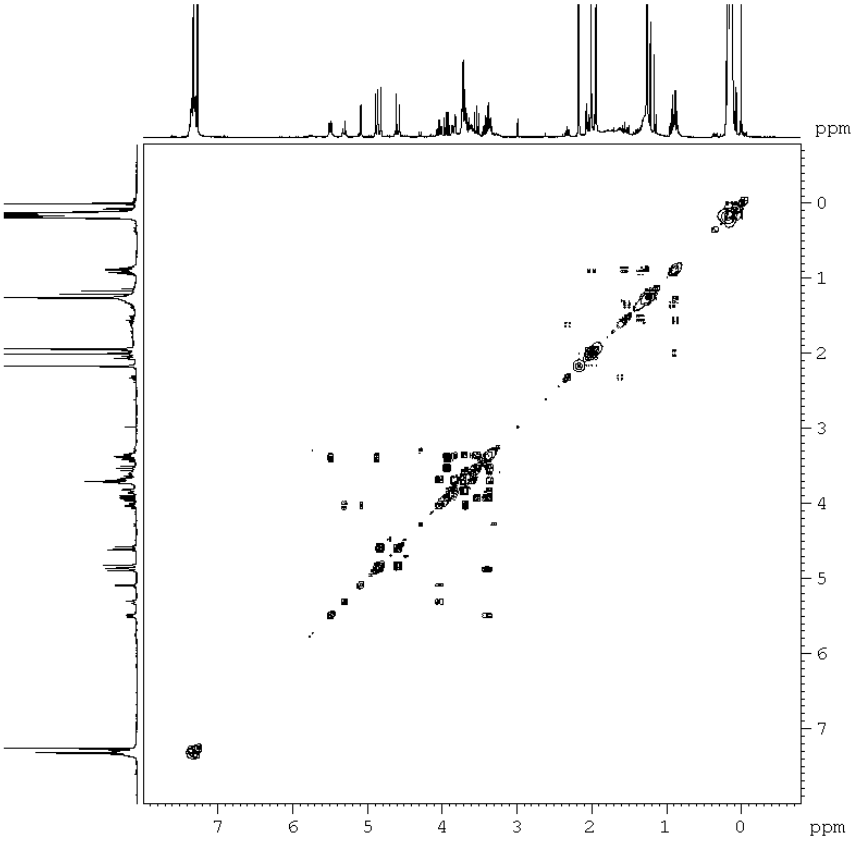

Figure 7.2 COSY of glycoside 5.37

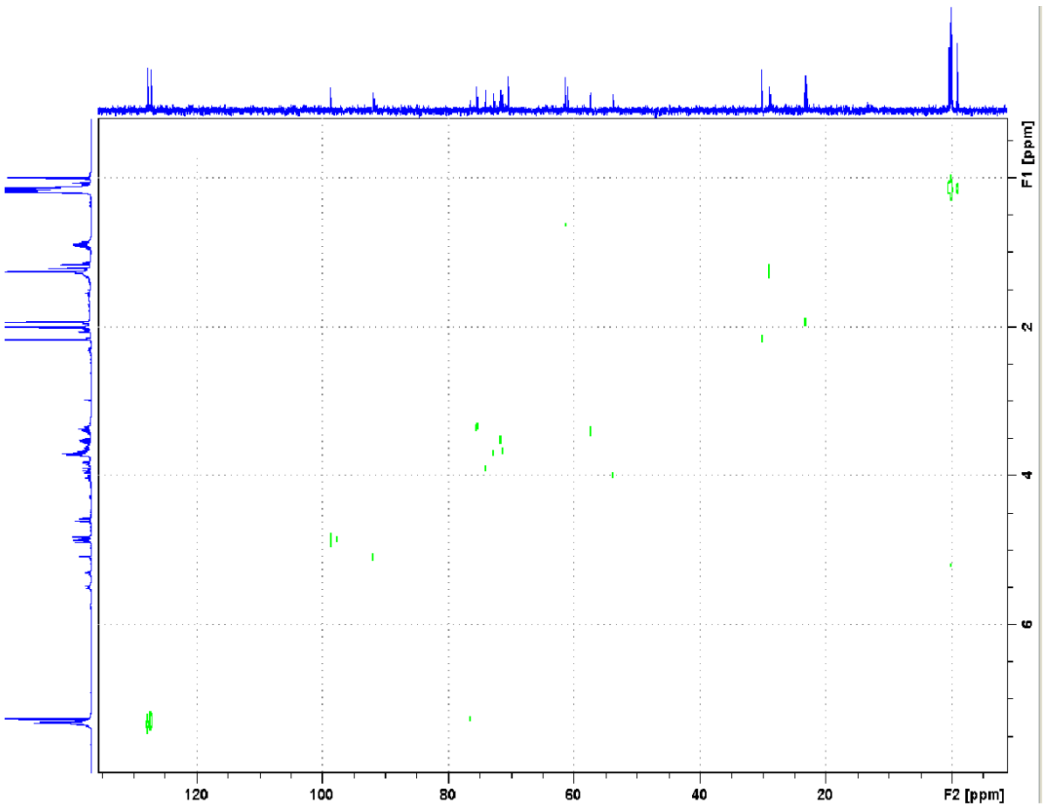

Figure 7.3 HSQC of glycoside 5.37

7.2 Appendix 2: Experimental Data for Attempted Reactions

Table 2.1 Attempted synthesis of 2.55 using acetyl chloride coupling methology

The free acid **2.54** (100 mg, 0.14 mmol) was dissolved in anhydrous DCM (5 mL) and placed under a N_2 atmosphere at 0 °C, in the presence of 3.4 Å molecular sieves. Oxalyl chloride (0.01 mL, 0.15 mmol) and DMF (0.005 mL) were added to the reaction mixture. This was allowed to stir at 0 °C for 1 h. A solution of tetradecylamine (29 mg, 0.14 mmol) and pyridine (0.012 mL, 0.15 mmol) in DCM (3 mL) was added dropwise to the reaction mixture, which was allowed to return to rt. The reaction mixture was stirred at rt for 4.5 h, then the solvent was evaporated under reduced pressure. The remaining residue was dissolved in DCM, and washed with 1.0 M HCl. The organic layer was evaportated using a rotary evaporator. This reaction failed to yield the desired product.

Scheme 2.17 Attempted direct glycosylation of acceptor 2.63

Imidate donor **2.34** (18 mg, 0.03 mmol) and lipid acceptor **2.63** (11 mg, 0.02 mmol) were dissolved in anhydrous DCM (5 mL) under a N_2 atmosphere, in the presence of 3.4 Å molecular sieves. To this BF_3OEt_2 (0.002 mL, 0.01 mmol) was added, and the reaction mixture was allowed to stir at rt for 3 h. The solvent was evaporated under reduced pressure to leave a white oily solid. The desired product was not synthesised, and hemiacetal **2.33** and lipid starting material **2.63** were recovered.

Scheme 2.21 *N*-Cbz removal from Troc protected derivative 2.67

Troc protected derivative **2.67** (230 mg, 0.3 mmol) was dissolved in EtOAc (13 mL). Pd/C 10 % (w/w) (100 mg) was added and the reaction mixture was placed under a H_2 atmosphere, then stirred at rt overnight. The reaction did not proceed with recovery of starting material. The reaction mixture was filtered to remove the Pd/C, then the experiment was repeated for a further 24 h. Full recovery of starting material **2.67** was achieved, with non of the desired product synthesised.

Table 4.1 Attempted tritylation of 4.1

The Troc protected glucosamine **4.1** (400 mg, 1.1 mmol) was dissolved in dry pyridine (15 mL). Et_3N (0.02 mL, 0.12 mmol) and TrCl (379 mg, 1.4 mmol) was added to the reaction mixture. This was stirred at 70 °C for 4 h. The reaction mixture

was cooled to 0 °C, then Ac_2O (0.64 mL, 6.8 mmol) was added slowly. The reaction mixture was allowed to return to rt, then stirred at rt overnight. The solvent was evaporated under reduced pressure, and the remaining residue was dissolved in DCM, and washed with brine. The organic layer was dried ($MgSO_4$), and filtered, then concentrated under reduced pressure. The crude product was purified by column chromatography (Hex:EtOAc, 2:1) to give protected glucosamine derivative **4.2** as a clear oil (83 mg, 5 %), and mainly the acetylated derivative **2.26**.

Table 4.2 i) Attempted *O*-Fmoc protection of the C-6 position

Glycoside **4.7** (55 mg, 0.12 mmol) was dissolved in anhydrous pyridine (10 mL) under a N_2 atmosphere, and cooled to 0 °C. Fmoc-Cl (47 mg, 0.19 mmol) was added to the reaction mixture, and this was allowed to stir at 0 °C for 2 h. The reaction mixture was allowed to return to rt, then stirred for a further 4 h. Another equivalent of Fmoc-Cl was added (32 mg), and the reaction mixture was allowed to stir at rt overnight. Ac_2O (8 mL) was added, and the reaction mixture was allowed to stir for 4 h. The solvent was evaporated under reduced pressure, and the remaining residue was dissolved in DCM then washed with 1.0 M HCl, followed by a sat. solution of $NaHCO_3$. The organic layer was concentrated under reduced pressure. The desired product was not obtained from this experiment.

Table 4.2 ii) Attempted *O*-MOM protection of the C-6 position

Glycoside **4.7** (55 mg, 0.12 mmol) was dissolved in acetone (10 mL) and K_2CO_3 (62 mg, 0.45 mmol) was added. MOM-Br (0.14 mL mg, 0.17 mmol) was added dropwise to the reaction mixture, and this was heated at reflux (56 °C) overnight. The reaction mixture was allowed to return to rt, then MeOH (6 mL) was added to quench the remaining MOM-Br. The solvent was evaporated under reduced pressure, and the remaining reside dissolved in pyridine (6 Ml). Ac_2O (6 mL) was added, and the reaction mixture was allowed to stir at rt overnight. The solvent was evaporated under reduced pressure, and the remaining residue was dissolved in DCM then washed with 1.0 M HCl, followed by a sat. solution of $NaHCO_3$. The organic layer was concentrated under reduced pressure. The desired product was not obtained from this experiment.

Table 4.3 Attempted enzymatic deacetylation (general procedure)

Glycoside **3.4** (83 mg, 0.11 mmol) was dissolved in ethanol or ACN (10 mL). Phosphate buffer was added to adjust the pH of the reaction mixture to the desired value. Enzyme (CRL or CAL B) (42 mg) was added to the reaction mixture, and this was gently shaken in a temperature controlled water bath (temperature range from 20 → 50 °C) for 2 days. None of these enzymatic experiments yielded the desired product, with full recovery of starting material **3.4** in all cases.

Table 4.4 i) Attempted chemical deacetylation using DBTO

Glycoside **3.4** (22 mg, 0.03 mmol) was dissolved in MeOH (5 mL) and DBTO (7.3 mg, 0.03 mmol) was added. The reaction mixture was heated to 50 °C and allowed to stir for 3 h. The reaction mixture was allowed to return to rt, then stirred overnight. The reaction had not gone to completion, and was again heated to 50 °C, and stirred for 3 h. Partial deacetylation was observed, with mainly the starting material recovered.

Table 4.4 ii) Attempted chemical deacetylation using KCN

Glycoside **3.4** (22 mg, 0.03 mmol) was dissolved in MeOH (5 mL) and cooled to 0 °C. KCN (5.7 mg, 0.09 mmol) was added and the reaction mixture was stirred at 0 °C for 0.5 h. The reaction mixture was allowed to return to rt, then stirred for 1.5 h. The solvent was evaporated under reduced pressure. The desired product was not obtained under these reaction conditions.

Scheme 4.7 Attempted introduction of azide functionality into 4.18

Tosyl protected glycoside **4.18** (20 mg, 0.03 mmol) was dissolved in DMF (5 mL) and NaN_3 (18 mg, 0.3 mmol) was added. The reaction mixture was heated to 70 °C and allowed to stir for 2.5 h. The solvent was evaporated under reduced pressure, and the remaining residue was purified by column chromatography (DCM:MeOH, 15:1 to 10:1 to 8:2). The desired product was not synthesised, and removal of the Fmoc group was noted by NMR.

Scheme 4.9 Attempted introduction of linker attached azide into 4.23 using TBTU/HOBt methodology

TMS protected glycoside **4.23**

Azido propionic acid **4.21** (110 mg, which still contained some MeCN) was dissolved in anhydrous DCM (3 mL) under N_2, and cooled to 0 °C. HOBt (17 mg, 0.13 mmol), TBTU (41 mg, 0.13 mmol) and DIPEA (0.02 mL, 0.13 mmol) were added to the reaction mixture, and this was allowed to stir for 5 mins. A solution of the crude TMS protected glycoside, **4.23** (45 mg, 0.06 mmol) in anhydrous DCM was added slowly to the reaction mixture. This was stirred at 0 °C for 1.5 h, and then allowed to return to rt. The reaction mixture was stirred at rt overnight, and then washed with H_2O. The organic layer was concentrated under reduced pressure to almost dryness. The remaining oil was purified by column chromatography (DCM:MeOH, 15:1 to 9:1). The desired product was not synthesised under these reaction conditions.

Chapter 8: Bibliography

1. Varki, A., *Biological roles of oligosaccharides: All of the theories are correct.* Glycobiology 1993, **3**(2): p. 97-130.
2. M. E. Taylor and Drickamer, K., *Introduction to glycobiology*. 3rd ed. 2011, New York: Oxford University Press Inc.
3. Lindhorst, T.K., *Essentials of carbohydrate chemistry and biochemistry*. 3rd ed. 2007, Weinheim: John Wiley and Sons.
4. van Kasteren, S.I., Kramer, H.B., Gamblin, D.P., and Davis, B.G., *Site-selective glycosylation of proteins: creating synthetic glycoproteins.* Nat. Protoc., 2007, **2**(12): p. 3185-3194.
5. Bongat, A.F.G. and Demchenko, A.V., *Recent trends in the synthesis of O-glycosides of 2-amino-2-deoxysugars.* Carbohydr. Res., 2007, **342**(3-4): p. 374-406.
6. Galan, M.C., Benito-Alifonso, D., and Watt, G.M., *Carbohydrate chemistry in drug discovery.* Org. Biomol. Chem., 2011, **9**(10): p. 3598-3610.
7. Zhu, X. and Schmidt, R.R., *New principles for glycoside-bond formation.* Angew Chem Int Ed Engl, 2009, **48**(11): p. 1900-34.
8. Dube, D.H. and Bertozzi, C.R., *Glycans in cancer and inflammation - potential for therapeutics and diagnostics.* Nat. Rev. Drug Discovery 2005, **4**(6): p. 477-488.
9. Huang, C.-Y., Thayer, D.A., Chang, A.Y., Best, M.D., Hoffmann, J., Head, S., and Wong, C.-H., *Carbohydrate microarray for profiling the antibodies interacting with Globo H tumor antigen.* Proc. Natl. Acad. Sci. U. S. A., 2006, **103**(1): p. 15-20.
10. Suzuki-Anekoji, M., Suzuki, M., Kobayashi, T., Sato, Y., Nakayama, J., Suzuki, A., Bao, X., Angata, K., and Fukuda, M., *HNK-1 glycan functions as a tumor suppressor for astrocytic tumor.* J. Biol. Chem., 2011, **286**(37): p. 32824-32833, S32824/1-S32824/9.
11. El Ashry, E.S.H. and Aly, M.R.E., *Synthesis and biological relevance of N-acetylglucosamine-containing oligosaccharides.* Pure Appl. Chem., 2007, **79**(12): p. 2229-2242.
12. Yan, Y., Wanshun, L., Baoqin, H., Changhong, W., Chenwei, F., Bing, L., and Liehuan, C., *The antioxidative and immunostimulating properties of D-glucosamine.* Int Immunopharmacol 2007, **7**(1): p. 29-35.
13. Nakamura, H., *Application of glucosamine on human disease-Osteoarthritis.* Carbohydr. Polym., 2011, **84**(2): p. 835-839.
14. Torres, C.-R. and Hart, G.W., *Topography and polypeptide distribution of terminal N-acetylglucosamine residues on the surfaces of intact lymphocytes. Evidence for O-linked GlcNAc.* J. Biol. Chem., 1984, **259**(5): p. 3308-17.
15. Hart, G.W., Housley, M.P., and Slawson, C., *Cycling of O-linked β-N-acetylglucosamine on nucleocytoplasmic proteins.* Nature (London, U. K.), 2007, **446**(7139): p. 1017-1022.
16. Xu, W., Yang, S., Bhadury, P., He, J., He, M., Gao, L., Hu, D., and Song, B., *Synthesis and bioactivity of novel sulfone derivatives containing 2,4-dichlorophenyl substituted 1,3,4-oxadiazole/thiadiazole moiety as chitinase inhibitors.* Pestic. Biochem. Physiol., 2011, **101**(1): p. 6-15.

17. Lane, J.A., Mehra, R.K., Carrington, S.D., and Hickey, R.M., *Development of biosensor-based assays to identify anti-infective oligosaccharides.* Anal. Biochem., 2011, **410**(2): p. 200-205.
18. Butkinaree, C., Park, K., and Hart, G.W., *O-linked β-N-acetylglucosamine (O-GlcNAc): Extensive crosstalk with phosphorylation to regulate signaling and transcription in response to nutrients and stress.* Biochim. Biophys. Acta, Gen. Subj., 2010, **1800**(2): p. 96-106.
19. Fang, B. and Miller, M.W., *Use of Galactosyltransferase to Assess the Biological Function of O-linked N-Acetyl-D-Glucosamine: A Potential Role for O-GlcNAc during Cell Division.* Exp. Cell Res., 2001, **263**(2): p. 243-253.
20. O'Donnell, N., Zachara, N.E., Hart, G.W., and Marth, J.D., *Ogt-dependent X-chromosome-linked protein glycosylation is a requisite modification in somatic cell function and embryo viability.* Mol. Cell. Biol., 2004, **24**(4): p. 1680-1690.
21. Zachara, N.E. and Hart, G.W., *Cell signaling, the essential role of O-GlcNAc!* Biochim. Biophys. Acta, Mol. Cell Biol. Lipids 2006, **1761**(5-6): p. 599-617.
22. Griffith, L.S. and Schmitz, B., *O-linked N-acetylglucosamine levels in cerebellar neurons respond reciprocally to perturbations of phosphorylation.* Eur. J. Biochem., 1999, **262**(3): p. 824-831.
23. Hu, P., Shimoji, S., and Hart, G.W., *Site-specific interplay between O-GlcNAcylation and phosphorylation in cellular regulation.* FEBS Lett., 2010, **584**(12): p. 2526-2538.
24. Rechsteiner, M. and Rogers, S.W., *PEST sequences and regulation by proteolysis.* Trends Biochem. Sci., 1996, **21**(7): p. 267-271.
25. Garner, K., Li, M., Ugwuanya, N., and Cockcroft, S., *The phosphatidylinositol transfer protein RdgB-β binds 14-3-3 via its unstructured C-terminus, whereas its lipid-binding domain interacts with the integral membrane protein ATRAP (angiotensin II type I receptor-associated protein).* Biochem. J., 2011, **439**(1): p. 97-111.
26. Cheng, X. and Hart, G.W., *Alternative O-glycosylation/O-phosphorylation of serine-16 in murine estrogen receptor-β. Post-translational regulation of turnover and transactivation activity.* J. Biol. Chem., 2001, **276**(13): p. 10570-10575.
27. Sayat, R., Leber, B., Grubac, V., Wiltshire, L., and Persad, S., *O-GlcNAc-glycosylation of β-catenin regulates its nuclear localization and transcriptional activity.* Exp. Cell Res., 2008, **314**(15): p. 2774-2787.
28. Rajamani, U., Joseph, D., Roux, S., and Essop, M.F., *The hexosamine biosynthetic pathway can mediate myocardial apoptosis in a rat model of diet-induced insulin resistance.* Acta Physiol., 2011, **202**(2): p. 151-157.
29. Fernandez-Gonzalez, M., Boutureira, O., Bernardes, G.J.L., Chalker, J.M., Young, M.A., Errey, J.C., and Davis, B.G., *Site-selective chemoenzymatic construction of synthetic glycoproteins using endoglycosidases.* Chem. Sci., 2010, **1**(6): p. 709-715.
30. Hudak, J.E., Yu, H.H., and Bertozzi, C.R., *Protein glycoengineering enabled by the versatile synthesis of aminooxy glycans and the genetically encoded aldehyde tag.* J. Am. Chem. Soc., 2011, **133**(40): p. 16127-16135.

31. Morales-Serna, J.A., Boutureira, O., Diaz, Y., Matheu, M.I., and Castillon, S., *Recent advances in the glycosylation of sphingosines and ceramides.* Carbohydr. Res., 2007, **342**(12-13): p. 1595-1612.
32. Kolter, T., *A view on sphingolipids and disease.* Chem. Phys. Lipids 2011, **164**(6): p. 590-606.
33. Zhu, Y., Gumlaw, N., Karman, J., Zhao, H., Zhang, J., Jiang, J.-L., Maniatis, P., Edling, A., Chuang, W.-L., Siegel, C., Shayman, J.A., Kaplan, J., Jiang, C., and Cheng, S.H., *Lowering glycosphingolipid levels in CD4+ T cells attenuates T cell receptor signaling, cytokine production, and differentiation to the Th17 lineage.* J. Biol. Chem., 2011, **286**(17): p. 14787-14794.
34. Ciarlo, L., Manganelli, V., Garofalo, T., Matarrese, P., Tinari, A., Misasi, R., Malorni, W., and Sorice, M., *Association of fission proteins with mitochondrial raft-like domains.* Cell Death Differ., 2010, **17**(6): p. 1047-1058.
35. Posse de Chaves, E. and Sipione, S., *Sphingolipids and gangliosides of the nervous system in membrane function and dysfunction.* FEBS Lett., 2010, **584**(9): p. 1748-1759.
36. Sonnino, S., Mauri, L., Chigorno, V., and Prinetti, A., *Gangliosides as components of lipid membrane domains.* Glycobiology 2007, **17**(1): p. 1R-13R.
37. Lopez, P.H.H. and Schnaar, R.L., *Gangliosides in cell recognition and membrane protein regulation.* Curr. Opin. Struct. Biol., 2009, **19**(5): p. 549-557.
38. Schnaar, R.L., *Brain gangliosides in axon-myelin stability and axon regeneration.* FEBS Lett., 2010, **584**(9): p. 1741-1747.
39. Walkley, S.U. and Vanier, M.T., *Secondary lipid accumulation in lysosomal disease.* Biochim. Biophys. Acta, Mol. Cell Res., 2009, **1793**(4): p. 726-736.
40. Pannuzzo, G., Cardile, V., Costantino-Ceccarini, E., Alvares, E., Mazzone, D., and Perciavalle, V., *A galactose-free diet enriched in soy isoflavones and antioxidants results in delayed onset of symptoms of Krabbe disease in twitcher mice.* Mol. Genet. Metab., 2010, **100**(3): p. 234-240.
41. Roeske-Nielsen, A., Buschard, K., Maanson, J.E., Rastam, L., and Lindblad, U., *A variation in the cerebroside sulfotransferase gene is linked to exercise-modified insulin resistance and to type 2 diabetes.* Exp. Diabetes Res., 2009: p. 5.
42. Esteves, A.I.S., Nicolai, M., Humanes, M., and Goncalves, J., *Sulfated polysaccharides in marine sponges: extraction methods and anti-HIV activity.* Mar. Drugs, 2011, **9**: p. 139-153.
43. Yoshida, H., Ikeda, K., Achiwa, K., and Hoshino, H., *Synthesis of sulfated cerebroside analogs having mimics of ceramide and their anti-human immunodeficiency virus type 1 activities.* Chem. Pharm. Bull., 1995, **43**(4): p. 594-602.
44. Meyers, R.A., *Immunology; From cell biology to disease*. 1st ed. 2007, Weinheim: Wiley-VCH.
45. Terabe, M. and Berzofsky, J.A., *The role of NKT cells in tumor immunity.* Adv. Cancer Res., 2008, **101**: p. 277-348.
46. Wu, L. and Van Kaer, L., *Natural killer T cells and autoimmune disease.* Curr. Mol. Med., 2009, **9**(1): p. 4-14.
47. Bendelac, A., Savage, P.B., and Teyton, L., *The biology of NKT cells.* Annu. Rev. Immunol., 2007, **25**: p. 297-336.

48. Silk, J.D., Salio, M., Brown, J., Jones, E.Y., and Cerundolo, V., *Structural and functional aspects of lipid binding by CD1 molecules.* Annu Rev Cell Dev Biol, 2008, **24**: p. 369-95.
49. Florence William, C., Bhat Rakesh, K., and Joyce, S., *CD1d-restricted glycolipid antigens: presentation principles, recognition logic and functional consequences.* Expert Rev Mol Med 2008, **10**: p. e20.
50. Zhou, L.-d., Zhang, Q.-h., Zhang, Y., Liu, J., and Cao, Y.-m., *The shiitake mushroom-derived immuno-stimulant lentinan protects against murine malaria blood-stage infection by evoking adaptive immune-responses.* Int. Immunopharmacol., 2009, **9**(4): p. 455-462.
51. Sakuishi, K., Oki, S., Araki, M., Porcelli, S.A., Miyake, S., and Yamamura, T., *Invariant NKT cells biased for IL-5 production act as crucial regulators of inflammation.* J. Immunol., 2007, **179**(6): p. 3452-3462.
52. Blomqvist, M., Rhost, S., Teneberg, S., Loefbom, L., Oesterbye, T., Brigl, M., Mansson, J.-E., and Cardell, S.L., *Multiple tissue-specific isoforms of sulfatide activate CD1d-restricted type II NKT cells.* Eur. J. Immunol., 2009, **39**(7): p. 1726-1735.
53. Venkataswamy, M.M. and Porcelli, S.A., *Lipid and glycolipid antigens of CD1d-restricted natural killer T cells.* Semin. Immunol., 2010, **22**(2): p. 68-78.
54. Yin, N., Long, X., Goff, R.D., Zhou, D., Cantu, C., III, Mattner, J., Saint Mezard, P., Teyton, L., Bendelac, A., and Savage, P.B., *α-Anomers of iGb3 and Gb3 stimulate cytokine production by Natural Killer T Cells.* ACS Chem. Biol., 2009, **4**(3): p. 191-197.
55. Gapin, L., *iNKT cell autoreactivity: what is 'self' and how is it recognized?* Nat. Rev. Immunol., 2010, **10**(4): p. 272-277.
56. Brennan, P.J., Tatituri, R.V.V., Brigl, M., Kim, E.Y., Tuli, A., Sanderson, J.P., Gadola, S.D., Hsu, F.-F., Besra, G.S., and Brenner, M.B., *Invariant natural killer T cells recognize lipid self antigen induced by microbial danger signals.* Nat. Immunol., 2011, **12**(12): p. 1202-1211.
57. Stanic, A.K., De Silva, A.D., Park, J.-J., Sriram, V., Ichikawa, S., Hirabyashi, Y., Hayakawa, K., Van Kaer, L., Brutkiewicz, R.R., and Joyce, S., *Defective presentation of the CD1d1-restricted natural Va14Ja18 NKT lymphocyte antigen caused by β-D-glucosylceramide synthase deficiency.* Proc. Natl. Acad. Sci. U. S. A., 2003, **100**(4): p. 1849-1854.
58. Adar, T. and Ilan, Y., *β-Glycosphingolipids as immune modulators.* J. Immunotoxicol., 2008, **5**(2): p. 209-220.
59. van den Heuvel, M.J., Garg, N., Van Kaer, L., and Haeryfar, S.M.M., *NKT cell costimulation: Experimental progress and therapeutic promise.* Trends Mol. Med., 2011, **17**(2): p. 65-77.
60. Van Kaer, L., *α-Galactosylceramide therapy for autoimmune diseases: prospects and obstacles.* Nat. Rev. Immunol., 2005, **5**(1): p. 31-42.
61. Tupin, E., Nicoletti, A., Elhage, R., Rudling, M., Ljunggren, H.-G., Hansson, G.K., and Berne, G.P., *CD1d-dependent activation of NKT cells aggravates atherosclerosis.* J. Exp. Med., 2004, **199**(3): p. 417-422.
62. Miyamoto, K., Miyake, S., and Yamamura, T., *A synthetic glycolipid prevents autoimmune encephalomyelitis by inducing Th2 bias of natural killer T cells.* Nature (London, U. K.) 2001, **413**(6855): p. 531-534.
63. Oki, S., Chiba, A., Yamamura, T., and Miyake, S., *The clinical implication and molecular mechanism of preferential IL-4 production by modified*

glycolipid-stimulated NKT cells. J. Clin. Invest., 2004, **113**(11): p. 1631-1640.

64. Henon, E., Dauchez, M., Haudrechy, A., and Banchet, A., *Molecular dynamics simulation study on the interaction of KRN 7000 and three analogues with human CD1d.* Tetrahedron 2008, **64**(40): p. 9480-9489.
65. Goff, R.D., Gao, Y., Mattner, J., Zhou, D., Yin, N., Cantu, C., III, Teyton, L., Bendelac, A., and Savage, P.B., *Effects of lipid chain lengths in α-galactosylceramides on cytokine release by Natural Killer T cells.* J. Am. Chem. Soc., 2004, **126**(42): p. 13602-13603.
66. Veerapen, N., Reddington, F., Salio, M., Cerundolo, V., and Besra, G.S., *Synthesis of truncated analogues of the iNKT cell agonist, α-galactosyl ceramide (KRN7000), and their biological evaluation.* Bioorg. Med. Chem., 2011, **19**(1): p. 221-228.
67. Kenna, T., Mason, L.G., Porcelli, S.A., Koezuka, Y., Hegarty, J.E., O'Farrelly, C., and Doherty, D.G., *NKT Cells from normal and tumor-bearing human livers are phenotypically and functionally distinct from murine NKT cells.* J. Immunol., 2003, **171**(4): p. 1775-1779.
68. Fujio, M., Wu, D., Garcia-Navarro, R., Ho, D.D., Tsuji, M., and Wong, C.-H., *Structure-based discovery of glycolipids for CD1d-mediated NKT cell activation: Tuning the adjuvant versus immunosuppression activity.* J. Am. Chem. Soc., 2006, **128**(28): p. 9022-9023.
69. Fan, G.-T., Pan, Y.-s., Lu, K.-C., Cheng, Y.-P., Lin, W.-C., Lin, S., Lin, C.-H., Wong, C.-H., Fang, J.-M., and Lin, C.-C., *Synthesis of α-galactosyl ceramide and the related glycolipids for evaluation of their activities on mouse splenocytes.* Tetrahedron 2005, **61**(7): p. 1855-1862.
70. Schmieg, J., Yang, G., Franck, R.W., and Tsuji, M., *Superior protection against malaria and melanoma metastases by a C-glycoside analogue of the natural killer T cell ligand α-galactosylceramide.* J. Exp. Med., 2003, **198**(11): p. 1631-1641.
71. Li, X., Chen, G., Garcia-Navarro, R., Franck, R.W., and Tsuji, M., *Identification of C-glycoside analogues that display a potent biological activity against murine and human invariant natural killer T cells.* Immunology 2009, **127**(2): p. 216-225.
72. Hogan, A.E., O'Reilly, V., Dunne, M.R., Dere, R.T., Zeng, S.G., O'Brien, C., Amu, S., Fallon, P.G., Exley, M.A., O'Farrelly, C., Zhu, X., and Doherty, D.G., *Activation of human invariant natural killer T cells with a thioglycoside analogue of α-galactosylceramide.* Clin. Immunol. (Amsterdam, Neth.) 2011, **140**(2): p. 196-207.
73. Ben Ya'acov, A., Lalazar, G., Livovsky, D.M., Kanovich, D., Axelrod, E., Preston, S., Schwarzmann, G., and Ilan, Y., *Decreased STAT-1 phosphorylation by a thio analogue of β-glucosylceramide is associated with altered NKT lymphocyte polarization.* Mol. Immunol., 2009, **47**(2-3): p. 526-533.
74. Pellicci, D.G., Clarke, A.J., Patel, O., Mallevaey, T., Beddoe, T., Le Nours, J., Uldrich, A.P., McCluskey, J., Besra, G.S., Porcelli, S.A., Gapin, L., Godfrey, D.I., and Rossjohn, J., *Recognition of β-linked self glycolipids mediated by natural killer T cell antigen receptors.* Nat. Immunol., 2011, **12**(9): p. 827-833.

75. Yu, E.D., Girardi, E., Wang, J., and Zajonc, D.M., *Cutting edge: Structural basis for the recognition of β-linked glycolipid antigens by Invariant NKT cells.* J. Immunol., 2011, **187**(5): p. 2079-2083.
76. Kobayashi, E., Motoki, K., Yamaguchi, Y., Uchida, T., Fukushima, H., and Koezuka, Y., *Enhancing effects of α-, β-monoglycosylceramides on natural killer cell activity.* Bioorg. Med. Chem., 1996, **4**(4): p. 615-619.
77. Oku, H., Li, C., Shimatani, M., Iwasaki, H., Toda, T., Okabe, T., and Watanabe, H., *Tumor specific cytotoxicity of β-glucosylceramide: structure-cytotoxicity relationship and anti-tumor activity in vivo.* Cancer Chemother. Pharmacol., 2009, **64**(3): p. 485-496.
78. Trappeniers, M., Van Beneden, K., Decruy, T., Hillaert, U., Linclau, B., Elewaut, D., and Van Calenbergh, S., *6'-Derivatised α-GalCer Analogues Capable of Inducing Strong CD1d-Mediated Th1-Biased NKT Cell Responses in Mice.* J. Am. Chem. Soc., 2008, **130**(49): p. 16468-16469.
79. Aspeslagh, S., Li, Y.-L., Yu, E.D., Pauwels, N., Trappeniers, M., Girardi, E., Decruy, T., Van Beneden, K., Venken, K., Drennan, M., Leybaert, L., Wang, J., Franck, R.W., Van Calenbergh, S., Zajonc, D.M., and Elewaut, D., *Galactose-modified iNKT cell agonists stabilized by an induced fit of CD1d prevent tumour metastasis.* EMBO J., 2011, **30**(11): p. 2294-2305.
80. O'Konek, J.J., Illarionov, P., Khursigara, D.S., Ambrosino, E., Izhak, L., Castillo, B.F., II, Raju, R., Khalili, M., Kim, H.-Y., Howell, A.R., Besra, G.S., Porcelli, S.A., Berzofsky, J.A., and Terabe, M., *Mouse and human iNKT cell agonist β-mannosylceramide reveals a distinct mechanism of tumor immunity.* J. Clin. Invest., 2011, **121**(2): p. 683-694.
81. Silk, J.D., Salio, M., Reddy, B.G., Shepherd, D., Gileadi, U., Brown, J., Masri, S.H., Polzella, P., Ritter, G., Besra, G.S., Jones, E.Y., Schmidt, R.R., and Cerundolo, V., *Cutting edge: nonglycosidic CD1d lipid ligands activate human and murine invariant NKT cells.* J Immunol, 2008, **180**(10): p. 6452-6.
82. Banchet-Cadeddu, A., Henon, E., Dauchez, M., Renault, J.-H., Monneaux, F., and Haudrechy, A., *The stimulating adventure of KRN 7000.* Org. Biomol. Chem., 2011, **9**(9): p. 3080-3104.
83. Ikeda, K., Asahara, T., Achiwa, K., and Hoshino, H., *Synthesis of N-acetylglucosaminyl- and N-acetylgalactosaminylceramides as cerebroside analogs and their anti-human immunodeficiency virus type 1 activities.* Chem. Pharm. Bull., 1997, **45**(2): p. 402-405.
84. Huang, L.-D., Lin, H.-J., Huang, P.-H., Hsiao, W.-C., Raghava Reddy, L.V., Fu, S.-L., and Lin, C.-C., *Synthesis of serine-based glycolipids as potential TLR4 activators.* Org. Biomol. Chem., 2011, **9**(7): p. 2492-2504.
85. Faroux-Corlay, B., Greiner, J., Terreux, R., Cabrol-Bass, D., Aubertin, A.-M., Vierling, P., and Fantini, J., *Amphiphilic anionic analogues of galactosylceramide: Synthesis, anti-HIV-1 activity, and gp120 binding.* J. Med. Chem., 2001, **44**(13): p. 2188-2203.
86. Fukunaga, K., Yoshida, M., Nakajima, F., Uematsu, R., Hara, M., Inoue, S., Kondo, H., and Nishimura, S.-I., *Design, synthesis, and evaluation of β-galactosylceramide mimics promoting β-glucocerebrosidase activity in keratinocytes.* Bioorg. Med. Chem. Lett., 2003, **13**(5): p. 813-815.
87. Sahha, U.K. and Schmidt, R.R., *Glycosylimidates. Part 77. Efficient synthesis of O-(2-acetamido-2-deoxy-β-D-glucopyranosyl)-serine and -*

threonine building blocks for glycopeptide formation. J. Chem. Soc., Perkin Trans. 1 : Organic and Bio-Organic Chemistry, 1997(12): p. 1855-1860.

88. Clemens, J.J., Davis, M.D., Lynch, K.R., and MacDonald, T.L., *Synthesis of para-alkyl aryl amide analogues of sphingosine-1-phosphate: discovery of potent S1P receptor agonists.* Bioorg. Med. Chem. Lett., 2003, **13**(20): p. 3401-3404.
89. Dullenkopf, W., Castro-Palomino, J.C., Manzoni, L., and Schmidt, R.R., *Glycosyl imidates. Part 77. N-trichloroethoxycarbonyl-glucosamine derivatives as glycosyl donors.* Carbohydr. Res., 1996, **296**: p. 135-147.
90. Salvador, L.A., Elofsson, M., and Kihlberg, J., *Preparation of building blocks for glycopeptide synthesis by glycosylation of Fmoc amino acids having unprotected carboxyl groups.* Tetrahedron 1995, **51**(19): p. 5643-56.
91. Pazynina, G., Nasonov, V., Belyanchikov, I., Brossmer, R., Maisel, M., Tuzikov, A., and Bovin, N., *Koenigs-Knorr glycosylation with neuraminic acid derivatives.* Int. J. Carbohydr. Chem., 2010: p. 594247, 8 pp.
92. Davis, B.G., *Recent developments in oligosaccharide synthesis.* Perkin 1 2000(14): p. 2137-2160.
93. Davis, B.G. and Fairbanks, A.J., *Carbohydrate chemistry*. 1st ed. Oxford Chemistry Primers. 2002, New York: Oxford University Press.
94. Imoto, M., Yoshimura, H., Yamamoto, M., Shimamoto, T., Kusumoto, S., and Shiba, T., *Chemical synthesis of a biosynthetic precursor of lipid A with a phosphorylated tetraacyl disaccharide structure.* Bull. Chem. Soc. Jpn., 1987, **60**(6): p. 2197-204.
95. Kamst, E., Zegelaar-Jaarsveld, K., van der Marel, G.A., van Boom, J.H., Lugtenberg, B.J.J., and Spaink, H.P., *Chemical synthesis of N-acetylglucosamine derivatives and their use as glycosyl acceptors by the Mesorhizobium loti chitin oligosaccharide synthase NodC.* Carbohydr. Res., 1999, **321**(3-4): p. 176-189.
96. Joullie, M.M. and Lassen, K.M., *Evolution of amide bond formation.* ARKIVOC (Gainesville, FL, U. S.) 2010(8): p. 189-250.
97. Reid, G.E. and Simpson, R.J., *Automated solid-phase peptide synthesis: use of 2-(1H-benzotriazol-1-yl)-1,1,3,3-tetramethyluronium tetrafluoroborate for coupling of tert-butyloxycarbonyl amino acids.* Anal. Biochem., 1992, **200**(2): p. 301-9.
98. Abdelmoty, I., Albericio, F., Carpino, L.A., Foxman, B.M., and Kates, S.A., *Structural studies of reagents for peptide bond formation: Crystal and molecular structures of HBTU and HATU.* Lett. Pept. Sci., 1994, **1**(2): p. 57-67.
99. Jones, J., *Amino acid and peptide synthesis*. 2nd ed. Oxford Chemistry Primers. 2002, New York: Oxford University Press Inc.
100. Baumann, K., Kowalczyk, D., and Kunz, H., *Total synthesis of the glycopeptide recognition domain of the P-selectin glycoprotein ligand 1.* Angew Chem Int Ed Engl, 2008, **47**(18): p. 3445-9.
101. Seitz, O., *Glycopeptide synthesis and the effects of glycosylation on protein structure and activity.* ChemBioChem 2000, **1**(4): p. 214-246.
102. Ramesh, R., De, K., and Chandrasekaran, S., *An efficient synthesis of dehydroamino acids and dehydropeptides from O-Cbz and O-Eoc derivatives of serine and threonine.* Tetrahedron 2007, **63**(42): p. 10534-10542.
103. Ferreira, P.M.T., Monteiro, L.S., Pereira, G., Ribeiro, L., Sacramento, J., and Silva, L., *Reactivity of dehydroamino acids and dehydrodipeptides towards*

N-bromosuccinimide: synthesis of β-bromo- and β, β-dibromodehydroamino acid derivatives and of substituted 4-imidazolidinones. Eur. J. Org. Chem., 2007(35): p. 5934-5949.

104. Zhu, X. and Schmidt, R.R., *Selective conversion of N-trichloroethoxycarbonyl (Troc) groups into N-acetyl groups in the presence of N-tert-butoxycarbonyl (Boc) protecting groups.* Synthesis 2003(8): p. 1262-1266.
105. Yoshiizumi, K., Nakajima, F., Dobashi, R., Nishimura, N., and Ikeda, S., *Studies on scavenger receptor inhibitors. Part 1: synthesis and structure-activity relationships of novel derivatives of sulfatides.* Bioorg. Med. Chem., 2002, **10**(8): p. 2445-2460.
106. Petrasca, A., *Characterisation of the stimulatory properties of synthetic glycolipids for human invariant natural killer T cells*, 2011, Trinity College Dublin, M.Sc. Thesis.
107. Aktas, E., Kucuksezer, U.C., Bilgic, S., Erten, G., and Deniz, G., *Relationship between CD107a expression and cytotoxic activity.* Cell. Immunol., 2009, **254**(2): p. 149-154.
108. Grewal, I.S. and Flavell, R.A., *CD40 and CD154 in cell-mediated immunity.* Annu. Rev. Immunol., 1998, **16**: p. 111-135.
109. O'Reilly, V., Zeng Shijuan, G., Bricard, G., Atzberger, A., Hogan Andrew, E., Jackson, J., Feighery, C., Porcelli Steven, A., and Doherty Derek, G., *Distinct and overlapping effector functions of expanded human CD4, CD8α and CD4CD8α Invariant Natural Killer T Cells.* PLoS One, 2011, **6**(12): p. e28648.
110. Kornbluth, R.S. and Stone, G.W., *Immunostimulatory combinations: designing the next generation of vaccine adjuvants.* J. Leukocyte Biol., 2006, **80**(5): p. 1084-1102.
111. Slobedman, B., Barry, P.A., Spencer, J.V., Avdic, S., and Abendroth, A., *Virus-encoded homologs of cellular interleukin-10 and their control of host immune function.* J. Virol., 2009, **83**(19): p. 9618-9629.
112. *http://www.alzheimer.ie/eng/Alzheimer-Dementia/Dementia-and-Alzheimer's-disease/Alzheimer*. 04/01/2012].
113. Alzheimer, A., Stelzmann, R.A., Schnitzlein, H.N., and Murtagh, F.R., *An English translation of Alzheimer's 1907 paper, "Uber eine eigenartige Erkankung der Hirnrinde".* Clin Anat, 1995, **8**(6): p. 429-31.
114. Shankar, G.M., Li, S., Mehta, T.H., Garcia-Munoz, A., Shepardson, N.E., Smith, I., Brett, F.M., Farrell, M.A., Rowan, M.J., Lemere, C.A., Regan, C.M., Walsh, D.M., Sabatini, B.L., and Selkoe, D.J., *Amyloid-β protein dimers isolated directly from Alzheimer's brains impair synaptic plasticity and memory.* Nat. Med. (N. Y., NY, U. S.), 2008, **14**(8): p. 837-842.
115. Brunden, K.R., Trojanowski, J.Q., and Lee, V.M., *Advances in tau-focused drug discovery for Alzheimer's disease and related tauopathies.* Nat Rev Drug Discov, 2009, **8**(10): p. 783-93.
116. Nyakas, C., Granic, I., Halmy, L.G., Banerjee, P., and Luiten, P.G.M., *The basal forebrain cholinergic system in aging and dementia. Rescuing cholinergic neurons from neurotoxic amyloid-β42 with memantine.* Behav. Brain Res., 2011, **221**(2): p. 594-603.
117. Teipel, S.J., Buchert, R., Thome, J., Hampel, H., and Pahnke, J., *Development of Alzheimer-disease neuroimaging-biomarkers using mouse*

models with amyloid-precursor protein-transgene expression. Prog. Neurobiol. (Oxford, U. K.), 2011, **95**(4): p. 547-556.

118. Drechsel, D.N., Hyman, A.A., Cobb, M.H., and Kirschner, M.W., *Modulation of the dynamic instability of tubulin assembly by the microtubule-associated protein tau.* Mol Biol Cell, 1992, **3**(10): p. 1141-54.
119. Mazanetz, M.P. and Fischer, P.M., *Untangling tau hyperphosphorylation in drug design for neurodegenerative diseases.* Nat Rev Drug Discov, 2007, **6**(6): p. 464-79.
120. Arnold, C.S., Johnson, G.V.W., Cole, R.N., Dong, D.L.Y., Lee, M., and Hart, G.W., *The microtubule-associated protein tau is extensively modified with O-linked N-acetylglucosamine.* J. Biol. Chem., 1996, **271**(46): p. 28741-28744.
121. Dias, W.B. and Hart, G.W., *O-GlcNAc modification in diabetes and Alzheimer's disease.* Mol. BioSyst., 2007, **3**(11): p. 766-772.
122. Goedert, M., Wischik, C.M., Crowther, R.A., Walker, J.E., and Klug, A., *Cloning and sequencing of the cDNA encoding a core protein of the paired helical filament of Alzheimer disease: identification as the microtubule-associated protein tau.* Proc. Natl. Acad. Sci. U. S. A., 1988, **85**(11): p. 4051-5.
123. Goedert, M., Spillantini, M.G., Jakes, R., Rutherford, D., and Crowther, R.A., *Multiple isoforms of human microtubule-associated protein tau: sequences and localization in neurofibrillary tangles of Alzheimer's disease.* Neuron, 1989, **3**(4): p. 519-26.
124. Lee, V.M.Y., Goedert, M., and Trojanowski, J.Q., *Neurodegenerative tauopathies.* Annu. Rev. Neurosci., 2001, **24**: p. 1121-1159.
125. Anderton, B.H., Betts, J., Blackstock, W.P., Brion, J.P., Chapman, S., Connell, J., Dayanandan, R., Gallo, J.M., Gibb, G., Hanger, D.P., Hutton, M., Kardalinou, E., Leroy, K., Lovestone, S., Mack, T., Reynolds, C.H., and Van Slegtenhorst, M., *Sites of phosphorylation in tau and factors affecting their regulation.* Biochem Soc Symp, 2001(67): p. 73-80.
126. Matsuo, E.S., Shin, R.-W., Billingsley, M.L., Van deVoorde, A., O'Connor, M., Trojanowski, J.Q., and Lee, V.M.Y., *Biopsy-derived adult human brain tau is phosphorylated at many of the same sites as Alzheimer's disease paired helical filament tau.* Neuron, 1994, **13**(4): p. 989-1002.
127. Roberson, E.D., Scearce-Levie, K., Palop, J.J., Yan, F., Cheng, I.H., Wu, T., Gerstein, H., Yu, G.-Q., and Mucke, L., *Reducing endogenous Tau ameliorates amyloid β-induced deficits in an Alzheimer's disease mouse model.* Science (Washington, DC, U. S.), 2007, **316**(5825): p. 750-754.
128. Small, S.A. and Duff, K., *Linking Aβ and tau in late-onset Alzheimer's disease: a dual pathway hypothesis.* Neuron, 2008, **60**(4): p. 534-542.
129. Vossel, K.A., Zhang, K., Brodbeck, J., Daub, A.C., Sharma, P., Finkbeiner, S., Cui, B., and Mucke, L., *Tau reduction prevents Aβ-induced defects in axonal transport.* Science (Washington, DC, U. S.), 2010, **330**(6001): p. 198.
130. Han, D., Qureshi, H.Y., Lu, Y., and Paudel, H.K., *Familial FTDP-17 Missense Mutations Inhibit Microtubule Assembly-promoting Activity of Tau by Increasing Phosphorylation at Ser202 in Vitro.* J Biol Chem, 2009, **284**(20): p. 13422-33.
131. Bramblett, G.T., Goedert, M., Jakes, R., Merrick, S.E., Trojanowski, J.Q., and Lee, V.M.Y., *Abnormal tau phosphorylation at Ser396 in Alzheimer's disease recapitulates development and contributes to reduced microtubule binding.* Neuron, 1993, **10**(6): p. 1089-99.

132. Pritchard, S.M., Dolan, P.J., Vitkus, A., and Johnson, G.V.W., *The toxicity of tau in Alzheimer disease: turnover, targets and potential therapeutics.* J. Cell. Mol. Med., 2011, **15**(8): p. 1621-1635.
133. Steinhilb, M.L., Dias-Santagata, D., Mulkearns, E.E., Shulman, J.M., Biernat, J., Mandelkow, E.-M., and Feany, M.B., *S/P and T/P phosphorylation is critical for tau neurotoxicity in Drosophila.* J. Neurosci. Res., 2007, **85**(6): p. 1271-1278.
134. Ishihara, T., Hong, M., Zhang, B., Nakagawa, Y., Lee, M.K., Trojanowski, J.Q., and Lee, V.M., *Age-dependent emergence and progression of a tauopathy in transgenic mice overexpressing the shortest human tau isoform.* Neuron, 1999, **24**(3): p. 751-62.
135. Santacruz, K., Lewis, J., Spires, T., Paulson, J., Kotilinek, L., Ingelsson, M., Guimaraes, A., DeTure, M., Ramsden, M., McGowan, E., Forster, C., Yue, M., Orne, J., Janus, C., Mariash, A., Kuskowski, M., Hyman, B., Hutton, M., and Ashe, K.H., *Tau suppression in a neurodegenerative mouse model improves memory function.* Science, 2005, **309**(5733): p. 476-81.
136. Arrasate, M., Mitra, S., Schweitzer, E.S., Segal, M.R., and Finkbeiner, S., *Inclusion body formation reduces levels of mutant huntingtin and the risk of neuronal death.* Nature (London, U. K.), 2004, **431**(7010): p. 805-810.
137. Zhang, B., Maiti, A., Shively, S., Lakhani, F., McDonald-Jones, G., Bruce, J., Lee, E.B., Xie, S.X., Joyce, S., Li, C., Toleikis, P.M., Lee, V.M.Y., and Trojanowski, J.Q., *Microtubule-binding drugs offset tau sequestration by stabilizing microtubules and reversing fast axonal transport deficits in a tauopathy model.* Proc. Natl. Acad. Sci. U. S. A., 2005, **102**(1): p. 227-231.
138. Matsuoka, Y., Gray, A.J., Hirata-Fukae, C., Minami, S.S., Waterhouse, E.G., Mattson, M.P., LaFerla, F.M., Gozes, I., and Aisen, P.S., *Intranasal NAP administration reduces accumulation of amyloid peptide and tau hyperphosphorylation in a transgenic mouse model of Alzheimer's disease at early pathological stage.* J. Mol. Neurosci., 2007, **31**(2): p. 165-170.
139. Renna, M., Jimenez-Sanchez, M., Sarkar, S., and Rubinsztein, D.C., *Chemical Inducers of autophagy that enhance the clearance of mutant proteins in neurodegenerative diseases.* J. Biol. Chem., 2010, **285**(15): p. 11061-11067.
140. Rodriguez-Navarro, J.A., Rodriguez, L., Casarejos, M.J., Solano, R.M., Gomez, A., Perucho, J., Cuervo, A.M., Garcia de Yebenes, J., and Mena, M.A., *Trehalose ameliorates dopaminergic and tau pathology in parkin deleted/tau overexpressing mice through autophagy activation.* Neurobiol. Dis., 2010, **39**(3): p. 423-438.
141. Boimel, M., Grigoriadis, N., Lourbopoulos, A., Haber, E., Abramsky, O., and Rosenmann, H., *Efficacy and safety of immunization with phosphorylated tau against neurofibrillary tangles in mice.* Exp. Neurol., 2010, **224**(2): p. 472-485.
142. Schirmer, R.H., Adler, H., Pickhardt, M., and Mandelkow, E., *"Lest we forget you - methylene blue ..."*. Neurobiol. Aging, 2011, **32**(12): p. 2325 e7-2325 e16.
143. Cuny, G.D., *Kinase inhibitors as potential therapeutics for acute and chronic neurodegenerative conditions.* Curr. Pharm. Des., 2009, **15**(34): p. 3919-3939.

144. Wang, Z., Pandey, A., and Hart, G.W., *Dynamic interplay between O-linked N-acetylglucosaminylation and glycogen synthase kinase-3-dependent phosphorylation.* Mol. Cell. Proteomics, 2007, **6**(8): p. 1365-1379.
145. Steinacker, P., Klafki, H., Lehnert, S., Jesse, S., v. Arnim, C.A.F., Tumani, H., Pabst, A., Kretzschmar, H.A., Wiltfang, J., and Otto, M., *ERK2 is Increased in cerebrospinal fluid of Creutzfeldt-Jakob Disease patients.* J. Alzheimer's Dis., 2010, **22**(1): p. 119-128.
146. Zeitlin, R., Patel, S., Burgess, S., Arendash, G.W., and Echeverria, V., *Caffeine induces beneficial changes in PKA signaling and JNK and ERK activities in the striatum and cortex of Alzheimer's transgenic mice.* Brain Res., 2011, **1417**: p. 127-136.
147. Su, S.C. and Tsai, L.-H., *Cyclin-dependent kinases in brain development and disease.* Annu. Rev. Cell Dev. Biol., 2011, **27**: p. 465-491.
148. Sato, K., Minegishi, S., Takano, J., Plattner, F., Saito, T., Asada, A., Kawahara, H., Iwata, N., Saido, T.C., and Hisanaga, S.-i., *Calpastatin, an endogenous calpain-inhibitor protein, regulates the cleavage of the Cdk5 activator p35 to p25.* J. Neurochem., 2011, **117**(3): p. 504-515.
149. Jain, P., Flaherty, P.T., Yi, S., Chopra, I., Bleasdell, G., Lipay, J., Ferandin, Y., Meijer, L., and Madura, J.D., *Design, synthesis, and testing of an 6-O-linked series of benzimidazole based inhibitors of CDK5/p25.* Bioorg. Med. Chem., 2011, **19**(1): p. 359-373.
150. Mapelli, M., Massimiliano, L., Crovace, C., Seeliger, M.A., Tsai, L.-H., Meijer, L., and Musacchio, A., *Mechanism of CDK5/p25 binding by CDK inhibitors.* J. Med. Chem., 2005, **48**(3): p. 671-679.
151. Wen, Y., Planel, E., Herman, M., Figueroa, H.Y., Wang, L., Liu, L., Lau, L.-F., Yu, W.H., and Duff, K.E., *Interplay between cyclin-dependent kinase 5 and glycogen synthase kinase 3β mediated by neuregulin signaling leads to differential effects on Tau phosphorylation and amyloid precursor protein processing.* J. Neurosci., 2008, **28**(10): p. 2624-2632.
152. Zhang, J. and Herrup, K., *Nucleocytoplasmic Cdk5 is involved in neuronal cell cycle and death in post-mitotic neurons.* Cell Cycle, 2011, **10**(8): p. 1208-1214.
153. Zhang, J., Yang, P.L., and Gray, N.S., *Targeting cancer with small molecule kinase inhibitors.* Nat. Rev. Cancer, 2009, **9**(1): p. 28-39.
154. Fischer, P.M., *The design of drug candidate molecules as selective inhibitors of therapeutically relevant protein kinases.* Curr. Med. Chem., 2004, **11**(12): p. 1563-1583.
155. Garuti, L., Roberti, M., and Bottegoni, G., *Non-ATP competitive protein kinase inhibitors.* Curr. Med. Chem., 2010, **17**(25): p. 2804-2821.
156. Chico, L.K., Van Eldik, L.J., and Watterson, D.M., *Targeting protein kinases in central nervous system disorders.* Nat Rev Drug Discov, 2009, **8**(11): p. 892-909.
157. Plotkin, B., Kaidanovich, O., Talior, I., and Eldar-Finkelman, H., *Insulin mimetic action of synthetic phosphorylated peptide inhibitors of glycogen synthase kinase-3.* J. Pharmacol. Exp. Ther., 2003, **305**(3): p. 974-980.
158. Spittaels, K., Van den Haute, C., Van Dorpe, J., Geerts, H., Mercken, M., Bruynseels, K., Lasrado, R., Vandezande, K., Laenen, I., Boon, T., Van Lint, J., Vandenheede, J., Moechars, D., Loos, R., and Van Leuven, F., *Glycogen synthase kinase-3β phosphorylates protein tau and rescues the axonopathy in*

the central nervous system of human four-repeat tau transgenic mice. J. Biol. Chem., 2000, **275**(52): p. 41340-41349.

159. Gomez-Sintes, R., Hernandez, F., Lucas, J.J., and Avila, J., *GSK-3 mouse models to study neuronal apoptosis and neurodegeneration.* Front. Mol. Neurosci., 2011, **4**(Nov.): p. 45.
160. Gong, C.X. and Iqbal, K., *Hyperphosphorylation of microtubule-associated protein tau: a promising therapeutic target for Alzheimer disease.* Curr. Med. Chem., 2008, **15**(23): p. 2321-2328.
161. Dajani, R., Fraser, E., Roe, S.M., Young, N., Good, V., Dale, T.C., and Pearl, L.H., *Crystal structure of glycogen synthase kinase 3β: structural basis for phosphate-primed substrate specificity and autoinhibition.* Cell (Cambridge, MA, U. S.), 2001, **105**(6): p. 721-732.
162. Martinez, A., Alonso, M., Castro, A., Perez, C., and Moreno, F.J., *First non-ATP competitive Glycogen Synthase Kinase 3β (GSK-3β) inhibitors: Thiadiazolidinones (TDZD) as potential drugs for the treatment of Alzheimer's disease.* J. Med. Chem., 2002, **45**(6): p. 1292-1299.
163. Eldar-Finkelman, H. and Martinez, A., *GSK-3 inhibitors: preclinical and clinical focus on CNS.* Front. Mol. Neurosci., 2011, **4**(Oct.): p. 32.
164. Selenica, M.L., Jensen, H.S., Larsen, A.K., Pedersen, M.L., Helboe, L., Leist, M., and Lotharius, J., *Efficacy of small-molecule glycogen synthase kinase-3 inhibitors in the postnatal rat model of tau hyperphosphorylation.* Br. J. Pharmacol., 2007, **152**(6): p. 959-979.
165. Stukenbrock, H., Mussmann, R., Geese, M., Ferandin, Y., Lozach, O., Lemcke, T., Kegel, S., Lomow, A., Burk, U., Dohrmann, C., Meijer, L., Austen, M., and Kunick, C., *9-Cyano-1-azapaullone (Cazpaullone), a Glycogen Synthase Kinase-3 (GSK-3) inhibitor activating pancreatic β cell protection and replication.* J. Med. Chem., 2008, **51**(7): p. 2196-2207.
166. Chen, Q., Cui, W., Cheng, Y., Zhang, F., and Ji, M., *Studying the mechanism that enables paullones to selectively inhibit glycogen synthase kinase 3 rather than cyclin-dependent kinase 5 by molecular dynamics simulations and free-energy calculations.* J. Mol. Model., 2011, **17**(4): p. 795-803.
167. Martinez, A. and Perez, D.I., *GSK-3 inhibitors: a ray of hope for the treatment of Alzheimer's disease?* J Alzheimers Dis, 2008, **15**(2): p. 181-91.
168. Hampel, H., Ewers, M., Buerger, K., Annas, P., Moertberg, A., Bogstedt, A., Froelich, L., Schroeder, J., Schoenknecht, P., Riepe, M.W., Kraft, I., Gasser, T., Leyhe, T., Moeller, H.-J., Kurz, A., and Basun, H., *Lithium trial in Alzheimer's disease: a randomized, single-blind, placebo-controlled, multicenter 10-week study.* J. Clin. Psychiatry (Memphis, TN, U. S.), 2009, **70**(6): p. 922-931.
169. Eldar-Finkelman, H. and Eisenstein, M., *Peptide inhibitors targeting protein kinases.* Curr. Pharm. Des., 2009, **15**(21): p. 2463-2470.
170. Chen, G., Bower, K.A., Ma, C., Fang, S., Thiele, C.J., and Luo, J., *Glycogen synthase kinase 3β (GSK3β) mediates 6-hydroxydopamine-induced neuronal death.* Faseb J., 2004, **18**(10): p. 1162-1164, 10 1096/fj 04-1551fje.
171. Licht-Murava, A., Plotkin, B., Eisenstein, M., and Eldar-Finkelman, H., *Elucidating substrate and inhibitor binding sites on the surface of GSK-3β and the refinement of a competitive inhibitor.* J. Mol. Biol., 2011, **408**(2): p. 366-378.

172. Coin, I., Beyermann, M., and Bienert, M., *Solid-phase peptide synthesis: from standard procedures to the synthesis of difficult sequences.* Nat. Protoc., 2007, **2**(12): p. 3247-3256.
173. *Amino acids, peptides and proteins in organic chemistry*, ed. A.B. Hughes. Vol. 3. 2011, Weinheim: Wiley-VCH.
174. Mende, F. and Seitz, O., *9-Fluorenylmethoxycarbonyl-based solid-phase synthesis of peptide α-thioesters.* Angew. Chem., Int. Ed., 2011, **50**(6): p. 1232-1240.
175. Herzner, H., Reipen, T., Schultz, M., and Kunz, H., *Synthesis of glycopeptides containing carbohydrate and peptide recognition motifs.* Chem. Rev. (Washington, D. C.), 2000, **100**(12): p. 4495-4537.
176. Werz, D.B., Castagner, B., and Seeberger, P.H., *Automated synthesis of the tumor-associated carbohydrate antigens Gb-3 and Globo-H: Incorporation of α-galactosidic linkages.* J. Am. Chem. Soc., 2007, **129**(10): p. 2770-2771.
177. Polt, R., Szabo, L., Treiberg, J., Li, Y., and Hruby, V.J., *General methods for α- or β-O-Ser/Thr glycosides and glycopeptides. Solid-phase synthesis of O-glycosyl cyclic enkephalin analogs.* J. Am. Chem. Soc., 1992, **114**(26): p. 10249-58.
178. Schlummer, S., Vetter, R., Kuder, N., Henkel, A., Chen, Y.-X., Li, Y.-M., Kuhlmann, J., and Waldmann, H., *Influence of serine O-glycosylation or O-phosphorylation close to the vJun nuclear localisation sequence on nuclear import.* ChemBioChem 2006, **7**(1): p. 88-97.
179. Albericio, F., *Developments in peptide and amide synthesis.* Curr. Opin. Chem. Biol., 2004, **8**(3): p. 211-221.
180. Gude, M., Ryf, J., and White, P.D., *An accurate method for the quantitation of Fmoc-derivatized solid phase supports.* Lett. Pept. Sci., 2003, **9**(4-5): p. 203-206.
181. Aitken, A. and Learmonth, M., *Protein determination by UV absorption.* Protein Protoc. Handb., 1996: p. 3-6.
182. Kuipers, B.J.H. and Gruppen, H., *Prediction of molar extinction coefficients of proteins and peptides using UV absorption of the constituent amino acids at 214 nm to enable quantitative reverse phase high-performance-liquid chromatography-mass spectrometry analysis.* J. Agric. Food Chem., 2007, **55**(14): p. 5445-5451.
183. Kunz, H., *Glycopeptides of biological interest: a challenge for chemical synthesis.* Pure Appl. Chem., 1993, **65**(6): p. 1223-32.
184. Buskas, T., Ingale, S., and Boons, G.-J., *Glycopeptides as versatile tools for glycobiology.* Glycobiology, 2006, **16**(8): p. 113R-136R.
185. Rawe, S.L., Zaric, V., O'Boyle, K.M., and Murphy, P.V., *N-Glycosyl-thiophene-2-carboxamides: Effects on endothelial cell growth in the presence and absence of bFGF-A significant increase in potency using per-O-acetylated sugar analogues.* Bioorg. Med. Chem. Lett., 2006, **16**(5): p. 1316-1319.
186. Meutermans, W., Le, G.T., and Becker, B., *Carbohydrates as scaffolds in drug discovery.* ChemMedChem, 2006, **1**(11): p. 1164-1194.
187. Sletten, E.M. and Bertozzi, C.R., *Bioorthogonal chemistry: Fishing for selectivity in a sea of functionality.* Angew. Chem., Int. Ed., 2009, **48**(38): p. 6974-6998.
188. Boyce, M., Carrico, I.S., Ganguli, A.S., Yu, S.-H., Hangauer, M.J., Hubbard, S.C., Kohler, J.J., and Bertozzi, C.R., *Metabolic cross-talk allows labeling of*

O-linked β-N-acetylglucosamine-modified proteins via the N-acetylgalactosamine salvage pathway. Proc. Natl. Acad. Sci. U. S. A., 2011, **108**(8): p. 3141-3146, S3141/1-S3141/10.

189. Bennett, C.S., Dean, S.M., Payne, R.J., Ficht, S., Brik, A., and Wong, C.-H., *Sugar-assisted glycopeptide ligation with complex oligosaccharides: Scope and limitations.* J. Am. Chem. Soc., 2008, **130**(36): p. 11945-11952.
190. Sarkar, S. and Sucheck, S.J., *Comparing the use of 2-methylenenaphthyl, 4-methoxybenzyl, 3,4-dimethoxybenzyl and 2,4,6-trimethoxybenzyl as N-H protecting groups for p-tolyl 2-acetamido-3,4,6-tri-O-acetyl-2-deoxy-1-thio-β-D-glucosides.* Carbohydr. Res., 2011, **346**(3): p. 393-400.
191. Fleming, I. and Mason, J.B., *Product from the reaction of pyridine with acetic anhydride.* J. Chem. Soc. C, 1969(18): p. 2509-10.
192. Abramov, M., Schepers, G., Van Aerschot, A., and Herdewijn, P., *Fmoc-protected altritol phosphoramidite building blocks and their application in the synthesis of altritol nucleic acids (ANAs).* Eur. J. Org. Chem., 2007(9): p. 1446-1456.
193. Vogel, S. and Heilmann, J., *Synthesis, Cytotoxicity, and Antioxidative Activity of Minor Prenylated Chalcones from Humulus lupulus.* J. Nat. Prod., 2008, **71**(7): p. 1237-1241.
194. Gudino, E.D., Iribarren, A.M., and Iglesias, L.E., *Candida antarctica B lipase-catalysed alcoholysis of peracetylated alkyl D-ribofuranosides.* Biocatal. Biotransform., 2010, **28**(4): p. 267-271.
195. Filice, M., Bavaro, T., Fernandez-Lafuente, R., Pregnolato, M., Guisan, J.M., Palomo, J.M., and Terreni, M., *Chemo-biocatalytic regioselective one-pot synthesis of different deprotected monosaccharides.* Catal. Today 2009, **140**(1-2): p. 11-18.
196. Perez, J.A., Trujillo, J.M., Lopez, H., Aragon, Z., and Boluda, C., *Regioselective enzymatic acylation and deacetylation of secoiridoid glucosides.* Chem. Pharm. Bull., 2009, **57**(8): p. 882-884.
197. Singh, S.K., Sharma, V.K., Olsen, C.E., Wengel, J., Parmar, V.S., and Prasad, A.K., *Biocatalytic Separation of N-7/N-9 Guanine Nucleosides.* J. Org. Chem., 2010, **75**(22): p. 7932-7935.
198. Troiani, V., Cluzeau, J., and Casar, Z., *Application of chemoselective pancreatin powder-catalyzed deacetylation reaction in the synthesis of key statin side chain intermediate (4R,6S)-4-(tert-butyldimethylsilyloxy)-6-(hydroxymethyl)tetrahydropyran-2-one.* Org. Process Res. Dev., 2011, **15**(3): p. 622-630.
199. Velasco-Torrijos, T., *Towards a second generation of macrotricyclic receptors for carbohydrate recognition,* PhD thesis, 2002, University of Bristol.
200. Wang, S.-M., Zhu, W.-G., Kang, J.-X., Liu, H.-M., Chen, J.-M., Li, C.-P., and Zhang, K., *ESIMS and NMR studies on the selective deprotection of acetylated glucosides by dibutyltin oxide.* Carbohydr. Res., 2011, **346**(2): p. 203-209.
201. Gurjar, M.K., Mondal, D., Ravindranadh, S.V., and Chorghade, M.S., *Clay-mediated selective hydrolysis of 5'-O-acetyl-2',3'-isopropylidene/cyclohexylidene nucleosides.* Synth. Commun., 2006, **36**(16): p. 2321-2327.
202. Gonzalez, A.G., Brouard, I., Leon, F., Padron, J.I., and Bermejo, J., *A facile chemoselective deacetylation in the presence of benzoyl and p-bromobenzoyl*

groups using p-toluenesulfonic acid. Tetrahedron Lett., 2001, **42**(18): p. 3187-3188.
203. Jung, M.E. and Koch, P., *An efficient synthesis of the protected carbohydrate moiety of Brasilicardin A.* Org. Lett., 2011, **13**(14): p. 3710-3713.
204. Yeom, C.-E., Lee, S.Y., Kim, Y.J., and Kim, B.M., *Mild and chemoselective deacetylation method using a catalytic amount of acetyl chloride in methanol.* Synlett, 2005(10): p. 1527-1530.
205. Wong, C.-H., Hendrix, M., Manning, D.D., Rosenbohm, C., and Greenberg, W.A., *A library approach to the discovery of small molecules that recognize RNA: Use of a 1,3-hydroxyamine motif as core.* J. Am. Chem. Soc., 1998, **120**(33): p. 8319-8327.
206. Mayer, A., Gloster, T.M., Chou, W.K., Vocadlo, D.J., and Tanner, M.E., *6''-Azido-6''-deoxy-UDP-N-acetylglucosamine as a glycosyltransferase substrate.* Bioorg. Med. Chem. Lett., 2011, **21**(4): p. 1199-1201.
207. Lieber, E., Rao, C.N.R., Chao, T.S., and Hoffman, C.W.W., *Infrared spectra of organic azides.* Anal. Chem., 1957, **29**: p. 916-18.
208. Brabez, N., Lynch, R.M., Xu, L., Gillies, R.J., Chassaing, G., Lavielle, S., and Hruby, V.J., *Design, synthesis, and biological studies of efficient multivalent melanotropin ligands: Tools toward melanoma diagnosis and treatment.* J. Med. Chem., 2011, **54**(20): p. 7375-7384.
209. Grandjean, C., Boutonnier, A., Guerreiro, C., Fournier, J.-M., and Mulard, L.A., *On the preparation of carbohydrate-protein conjugates using the traceless staudinger ligation.* J. Org. Chem., 2005, **70**(18): p. 7123-7132.
210. Fernandez, C., Nieto, O., Rivas, E., Montenegro, G., Fontenla, J.A., and Fernandez-Mayoralas, A., *Synthesis and biological studies of glycosyl dopamine derivatives as potential antiparkinsonian agents.* Carbohydr. Res., 2000, **327**(4): p. 353-365.
211. Mayato, C., Dorta, R.L., and Vazquez, J.T., *Methyl esters: an alternative protecting group for the synthesis of O-glycosyl amino acid building blocks.* Tetrahedron Lett., 2008, **49**(8): p. 1396-1398.
212. Rautio, J., Laine, K., Gynther, M., and Savolainen, J., *Prodrug approaches for CNS delivery.* AAPS J., 2008, **10**(1): p. 92-102.
213. Beaumont, K., Webster, R., Gardner, I., and Dack, K., *Design of ester prodrugs to enhance oral absorption of poorly permeable compounds: Challenges to the discovery scientist.* Curr. Drug Metab., 2003, **4**(6): p. 461-485.
214. Sola, R.J. and Griebenow, K., *Glycosylation of therapeutic proteins an effective strategy to optimize efficacy.* BioDrugs 2010, **24**(1): p. 9-21.
215. Graham, P.L., *An introduction to Medicinal Chemistry*. 3rd ed. 2005, New York: Oxford University Press Inc.
216. Caliceti, P. and Veronese, F.M., *Pharmacokinetic and biodistribution properties of poly(ethylene glycol)-protein conjugates.* Adv. Drug Delivery Rev., 2003, **55**(10): p. 1261-1277.
217. Khondee, S., Olsen, C., Zeng, Y., Middaugh, C.R., and Berkland, C., *Noncovalent PEGylation by Polyanion Complexation as a Means To Stabilize Keratinocyte Growth Factor-2 (KGF-2).* Biomacromolecules 2011, **12**(11): p. 3880-3894.
218. Gantt, R.W., Peltier-Pain, P., and Thorson, J.S., *Enzymatic methods for glyco(diversification/randomization) of drugs and small molecules.* Nat. Prod. Rep., 2011, **28**(11): p. 1811-1853.

219. Larrosa, M., Tome-Carneiro, J., Yanez-Gascon, M.J., Alcantara, D., Selma, M.V., Beltran, D., Garcia-Conesa, M.T., Urban, C., Lucas, R., Tomas-Barberan, F., Morales, J.C., and Espin, J.C., *Preventive oral treatment with resveratrol pro-prodrugs drastically reduce colon inflammation in rodents.* J. Med. Chem., 2010, **53**(20): p. 7365-7376.
220. Tietze, L.F., von Hof, J.M., Mueller, M., Krewer, B., and Schuberth, I., *Glycosidic prodrugs of highly potent bifunctional duocarmycin derivatives for selective treatment of cancer.* Angew. Chem., Int. Ed., 2010, **49**(40): p. 7336-7339, S7336/1-S7336/33.
221. de Lange, E.C.M., *Potential role of ABC transporters as a detoxification system at the blood-CSF barrier.* Adv. Drug Delivery Rev., 2004, **56**(12): p. 1793-1809.
222. Patrick, G.L., *An introduction to medicinal chemistry*. 3rd ed. 2005, New York: Oxford University Press.
223. Pardridge William, M., *The blood-brain barrier: bottleneck in brain drug development.* NeuroRx, 2005, **2**(1): p. 3-14.
224. Begley, D.J., *Delivery of therapeutic agents to the central nervous system: the problems and the possibilities.* Pharmacol. Ther., 2004, **104**(1): p. 29-45.
225. Cura, A.J. and Carruthers, A., *Acute Modulation of Sugar Transport in Brain Capillary Endothelial Cell Cultures during Activation of the Metabolic Stress Pathway.* J. Biol. Chem., 2010, **285**(20): p. 15430-15439.
226. Cunningham, P., Afzal-Ahmed, I., and Naftalin, R.J., *Docking studies show that D-glucose and quercetin slide through the transporter GLUT1.* J. Biol. Chem., 2006, **281**(9): p. 5797-5803.
227. Liu, Y., Liu, F., Grundke-Iqbal, I., Iqbal, K., and Gong, C.-X., *Brain glucose transporters, O-GlcNAcylation and phosphorylation of tau in diabetes and Alzheimer's disease.* J. Neurochem., 2009, **111**(1): p. 242-249.
228. Gynther, M., Ropponen, J., Laine, K., Leppanen, J., Haapakoski, P., Peura, L., Jarvinen, T., and Rautio, J., *Glucose Promoiety Enables Glucose Transporter Mediated Brain Uptake of Ketoprofen and Indomethacin Prodrugs in Rats.* J. Med. Chem., 2009, **52**(10): p. 3348-3353.
229. Farrell, C.L. and Pardridge, W.M., *Blood-brain barrier glucose transporter is asymmetrically distributed on brain capillary endothelial lumenal and ablumenal membranes: an electron microscopic immunogold study.* Proc. Natl. Acad. Sci. U. S. A., 1991, **88**(13): p. 5779-83.
230. Fan, W., Wu, Y., Li, X.-K., Yao, N., Li, X., Yu, Y.-G., and Hai, L., *Design, synthesis and biological evaluation of brain-specific glucosyl thiamine disulfide prodrugs of naproxen.* Eur. J. Med. Chem., 2011, **46**(9): p. 3651-3661.
231. Golan, D.E., *Principles of pharmacology: the pathophysiologic basis of drug therapy*. 2nd ed. 2008, Philadelphia: Lippincott, Williams and Wilkins.
232. WHO, *Neuroscience of psychoactive substance use and dependence*. 1st ed. 2004, Geneva: WHO.
233. Miyake, N., Thompson, J., Skinbjerg, M., and Abi-Dargham, A., *Presynaptic dopamine in schizophrenia.* CNS Neurosci. Ther., 2010, **17**(2): p. 104-109.
234. Dalpiaz, A., Filosa, R., de Caprariis, P., Conte, G., Bortolotti, F., Biondi, C., Scatturin, A., Prasad, P.D., and Pavan, B., *Molecular mechanism involved in the transport of a prodrug dopamine glycosyl conjugate.* Int. J. Pharm., 2007, **336**(1): p. 133-139.

235. Mosley, A.D., Romaine, D.S., and Samii, A., *The encyclopedia of Parkinson's Disease*. 2nd ed. 2010, New York: Facts on File, inc.
236. Santini, E., Valjent, E., and Fisone, G., *Parkinson's disease: levodopa-induced dyskinesia and signal transduction.* FEBS J., 2008, **275**(7): p. 1392-1399.
237. Malvindi, M.A., Di Corato, R., Curcio, A., Melisi, D., Rimoli, M.G., Tortiglione, C., Tino, A., George, C., Brunetti, V., Cingolani, R., Pellegrino, T., and Ragusa, A., *Multiple functionalization of fluorescent nanoparticles for specific biolabeling and drug delivery of dopamine.* Nanoscale, 2011, **3**(12): p. 5110-5119.
238. Fernandez, C., Nieto, O., Fontenla, J.A., Rivas, E., de Ceballos, M.L., and Fernandez-Mayoralas, A., *Synthesis of glycosyl derivatives as dopamine prodrugs: Interaction with glucose carrier GLUT-1*. Org. Biomol. Chem., 2003, **1**(5): p. 767-771.
239. Bonina, F., Puglia, C., Rimoli, M.G., Melisi, D., Boatto, G., Nieddu, M., Calignano, A., La Rana, G., and De Caprariis, P., *Glycosyl derivatives of dopamine and L-dopa as Anti-Parkinson prodrugs: Synthesis, pharmacological activity and in vitro stability studies.* J. Drug Targeting 2003, **11**(1): p. 25-36.
240. Yoon, S.-H., Bruce Fulton, D., and Robyt, J.F., *Synthesis of dopamine and L-DOPA-α-glycosides by reaction with cyclomaltohexaose catalyzed by cyclomaltodextrin glucanyltransferase.* Carbohydr. Res., 2009, **344**(17): p. 2349-2356.
241. Trapani, A., De Giglio, E., Cafagna, D., Denora, N., Agrimi, G., Cassano, T., Gaetani, S., Cuomo, V., and Trapani, G., *Characterization and evaluation of chitosan nanoparticles for dopamine brain delivery.* Int. J. Pharm., 2011, **419**(1-2): p. 296-307.
242. Carafa, M., Marianecci, C., Di Marzio, L., De Caro, V., Giandalia, G., Giannola, L.I., and Santucci, E., *Potential dopamine prodrug-loaded liposomes: preparation, characterization, and in vitro stability studies.* J. Liposome Res., 2010, **20**(3): p. 250-257.
243. Ohtsuki, S., Yamaguchi, H., Kang, Y.-S., Hori, S., and Terasaki, T., *Reduction of L-type amino acid transporter 1 mRNA expression in brain capillaries in a mouse model of Parkinson's disease.* Biol. Pharm. Bull., 2010, **33**(7): p. 1250-1252.
244. Barwell, N.P. and Davis, A.P., *Substituent Effects in Synthetic Lectins - Exploring the Role of CH-π Interactions in Carbohydrate Recognition.* J. Org. Chem., 2011, **76**(16): p. 6548-6557.
245. Witschi, M.A. and Gervay-Hague, J., *Selective Acetylation of per-O-TMS-Protected Monosaccharides.* Org. Lett., 2010, **12**(19): p. 4312-4315.
246. Slebioda, M., Wodecki, Z., and Kolodziejczyk, A.M., *Formation of optically pure N-acyl-N,N'-dicyclohexylurea in N,N'-dicyclohexylcarbodiimide-mediated peptide synthesis.* Int. J. Pept. Protein Res., 1990, **35**(6): p. 539-41.
247. Katoh, A., Ohkanda, J., Itoh, Y., and Mitsuhashi, K., *N-hydroxyamide-containing heterocycles. New effective additives for peptide synthesis by the dicyclohexylcarbodiimide method.* Chem. Lett., 1992(10): p. 2009-12.
248. Ulrich, H., *Chemistry and Technology of Carbodiimides*. 1st ed. 2007, London: John Wiley and Sons.

249. Xia, J., Alderfer, J.L., Srikrishnan, T., Chandrasekaran, E.V., and Matta, K.L., *A convergent synthesis of core 2 branched sialylated and sulfated oligosaccharides.* Bioorg. Med. Chem., 2002, **10**(11): p. 3673-3684.
250. Kocienski, P.J., *Protecting Groups*. 3rd ed. 2005, Stuttgart: Thieme.
251. Aguilera, B., Fernandez-Mayoralas, A., and Jaramillo, C., *Use of cyclic sulfamidates derived from D-allosamine in nucleophilic displacements: scope and limitations.* Tetrahedron 1997, **53**(16): p. 5863-5876.
252. Gottlieb, H.E., Kotlyar, V., and Nudelman, A., *NMR chemical shifts of common laboratory solvents as trace impurities.* J. Org. Chem., 1997, **62**(21): p. 7512-7515.
253. Tummatorn, J., Albiniak, P.A., and Dudley, G.B., *Synthesis of benzyl esters using 2-benzyloxy-1-methylpyridinium triflate.* J. Org. Chem., 2007, **72**(23): p. 8962-8964.
254. Ellervik, U. and Magnusson, G., *Glycosylation with N-Troc-protected glycosyl donors.* Carbohydr Res, 1996, **280**(2): p. 251-60.
255. Johnson, D.A. and Sowell, C.G., *Aminoalkyl glucosaminide phosphate compounds and their use as adjuvants and immunoeffectors*, 2001, (Corixa Corporation, USA). Application: US. p. 44 pp , Cont -in-part of U S 6,113,918.
256. Sudibya, H.G., Ma, J., Dong, X., Ng, S., Li, L.-J., Liu, X.-W., and Chen, P., *Interfacing glycosylated carbon-nanotube-network devices with living cells to detect dynamic secretion of biomolecules.* Angew. Chem., Int. Ed., 2009, **48**(15): p. 2723-2726.
257. Paulsen, H. and Helpap, B., *Building blocks of oligosaccharides. Part XCVI. Synthesis and partial structures of the N-glycoproteins of the complex type.* Carbohydr. Res., 1991, **216**: p. 289-313.
258. Antoon, J.W., Liu, J., Gestaut, M.M., Burow, M.E., Beckman, B.S., and Foroozesh, M., *Design, Synthesis, and Biological Activity of a Family of Novel Ceramide Analogues in Chemoresistant Breast Cancer Cells.* J. Med. Chem., 2009, **52**(18): p. 5748-5752.
259. Huang, Y., Dey, S., Zhang, X., Soennichsen, F., and Garner, P., *The α-helical peptide nucleic acid concept: Merger of peptide secondary structure and codified nucleic acid recognition.* J. Am. Chem. Soc., 2004, **126**(14): p. 4626-4640.
260. Higashi, K., Nakayama, K., Shioya, E., and Kusama, T., *Direct transformation of O-glycoside into glycosyl bromide with the combination of trimethylsilyl bromide and zinc bromide.* Chem. Pharm. Bull., 1991, **39**(10): p. 2502-4.
261. Bera, S. and Linhardt, R.J., *Design and synthesis of unnatural heparosan and chondroitin building blocks.* J. Org. Chem., 2011, **76**(9): p. 3181-3193.
262. Meng, Y., Guo, Y., Ling, Y., Zhao, Y., Zhang, Q., Zhou, X., Ding, F., and Yang, Y., *Synthesis and protective effects of aralkyl alcoholic 2-acetamido-2-deoxy-β-D-pyranosides on hypoglycemia and serum limitation induced apoptosis in PC12 cell.* Bioorg. Med. Chem., 2011, **19**(18): p. 5577-5584.
263. Robyt, J.F., *Essentials of carbohydrate chemistry*. 1st ed. 1998, New York: Springer-Verlag New York, Inc.